Grasas y aceites

International Journal of Fats and Oils

Volumen 72 | Nº 3 | July-September 2021 | Sevilla (España) | ISSN-L: 0017-3495

CSIC
INSTITUTO DE LA GRASA

CONSEJO SUPERIOR DE INVESTIGACIONES CIENTÍFICAS

Grasas y aceites

International Journal of Fats and Oils

Volume 72 • N.º 3 **July-September 2021** Sevilla (España) ISSN-L: 0017-3495

MINISTERIO DE CIENCIA E INNOVACIÓN

CSIC

CONSEJO SUPERIOR DE INVESTIGACIONES CIENTÍFICAS

Volume 72 • N.º 3 **July-September 2021** Sevilla (España) ISSN-L: 0017-3495

GRASAS Y ACEITES
REVISTA PUBLICADA POR EL INSTITUTO DE LA GRASA, CSIC

La revista *Grasas y Aceites (Grasas Aceites)*, de periodicidad trimestral, es una publicación dedicada a la información científica y técnica sobre grasas comestibles y sus derivados.
Publica trabajos de investigación originales, artículos de información, notas de laboratorio, trabajos de revisión así como bibliografía sobre revistas, patentes o libros. El campo que cubre se refiere fundamentalmente a frutos y semillas oleaginosas, materias grasas, productos afines o derivados y aceitunas de mesa. Igualmente, incluye trabajos relacionados con subproductos de todas las materias anteriores y el tratamiento de las aguas residuales de las industrias correspondientes. Los originales recibidos son evaluados por el Consejo de Redacción y por evaluadores externos.
Se publica desde 1.991 en edición electrónica, modelo acceso abierto en:
http://grasasyaceites.revistas.csic.es.

Grasas y Aceites (Grasas Aceites) is a quarterly published journal devoted to scientific and technological information on the field of edible fat and oils and their derivatives.
Grasas y Aceites publishes full research articles, research notes, reviews as well as information on references, patents, and books. Grasas y Aceites covers the following fields: oleaginous fruit and seeds, edible fatty materials as well as related products and their derivatives, including table olives. It also accept works related to by-products from all the previous materials and the handling and treatment of the wastewaters from the corresponding industries. Originals are always reviewed by the Editorial Board and by qualified experts.
There is since 1.991 an electronic edition, open access model, at:
http://grasasyaceites.revistas.csic.es

REDACCIÓN E INFORMACIÓN

Revista Grasas y Aceites
INSTITUTO DE LA GRASA, CSIC
Universidad Pablo de Olavide - Edificio 46
Ctra. de Utrera, km. 1 - 41013, Sevilla (Spain)
Tel.: +34 954 611 550
e-mail: grasasyaceites@ig.csic.es
http://grasasyaceites.revistas.csic.es

DISTRIBUTION, SALES and SUBSCRIPTIONS

Editorial CSIC / CSIC Press
c/ Vitruvio 8
28006 Madrid
Tel: +34 915 681 402
Email: publ@csic.es
editorial.csic.es

Librería Científica del CSIC
Calle de Serrano, 123 28006 Madrid
Telf.: +34 915 680 051
E-mail: libreria@csic.es

Sale of Printed edition available until 2013 at:
http://editorial.csic.es/publicaciones/revista/17/1/10/grasas-y-aceites.html:
Subscription to the Digital Collection as PDF available since 2011 through the following associated plataforms: Casalini Libri s.p.a., Digitalia US, e-Libro.net and e-Libro.com

SERVICIO DE INFORMACIÓN

Los artículos publicados por Grasas y Aceites son recogidos, entre otras, por las siguientes bases de datos: C.A.S. Chemical Abstracts Services (USA), I.A.L.I.N.E. (Francia), C.A.B.S. Current Awareness in Biological Sciences (Gran Bretaña), F.S.T.A. Food Science and Technology Abstracts (USA-Gran Bretaña), BIOSIS Biological Abstracts (USA), SCISEARCH Science Citation Index Search (USA), SWETS (Holanda), CAB Commowealth Agricultural Bureaux (Gran Bretaña), OSTI Office of Scientific and Technological Information (USA), FOODS-ADLIBRA (USA), PASCAL (Francia), A.A. Analytical Abstract (Gran Bretaña), Cambridge Scientific Abstracts (USA), Current Contents (USA), Deutsche Gessellscharft für Fettiwissenschaft (Alemania), ICYT Índice Español de Ciencia y Tecnología España) y en el CINDOC.

Cada autor es responsable del contenido de sus respectivos trabajos.
El Consejo Superior de Investigaciones Científicas no se hace responsable, en ningún caso, de la credibilidad y autenticidad de los trabajos.
Los originales de la revista Grasas y Aceites, publicados en papel y en versión electrónica, son de propiedad del Consejo Superior de Investigaciones Científicas, siendo necesario citar la procedencia en cualquier reproducción parcial o total.

Authors take full responsibility for all statements or opinions included in their papers.
CSIC does not assume any liability with respect to the credibility or authenticity of the contributions.
Articles appeared in Grasas y Aceites, both in the printed and the electronic versions, are property of the CSIC and it is needed to cite the origin of the article in any total or partial reproduction.

ISSN-L: 0017-3495
NIPO (en línea): 833-20-022-X
Depósito legal: M 862-1958
Impreso en España - Printed in Spain.
En esta edición se ha utilizado papel ecológico sometido a un proceso de blanqueado TCF, cuya fibra procede de bosques gestionados de forma sostenible.
Maquetación: Editorial MIC

Volume 72 • N.º 3 **July-September 2021** Sevilla (España) ISSN-L: 0017-3495

Grasas y aceites

CONTENIDO

Investigación

CONTENTS

Research

GRASAS Y ACEITES 72 (3)
July-September 2021, e415
ISSN-L: 0017-3495
https://doi.org/10.3989/gya.0329201

Cold-pressed cactus pear seed oil: Quality and stability

M. de Wit[a, ✉], V.K. Motsamai[a] and A. Hugo[a]

[a]Department of Microbial, Biochemical and Food Biotechnology, University of the Free State, P.O. Box 339, Bloemfontein, 9301, South Africa
✉Corresponding author: dewitm@ufs.ac.za

Submitted: 11 March 2020; Accepted: 04 June 2020; Published online: 14 September 2021

SUMMARY: Cold-pressed seed oil from twelve commercially produced cactus pear cultivars was assessed for oil yield, fatty acid composition, physicochemical properties, quality and stability. Large differences in oil content, fatty acid composition and physicochemical properties (IV, PV, RI, tocopherols, ORAC, % FFA, OSI and induction time) were observed. Oil content ranged between 2.51% and 5.96% (Meyers and American Giant). The important fatty acids detected were C16:0, C18:0, C18:1c9 and C18:2c9,12, with C18:2c9,12, the dominating fatty acid, ranging from 58.56–65.73%, followed by C18:1c9, ranging between 13.18–16.07%, C16:0, which ranged between 10.97 - 15.07% and C18:0, which ranged between 2.62–3.18%. Other fatty acids such as C14:0, C16:1c9, C17:0, C17:1c10, C20:0, C18:3c9,12,15 and C20:3c8,11,14 were detected in small amounts. The quality parameters of the oils were strongly influenced by oil content, fatty acid composition and physicochemical properties. Oil content, PV, % FFA, RI, IV, tocopherols, ORAC and *ρ*-anisidine value were negatively correlated with OSI. C18:0; C18:1c9; C18:2c9,12; MUFA; PUFA; *n*-6 and PUFA/SFA were also negatively correlated with OSI. Among all the cultivars, American Giant was identified as the paramount cultivar with good quality traits (oil content and oxidative stability).

***KEYWORDS**: Antioxidants; Induction time; Oxidation; Prickly pear; Yield*

RESUMEN: ***Aceite de semilla de nopal prensado en frío: calidad y estabilidad.*** Se evaluó el rendimiento de aceite, la composición en ácidos grasos, las propiedades fisicoquímicas, la calidad y la estabilidad del aceite de semilla prensadas en frío de doce cultivares de nopal producidos comercialmente. Se observaron grandes diferencias en el contenido de aceite, la composición en ácidos grasos y las propiedades fisicoquímicas (IV, PV, RI, tocoferoles, ORAC, % FFA, OSI y tiempo de inducción). El contenido de aceite varió entre 2,51–5,96% (Meyers y American Giant). Los ácidos grasos mayoritarios fueron C16:0, C18:0, C18:1c9 y C18:2c9,12, siendo el C18:2c9,12 el mayoritario con porcentajes entre 58,56–65,73, seguido de C18:c9 que varía entre 13,18–16,07%, C16:0, 10,97-15.07% y C18:0 entre 2,62-3,18%. Otros ácidos grasos, tales como C14:0, C16:1c9, C17:1c10, C20:0, C18:3c9,12,15 y C20:3c8,11,14 se detectaron en pequeñas cantidades. Los parámetros de calidad de los aceites estuvieron estrechamente influenciados por el contenido total de aceite, la composición de ácidos grasos y las propiedades fisicoquímicas. El contenido de aceite, PV, % FFA, RI, IV, tocoferoles, ORAC y el valor de *ρ*-anisidina se correlacionaron negativamente con OSI. C18:0; C18:1c9; C18: 2c9,12; MUFA; PUFA; n-6 y PUFA / SFA también se correlacionaron negativamente con OSI. Entre todos los cultivares, American Giant fue identificado como el cultivar primordial con rasgos de buena calidad (contenido de aceite y estabilidad oxidativa).

***PALABRAS CLAVE:** Antioxidantes; Higo chumbo; Oxidación; Rendimiento; Tiempo de inducción*

Citation/Cómo citar este artículo: Wit M de, Motsamai VK, Hugo A. 2021. Cold-pressed cactus pear seed oil: Quality and stability. *Grasas Aceites* 72 (3), e415. https://doi.org/10.3989/gya.0329201

1. INTRODUCTION

Edible cold-pressed oils are functional products because of their bioactive substances such as polyunsaturated fatty acids, tocopherols, sterols, phenols, carotenoids and chlorophyll. These oils have specific characteristics which provide additional health benefits (Boskou, 2017). The use of non-traditional cold-pressed oils to be introduced into the cosmetic and nutraceutical markets is expected to increase. Recently, research on oils from fig seeds from Morocco (Hssaini *et al*., 2020), lentisk and skeels from Algeria (Brahmi *et al*., 2020) as well as milk thistle oil and their functional properties were reported. Cactus pear seed oil has been viewed as an important vegetable oil because of its related quality composition factors, namely high concentrations of important fatty acids, for example, linoleic acid (C18:2c9,12) (C18:2 n-6); vitamin E (100 mg/100g) and sterols (1 g/100g) (Ennouri *et al.*, 2005). In the past, oil quality was estimated based on oil yield and fatty acid composition alone. Lately, in addition to fatty acid composition, the natural antioxidants, tocopherols and sterols are additional important components which define oil quality (Fernández-Martínez *et al*., 2004). Oil quality has been transformed by the development of oil with enhanced nutritional and functional properties, and these modifications are incorporated when breeding for increased quantities of C18:2c9,12.

Cold-pressed cactus pear seed oil is characterized by a high content of unsaturated fatty acids (Sawaya and Khan, 1982). Past research has demonstrated that vegetable oil with the highest unsaturation level is most likely to undergo autoxidation. Martínez *et al*. (2011) reported that there are elements that can potentially affect the stability and quality of oil in a negative way, for example light, heat, metals, free fatty acids, tocopherols, phospholipids and waxes which contain pro or antioxidant properties. Hydrolytic reactions which are catalyzed by lipases and react with atmospheric oxygen (autoxidation) are a major cause of nutritional and oil quality losses. Naz *et al*. (2004) explained oxidation as an autocatalytic series of reactions that requires low activation energy. These authors also reported that fatty acid composition and the presence of antioxidants in vegetable oil influences oxidation. Lajara *et al.* (1990) and Izquierdo *et al*. (2009) reported that oils containing high contents of oleic acid (C18:1c9) will possibly have greater stability against oxidation and are favored for improved shelf-life. Naz *et al*. (2004) further reported that to minimize the effect of hydrolytic reactions, cold storage and proper packaging must be applied. Martínez *et al*. (2011) stated that the oxidative stability of cold-pressed oils is usually measured by the level of peroxide and *ρ*-anisidine values. The level of unsaturation (polyunsaturated fatty acids) (PUFA), especially the level of α-linoleic acid (C18:2c9,12) and the amounts of antioxidants may perhaps limit the stability of these oils. Tocopherols are reported to be strong antioxidants which can scavenge peroxyl radicals. Choe and Min (2006) indicated that the stability of these oils is commonly set for 6 months or a year. Normand *et al.* (2006) stated that oils with high tocopherol contents have greater stability. Cold-pressed cactus pear seed oil was reported to have higher contents (94.6 mg/100g) of tocopherols than olive oil (22 mg/100g), soybean oil (49 mg/100g) and sunflower oil (49 mg/100g), and close to those of argan oil (85 mg/100g) (Zine *et al*., 2013).

Cactus pear seed oil is a promising source of polyunsaturated fatty acids (PUFA), with significant levels of carotenoids and γ-tocopherols which can be used as antioxidants to preserve lipid components and serve as functional ingredients (Loizzo *et al*., 2019). Proper utilization of this seed by-product can generate up to 1220€ income per ton and is therefore a potentially new economic source (Ciriminna *et al*., 2017). According to Regalado-Rentería *et al. (*2018) prickly pear seed oils are rich in functional metabolites and linoleic fatty acids. Furthermore, this oil could be used in foods as a nutritional supplement, as well as an ingredient in cosmetics and pharmaceuticals. A major advantage is that the residual oilcake can be directly used in animal feed or other secondary products.

Recent research on the oil quality of seed oil from different colored cactus pear fruit seed oil found that cultivar played a major role in the composition of the oils (Regalado-Rentería *et al.,* 2018). Furthermore, oil content and the composition of oils from different origins were reported to indicate differences between cultivars from Sicily and those from Algeria and Morocco; while similarities occurred between cultivars from Sicily and Tunisia, indicating an origin/environment effect (Ghazi *et al.*, 2013; Ciriminna *et al*., 2017; Regalado-Rentería *et al.,*

2018; Loizzo *et al*., 2019). In addition, the effect of different species, e.g. *Opuntia dillenii,* on oil quality was reported. New studies on *O. ficus-indica* seed oils from countries such as Greece (Karabagias *et al*., 2020) and Saudi Arabia (Koshak *et al*., 2020) have been undertaken very recently.

In a previous study done by de Wit *et al*. (2017), the quality aspects of chemically extracted (Soxhlet extraction) seed oils from a few selected cultivars were quantitatively analyzed. The current study focused on the oil yield, composition, quality and stability of cold-pressed seed oil of commercially produced *Opuntia ficus-indica* cultivars. *O. robusta* seed was included as a reference and for comparison purposes. The aim of this study was to determine the quality and oxidative stability of cold-pressed cactus pear seed oil from 12 chosen cultivars. The quality attributes assessed included oil content, fatty acid composition, refractive index, tocopherols, oxygen radical antioxidant capacity, peroxide value and ρ-anisidine value; while stability tests included the oxidative stability index (OSI), as well as induction time extrapolated at 25 and 30 °C.

2. MATERIALS AND METHODS

2.1. Seed material used

Fruit from selected cultivars growing at an experimental orchard outside Bloemfontein (29.0852 °S, 26.1596 °E) was collected during the 2014, 2015 and 2016 seasons. Twelve cultivars, namely Algerian, American Giant, Ficus-Indice, Gymno Carpo, Meyers, Morado, Nudosa, Ofer, Tormentosa, Van As and Zastron were chosen. These *O. ficus-indica* cultivars are commercially produced for fresh fruit consumption. The *O. robusta* cultivar, Robusta, represents a different species and was included because it is commonly found and cultivated as animal fodder in South Africa. The fruit collection was done when the fruit reached 50% color break stage and ±75 kg of fruit per cultivar were collected to produce 2-3 kg of seeds. The seeds were extracted with an industrial liquidizer (Ingram Engineering, Zastron, South Africa) which separates the seeds from the pulp and peels. The seeds were washed with water and collected in a rotating sieved drum. The seeds were then dried under direct sunlight for 2-3 days on shade-netting, placed ± 1 m from the ground to allow for sufficient ventilation. The seeds were manually turned regularly. The drying process aimed to dry out any pulp tissue left on the seed surfaces for easy removal and cleaning before pressing. In a previous study done by de Wit *et al.* (2016), the moisture content in seeds varied from ~3% to ~7.2% due to variations in location, season and especially rainfall. The dried seeds were then vacuum-packed and stored in a freezer at -18 ºC until further analysis.

2.2. Seed oil extraction (cold-pressing)

The dried seeds from all cultivars for each season were cold-pressed in a Komet DD85G twin screw plant oil press (Oekotek, IBG Monforts, Germany) at Nattrend/Bauma Investments CC commercial oil pressing laboratory in Montana Park, Pretoria. The oil extracted using the Komet cold-pressing system is subjected to low temperatures and therefore top-quality vegetable oil which can be utilized for human consumption without any further treatment depending on the raw material used (Schramm, 2016; pers. comm.). The oilcake extrudes out of the oil press in the shape of pellets. The oil was then stored in amber screw-cap 50 ml plastic bottles for one week at room temperature before analysis. The oil analysis for each cultivar for each of the three seasons was done in triplicate.

2.3. Oil yield

The oil yield from the seeds of each cultivar from each season was determined according to the formula:

Oil yield (%) = Mass of oil (g) / Mass of cactus pear seed (g) x 100

2.4. Physico-chemical properties

2.4.1. Fatty acid composition (fatty acid methyl esters) (FAME)

Approximately 20 mg of total lipid (from cold-pressed oil) were transferred to a Teflon-lined screw-top test tube with a glass pasteur pipette. Fatty acids were methylated to methyl esters by using 0.5 N sodium hydroxide (NaOH) in methanol and 14% boron trifluoride in methanol (Park and Goins, 1994). The fatty acid methyl esters (FAME) were quantified using a Varian 430 gas chromatograph with flame ionization detector with a fused silica capillary column (Chrompack CPSIL 88, 100 m length, 0.25 mm ID, 0.2 mm film thickness). Column

temperature was 40–230 °C (held 2 minutes; 4 °C/ minute; held 10 minutes). Fatty acid methyl esters in hexane (1ml) were injected into the column using a Varian CP8400 Auto-sampler with a split ratio of 100:1. The injection port as well as the detector were maintained at 250 °C. The carrier gas was hydrogen, at 45 psi. The makeup gas was nitrogen. Galaxy Star Chromatography Software was used to record the chromatograms. The peaks were identified by comparing the relative retention times of FAME peaks from samples with that of standards from Supelco (Supelco 37 Component Fame Mix 47885-U, Sigma-Aldrich Aston Manor, Pretoria, South Africa). Fatty acids were expressed as the relative percentage of each individual fatty acid as a percentage of the total of all fatty acids in the sample. The following fatty acid ratios and combinations were calculated from the fatty acid data: total saturated fatty acids (SFA), total mono-unsaturated fatty acids (MUFA), total polyunsaturated fatty acids (PUFA), total omega-6, total omega-3 fatty acid content and the PUFA/SFA (P/S) ratio.

2.4.2. Refraction index (RI)

Refractive Index (RI) was determined according to the Association of Official Analytical Chemists' (AOAC), official method 921.08 (AOAC, 2000) with an Abbè programmed advanced refractometer from ATAGO® (Model RX 5000α) at 40 °C.

2.4.3. Iodine value (IV)

Hanus iodine Value (IV) was determined by the AOAC official method 920.158 (AOAC, 2000), which consists of adding a mixture of iodine and bromine in glacial acetic acid and measuring the excess of unused halogen by titration with sodium thiosulfate.

2.4.4. Tocopherols

High performance liquid chromatography (HPLC) was used to determine the tocopherol amount in each sample using Shimadzu CR8A instruments (Champ sur Marne, France) equipped with a C18-Varian column (25 cm x 4 mm; Varian Incorporated, Middleburg, Netherlands). One gram of each oil sample was added to 5 mL of ethanol (EtOH), filtered (45µm) into a HPLC vial at 25 ºC. HPLC was carried out with an injection volume of 20 µL, a flow rate of 1 ml/min and estimated at UV of 296 nm. The mobile stages were: mobile stage A (Acetonitrile: Methanol: Isopropanol: Water (45:45:5:5, v/v/v/v)) and mobile stage B (Acetonitrile: Methanol: Isopropanol (50:45:5, v/v/v)).

2.4.5. Oxygen Radical Antioxidant Capacity (ORAC)

For the Oxygen Radical Antioxidant Capacity (ORAC) analysis, the method of Prior *et al*. (2003) was used, where samples (10 g each) were diluted with 80% methanol in H_2O (1:1 w/v), and then vortexed for 2 minutes at room temperature and centrifuged for 10 minutes at 500 X g. The peroxyl radicals were generated with 2, 2'-Azobis (2-amidinopropane) dihydrochlorine (AAPH) and B-phycoerythrin (B-PE) was used as the detector of radical activity. The final reaction mixture was prepared in 10-mm-wide quartz cuvettes as follows: 1600 µL of 0.04 µM B-PE in 0.0075 M sodium (Na) – potassium (K) phosphate buffer at pH 7.0 and 200 µL of 50 µM Trolox (6-hydroxy-2,5,7,8-tetramethylchroman -2-carboxylic acid). Phosphate buffer was used as a blank (200 µL of methanol, diluted 1:20 (v/v) with 0.075 M Na-K, at pH 7.0 and Trolox (β and γ tocopherol analogue) as the standards during each run. Samples were pre-incubated at 37 ºC for 15 min. AAPH was added. Flourescence was measured and measurements were recorded every 5 minutes for 35 minutes at 570 nm until a steady state (plateau) of fluorescence decay was reached. The results were then calculated and expressed as µmol of Trolox equivalent (TE). The analyses were done in triplicate.

2.5. Determination of oxidative stability

2.5.1. Free Fatty Acids (FFA)

Free fatty acids were determined according to the method of Pearson (1973), which involves the titration of the oil in an alcoholic medium against potassium hydroxide using phenolphthalein as indicator.

2.5.2. Peroxide value (PV)

Peroxide value was determined by the official method of the AOAC 965.33 (AOAC, 2000). Peroxide value determines hydrogen peroxide, a primary oxidation product, and involves peroxides liberating iodine from potassium iodide by calculating the amount of sodium thiosulfate consumed.

2.5.3. ρ-Anisidine value (ρ-AV)

The *ρ*-AV was determined using the technique of Hamilton and Hamilton (1992). It determines the amounts of aldehydes and ketones during secondary oxidation by reaction with *ρ*-Anisidine (4-methoxyaniline) using a spectrophotometer at 350 nm.

2.5.4. Oxidative Stability index (OSI)

The oxidative stability index (OSI) was determined using the AOAC OSI official method Cd 12b-92 (AOAC, 2000) with a Rancimat 743 apparatus from Metrohm. Three samples were tested per cultivar.

2.5.5. Extrapolated induction time (Shelf-life prediction at 25 and 30 °C)

The oxidative stability index (OSI) was determined using the AOAC OSI official method Cd 12b-92 (AOAC, 2000) with a Rancimat 743 apparatus from Metrohm. Three samples were tested per cultivar. Oxidative stability index (OSI) values were determined at 100, 110, 120 and 130 °C for each sample in duplicate. The extrapolation function of the Rancimat 743 apparatus was used to predict induction times at 25 and 30 °C (Rancimat Manual, 2009) according to the formula:

Predicted induction time = $A \times e^{(BXT)}$

2.6. Statistical analysis

Seed were selected from each of the 2014, 2015 and 2016 harvest. Oil yield was determined for each cultivar for each season. Each measurement was made in triplicate on oil from each cultivar per year. Data were captured for the three years and were reported as average ± standard deviation using NCSS Statistical Software package, version 11.0.20). The Pearson correlation analysis was done to determine the link between the physico-chemical properties of the oil (NCSS Statistical Software package, version 11.0.20).

3. RESULTS AND DISCUSSION

3.1. Oil yield

Seed oil content ranged from 2.51 to 5.96% (Meyers and American Giant), respectively (Figure 1). Gymno Carpo and Morado were amongst those which attained the lowest oil contents (2.72 and 2.78%). In a previous limited study, the chemical extraction of seed oils from only seven selected cultivars by de Wit *et al*. (2017), the oil content ranged from 5.65–8.09%. A subsequent elaborated study on seed oil from 42 cultivars by de Wit *et al*. (2018) reported oil contents ranging from 4.09–8.76%. The lower yield values reported in the current study were expected since the oil was recovered by pressing and not by chemical extraction as in the above-

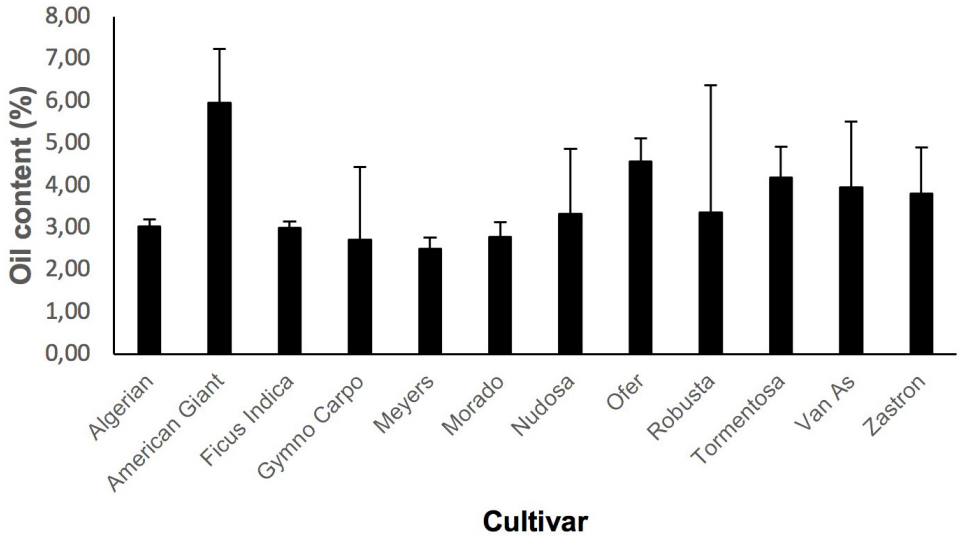

Figure 1. Oil yield (%) of cold-pressed oil for all 12 cultivars. Oil yield was expressed as % Oil yield = Mass of oil (g) / Mass of cactus pear seed (g) x 100. Values in the Figure are mean ±SD of triplicate analyses.

mentioned studies. American Giant also obtained the highest oil content in the study of 42 cultivars by de Wit *et al*. (2018). The values obtained in the current study agree with those reported for the same commercial South African cactus pear cultivars from the Limpopo Province by Labuschagné and Hugo (2010) (2.24 to 5.69%). That study did not include American Giant.

It was also found by Ortega-Ortega *et al*. (2017), Ramírez-Moreno *et al*. (2017), Regalado-Rentería *et al.* (2018) and Loizzo *et al*. (2019) that extraction method had an effect on the oil yield of cactus pear seeds. These authors and others, e.g. Ciriminna *et al*. (2017) also reported the effect of variety and species on the oil yield of cactus pear seeds. High yields of 9.3– 9.5 g oil per 100 g seed were reported for Sicilian cactus pears (*O. ficus-indica*) extracted with hexane by the Soxhlet method, while Ultra-Sound Assisted extraction yielded 5.4–5.6 g/100 g. The highest yields were found in the Turkish and Moroccan varieties (≈ 14 g/100 g seed) (Chougui *et al*., 2013). Lower values than those were reported for Algerian (7.3–9.3 g/100 g seed) and Tunisian fruit seed oils (Chougui *et al*., 2013). The lowest values were found for the Greek wild *O. ficus-indica* variety (yellow to green fruit) of 5.4%, which was also obtained by cold-pressing (Karabagias *et al.*, 2020). Slightly higher yields were reported for *O. microdasys* (Engelm) (9.2%) and *O. macrorhiza* (11.3%) from Tunisia (Chahdoura *et al.*, 2015). Maceration-Percolation (MP) extraction was used by Regalado-Rentería *et al*. (2018) to yield oil contents of up to 15.5% from *O. robusta* species (14.54 - 15.54%). Oil yields for other prickly pear varieties included *O. albicarpa* (8.72%), *O. magacantha* (6.16 – 7.63%), *O. matudae* (9.68%), *O. streptacantha* (10.55 – 11.64%) and *O. dillenii* (6.5%) (Ali Asaad *et al*., 2019).

Fruit color was also indicated as a factor influencing oil yield, e.g. Ramírez-Moreno *et al*. (2017) reported higher yields from a green cultivar compared to a red cultivar. American Giant from the current study is also a green cultivar. These results support research that pointed out that cultivar, crop, environment and origin (rainfall, soil type and soil nutrients, light, temperature) and extraction method, including extraction solvents (hexane > ethanol > ethyl acetate) influence oil yields. According to Karabagias *et al*. (2020), the most important factors are variety and extraction process.

3.2. Physico-chemical properties

3.2.1. Fatty acid composition

The fatty acid compositions of cold-pressed oil from a selection of cactus pear cultivars are shown in Table 1. According to the results presented, there are considerable variations in the fatty acid percentage of the selected cultivars. The dominating fatty acids identified (in decreasing order) were linoleic acid (C18:2 n-6) (C18:2c9,12); oleic acid (C18:1 n-9) (C18:1c9); palmitic acid (C16:0) and stearic acid (C18:0); while palmitoleic acid (C16:1 n-9) (C16:1c9), α-linolenic acid (C18:3 n-3) (C18:3c9,12,15), arachidic acid (C20:0) and lignoceric acid (C24:0) were notable in small amounts in all cultivars. C16:0, C18:0, C18:1c9 and C18:2c9, 12 were the only fatty acids detected at levels of more than 1%. This is in accordance with the results of various authors who reported that cactus pear seed oil contained primarily unsaturated fatty acids namely linoleic and oleic acid, and with a lower but significant content of palmitic and stearic fatty acids (Chougui *et al*., 2013; Ciriminna *et al*., 2017; Ortega-Ortega *et al*., 2017; Ramírez-Moreno *et al.*, 2017, Regalado-Rentería *et al*., 2018; Loizzo *et al.,* 2019). A completely different profile was found for the Greek *O. ficus-indica* which included butyric acid (C4:0), palmitic acid, stearic acid and oleic acid as the main fatty acids (Karabagias *et al*., 2020).

The C18:2c9,12 content varied from 58.56% (Nudosa) to 65.18% (Robusta) (Table 1). A slightly larger range for C18:2c9,12 between 57.75–67.32% was reported by de Wit *et al*. (2017) and de Wit *et al*. (2018) (56.86–65.21%). Labuschagné and Hugo (2010) also reported comparable results for fatty acid profiles with unsaturated fatty acids (C18:2c9,12) ranging between 57.75–67.32%. Linoleic acid (omega-6) is an essential fatty acid and a precursor of arachidonic acid (AA) biosynthesis which is the substrate for eicosanoid synthesis (Ghazi *et al*., 2013). Both present a hypocholesterolemic effect and inhibit colon cancer. Omega-6 PUFA is the source of inflammatory mediators' prostaglandins (PGE) and leukotrienes. Consumption of oleic acid (n-9) and α-linolenic acid (n-3) act as AA antagonists and reduces the production of inflammatory mediators (Koshak *et al*., 2020). Higher levels were found in *O. microdasys* (Engelm) and *O. macrorhiza* as well as *O. dillenii* (> 70%) (Ghazi *et al*., 2013; Chahdoura *et al*., 2015; Ali Alsaad *et al*., 2019); while the current results

Table 1. Fatty acid composition of oil from 12 selected cold-pressed cactus pear cultivars (fatty acids were expressed as the proportion of each individual fatty acid to the total of all fatty acids present in the sample). Values in the Table are mean ±SD of triplicate analyses.

Cultivar	Fatty acids														
	Myristic	Palmitic	Palmiteloleic	Margaric	Heptadecenoic	Stearic	Oleic	Vaccenic	Linoleic	Arachidic	Eicosenoic	α-Linolenic	Eicosatrienoic (8,11,14)	Eicosatrienoic (11, 14, 17)	Lignoceric
Algerian	0.06 ± 0.01	12.54 ± 0.05	0.55 ± 0.01	0.01 ± 0.01	0.03 ± 0.01	3.04 ± 0.01	13.86 ± 0.02	5.87 ± 0.01	63.29 ± 0.09	0.22 ± 0.01	0.03 ± 0.04	0.23± 0.20	0.12 ± 0.01	0.05 ± 0.06	0.08 ± 0.01
American Giant	0.05 ± 0.01	10.97 ± 0.05	0.38 ± 0.01	0.02 ± 0.01	0.01 ± 0.01	3.74 ± 0.01	16.37 ± 0.02	5.14 ± 0.01	62.49 ± 0.18	0.28± 0.01	0.10 ± 0.01	0.21 ± 0.04	0.14 ± 0.01	0.02 ± 0.01	0.08 ± 0.02
Ficus-Indice	0.06 ± 0.01	12.05 ± 0.08	0.56 ± 0.01	0.01 ± 0.01	0.02 ± 0.01	2.86 ± 0.02	15.74 ± 0.01	6.21 ± 0.02	61.66 ± 0.01	0.22 ± 0.01	0.05 ± 0.04	0.35± 0.01	0.12 ± 0.01	0.02 ± 0.01	0.07 ± 0.02
Gymno Carpo	0.05 ± 0.01	13.24 ± 0.05	0.62 ± 0.01	0.02 ± 0.01	0.05 ± 0.01	2.62 ± 0.01	12.22 ± 0.02	6.16 ± 0.01	64.10 ± 0.03	0.21 ± 0.01	0.08 ± 0.01	0.32 ± 0.01	0.12 ± 0.01	0.14 ± 0.01	0.07 ± 0.01
Meyers	0.06 ± 0.01	12.31 ± 0.18	0.81 ± 0.01	0.02 ± 0.01	0.03 ± 0.01	3.18 ± 0.01	15.61 ± 0.04	6.53 ± 0.02	60.68 ± 0.28	0.26 ± 0.01	0.12 ± 0.22	0.18 ± 0.01	0.15 ± 0.01	0.02 ± 0.01	0.10 ± 0.01
Morado	0.06 ± 0.01	12.77 ± 0.06	0.59 ± 0.01	0.01 ± 0.01	0.03 ± 0.01	2.81 ± 0.01	13.51 ± 0.01	6.05 ± 0.02	63.28 ± 0.07	0.21 ± 0.01	0.05 ± 0.05	0.36± 0.18	0.11 ± 0.01	0.09 ± 0.07	0.07 ± 0.01
Nudosa	0.07 ± 0.01	15.07 ± 0.07	0.75 ± 0.04	0.02 ± 0.01	0.05 ± 0.01	3.01 ± 0.05	15.78 ± 0.16	5.69 ± 0.07	58.56 ± 0.07	0.26 ± 0.01	0.02 ± 0.03	0.35± 0.01	0.22 ± 0.14	0.11 ± 0.08	0.07 ± 0.01
Ofer	0.06 ± 0.01	12.65 ± 0.21	0.61 ± 0.01	0.02 ± 0.01	0.03 ± 0.01	2.81 ± 0.02	14.98 ± 0.04	6.17 ± 0.02	61.83 ± 0.13	0.22 ± 0.01	0.07 ± 0.01	0.35 ± 0.01	0.12 ± 0.01	0.02 ± 0.01	0.08 ± 0.01
Robusta	0.04 ± 0.01	11.93 ± 0.18	0.41 ± 0.01	0.03 ± 0.01	0.02 ± 0.01	2.68 ± 0.02	13.46 ± 0.06	5.48 ± 0.02	65.18 ± 0.11	0.21 ± 0.01	0.11 ± 0.19	0.22 ± 0.19	0.13 ± 0.01	0.02 ± 0.01	0.07 ± 0.01
Tormentosa	0.06 ± 0.01	12.19 ± 0.04	0.59 ± 0.01	0.02 ± 0.01	0.03 ± 0.01	3.07 ± 0.01	14.99 ± 0.03	6.04 ± 0.09	62.14 ± 0.09	0.24 ± 0.01	0.05 ± 0.05	0.35 ± 0.01	0.13 ± 0.01	0.02 ± 0.01	0.08 ± 0.01
Van As	0.06 ± 0.01	11.80 ± 0.11	0.58 ± 0.01	0.01 ± 0.01	0.02 ± 0.01	2.98 ± 0.01	16.07 ± 0.05	6.30 ± 0.02	61.29 ± 0.10	0.24 ± 0.01	0.17 ± 0.16	0.24 ± 0.20	0.14 ± 0.01	0.02 ± 0.01	0.09 ± 0.01
Zastron	0.06 ± 0.01	11.71 ± 0.07	0.38 ± 0.01	0.02 ± 0.01	0.02 ± 0.01	2.70 ± 0.01	13.18 ± 0.04	5.36 ± 0.01	65.73 ± 0.14	0.20 ± 0.01	0.19 ± 0.15	0.24 ± 0.21	0.11 ± 0.01	0.04 ± 0.05	0.07 ± 0.01

are in agreement with the levels reported for *O. ficus-indica* varieties from Sicily, Saudi Arabia, Turkey and Tunisia (Ghazi *et al*., 2013; Ciriminna *et al*., 2017; Loizzo *et al.,* 2019). Astiasarán and Candela (2000) reported a comparable study on PUFAs (C18:2c9,12) content of various vegetable oils, i.e. soy oil which obtained 48.7%, corn oils (47.7%), sesame oils (44.5%), sunflower oil (49.7%), olive oil ranging from 3.5–21% and cotton oils with 50%. These values are all significantly lower than the values obtained in this current study, implying that cactus pear is the best in terms of oil PUFA yield. PUFAs are able to alleviate symptoms of diseases such as coronary heart disease, stroke and rheumatoid arthritis.

The highest amount of C18:1c9 was detected for American Giant with 16.37% compared with Gymno Carpo, which demonstrated the lowest amount with 12.22%. Robusta contained 13.46% C18:1c9. The highest value for vaccenic acid (C18:1 n-7) (C18:1c7) was observed for Meyers (6.53%) and the lowest for American Giant (5.14%). Robusta (*O. robusta*) obtained 5.48%. Loizzo *et al.* (2019) reported values ranging from 15.8 – 18.1% for C18:1c9 from two *O. ficus-indica* cultivars (red and yellow) extracted by two different methods (Soxhlet and Ultrasound-Assisted). These authors reported values ranging between 4.3% and 5.1% for C18:1c7. The values for C18:1c9 reported by these authors were higher than in the current study, while the C18:1c7 values were somewhat lower than the current study's values. Ciriminna *et al.* (2017) obtained a higher content of vaccenic acid (6.29%) for yellow Sicilian *Opuntia ficus-indica* seed oil, while Chougui *et al.* (2013) reported no vaccenic acid in yellow Algerian fruit. A vaccenic acid content of 4.83% was reported by Tlili *et al.* (2011) for Tunisian cactus pears. Interestingly, seed oil from *O. ficus-indica* from Marocco had no oleic acid (Ghazi *et al*., 2013).

The saturated fatty acid (SFA) palmitic acid (C16:0) ranged between 10.97 and 15.07% and stearic acid (C18:0) ranged between 2.62 and 3.74%. American Giant obtained the lowest content of C16:0 (Table 1) and the highest oil percentage (Figure 1). These C16:0 values are slightly lower than those reported by de Wit *et al*. (2017) which ranged between 12.90 and 17.83% (Monterey and Nudosa, respectively) and the range reported by de Wit *et al*. (2018) namely 12.72–16.05%. The C18:0 content varied between 2.62% (Gymno Carpo) and 3.74% (American Giant) (Table 1), indicating only slight variation in C18:0 levels. Similar values were reported for chemically extracted oil as reported by

Table 2. Fatty acid ratios of oil from 12 selected cold-pressed cactus pear cultivars (fatty acids were expressed as the proportion of each individual fatty acid to the total of all fatty acids present in the sample). Values in the Table are mean ±SD of triplicate analyses.

Cultivar	Saturated fatty acids (SFA)	Monounsaturated fatty acids (MUFA)	Polyunsaturated fatty acids (PUFA)	Omega-6 fatty acids	Omega-3 Fatty acids	PUFA/SFA
Algerian	15.96 ± 0.06	20.34± 0.05	63.70± 0.10	63.42± 0.09	0.28± 0.14	3.99± 0.02
American Giant	15.13 ± 0.04	22.00± 0.01	62.87± 0.05	62.64± 0.18	0.23± 0.14	4.16± 0.01
Ficus-Indice	15.27± 0.05	22.58± 0.06	62.15± 0.01	61.78± 0.01	0.37± 0.01	4.07± 0.01
Gymno Carpo	16.21± 0.06	19.13± 0.03	64.67± 0.03	64.21± 0.03	0.46± 0.01	3.99± 0.02
Meyers	15.94± 0.16	23.10± 0.25	60.87± 0.07	60.83± 0.28	0.20± 0.18	3.81± 0.03
Morado	15.91± 0.07	20.24± 0.04	63.85± 0.04	63.40± 0.07	0.46± 0.07	4.01± 0.02
Nudosa	18.50± 0.05	22.28± 0.24	59.23± 0.24	58.78± 0.20	0.45± 0.07	3.20± 0.02
Ofer	15.83± 0.19	21.84± 0.05	62.32± 0.14	61.96± 0.14	0.37± 0.01	3.94± 0.05
Robusta	14.96± 0.17	19.48± 0.14	65.55± 0.31	65.32± 0.12	0.24± 0.19	4.38± 0.07
Tormentosa	15.66± 0.04	21.69± 0.05	62.65± 0.08	62.27± 0.09	0.37± 0.01	4.00± 0.01
Van As	15.18± 0.10	23.14± 0.1	61.68± 0.10	61.43± 0.11	0.25± 0.20	4.06± 0.02
Zastron	14.76± 0.07	19.12± 0.15	66.13± 0.11	65.84± 0.07	0.28± 0.24	4.48± 0.02

Values in the Table are mean ±SD of triplicate analyses.

de Wit *et al*. (2017) (2.21–3.39%) and de Wit *et al*. (2018) (2.4–4.01%). These results are in agreement to those of Loizza *et al*. (2019) who found that fatty acid content is not affected by extraction method but by variety. Interestingly, Regalado-Rentería *et al*. (2018) found that oil extracted by cold-pressing was richer in UFA and poorer in SFA than oils extracted with solvents. Regarding SFA, the palmitic acid (5.12%) and stearic acid (7.51%) found in *O. dillenii* presented the main saturated fatty acid (> 22%). These are even higher than the SFA found in soy (~3%) (Ali Alsaad *et al*., 2019). Stearic acid has a neutral effect on LDL.

3.2.2. Fatty acid ratios

According to Table 2 SFA ranged from 14.76 (Zastron) to 18.50% (Nudosa). The results for the fatty acid composition presented in Table 1 show that C16:0 and C18:0 were observed to be marginally lower than those reported in the publication of de Wit *et al. (*2017) (16.59–20.65%) and de Wit *et al*. (2018) (16.19–19.12%) yet higher than those obtained by Ennouri *et al*. (2005). These fatty acids will influence SFA ratios, since they are the main contributors to SFA. The stage of development of the fruit may be the cause of variation in fatty acid composition, but in this study the fruits were all picked at the same maturity stage (50% color break), although genotype, climate and weather, as well as environmental effects may be the reason behind this variation. According to de Wit *et al.* (2017), weather conditions, particularly were the main factors contributing to variations in fatty acid composition and oil percentage.

Total MUFA ranged between 19.12 and 23.10%, which corresponds to that reported by de Wit *et al*. (2017) (15.78–23.30%) and de Wit *et al*. (2018) (17.4–23.61%). Gymno Carpo and Zastron obtained the lowest MUFA contents (19.13% and 19,12%) (Table 2), while Meyers and Van As showed the highest contents of MUFA (23.14% and 23.10%), respectively. MUFA, such as C18:1c9, ranged between 12.22% (Gymno Carpo) and 16.07% (Van As) (Table 1). Oil containing high concentration of C18:1c9 has been reported to be more stable to oxidation, which is desired for improved shelf-life (Lajara *et al*., 1990).

PUFA was established as the most prominent fatty acid ratio ranging between 59.23 (Nudosa) and 66.13% (Zastron). PUFA from de Wit *et al.* (2017) was at the lower range and ranged from 55.98 – 67.62%. C18:2c9,12 was established as the dominating PUFA with the lowest level of 58.56% for Nudosa and the highest level of 65.18% for Robusta (Table 1), with C20:3c9,12,15 (0.22 to 0.35%) and C20:3c8,11,14 (0.13 to 0.22%) occurring at very low levels.

Table 3. Physicochemical properties of oil from 12 selected cold-pressed cactus pear cultivars analyzed one week after pressing.

Cultivar	Peroxide Value (meq O2/1000 g fat)	% Free Fatty Acids	ρ-Anisidine value (mmol/kg)	Refraction Index at 40 ˚C	Iodine Value	β + γ Tocopherol (mg/100g)	ORAC[1]	OSI[2]	Induction Time extrapolated to 25 ˚C (Years)	Induction Time extrapolated to 30 ˚C (Years)
Algerian	4.23 ± 0.48	3.21 ± 0.04	4.08 ± 0.37	1.4666 ± 0.0001	121.60 ± 4.12	58.27 ± 2.47	5.28 ± 0.43	2.31 ± 0.14	0.52 ± 0.01	0.35 ± 0.01
American Giant	3.02 ± 0.02	1.21 ± 0.03	1.37 ± 0.14	1.4666 ± 0.0001	125.45 ± 2.09	54.19 ± 2.96	4.70 ± 0.25	2.19 ± 0.04	3.44 ± 0.01	2.08 ± 0.01
Ficus-Indice	3.65 ± 0.18	2.19 ± 0.06	2.73 ± 0.21	1.4666 ± 0.0001	123.84 ± 2.09	59.36 ± 7.61	4.54 ± 0.27	3.17 ± 0.09	0.73 ± 0.01	0.49 ± 0.01
Gymno Carpo	5.87 ± 0.02	2.32 ± 0.01	1.00 ± 0.02	1.4666 ± 0.0001	122.32 ± 0.60	55.43 ± 6.05	4.10 ± 0.25	2.54 ± 0.01	2.69 ± 0.01	1.66 ± 0.01
Meyers	4.81 ± 0.12	1.63 ± 0.03	1.42 ± 0.32	1.4664 ± 0.0003	123.07 ± 1.17	59.78± 2.04	3.87± 0.06	1.88± 0.01	4.15± 0.01	2.46± 0.01
Morado	4.19 ± 0.24	1.15 ± 0.01	1.40 ± 0.42	1.4666 ± 0.0001	123.32 ± 0.28	61.31 ± 3.33	4.01 ± 0.18	2.46 ± 0.06	2.14 ± 0.01	1.33 ± 0.01
Nudosa	4.49 ± 1.24	1.74 ± 0.09	1.58 ± 0.12	1.4659 ± 0.0001	123.92 ± 6.36	51.69 ± 4.26	4.14 ± 0.09	2.95 ± 0.10	2.74 ± 0.01	1.69 ± 0.01
Ofer	4.72 ± 0.01	1.19 ± 0.02	1.64 ± 0.36	1.4666 ± 0.0001	122.64 ± 1.18	61.47 ± 1.65	4.30 ± 0.49	2.92 ± 0.02	1.64 ± 0.01	1.04 ± 0.01
Robusta	5.06 ± 0.78	3.41 ± 0.09	1.95 ± 0.54	1.4665 ± 0.0002	122.85 ± 3.85	55.30 ± 9.38	5.07 ± 0.51	2.25 ± 0.01	3.56 ± 0.01	2.16 ± 0.01
Tormentosa	5.80 ± 0.38	3.22 ± 0.03	0.98 ± 0.54	1.4664 ± 0.0001	120.58 ± 2.22	58.45 ± 4.70	4.20 ± 0.41	1.91 ± 0.08	9.40 ± 0.01	5.30 ± 0.01
Van As	3.60 ± 0.41	4.30 ± 0.02	2.94 ± 0.17	1.4664 ± 0.0001	120.59 ± 1.93	59.95 ± 5.74	5.08 ± 0.22	1.78 ± 0.08	2.14 ± 0.01	1.31 ± 0.01
Zastron	5.72 ± 0.58	2.75 ± 0.06	1.94 ± 0.55	1.4668 ± 0.0001	127.43 ± 1.13	56.70 ± 1.37	5.37 ± 0.05	1.74 ± 0.07	4.73 ± 0.01	2.76 ± 0.01

Values in the Table are mean ±SD of triplicate analyses.
1 Oxygen radical antioxidant capacity (µmol Trolox equivalents/g)
2 Oxidative stability Index at 110 ˚C (Hour)

Omega-6 (n-6) fatty acids ranged from 58.78-65.84% (Nudosa and Zastron, respectively). All the cultivars, with the exception of Nudosa, contained n-6 contents at above 60%. Nudosa attained the lowest concentration of n-6 fatty acid ratio with 58.78% (Table 2). Zastron had the highest contents of PUFA and n-6 but obtained the lowest content of MUFA. These contents were found to be slightly higher compared to results from de Wit *et al*. (2017) (55.98 – 67.45%). Pardo *et al*. (2009) concluded that cactus pear seed oils are good sources of omega-6 fatty acids.

The omega-3 (n-3) fatty acid ratio occurred at very low levels (Table 2). The contents ranged from 0.20 (Meyers) - 0.46% (Gymno Carpo), respectively. Omega-3 (n-3) fatty acids, such as C18:3c9,12,15 (C18:3 n-3) occurred at a very low level and ranged from 0.18 - 0.36% (Meyers and Morado in Table 2).

The PUFA/SFA ratio is used to measure the level of unsaturation and is taken as an instrument to measure the oil's tendency to undergo autoxidation. The PUFA/SFA ratio ranged from 3.20 - 4.48% with Zastron occurring in the highest amount and Nudosa at the lowest level (Table 2). American Giant, Ficus-Indice, Morado, Robusta, Tormentosa, van As and Zastron also attained PUFA/SFA contents above 4%. Zastron was also amongst those that had the highest content of C18:2c9,12, while Nudosa occurred at the lowest level (Table 1). *O. dillenii* presented a ratio of 3.22.

The results for the physicochemical properties of the oil from cactus pear cultivars are presented in Table 3.

3.2.3. Refraction index (RI)

The RI values of the oils increase as a result of autoxidation. The RI depends on the chemical composition and temperature of the oil. It also increases with degree of saturation (Brahmi *et al*., 2020) and secondary functions on fatty acid chains. As indicated by the RI values presented in Table 3, little differences were observed among the RI values for all cultivars. The RI values ranged from 1.4659–1.4668 (Nudosa and Zastron). The higher the level of unsaturation, the higher the levels of RI and IV, for example, Zastron obtained the highest RI value (1.4668) and high PUFA content (66.08%) as well as high IV (127.43). Oils with a high unsaturation degree are more likely to undergo autoxidation and tend to oxidize easily when used at high temperatures, for example, PUFA (C18:2c9,12) oxidized ± 50 times faster than C18:1c9 (MUFA). Therefore, an increased RI value could be expected as a result of exposure to heat and light.

American Giant and Gymno Carpo were also amongst the cultivars with high PUFA, RI value and

IV value (Tables 2 and 3). Furthermore, the higher the MUFA content (C18:1c9), the lower the RI and IV-values, for example, Van As attained a higher content of MUFA (23.14%), a low RI value of 1.4664 as well as a low IV value of 120.59 (Tables 2 and 3). These results fall within a similar range (1.464 RI) to those reported by Gharby *et al*. (2011). Previous literature reported a higher RI value of 1.4831 in cactus pear seed oil, 1.473 in rape seed oil, and 1.475 in *Opuntia ficus-indica* (Ennouri *et al*., 2005). Other studies reported slightly lower RI values ranging between 1.4658 and 1.4676 (de Wit *et al*., 2017).

Valuable information can be obtained by determining the density of the oils. Density gives information on the nature of fatty acids, such as chain length, unsaturation degree, and functional groups. Density will also be influenced by the composition and temperature of the oil. Together with RI, it can also indicate the purity of the oil (Brahmi *et al*., 2020). It is therefore recommended to include density analyses in future studies.

3.2.4. Iodine value (IV)

Iodine value is an indication of the total number of double bonds. The iodine value (IV) ranged from 120.58–127.43 (Tormentosa and Zastron). Zastron obtained the highest IV (number of gram iodine absorbed by 100g of oil) of 127.43 followed by American Giant (125.45), Morado (123.32) and Nudosa (123.92). Tormentosa recorded the lowest IV of 120.58 (Table 3). According to Table 2, Zastron and American Giant attained the highest PUFAs (high unsaturation level) as well as high IV and low MUFA content while Nudosa obtained the smallest content of PUFA. The values in this study are higher than those reported by Karleskind and Wolff (1992) ranging from 105.5–107.38 (cactus pear seed oils). De Wit *et al*. (2017) reported slightly lower iodine values ranging between 110.68 (Nudosa) and 126.82 (Robusta).

Since IV measures the unsaturation of oils, it can also be an indication of the stability of the oil since a high degree of unsaturation suggests a high susceptibility to oxidation. Low IV therefore indicates more resistance to oxidation because of increased saturation and vice versa (de Wit *et al*., 2017).

3.2.5. Tocopherols

Vegetable oils are the most important dietary source of tocopherols. Tocopherols are phenolic compounds that are naturally occurring antioxidants that present biological activity (Ali Alsaad *et al*., 2019). Fernández-Martinez *et al*. (2004) indicated that fatty acids, natural antioxidants, tocopherols and sterols are the key constituents that define oil quality. Normand *et al*. (2006) stated that oils with high tocopherols have greater stability to oxidation. Tocopherols are natural antioxidants in plant foods, particularly those that contain high levels of PUFA as they are able to scavenge lipid peroxyl radicals of unsaturated lipid molecules, inhibiting the propagation of lipid peroxidation.

β and γ tocopherols ranged between 61.47 and 51.69 mg/100g (Table 3). Ofer obtained a higher content of β and γ tocopherols (51.69 mg/100g) followed by Morado (61.31 mg/100g), which means that Ofer and Morado will be more stable to oxidation compared to Nudosa (51.69 mg/100g). The values obtained in the current study are comparable to those reported by Chu *et al*. (2002) with cold-pressed cactus pear seed oil at 94.6 mg/100g, argan oil at 85.0 mg/100g, olive oil at 22.0 mg/100g, soybean at 65.0 mg/100g and sunflower oil at 49.0 mg/100g. Morales *et al*. (2012) found values of 140–220 µg/100 g.

Tocopherol contents are influenced by the extraction method (Loizzo *et al*., 2019). Red cultivars were found to contain higher contents than the yellow cultivars and were mainly in the form of γ-tocopherol. In Moroccan cactus pear seed oil, vitamin E was only present as γ-tocopherol (1.23%) (Ghazi *et al*., 2013). Regalado-Rentería *et al*. (2018) found a tendency for metabolites such as γ-tocopherol to be higher in cold-pressed oils than oils extracted with solvents. These authors reported γ-tocopherol values between 1.71 and 13.86 mg/100 g oil. During the analysis of anti-inflammatory compounds of *O. ficus-indica* seed oils from Saudi-Arabia, β-tocopherol contents of 1.56% were found. This oil was extracted with hexane (Boshak *et al*., 2020).

3.2.6. Oxygen radical antioxidant capacity (ORAC)

Lipid oxidation is a process which is initiated by free radical reactions at the double bonds of unsaturated fatty acids and has been reported to be the key factor in the quality deterioration of edible oils since it modifies the chemical, sensory and nutritional properties of the oils. Márquez-

Ruiz *et al*. (1996) pointed out that autoxidation is another key factor that leads to the development of quality loss in refined oils during storage. The 2,2-diphenyl-1-picrylhydrazyl (DPPH) assay is normally used to predict the stability of cold-pressed oils against oxidation. Most of the literature cited included the use of the DPPH and 2,2'-azino-bis-3-ethylbenzthiazoline-6-sulphonic acid (ABTS) methods. Cao *et al*. (1996) reported the determination of total antioxidant capacity using the ORAC method, which is currently being used to determine the total antioxidant capacity and measures the plant extract's ability to scavenge peroxyl radicals.

The oxidation of oils happens mainly at the sites of unsaturation and the oxidation rate mainly depends on the number of double bonds and their positions. Table 3 shows that Zastron had the highest antioxidant capacity with an ORAC value of 5.37 μmol/g, followed by Algerian with 5.28 μmol/g. Meyers had the lowest antioxidant capacity (3.87 μmol/g). Kuti (2004) reported higher values which ranged from 1.6–15.8 mMTE/g in yellow-skinned fruits and 1.7–49.2 mMTE/g in the purple-skinned fruits.

It was found by Ramírez-Moreno *et al*. (2017) that extraction solvent had a significant effect on the free radical scavenging capacity of the seed oil and that the green *O. ficus-indica* variety had a higher antioxidant activity regardless of the solvent used. The antioxidant activity of *O. ficus-indica* seed oil from Saudi-Arabia (Brahmi *et al*., 2020) showed a lower DPPH value in cold-pressed oil than in oils extracted by the Soxhlet method. Antioxidant activity was strongly correlated with the amounts of phenolic compounds, including polyphenols and flavonoids. *O. dillenii* seed oil from Iraq demonstrated a strong antioxidant capability due to its ability to reduce oxidation as determined by the DPPH method (Ali Alsaad *et al*., 2019), which reinforced the effect of variety on antioxidant activity.

3.3. Determination of oxidative stability

3.3.1. Free fatty acids (FFA)

The level of free fatty acids (FFA) in oils is measured by the acid value (AV) generated upon the hydrolytic degradation of lipid particles and is therefore an indicator of hydrolytic activity, which consequently adds to the decrease in the time span of usability of the oil. The maximum FFA content limit recommended for cold-pressed oil is 8%, 0.3% for refined oils and 5% for virgin palm oils according to the Codex Alimentarius Commission standard (Codex Alimentarius Commission, 2009). According to the results presented in Table 3, the FFA content ranged between 1.15 and 4.30% (Morado and Van As) and the % FFA of all cultivars was within the recommended limit, implying that cactus pear seed oil is of good quality from a FFA point of view. In a previous study, % FFA ranged between 2.49 and 5.08% in chemically extracted oil (de Wit *et al.*, 2017). The content in cold-pressed oil was thus lower. The production of FFA is a result of lipid hydrolysis which is triggered by chemical or enzymatic actions. Increased free fatty acid values are indicators of increased primary oxidation. Factors such as high temperature and humidity are accountable for an increase in FFA content in oils. An elevated acidity value of 21.2% was reported by Brahmi *et al.* (2020) for Algerian cold-pressed *O. ficus-indica* seed oil. This high value could be ascribed to the enzymatic hydrolysis of seeds during oil pressing, handling or processing, as well as elevated temperatures and the presence of water during the process. It was also mentioned by the authors that free fatty acids could be present since no refining of the oil took place, which could possibly remove acids as impurities.

3.3.2. Peroxide value (PV)

Martín-Polvillo *et al*. (2004) reported that peroxide value (PV) measures the level of hydroperoxide in the oil and is a valuable tool for the indication of a commencement period of oxidation. Furthermore, PV reaches the highest level during the progression of oxidation and following this stage (secondary oxidation), the decomposition rate of hydroperoxides surpasses the rate of their development. Peroxide value is also used to test oxidative rancidity in oils and fats (Karleskind and Wolff, 1992). It was reported that the acceptable PV value for cold pressed oil is < 15 meq $O_2 \cdot kg^{-1}$ (Codex Alimentarius Commission, 1999). According to the results presented in Table 3, all cultivars attained PV values of < 15 meq $O_2 \cdot kg^{-1}$, therefore PV value results are in agreement with the recommended value for cold-pressed oil of good quality.

PV ranged between 3.02 and 5.87. Although Gymno Carpo and Tormentosa were amongst the

cultivars with higher PV values (5.87 and 5.80), oxidation had not yet occurred in these cultivars since their PV values were still within the recommended limit of < 15 meq O_2.kg^{-1}, which indicates that a rancid taste was not yet noticeable (Table 3). Salvo *et al*. (2002) pointed out that a rancid taste in oils begins to be noticeable at PV values of 20–40 meq $O_2 \cdot kg^{-1}$. PUFAs are more susceptible to oxidation than MUFA and SFA. The higher PVs observed for Gymno Carpo and Tormentosa were probably a consequence of their higher unsaturation levels (Tables 1 and 2). American Giant had on average a PV of 3.02 meq $O_2 \cdot kg^{-1}$, which was the lowest compared to that of the other cultivars. Van As also had a relatively low PV value of 3.60 (Table 3). De Wit *et al*. (2017) reported PV values of chemically extracted cactus pear oils which were above the recommended limit and ranged between 9.5 and 23.30 meq $O_2 \cdot kg^{-1}$.

Karleskind and Wolff (1992) reported PV estimations of margarine containing *Opuntia ficus-indica* oil which were far below the levels permitted by the international benchmarks and ranged between 0.38 and 0.39 meq $O_2 \cdot kg^{-1}$. PV measures the extent of rancidity reactions during storage, and therefore indicates quality and stability. A PV of 12 meqO_2/kg was reported for Algerian *O. ficus-indica* cold-pressed seed oils (Koshak *et al*., 2020). PV is therefore affected by genetics, cultivars, growth conditions, soil geography, and harvesting routines as well as handling and storage.

3.3.3. ρ - Anisidine value (ρ-AV)

The *ρ*-AV was taken as a tool used to quantify secondary oxidation by surveying the measurement of unsaturated aldehydes as a result of the decomposition of hydroperoxides (Shahidi and Zhong, 2005). The *ρ*-AV is an indicator of oxidative rancidity in oils. The results presented in Table 3 demonstrate that the *ρ*-AV ranged between 0.98–4.08 mmol/kg for Tormentosa and Algerian, respectively. Algerian had the highest *ρ*-AV of 4.08 followed by Van As with *ρ*-AV of 2.94 mmol/kg. Tormentosa acquired the lowest *ρ*-AV content of 0.99 mmol/kg. The results demonstrated that there were only small differences among the *ρ*-AV of American Giant (1.37), Morado (1.40), Ofer (1.64) and Nudosa (1.58). Algerian recorded the highest ρ-Anisidine value and PV value, which is indicative of secondary oxidation products. The high *ρ*-AV may be due to their higher level of unsaturation. The recommended *ρ*-Anisidine value (*ρ*-AV) limit is < 10.0 mmol/kg (Codex Alimentarius Commission, 1999). The *ρ*-AV values obtained were within the acceptable limit (Table 3). Some of these *ρ*-AV values were higher than those reported in the literature which ranged from 0.02 - 3.73 mmol/kg (de Wit *et al*., 2017). Aldehydes made up the highest percentage of cactus pear seed oil volatiles (Karabagias *et al.*, 2020). Aldehydes are responsible for, among others, acrid, burnt-fat, fruit-like, fermented, nutty, deep fat, butter, chicken and fusty odors, flavors and smells. The butyric acid reported by Karabagias *et al*. (2020) is responsible for the buttery flavor of the cactus pear seed oil.

3.3.4. Oxidative stability index

The OSI value gives an indication of the resistance of lipids to oxidation and is also used for quality control of the oils, as well as an indication of the shelf-life of oils. The shorter the reaction time, the more susceptible the oil is to oxidation and therefore higher values will imply more resistance to oxidation. The values ranged between 1.78 and 3.17 h and were lower than the values obtained by de Wit *et al*. (2017), which ranged between 1.79 and 4.15 h. Ficus-Indice had the highest OSI value of 3.17 hours at 110 °C followed by Nudosa (2.92 hours) and Ofer (2.92 hours), implying that these cultivars were more resistant to oxidation reactions. Van As, which attained the highest content of C18:1c9 (Table 1), was determined to be the most favored oil since it is rich in oleic acid and oils rich in C18:1c9 have potential for combining the hypocholesterolemic effect and greater oxidative stability. Oils which are high in MUFA (C18:1c9) such as Nudosa (Table 2) are less susceptible to oxidative degradation and in this manner indicate potential for applications requiring high oxidative stability. Gharby *et al*. (2011) reported OSI of 7 hours at 110 °C for *Opuntia ficus-indica*, 31.23 hours for argan, 7.5 hours for olive oil and 5 hours for soybean and sunflower oil.

3.3.5. Extrapolation of induction time

Induction time extrapolated to 25 and 30 °C was done to predict the shelf-life of the oils based on OSI using Rancimat induction times (Rancimat Manual, 2009). The induction period is an indication of how long the oils will take to reach an end point or be

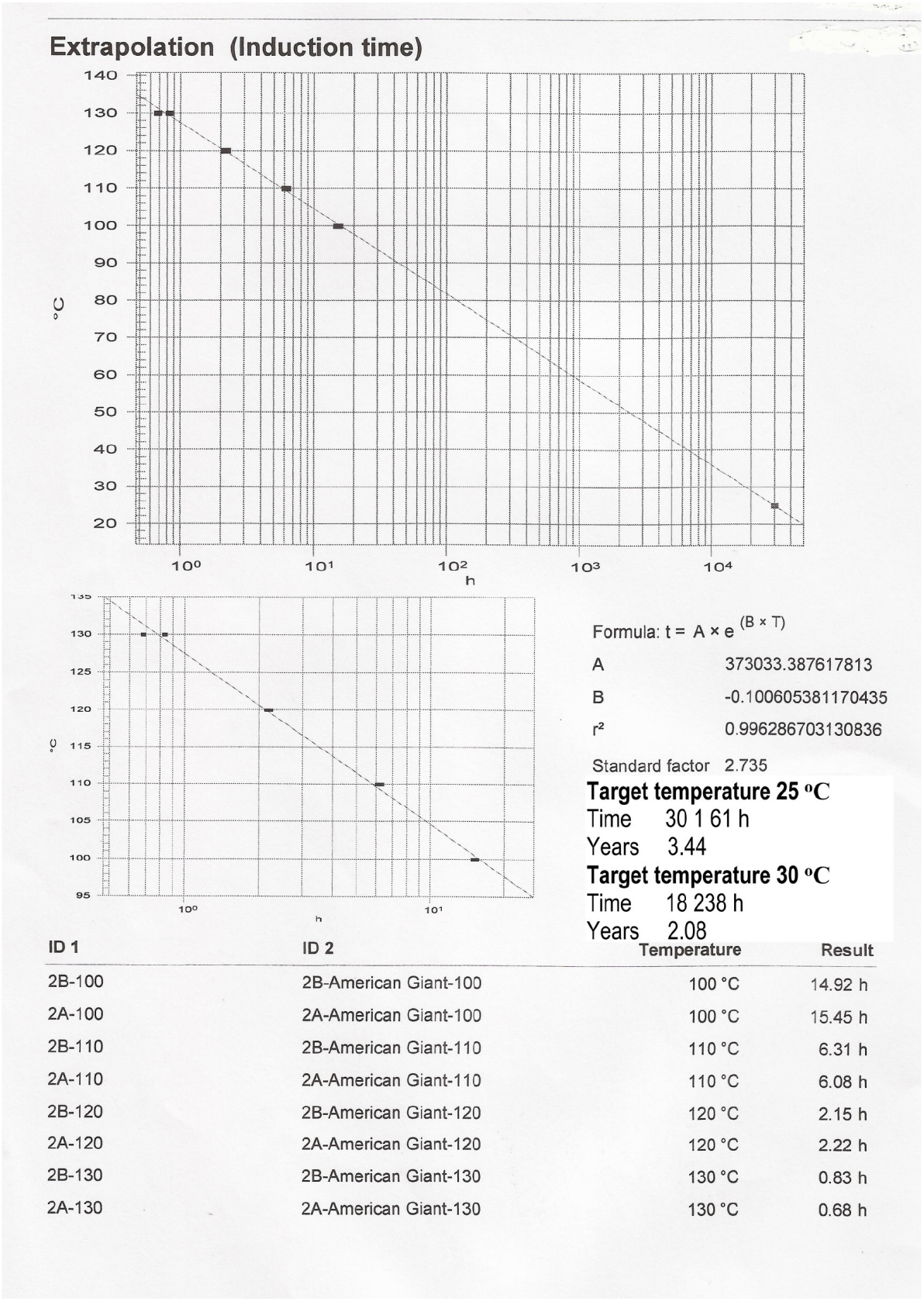

ID 1	ID 2	Temperature	Result
2B-100	2B-American Giant-100	100 °C	14.92 h
2A-100	2A-American Giant-100	100 °C	15.45 h
2B-110	2B-American Giant-110	110 °C	6.31 h
2A-110	2A-American Giant-110	110 °C	6.08 h
2B-120	2B-American Giant-120	120 °C	2.15 h
2A-120	2A-American Giant-120	120 °C	2.22 h
2B-130	2B-American Giant-130	130 °C	0.83 h
2A-130	2A-American Giant-130	130 °C	0.68 h

FIGURE 2. Predicted shelf-life of American Giant cold-pressed cactus pear seed oil stored at 25 and 30 ºC. The extrapolation function of the Rancimat 743 apparatus was used to predict induction times at 25 and 30 ºC according to the formula: Predicted induction time = A X e (BXT)

oxidized. American Giant is presented as an example in Figure 2. Induction time is also described as the time taken before the rapid increase in oxidation occurs and is used to make relative assessments on oxidative stability (Gharby *et al*., 2011).

The accelerated testing can then be extrapolated to real time conditions. Algerian was found to have a shorter induction time of 5 months, 2 weeks when extrapolated to 25 °C and 3 months, 5 weeks when extrapolated to 30 °C, implying that Algerian will have a shorter shelf-life compared to Tormentosa, with an anticipated time span of usability of 9 years and 4 months when extrapolated to 25 °C and 5 years 3 months when extrapolated to 30 °C (Table 3).

3.4. Pearson correlation analysis

A Pearson correlation analysis was conducted on fatty acid content, fatty acid ratios, physicochemical properties and OSI to establish the relationship among them (Table 4). A significant ($p < 0.001$) negative correlation (–0.6757) was observed between % FFA and OSI (Table 4). This means that cultivars which recorded high contents in % FFA had decreased OSI values or vice versa. This was observed in cultivars such as Algerian which attained a high content in % FFA (3.21%) and low OSI (2.31 h). Nudosa and Ofer possessed the lowest contents in % FFA and obtained the highest OSI values of 2.95 and 2.92 h. De Wit *et al*. (2017) reported higher % FFA results ranging from 2.49% (Tormentosa) with OSI of 3.91h - 5.08h (Algerian) with OSI of 4.15h and the % FFA was higher than the recommended limit, implying that there was increased primary oxidation. El Mannoubi *et al*. (2009) reported much lower % FFA results for cactus pear oil with 0.64%.

No significant correlations with OSI were observed for PV, % Oil, *ρ*-Anisidine value, Refraction Index or β + γ Tocopherols. A significant ($p < 0.01$) negative correlation (-0.5762) was observed between OSI and ORAC. An increase in ORAC initiated a decrease in the OSI value. This correlation was especially observed in Zastron and Algerian, whereby high ORAC values were observed for these cultivars along with low OSI values. This correlation shows that these cultivars are less stable to oxidation due to their higher degree of unsaturation. Both C16:0, C16:1c9 and C17:1c10 correlated significantly ($p < 0.001$, $p = 0.001$ and $p < 0.01$) with OSI, as in Nudosa, which obtained the highest content of C16:0 (15.22%) and the highest content of SFA (18.68%) (Tables 1 and 2).

A significant ($p < 0.001$) positive correlation (0.7409) was observed between C16:0 and OSI. This effect was observed for Nudosa, which obtained the highest content of C16:0 with 15.22% (Table 1) as well as the highest OSI value of 2.95 h (Table 3). A significant ($p < 0.001$) positive correlation (0.7230) was observed between OSI and SFA. An increase in SFA initiated an increase in OSI as in Nudosa, which had the highest SFA (18.68%, Table 3) with a high OSI value (2.95 h, Table 3).

C16:1c9 and C17:1c10 had a positive (0.6522 and 0.5690) significant ($p = 0.001$ and $p < 0.01$) correlation with the OSI. This effect was observed for Nudosa which obtained high C16:1c9 (0.75%) and C17:1c10 (0.05%) contents with OSI value of 2.95h. A negative (-0.7146) significant ($p < 0.001$) correlation between PUFA/SFA and OSI value existed. This effect was observed for Zastron, Van As and American Giant, which possessed the highest contents of PUFA/SFA (4.45%, 4.03% and 4.11%, Table 2) and obtained the lowest value of OSI (1.74 h, 1.78 h and 2.19 h, Table 3). With cold-pressing Algerian, American Giant and Ficus-Indice obtained the highest contents of C18:2c9,12 which resulted in a low oxidative stability index and made them less stable to oxidation. However, of these four cultivars, only American Giant had a low % FFA. The reason for the low OSI is the % FFA and the lower unsaturation level (secondary importance). Oil with high unsaturation is most likely to experience autoxidation.

As expected, a significant ($p < 0.001$) positive correlation (0.9996) was observed between OSI and induction time extrapolated to 25 °C and 30 °C. The length of induction time depends on the level of unsaturation of oil. Tormentosa recorded the highest predicted shelf-life at 25 and 30 °C and was also amongst those cultivars that obtained the high MUFA (C18:1c9) content (Tables 2 and 3). Oils with high MUFA contents (C18:1c9) are less susceptible to oxidation degradation and therefore these oils show great potential for applications requiring high oxidative stability.

ρ-Anisidine value had significant ($p < 0.01$) negative correlations (-0.5120 and -0.5297) with

Table 4. Pearson correlation analysis of the of the fatty acid content, fatty acid ratios, physicochemical properties and oxidative stability index, induction time extrapolated to 25 °C and induction time extrapolated to 30 °C of oil from selected cold-pressed cactus pear cultivars.

	OSI		Induction time extrapolated to 25 ºC		Induction time extrapolated to 30 ºC	
	Correlation coefficient (r)	Significance level (P)	Correlation coefficient (r)	Significance level (P)	Correlation coefficient (r)	Significance level (P)
Physicochemical properties:						
OSI (Oxidative stability index)	1.0000	-	-0.4616	0.0154	-0.4539	0.0174
Induction time extrapolated to 25 ºC	-0.4616	0.0154	1.0000	-	0.9996	P<0.001
Induction time extrapolated to 30 ºC	-0.4539	0.0174	0.9996	0.001	1.0000	-
% Oil	-0.1197	0.4869	0.1768	0.3024	0.1785	0.2975
PV (Peroxide Value)	-0.0620	0.7585	0.4585	0.0161	0.4569	0.0166
% FFA (Free Fatty Acids)	-0.6757	0.0001	0.2063	0.3019	0.1915	0.3387
ρ-Anisidine value	-0.1927	0.3355	-0.5120	0.0063	-0.5297	0.0045
RI (Refraction Index)	-0.4080	0.0346	-0.0312	0.8771	-0.0351	0.8619
IV (Iodine Value)	-0.0209	0.9174	-0.0180	0.9289	-0.0086	0.9661
β + γ Tocopherol	-0.1383	0.4915	-0.0747	0.7113	-0.0845	0.6753
ORAC (Oxygen radical antioxidant capacity)	-0.5762	0.0017	-0.1644	0.4125	-0.1749	0.3828
Fatty acid composition (%)						
C14:0 (Myristic acid)	0.2984	0.1306	-0.2782	0.1600	-0.2819	0.1542
C16:0 (Palmitic acid)	0.7409	0.001	-0.3072	0.1191	-0.3024	0.1253
C16:1c9 (Palmitelaidic acid)	0.6522	0.0002	-0.2109	0.2911	-0.2114	0.2897
C17:0 (Margaric acid)	0.1186	0.5556	0.2461	0.2159	0.2517	0.2053
C17:1c10 (Heptadecenoic)	0.5690	0.0020	-0.1896	0.3435	-0.1870	0.3503
C18:0 (Stearic acid)	-0.1058	0.5994	0.0253	0.9001	0.0273	0.8926
C18:1c9 (Oleic acid)	-0.0415	0.8370	0.2614	0.1879	0.2620	0.1867
C18:1c7 (Vaccenic acid)	-0,0554	0.7632	0.1345	0.2356	0.1643	0,3672
C18:2c9,12,16 (Linoleic acid)	-0.2590	0.1920	-0.1425	0.4783	-0.1455	0.4691
C20:0 (Arachidic acid)	0.0453	0.8224	0.0691	0.7321	0.0741	0.7135
C20:1 (Eicosenoic)	-0,0438	0.8141	0.1290	0.3452	0.2645	0.3176
C18:3c9,12,15 (α-Linolenic acid)	-0.0447	0.8249	0.1267	0.5290	0.1269	0.5283
C20:3c8,11,14 (Eicosatrienoic)	0.2705	0.1723	-0.0230	0.9093	-0.0172	0.9320
C20:3c11,14,17 (Eicosatrienoic)	0.3698	0.0576	-0.2043	0.3066	-0.1959	0.3275
C24:0 (Lignoceric acid)	-0.1651	0.4106	-0.0583	0.7727	-0.0671	0.7393
Fatty acid ratios (%)						
SFA (Saturated fatty acids)	0.7230	0.001	-0.3033	0.1241	-0.2977	0.1315
MUFA (Monounsaturated fatty acids)	-0.0150	0.9409	0.2517	0.2053	0.2524	0.2041
PUFA (Polyunsaturated fatty acids)	-0.2512	0.2062	-0.1450	0.4706	-0.1477	0.4622
n-6 (Omega-6)	-0.2562	0.1970	-0.1438	0.4743	-0.1467	0.4653
n-3 (Omega-3)	0.1962	0.3267	-0.0220	0.9131	-0.0165	0.9349
PUFA/SFA ratio	-0.7146	0.001	0.1709	0.3942	0.1658	0.4085

induction time extrapolated to 25 and 30 °C. This effect was observed for Algerian, which attained the lowest induction time extrapolated at both 25 and 30 °C but recorded the highest *ρ*-Anisidine value (Table 4). This cultivar is more likely to experience secondary oxidation (oxidative rancidity) due to its level of unsaturation (PUFA), hence it will have a shorter shelf-life.

4. CONCLUSIONS

The aim of the current study was to determine the oil content, fatty acid composition and physico-chemical quality parameters as well as the stability of cold-pressed seed oil from 12 commercially cultivated cultivars of cactus pear from the Bloemfontein, South Africa area. Large differences in oil content, fatty acid composition and physico-chemical properties (IV, PV, RI, tocopherols, ORAC, % FFA, OSI and induction time) were observed. The quality parameters of the oils were strongly influenced by the oil content, fatty acid composition and physicochemical properties. Quality traits were mainly compared to previous studies on chemically extracted oils from South African cactus pear seed oil.

The main findings pointed out that cold-pressed oils yielded lower oil contents than chemically extracted oils, while green-colored fruit had the highest yields – indicating the effect of cultivar and species. The fatty acids showed similar profiles to those in chemically extracted oils, although the main fatty acid, linoleic acid (C18:2), content was lower. In general, lower PUFA and SFA contents and higher MUFA contents were observed than in the chemically extracted oils. RI, IV and *ρ*-AV was higher than observed in chemically extracted oils, while the PV, FFA and OSI were lower (shorter) – indicating good quality and stable oils. Tocopherol content and antioxidant activity contributed to stability and quality. Extrapolated induction times indicated a shelf-life of up to ~3.5 years when stored at 25 ˚C.

Overall, American Giant, Ofer, Van As, Zastron and Nudosa have proved to be the best performing cultivars in such a way that they contain the highest oil content, antioxidant capacity as well as greater stability to oxidation. Among all the cultivars, American Giant has showed to be the paramount cultivar with good quality traits (oil content and oxidative stability).

Future research should focus on the measurement of total flavonoids, total phenolics and sterols, specifically β-sitosterol, as well as the composition of volatile compounds of seed oils. These would all attribute to regional and varietal identities of the oils. Further perspectives include application of the oils in food products, as well as measuring its ability to function as antioxidants and anti-microbial agents.

ACKNOWLEDGMENTS

The authors wish to express their sincere gratitude to the following people and institutions: Dr. H.J. Fouché from the ARC for providing the fruit; Mr. Fanie Rautenbach from CPUT for his assistance with the tocopherol and ORAC tests; the ARC-UFS-DUT collaborative consortium for funding of the project.

REFERENCES

Ali Alsaad AJ, Altemimi AB, Aziz SN, Lakhssassi N. 2019. Extraction and identification of cactus *Opuntia dillenii* seed oil and its added value for human health benefits. *Pharmacog. J.* **11** (3), 1-8. http://www.phcogj.com/v11/i3. https://doi.org/10.5530/pj.2019.3

AOAC. 2000. *Oils and fats*. In AOAC International Official Methods of Analysis, 17th Edition Association of Official Analytical Chemists, Gaithersburg.

Astiasarán I, Candela M. 2000. *Edible fats*. In: Astiasarán I. and Martínez JA (Eds) *Food Composition and Properties,* 2nd Ed. McGraw-Hill Interamericana, Madrid 109-133.

Boskou D. 2017. Edible cold pressed oils and their biologically active compounds. *J. Exp. Food Chem.* **3** (1), 1000e108. https://doi.org/10.4172/2472-0542.1000e108

Brahmi F, Haddad S, Bouamara K, Yalaoui-Guellal D, Prost-Camus E, Pais de Barros JP, Prost M, Atanasov AG, Madani K, Boulekbache-Makhlouf L, Lizard G. 2020. Comparison of chemical composition and biological activities of Algerian seed oils of *Pistacia lentiscus* L., *Opuntia ficus-indica* (L.) mill. and *Argania spinosa* L. skeels. *Ind. Crops Prod.* **151**, 1-12. https://doi.org/10.1016/j.indcrop.2020.112456

Cao G, Sofic E, Prior R. 1996. Antioxidant capacity of tea and common vegetables. *J. Agric. Food Chem.* **44**, 3426-3431. https://doi.org/10.1021/jf9602535

Choe E, Min DB. 2006. Mechanisms and factors for edible oil oxidation. *Comp. Rev. Food Sci. Tech*. **5**, 169-186. https://doi.org/10.1111/j.1541-4337.2006.00009.x

Chougui N, Tamendjari A, Hamidj W, Hallal S, Barras A, Richard T, Larbat R. 2013. Oil composition and characterization of phenolic compounds of *Opuntia ficus-indica* seeds. *Food Chem.* **193**, 796-803.

Chahdoura H, Barreira JCM, Barros L, Santos-Buelga C, Ferreira ICFR, Achour L. 2015. Seeds of *Opuntia* spp. as a novel high potential by-product: Phytochemical characterization and antioxidant activity. *Ind. Crops Prod*. **65**, 383-389. https://doi.org/10.1016/j.indcrop.2014.11.011

Chu BS, Baharin BS, Quek SY. 2002. Factors affecting pre- concentration of tocopherols and tocotrienols from palm fatty acid distillate by lipase-catalysed hydrolysis. *Food Chem.* **79** (1), 55-59.

Ciriminna R, Bongiorno D, Scurria A, Danzi C, Timpanaro G, Delisi R, Avellone G, Pagliaro M. 2017. Sicilian *Opuntia ficus-indica* seed oil: fatty acid composition and bio-economical aspects. *Eur. J. Lipid Sci. Tech.* **119** (11). https://doi.org/10.1002/ejlt.201700232.

Codex Alimentarius Commission. 1999. Joint FAO/WHO Food Standards Programme. Codex committee on fats and oils. Rome.

Codex Alimentarius Commission. 2009. Codex standard for named vegetable oils- CODEX STAN 210-1999, Food and Agricultural Organization of the United Nation and the World Health Organization Codex Alimentarius Commission.

Ennouri MM, Evelyne B, Laurence M, Hamadi A. 2005. Fatty acid composition and rheological behavior of prickly pear seed oils. *Food Chem.* **93**, 431-437. https://doi.org/10.1016/j.foodchem.2004.10.020

Fernández-Martínez JM, Velasco L, Pérez-Vich B. 2004. Progress in the genetic modification of sunflower oil quality. In: Proceedings of the 16th International Sunflower Conference, Fargo, ND, USA, 1-14.

Gharby S, Harhar H, Guillaume D, Haddad A, Matthäus B, Charrouf Z. 2011. Oxidative stability of edible argan oil: a two-year study. *LWT – Food Sci. Tech.* **44** (1), 1- 8. https://doi.org/10.1016/j.lwt.2010.07.003

Ghazi Z, Ramdani M, Fauconnier ML, El Mahi B, Cheikh R. 2013. Fatty acids sterols and vitamin E composition of seed oil of *Opuntia ficus-indica* and *Opuntia dillenii* from Marocco. *J. Mater. Environ. Sci.* **4** (6), 967-972. http://hdl.handle.net/2268/156950

Izquierdo NG, Aguirrezabal LAN, Andrade FH, Geroudet C, Valentinuzand O, Pereyra Iraola M. 2009. Intercepted solar radiation affects oil fatty acid composition in crop species. *Field Crop Res.* **114,** 66-74. https://doi.org/10.1016/j.fcr.2009.07.007

Hamilton RJ, Hamilton S. 1992. Lipid analysis: a practical approach. Oxford University Press.

Hssaini L, Hanine H, Charafi j, Razouk R, Elantari A, Ennahli S, Hernández F, Ouaabou R. 2020. First report on fatty acids composition, total phenolics and antioxidant activity in seeds oil of four fig cultivars (*Ficus carica* L.) grown in Marocco. *Oilseeds and Fats, Crops and Lipids* (*OCL*) **27** (8), 1-10. https://doi.org/10.1051/ocl/2020003

Karabagias VK, Karabagias IK, Gatzias I, Badeka AV. 2020. Prickly pear seed oil by shelf-grown cactus fruits: waste or maste? *Process* **8,** 132. https://doi.org/10.3390/pr8020132

Karleskind A, Wolff JP. 1996. *Oils and fats manual: A comprehensive treatise — properties, production, application*. A. Karleskind and J.-P. Wolff. (Eds.) 1527 pages. TEC and DOC Lavoisier, France, 1996. ISBN 1-898298-08-4. https://doi.org/10.1002/lipi.19970990608

Koshak AE, Abdallah HM, Esmat A, Rateb ME. 2020. Anti-inflammatory activity and chemical characterization of *Opuntia ficus-indica* seed oil cultivated in Saudi-Arabia. *Arab. J. Sci. Eng.* 1-8. https://doi.org/10.1007/s13369-020-04555-x

Kuti JO. 2004. Antioxidant compounds from four *Opuntia cactus* pear fruit varieties. *Food Chem*. **85**, 527-533. https://doi.org/10.1016/S0308-8146(03)00184-5

Labuschagne MT, Hugo A. 2010. Oil content and fatty acid composition of cactus pear seed compared with cotton and grape seed. *J. Food Biochem.* **34**, 93-100. https://doi.org/10.1111/j.1745-4514.2009.00266.x

Lajara JR, Diaz U, Quidiello RD. 1990. Definite influence of location and climatic conditions on the fatty acid composition of sunflower seed oil. *J. Am. Oil Chem. Soc.* **67** (10), 618-623. https://doi.org/10.1007/BF02540410

Loizzo MR, Bruno M, Balzano M, Giardinieri A, Pacetti D, Frega NG, Sicari V, Leporini M, Tundis R. 2019. Comparative chemical composition and bioactivity of *Opuntia ficus-indica* Sanguigna and Surfarina seed oils obtained by traditional and ultrasound-assisted extraction procedures *Eur. J. Lipid Sci. Tech*. **121**, 1800283. https://doi.org/10.1002/ejlt.201800283

Mannoubi I El, Barrek S, Skanji T, Casabianca H, Zarrouk H. 2009. Characterization of *Opuntia ficus-indica* seed oil from Tunisia. *Chem. Nat. Comp*. **45**, 616-620. https://doi.org/10.1007/s10600-009-9448-1

Márquez-Ruiz G, Martín-Polvillo M, Dobarganes MC. 1996. Quantitation of oxidised triglyceride monomers and dimers as a useful measurement for early and advanced stages of oxidation. *Grasas Aceites* **47**, 48-53.

Martín-Polvillo M, Márquez-Ruiz G, Dobarganes MC. 2004. Oxidative stability of sunflower oils differing in unsaturation degree during long-term storage at room temperature. *J. Am. Oil Chem. Soc.* **81**, 577-583. https://doi.org/10.1007/s11746-006-0944-1

Martínez M, Barrionuevo G, Nepote V, Grosso N, Maestri D. 2011. Sensory characterization and oxidative stability of walnut oil. *Int. J. Food Sci. Tech.* **46**, 1276-1281. https://doi.org/10.1111/j.1365-2621.2011.02618.x

Morales P, Ramírez-Moreno E, Sanchez-Mata, MC, Carvalho AM, Ferreira, ICFR. 2012. Nutritional and antioxidant properties of pulp and seeds of two xoconostle cultivars (*Opuntia joconostle* F.A.C. Weber ex Diguet and *Opuntia matudae* Scheinvar) of high consumption in Mexico. *Food Res. Int*. **46**, 279-285. https://doi.org/10.1016/j.foodres.2011.12.031

Naz S, Sheikh H, Siddiqi R, Sayeed SA. 2004. Oxidative stability of olive, corn and soybean oil under different conditions. *Food Chem.* **88**, 253-259. https://doi.org/10.1016/j.foodchem.2004.01.042

Normand L, Eskin NAM, Przybylski R. 2006. Comparison of the frying stability of regular and high oleic acid sunflower oils. *J. Am. Oil Chem. Soc.* **83**, 331-334. https://doi.org/10.1007/s11746-006-1208-9

NCCS 11 Statistical Software NCSS Version 11.0.20, LLC. Kaysville, Utah, USA, **2018.** ncss.com/software/ncss. Released 1 November 2018.

Ortega-Ortega MA, Cruz-Cansino SN, Alanís-García E, Delgado-Olivares L, Ariza-Ortega JA, Ramírez-Moreno E, de Jesús Manríquez-Torres J. 2017. Optimization of ultrasound extraction of cactus pear (*Opuntia ficus-indica*) seed oil based on antioxidant activity and evaluation of its antimicrobial activity. *J. Food Qual.* **2017**, 1-9. https://doi.org/10.1155/2017/9315360

Pardo JE, Fernandez E, Rubio M, Alvarruiz A, Alonso GL. 2009. Characterization of grape seed oil from different grape varieties (*Vitis vinifera*). *Eur. J. Lipid Sci. Tech*. **111** (2), 188-193. https://doi.org/10.1002/ejlt.200800052

Park, PW, Goins RE. 1994. *In situ* preparation of fatty acid methyl esters for analysis of fatty acid composition in foods. *J. Food Sc.* **59**, 1262-1266.

Pearson JR. 1973. Alteration of dietary fatty acids by human intestinal bacteria. *Proc. Nutri. Soc.* **32**, 8A-9A.

Prior RL, Hoang H, Gu L, Wu X, Bacchiocca M, Howard L, Hampsch-Woodill M, Huang D, Ou B, Jacob R. 2003. Assays for hydrophilic and lipophilic antioxidant capacity (oxygen radical absorbance capacity (ORACFL)) of plasma and other biological and food samples. *J. Agric. Food Chem.* **51** (11), 3273-3279. https://doi.org/10.1021/jf0262256

Ramírez-Moreno E, Cariño-Cortés R, del Socorro Cruz-Cansino N, Delgado-Olivares L, Ariza-Ortega LD, Montañez-Izquierdo VY, Hernández-Herrero MM, Filardo-Kerstupp T. 2017. Antioxidant and antimicrobial properties of cactus pear (*Opuntia*) seed oils *J. Food Qual*. 1-8. https://doi.org/10.1155/2017/3075907

Rancimat Manual. 2009. *Determination of the oxidative stability of the oils and fats*. Metrohm AG, CH-9101, Herisau, Switzerland.

Regalado-Rentería E, Aguirre-Rivera JR, González-Chávez MM, Sánchez-Sánchez R, Martínez-Gutiérrez F, Juárez-Flores BI. 2018. Assessment of extraction methods and biological value of seed oil from eight variants of prickly pear fruit (*Opuntia* spp.). *Waste Biomass. Valor*. https://doi.org/10.1007/s12649-018-0409-4

Salvo F, Galati E, Lo Curto S, Tripodo M. 2002. Study on the chemical characterization of lipid composition of *Opuntia ficus-indica* L. seed oil. *Acta Hort*. **581**, 283-289. https://doi.org/10.17660/ActaHortic.2002.581.33

Shahidi F, Zhong Y. 2005. Lipid oxidation: measurement methods. *In: Bailey's industrial oil and fat products*, 6th edition. John Wiley and Sons Incorporated, 357-385.

Sawaya WN, Khan P. 1982. Chemical characterization of prickly pear seed oil, *Opuntia ficus-indica J. Food Sci.* **47** (6), 2060-2061. https://doi.org/10.1111/j.1365-2621.1982.tb12946.x

Tlili N, Bargougui A, Elfalleh W, Triki A, Nasri N. 2011. Phenolic compounds, protein, lipid content and fatty acids compositions of cactus seeds. *J. Med. Plants Res.* **5**, 4519-4524.

Wit M de, Hugo A, Shongwe N. 2017. Quality assessment of seed oil from selected cactus pear cultivars (*Opuntia ficus-indica* and *O. robusta*). *J. Food Proc. Pres.* **41** (3), e12898 https://doi.org/10.1111/jfpp.12898

Wit M de, Hugo A, Shongwe N. 2018. South African cactus pear seed oil: a comprehensive study on 42 spineless Burbank *Opuntia ficus-indica* and *Opuntia robusta* cultivars. *Eur. J. Lipid Sci. Tech.* **120** (3), 1700343. https://doi.org/10.1002/ejlt.201700343

Zine S, Gharby S, El Hadek M. 2013. Physicochemical characterization of *Opuntia ficus-indica* seed oil from Morocco. *Biosci. Biotech. Res. Asia* **10** (1), 99-105. https://doi.org/10.13005/bbra/1099

GRASAS Y ACEITES 72 (3)
July-September 2021, e416
ISSN-L: 0017-3495
https://doi.org/10.3989/gya.0450201

Batoko plum (*Flacourtia inermis*) peel extract attenuates deteriorative oxidation of selected edible oils

N.E. Wedamulla✉ and W.A.J.P. Wijesinghe

Department of Export Agriculture, Faculty of Animal Science and Export Agriculture, Uva Wellassa University, Badulla, Sri Lanka.
✉Corresponding author: nishala.erandi@yahoo.com

Submitted: 28 April 2020; Accepted: 04 June 2020; Published online: 14 September 2021

SUMMARY: The oxidation of oils has an adverse effect on the organoleptic properties and shelf-life of stored oils. *Flacourtia inermis* is one of the underutilized fruits grown in Sri Lanka with promising antioxidant properties. *F. inermis* peel extract (FIPE) was used to retard rancidity in edible oils. The efficacy of added FIPE (500, 1000, 2000 ppm) on sunflower oil (SO) and virgin coconut oil (VCO) was monitored at 3-day intervals at 65 ± 5 °C against a positive control (α-tocopherol at 500 ppm level) using Free Fatty Acid (FFA) and Peroxide Value (PV). Oils without FIPE were used as the control. Antioxidant efficacy (IC_{50}) and Total Phenol Content (TPC) of FIPE were determined by DPPH assay and the Folin-Ciocalteu method. Fourier transform infrared spectroscopy was used to monitor the oxidative stability. The IC_{50} value and TPC of FIPE were 227.14 ± 4.12 μg·mL^{-1} and 4.87 ± 0.01 mg GAE/g extract, respectively. After 21 days, VCO (control) sample exhibited significantly ($p < 0.05$) higher FFA and PV than the treatments. FIPE exhibited comparable results with α-tocopherol. Conclusively, FIPE had strong antioxidant properties and thus, could be used as an alternative to α-tocopherol to improve the oxidative stability of virgin coconut oil and sunflower oil. However, only minor differences in the FTIR spectra were detected in treated and untreated virgin coconut and sunflower oil samples after 21 days storage at 65 ± 5 °C.

KEYWORDS: *Antioxidant efficacy; Coconut oil; Flacourtia inermis; Oxidative stability; Sunflower oil*

RESUMEN: ***Extracto de piel de ciruela Batoko (*Flacourtia inermis*) para atenuar el deterioro oxidativo de aceites comestibles seleccionados.*** La oxidación afecta negativamente a las propiedades organolépticas y a la vida útil de los aceites almacenados. *Flacourtia inermis* es una de las frutas infrautilizadas cultivadas en Sri Lanka con prometedoras propiedades antioxidantes. En este contexto, se utilizó el extracto de cáscara de *F. inermis* (FIPE) para retardar la rancidez de los aceites comestibles. La eficacia de FIPE añadido (500, 1000, 2000 ppm) a aceite de girasol (SO) y a aceite de coco virgen (VCO) se controló a intervalos de 3 días a 65 ± 5 °C frente a un control positivo (α-tocoferol a nivel de 500 ppm) y utilizando las determinaciones de acidez libre (FFA) e índice de peróxido (PV). Se usaron aceites sin FIPE como control. La eficacia antioxidante (IC50) y el contenido total de fenoles (TPC) de FIPE se midieron mediante el ensayo DPPH y el método de Folin-Ciocalteu. La espectroscopía infrarroja por transformada de Fourier se utilizó para controlar la estabilidad oxidativa. El valor de CI50 y el TPC de FIPE fueron 227,14 ± 4,12 μg·mL^{-1} y 4,87 ± 0,01 mg de extracto de GAE / g, respectivamente. Tras 21 días, la muestra de VCO (control) mostró valores significativamente más altos ($p < 0.05$) de FFA y PV que los tratamientos. FIPE exhibió resultados comparables con α-tocoferol. En conclusión, FIPE tiene fuertes propiedades antioxidantes, por lo que podría usarse como una alternativa al α-tocoferol para mejorar la estabilidad oxidativa de aceites de coco virgen y de girasol. Sin embargo, solo se mostraron diferencias menores en los espectros FTIR de las muestras de aceite de coco y girasol tratadas y no tratadas tras 21 días de almacenamiento a 65 ± 5 °C.

PALABRAS CLAVE: *Aceite de coco; Aceite de girasol; Eficacia antioxidante; Estabilidad oxidativa; Flacourtia inermis*

Citation/Cómo citar este artículo: Wedamulla NE, Wijesinghe WAJP. 2021. Batoko plum (*Flacourtia inermis*) peel extract attenuates deteriorative oxidation of selected edible oils. *Grasas Aceites* 72 (3), e416. https://doi.org/10.3989/gya.0450201

1. INTRODUCTION

Fats and oils play a vital role in the human diet owing to their nutritional value. Soybean, palm, rapeseed and sunflower oil are identified as the most widely consumed edible oils. Among them, sunflower oil is the second most widely used oil in Europe (Arshad and Amjad, 2012) and contains high amounts of vitamin E, essential fatty acids and a low level of saturated fat (Madhavi *et al*., 2010). Recently, virgin coconut oil (VCO) has drawn considerable attention from the scientific community as VCO contains a significant amount of medium-chain fatty acids *viz.* capric, caproic and caprylic acids which are proven to have antimicrobial and antiviral properties (Villarino *et al*., 2007).

Edible oils are subjected to oxidation during processing and storage via different chemical mechanisms *viz.* autoxidation and photosensitized oxidation (Choe and Min, 2006) which modifies organoleptic properties while affecting the shelf-life (Lercker and Rodriguez-Estrada, 2002) with a strong impact on the final quality of foods (Capuano *et al*., 2010). This lipid oxidation also contributes to decreasing the nutritional quality in addition to the production of rancid odors, unpleasant flavors and discoloration (Abdelazim *et al*., 2013). Thus, the oxidative stability of edible oils is one of the major concerns in the food industry; and oxidative stability is simply defined as "resistance to oxidation during processing and storage" (Guillén and Cabo, 2002).

There is a growing tendency toward using synthetic antioxidants such as butylated hydroxyanisole (BHA), butylated hydroxytoluene (BHT) and tert-butyl hydroquinone (TBHQ) to improve the oxidative stability of edible oils in order to overcome the adverse effects associated with lipid oxidation. However, an influx of literature has revealed that these compounds are associated with many health hazards, including cancer and carcinogenesis (Abdelazim *et al*., 2013). In light of this information, a surge of studies has been directed towards the addition of natural antioxidants in order to retard the rancidity of edible oils (Latha, 2009).

Natural antioxidants have drawn considerable attention owing to their potential role in preventing chronic diseases (Falowo *et al*., 2014). These antioxidants also inhibit or slow down the formation of free radicals and retard lipid oxidation by inhibiting the initiation or propagation of oxidative chain reactions (Latha, 2009). A number of local fruits grown in Sri Lanka has been identified as an excellent source of natural antioxidants. Moreover, many underutilized fruits exhibit greater amounts of promising antioxidant properties than commonly consumed fruits (Piyathunga *et al*., 2016).

The fruit from *Flacourtia inermis* (Sri Lankan name: *Lovi*) of the family Flacourtiaceae is one of the underutilized fruits grown in Sri Lanka with promising antioxidant properties (Jayasinghe *et al*., 2012; Alakolanga *et al*., 2014). The fruit is round, cherry-sized, and dark red when ripe with fruit juice which has a deep red color (Alakolanga *et al*., 2015). Though many studies have proven the antioxidant activity of *F. inermis* fruit, the studies directed to assess the efficacy of *F. inermis* as a natural antioxidant are still scarce. Thus, the present study aims to utilize FIPE to retard the rancidity of selected edible oils as the peels of many fruits get wasted during processing regardless of their promising bioactive properties.

2. MATERIALS AND METHODS

2.1. Materials

Sunflower oil and virgin coconut oil were obtained from a local market in Badulla, Sri Lanka. *F. inermis* (*Lovi*) fruits were collected from the Western province of Sri Lanka. All of the reagents and solvents used were of analytical reagent grade.

2.2. Extraction of natural antioxidants from the peel of *F. inermis* fruits

Freeze-dried fruit peel was ground to a fine powder using a laboratory grinder. Dried, powdered peel was sieved (mesh size; 1 mm) and stored at -18 °C temperature until extraction. Freeze dried peel powder (20 g) was dissolved in 200 mL of 70% aqueous ethanol and extracted using an ultrasonic cleaner (model UC -10 A, 40 kHz, Heater 50 w, Tank 2 L, Tank size L 180 * W 165* H 180 cm, China) at 40 ± 5 °C for 30 minutes. The extraction procedure was repeated twice. The combined filtrate was concentrated *in vacuo* at 40 ± 5 ºC. Concentrated crude extract was stored at -18 °C until analysis.

2.3. Determination of total phenol content (TPC)

Total phenol content was determined according to the method of ISO 14502-1 with slight modifications. First, crude extract was dissolved in 70% methanol to obtain a 60 $mg \cdot L^{-1}$ solution. Ten-

fold diluted Folin-Ciocalteu reagent (1.0 mL) was added to 200 µL plant extract and kept for 8 min. Then 800 µL of 7.5% (w/v) Na_2CO_3 (aq) were added and kept for 1 h. The absorbance was measured at a wavelength of 765 nm (UV /Visible SP-UV 50 VDB spectrophotometer). Gallic acid was used as a standard and a calibration curve was plotted using the absorbance values for gallic acid solution series. The phenolic content of plant extracts was calculated using the calibration curve and expressed as mg of gallic acid equivalents (GAE)/ g extract.

2.4. Determination of antioxidant activity

The crude extracts (150-325 ppm) were tested using the 2,2-diphenyl-1-picrylhydrazyl (DPPH) assay (Ali *et al*., 2018). Each solution (50 µL) was mixed with 50 µL of 4×10^{-4}M methanolic DPPH Solution and kept in the dark at room temperature for 20 min. The absorbance was measured at 517 nm using a microplate spectrophtometer (Multiskan Go, Version100.40, Thermo Fisher Scientific) against a reaction blank (50 µL of Methanol and 50 µL of the crude extract). A mixture of 50 µL of 4×10^{-4}M DPPH solution and 50 µL of methanol were used as a reaction control. Percent inhibition was calculated for each concentration and IC_{50} was calculated for crude extract. The following equation was used to calculate percent inhibition:

$$\text{Present Inhibition} = \frac{Ac - As}{Ac} \times 100$$

A_c: Absorbance of reaction control
A_s: Absorbance of the test sample

2.5. Sample preparation for storage of oils

Oil samples with crude extract were prepared at three different concentrations *viz* 500 ppm, 1000 ppm and 2000 ppm along with control (no added peel extract) and α-tocopherol (500 ppm) was used as positive control. First, oil sample was pre heated in a water bath at 50 °C for 3 hours. The crude extract of fruit peel was dissolved in a small amount of absolute ethanol (150 µL) to facilitate a uniform dispersion of extract in the oil. Oil samples with different concentrations of extracts were kept in an ultrasonic water bath at 60 °C for 30 min to obtain a homogenous dispersed sample. A storage study of the oils was conducted as per the method described by Besbes *et al*., 2004 with slight modifications. Treated oils were completely filled into glass bottles (volume 25 mL) wrapped with aluminum foil, sealed properly and stored in an oven at 65 ± 5 °C for 21 days. Oil samples were drawn for analysis at intervals of three days.

2.6. Determination of peroxide value (PV)

Peroxide values for the oil samples drawn at 3-day intervals were determined according to the standard procedures described as AOAC 965.33 (2016). Five grams of oil sample were dissolved in 30 mL of acetic acid: chloroform solution (3:2). Then, 0.5 mL of saturated KI solution were added and left to stand with occasional shaking for one minute and placed in the dark for 5 min. Then, 30 mL of distilled water were added and the mixture was titrated slowly with 0.01M sodium thiosulfate. A blank was made according to same procedure without the addition of oil. The peroxide value (meq $O_2 \cdot kg^{-1}$ of oil) of all samples was calculated according to the following equation:

$$\text{Peroxide value (mEq/kg)} = \frac{S \times M \times 1000}{\text{Sample weight (g)}}$$

Where,
S is the volume of $Na_2S_2O_3$ used (blank corrected)
M is the molarity of $Na_2S_2O_3$

2.7. Determination of free fatty acid (FFA) content

The free fatty acid contents of the oil samples drawn at 3-day intervals were determined according to the procedure described as AOAC 940.28 (2016). An accurately weighed oil sample was dissolved in 20 mL of previously neutralized absolute ethanol. The mixture was titrated with 0.05 M sodium hydroxide with the addition of phenolphthalein as indicator with vigorous shaking until a permanent faint pink color appeared and persisted for more than 1 min. The percentage of free fatty acids of each oil sample was calculated as oleic acid using the following equation:

$$\text{\% FFA (oleic acid)} = \frac{V \times C \times 282.46 \times 100}{M}$$

Where,
V is the volume of sodium hydroxide react in titration (mL)
C is the concentration of sodium hydroxide (M)
M is the mass of oil sample (g)

2.8. FTIR (Fourier transform infrared) analysis

The absorption spectra of oil samples before and after 21 days of storage were measured on a FTIR spectrometer (Bruker, Alpha-T, German) using Deuterated Triglycine Sulphate (DTGS) as detector. They were interfaced to a computer operating under Windows-based, and connected to OPUS (Version 7.5) software. The samples were placed in contact with attenuated total reflectance (ATR) element (platinum) at controlled ambient temperature. FTIR spectra were collected in the frequency of 4000-500 cm^{-1} by co-adding 64 scans and at resolution of 4 cm^{-1}. All spectra were rationed against a background of air spectrum.

2.9. Statistical analysis

Mean values of all data were obtained from triplicate determinations. Values were expressed are mean ± SD. Data were subjected to analysis of variance (ANOVA) according to the GLM (general linear model). Data processing was done by the Minitab 16.1 version of the computer software package.

3. RESULTS AND DISCUSSION

3.1. Antioxidant properties of *F. inermis* fruit peel extract

The antioxidant efficacy of plant extracts can be tested using a wide variety of methods. In the present study, the free radical scavenging capacity of FIPE was evaluated by DPPH assay and expressed as IC_{50}. Results of the present study revealed that the antioxidant activity of FIPE (227.14 ± 4.12 $\mu g \cdot mL^{-1}$) was significantly ($p < 0.05$) lower than that of α-tocopherol (29.80 ± 3.22 $\mu g \cdot mL^{-1}$). Alakolanga *et al*., (2015) observed comparatively high antioxidant activity (66.2 ppm) in the ethyl acetate extract of *F. inermis* whole fruit. However, the methanolic extract of the reported study exhibited comparatively low antioxidant activity (212.95 ppm). The disparity of the results may be due to the difference in the extraction technique employed and the fruit material used in the two studies.

In the present study sonication was used as the extraction technique to extract natural antioxidants from the peel of *lovi* fruit as it is reported to enhance the extraction of bioactive compounds from plants and their products (Annegowda *et al*., 2010). The present study used 30 min sonication time for the extraction as prolonged sonication led to the decomposition of the bioactive constituents, and most of the active constituents inside the cells are released into the solvent during the first few minutes (Annegowda *et al*., 2010).

3.2. Total phenol content of *F. inermis* fruit peel extract

The total phenol content of FIPE was determine using the Folin-Ciocalteau colorimetric method. The total phenolic content of a sample was calculated based on the calibration curve prepared using gallic acid as standard. The total phenol content of FIPE was 4.87 ± 0.01 mg GAE per g extract. However, the study carried out by Alakolanga and others (2015) reported the polyphenol content of *lovi* fruit as 1.28 g gallic acid equivalents per 100 g of fresh fruit.

The extraction of phenolic compounds from plant materials is influenced by several factors: chemical nature of the plant materials, method of extraction, particle size of the sample (plant material), storage time and conditions, and the presence of interfering substances. The solubility of phenolic compounds is governed by the type of solvent (polarity of the solvent) used, the degree of polymerization of phenolics, the interaction of phenolics with other food constituents and the formation of insoluble complexes (Naczk and Shahidi, 2004). Thus, considering all these factors and the literature (Liew *et al*., 2018), the present study used 70% ethanol as the solvent for extraction.

3.3. Variation in peroxide value (PV) during storage of oils

Peroxide value measures the formation of peroxide in the early stages of lipid oxidation. The present study measured the variation in peroxide value to determine the effect of FIPE addition on the oxidative stability of VCO and SO during storage at 65 ± 5 °C. The peroxide values for the VCO samples treated with FIPE are shown in Figure 1 along with the control and positive control α-tocopherol. The PV of all the oil samples increased during storage and thereby indicate the progression of lipid oxidation as PV is a good indicator of the extent of primary oxidative products formed in oils. Several studies have proven that the PV of VCO increased during storage at 63 °C (Rohman *et al*., 2011). However, the initial PV of the reported study was lower (0.42 ± 0.009 meq $O_2 \cdot kg^{-1}$ oil) than

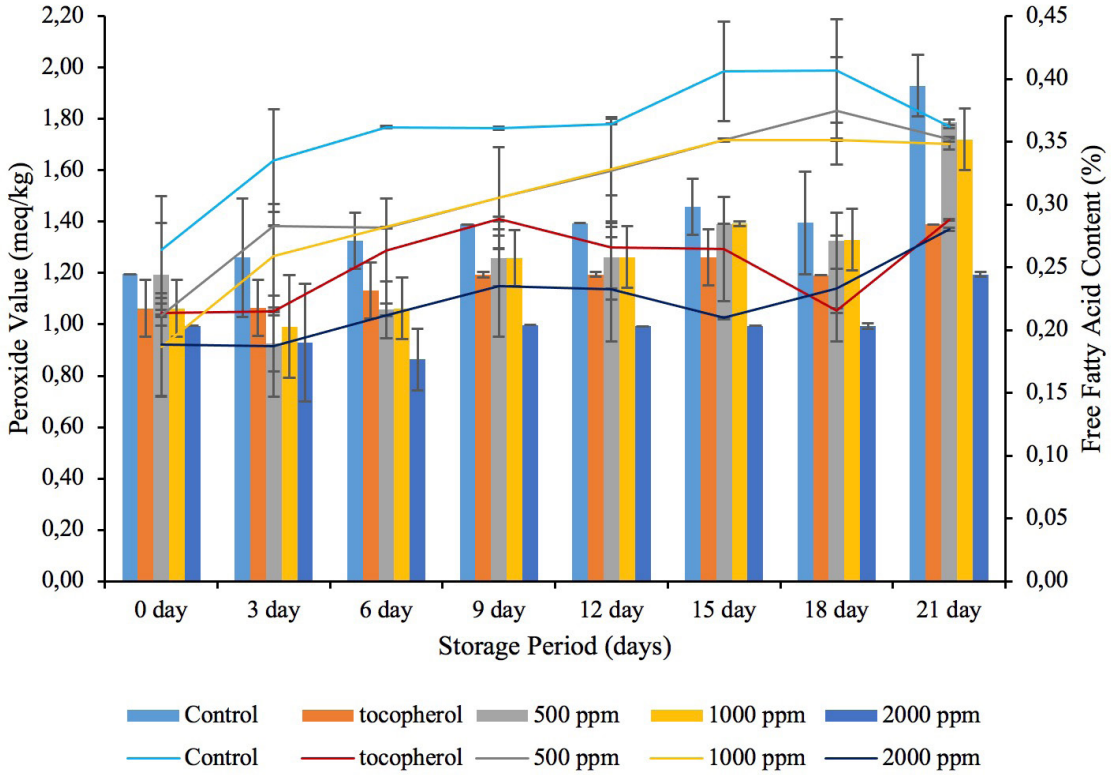

FIGURE 1. Variations in Peroxide Value and Free Fatty Acid Content in Virgin Coconut oil with added FIPE. Values are presented as mean ± SD of three determinations.

that of the present study (1.20 ± 0.00 meq $O_2 \cdot kg^{-1}$ oil). The peroxide values of treated samples and control samples showed no significant difference ($p > 0.05$) up to the third day of storage. From day 6 onwards the PV of the control and treated samples showed significant difference ($p < 0.05$); the PV value of the control sample was significantly ($p < 0.05$) higher than the 2000 ppm level of the extract-added VCO sample from day 6 onward. However, there was no significant difference between the control and 500 ppm and 1000 ppm levels of FIPE-added VCO samples after day 6 or day 18. The highest peroxide value (1.93 ± 0.12 meq $O_2 \cdot kg^{-1}$ oil) was observed for the control sample after 21 days storage.

Meanwhile, the lowest peroxide value (1.19 ± 0.01 meq $O_2 \cdot kg^{-1}$ oil) was reported for the VCO sample with 2000 ppm level of extract after 21 days of storage (Figure 1). There was no significant difference between the oil treated with α- tocopherol (1.39 ± 0.00 meq $O_2 \cdot kg^{-1}$ oil) and the oil treated with the 2000 ppm level of FIPE after 21 days of storage, which indicated excellent antioxidant capacity at higher concentration levels of FIPE.

The variation in the PV of sunflower oil treated with FIPE is illustrated in Figure 2. The PVs of all the tested oil samples were increased with time, which indicated the generation of hydroperoxides in sunflower oil (Szydłowska-Czerniak and Rabiej, 2018). The PVs of sunflower oil samples were higher than that of VCO owing to the high amount of unsaturated fatty acids present in SO which are more prone to oxidation (Wójcickiwt *et al*., 2015). The PV of oil samples treated with the 2000 ppm level of FIPE after 21 days of storage was 12.38 ± 0.46 meq/kg; while the control and α-tocopherol showed 28.30 ± 0.58 meq $O_2 \cdot kg^{-1}$ and 17.94 ± 0.35 meq $O_2 \cdot kg^{-1}$, respectively. However, there was no significant difference between the control and treatments until day 6. From day 9 onwards the PV of SO treated with the 2000 ppm level of FIPE was significantly ($p<0.05$) lower than that of the positive control, α-tocopherol. Moreover, there was no significant difference between SO with 500 ppm or 1000 ppm level of FIPE addition. However, the PV of the positive control was significantly lower than those of 500 ppm and 1000 ppm levels of

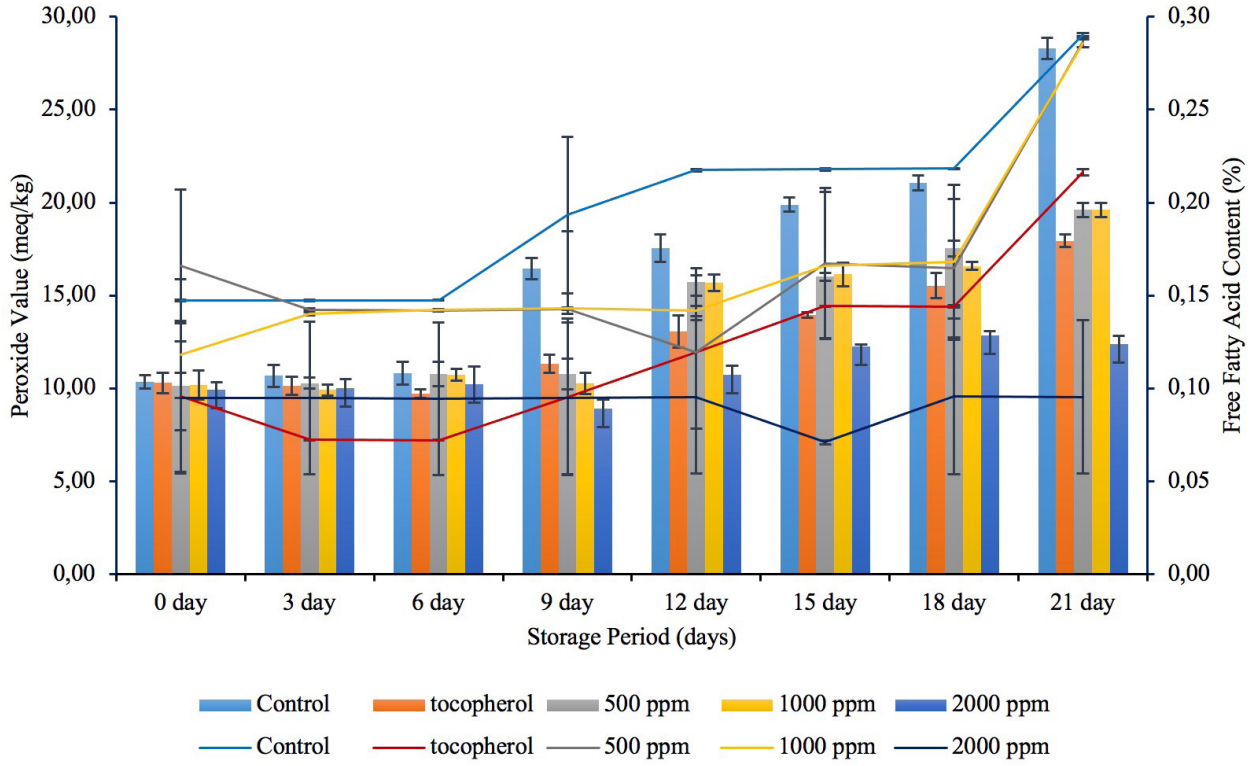

FIGURE 2. Variations in Peroxide Value and Free Fatty Acid Content in Sunflower oil with added FIPE. Values are presented as mean ± SD of three determinations.

FIPE-added SO samples, thus proving the efficacy of 2000 ppm level of FIPE addition in controlling the oxidation of SO.

3.4. Variation of free fatty acid (FFA) content during storage of oils

Free fatty acid content is one of the important quality parameters in oils, as FFA is responsible for the development of undesirable flavor and aroma in oils. These free fatty acids formed in oils from hydrolysis, oxidation due to free radical formation and cleavage of double bonds during frying (Ma *et al*., 2015). The free fatty acid content of VCO used for the study was relatively low (0.26 ± 0.04%) indicating that the initial quality of VCO used for the study was good. However, the FFA content in the present study was higher than that of the reported study (0.16 ± 0.002%) (Rohman *et al*., 2011). The variation in FFA contents in the VCO samples treated with FIPE are shown in Figure 1 along with the control and positive control, α-tocopherol. The FFA content in VCO treated with FIPE at the 2000 ppm level was significantly ($p < 0.05$) lower than that of the control after day 3. However, there was no significant difference between the FFA content of the 2000 ppm level of extract-added oil and the positive control after 3 days of storage. Initially, FFA content was not significantly different from the control and treated oil samples. However, with time the FFA contents in the oil samples were increased as shown in Figure 1. After 21 days of storage the VCO (control) sample exhibited the highest FFA content (0.36 ± 0.00 %); while the 2000 ppm level of extract-added oil sample contained the lowest FFA content (0.28 ± 0.00%). In addition, after 21 days of storage the FFA content of 2000 ppm level of extract-added sample was significantly lower than that of the positive control (0.29 ± 0.00%).

The initial FFA content of SO (0.15 ± 0.00%) used for the study was lower than that of VCO (0.26 ± 0.04%). A comparatively high initial FFA content of VCO could be attributed to the presence of free fatty acids, chlorophyll or products of oxidative degradation which impair the quality of the oil (Ma *et al*., 2015). Many studies were conducted to assess the effect of the addition of natural antioxidants on

the oxidative stability of SO (Carelli *et al*., 2005). The initial FFA content in the reported study (0.16%) was comparable to the present study. The FFA content of SO treated with the 2000 ppm level of extract was significantly ($p < 0.05$) lower than that of the control from day 3 onwards. However, there was no significant difference between oil treated with 2000 ppm level of extract and α-tocopherol until 21 days of storage. After 21 days of storage SO treated with the 2000 ppm level of FIPE exhibited the lowest FFA content (0.10 ± 0.04%); while oil treated with 500 ppm and 1000 ppm levels of extracts showed comparatively high FFA content (Figure 2). Moreover, there was no significant difference between the control and SO treated with 500 ppm and 1000 ppm extract levels after 21 days of storage.

3.5. FTIR analysis of stored edible oils

The influx of research studies was carried out on the potential applications of FTIR in monitoring the oxidation of edible oils (Van de *et al*., 1994). Thus, the present study used FTIR spectroscopy to monitor the oxidative changes occurring in treated and non-treated sunflower oil and virgin coconut oil after 21 days of storage. Figure 3 illustrates the FTIR spectra of non-treated VCO, VCO treated with the 2000 ppm level of FIPE and VCO treated with α-tocopherol. Among other edible oils VCO has a unique spectrum, as shown in Figure 3. In the spectra of VCO no peaks are identified at the region of 3008 cm^{-1} and 1655 cm^{-1} which is in agreement with previous studies (Rohman and CheMan, 2011). Peaks in the above-mentioned region represent the unsaturated double bonds and are used to express the degree of unsaturation of triglycerides. Since VCO contains very low levels of unsaturated fatty acids, the peak is hardly noticeable in this region (Rohman and CheMan, 2011).

Peaks appearing at 721, 962, 1744, 2852, 2927 and 3300 cm^{-1} were selected to compare the differences between the treated and non-treated VCO samples used for the study. All the VCO samples failed to show a peak at around 3444cm^{-1} (Figure 03), hence no evidence was detected for the

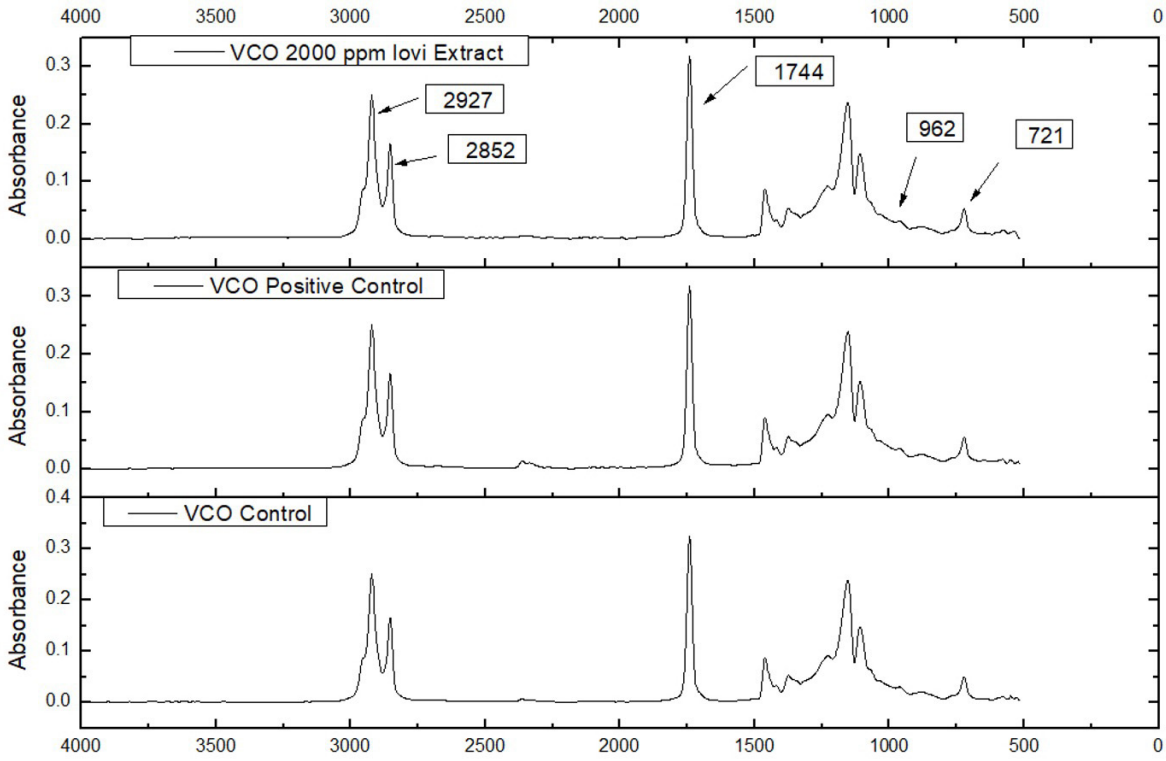

Wavenumber 2927, 2852, 1744, 962,721 corresponding respectively to the –C–H (CH_3) stretching, –C–H (CH_2) stretching, –C═O (ester) stretching, trans–CH═CH– bending and cis–CH═CH– bending according to Rohman and CheMan, 2011.

FIGURE 3. FTIR spectrum of treated and non-treated virgin coconut oils (VCO) after 21 days of storage

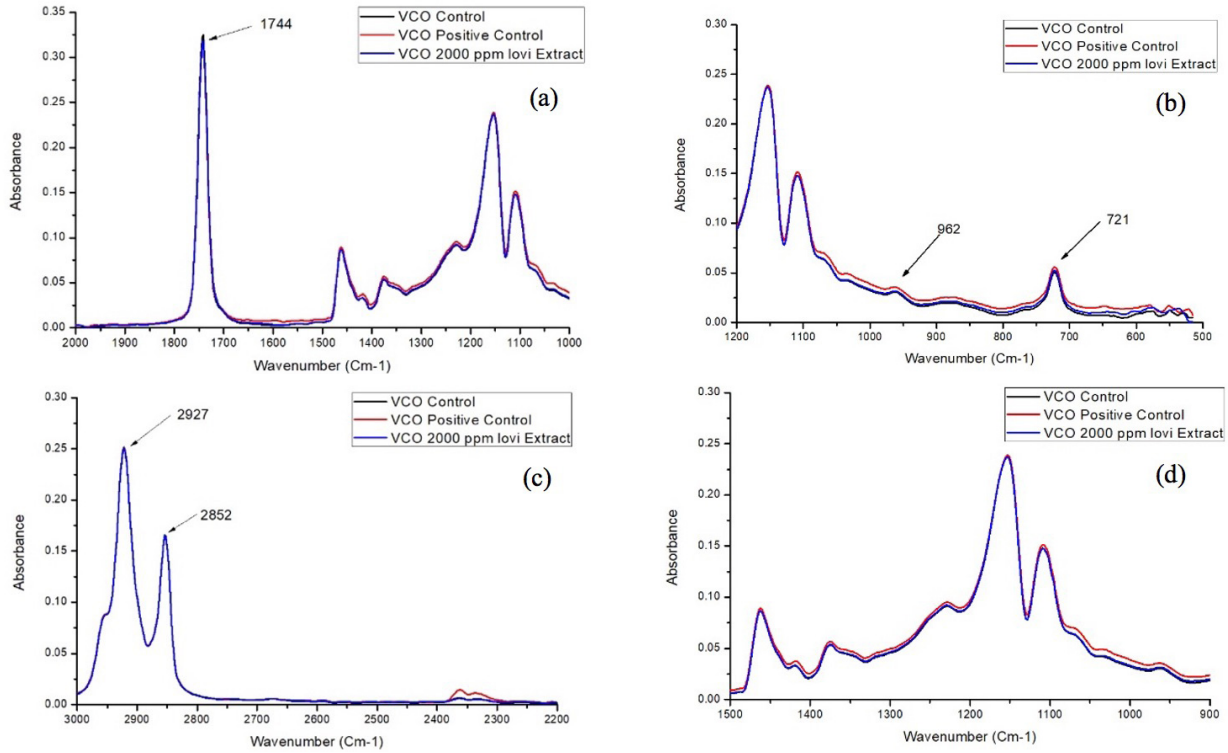

Wavenumber 2927, 2852, 1744, 962,721 corresponding respectively to the –C–H (CH_3) stretching, –C–H (CH_2) stretching, –C═O (ester) stretching, trans–CH═CH– bending and cis–CH═CH– bending according to Rohman and CheMan, 2011.

FIGURE 4. Magnification of FTIR spectra of virgin coconut oil (VCO) a) at region 2000 to 1000 cm^{-1} b) at region 1200 to 500 cm^{-1} c) at region 3000 to 2200 cm^{-1} d) at region 1500 to 900 cm^{-1}

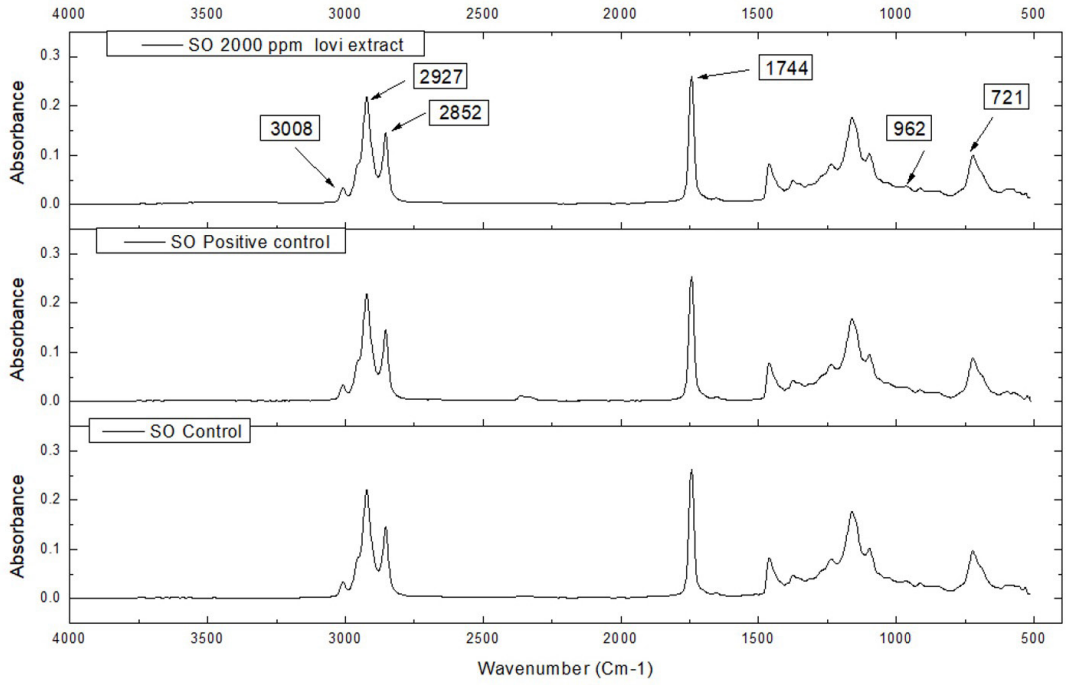

Wavenumber 3008, 2927, 2852, 1744, 962,721 corresponding respectively to the ═C–H (cis) stretching, –C–H (CH_3) stretching, –C–H (CH_2) stretching, –C═O (ester) stretching, trans–CH═CH– bending and cis–CH═CH– bending according to Rohman and CheMan, 2011.

FIGURE 5. FTIR spectra of treated and non-treated sunflower oil (SO) after 21 days of storage

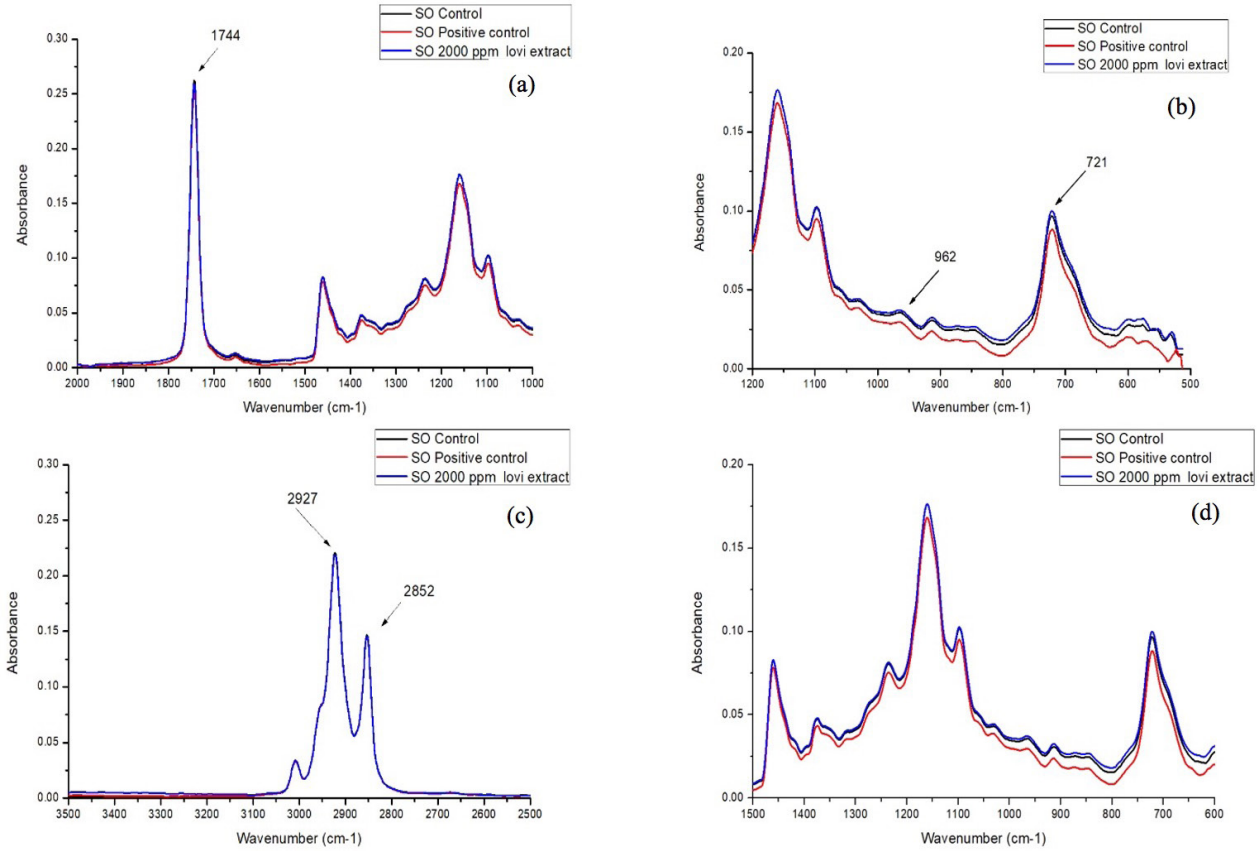

Wavenumber 2927, 2852, 1744, 962,721 corresponding respectively to the –C–H (CH3) stretching, –C–H (CH2) stretching, –C═O (ester) stretching, trans–CH═CH– bending and cis–CH═CH– bending according to Rohman and CheMan, 2011.

FIGURE 6. Magnification of FTIR spectra of sunflower oil (SO) a) at region 2000 to 1000 cm^{-1} b) at region 1200 to 500 cm^{-1} c) at region 3500 to 2500 cm^{-1} d) at region 1500 to 900 cm^{-1}

presence of hydroperoxides or free fatty acids which are formed in the thermal oxidation of oils. The carbonyl absorption of the triacylglyceol linkage is noticeable at 1744 cm^{-1}. However, a noticeable difference was not observed in VCO samples at this frequency (Figure 4 (a)). High intensity at 1744 cm^{-1} represents the high amounts of carbonyl compounds such as aldehydes, esters, ketones, and lactones present in the oils which formed during oxidation (Smith *et al.,* 2005). Moreover, added FIPE and α-tocopherol were not effective in lowering the intensity of carbonyl compounds (Figure 4 (a)). The peak at 962 cm^{-1} represents the bending vibration of CH functional groups of *trans* olefins. This peak serves as indicator of oxidative stability as the peak provides the information relevant to gradual *cis* to *trans* isomerization in the oxidized oil (Marina *et al*., 2013). There was a minor difference in the peak intensities of VCO at 962 cm^{-1}; the highest peak intensity represented the VCO treated with α- tocopherol followed by the VCO treated with the 2000 ppm level of FIPE and VCO without any treatment (Figure 4 (b)). The peak revealed in the 721 cm^{-1} region also displayed similar variation as the intensity variation in peak appeared in the 962 cm^{-1} region; the VCO sample stored for 21 days without any treatment exhibited the lowest intensity. The peaks appeared in the 2927 cm^{-1} and 2852 cm^{-1} regions also exhibited minor differences (Figure 4 (c)). One of the important regions of the FTIR spectra for VCO is the region of 1500 to 1000 cm^{-1}, which is also known as the finger print region (Marina *et al*., 2013). There is no noticeable difference revealed in the spectra of treated and non-treated VCO in this region (Figure 4 (d)).

Figure 5 illustrates the FTIR spectra of non-treated SO, SO treated with the 2000 ppm level of *lovi* peel extract and SO treated with α-tocopherol. In the

FTIR spectra of SO no peak is revealed at 3444 cm^{-1}, which represent the hydroperoxide functional group. With the progression of oxidation hydroperoxide formation increases and in relation to that, the intensity of the band revealed at 3444 cm^{-1} also increases gradually (Hamed and Allam, 2006). However, the spectra of SO revealed a peak at 3008 cm^{-1}, which represents the unsaturated double bond (Rohman and Man, 2011). Since SO contains comparatively high levels of unsaturated fatty acids the peak appeared in this region, but that peak is not revealed in the spectra of VCO.

Figure 6 illustrates the magnification of spectral ranges 2000-1000 cm^{-1}, 1200-500 cm^{-1}, 3500-2500 cm^{-1} and 1500-900 cm^{-1} in the FTIR spectra of treated and non-treated SO samples. Similar to the VCO a significant difference was not observed between the treated and non-treated SO samples at 1744 cm^{-1} (Figure 6 (a)). In non-oxidized oil this peak solely represents the ester carbonyl functional group of triglycerides and when the oil is oxidized, this peak overlaps with aldehydes, thereby producing a decrease in intensity (Guillén and Goicoechea, 2007). Figure 6(b) illustrates the differences in peak intensities between treated and non-treated SO samples at 962 cm^{-1}. The positive control, α-tocopherol, exhibits the lowest peak intensity. While the FIPE-added sample shows the highest peak intensity. This peak represents the gradual *cis* to *trans* isomerization in the oxidized oil, which increases with the progression of oxidation (Marina *et al*., 2013). Thus, α-tocopherol is effective in controlling the oxidation of SO since it exhibits the lowest peak intensity. The peak at 722 cm^{-1} was decreased with the progression of oxidation due to the loss of *cis* double bonds (Rohman and Che Man, 2013). The Figure 6(b) illustrates the differences in peak intensities at 722 cm^{-1}. As illustrated in the figure, the SO sample treated with FIPE extract exhibits the highest peak intensity and thereby represents the lowest rate of oxidation. Two peaks at 2853 and 2923 cm^{-1} remained unchanged. However, minor differences were observed in the peak intensities of treated and non-treated SO samples in the finger print region of the FTIR spectra (Figure 6(d)).

4. CONCLUSIONS

The present study concluded that the extract from the peel of *lovi* (*Flacourtia inermis*) has strong antioxidant activity with high total phenol content. Moreover, FIPE shows excellent protective effects against the oxidation of virgin coconut oil and sunflower at the 2000 ppm concentration level. The findings in the storage study have confirmed that the FIPE under the study conditions could be used as an alternative to α-tocopherol in order to improve the oxidative stability of virgin coconut oil and sunflower oil. However, only the minor differences were revealed in the FTIR spectra of treated and non-treated virgin coconut oil and sunflower oil samples after 21 days of storage at 65 ± 5 °C.

ACKNOWLEDGMENTS

This work was supported by the University Research Grant (UWU/RG/2018/004); Uva Wellasaa University, Badulla, Sri Lanka.

REFERENCES

Abdelazim AA, Mahmoud A, Ramadan-Hassanien MF. 2013. Oxidative stability of vegetable oils as affected by sesame extracts during accelerated oxidative storage. *J. Food Sci. Technol.* **50**, 868-878. https://doi.org/10.1007/s13197-011-0419-8

Alakolanga AGAW, Siriwardane AMDA, Kumar NS, Jayasinghe L, Jaiswal R, Kuhnert N. 2014. LC-MS^n identification and characterization of the phenolic compounds from the fruits of *Flacourtia indica* (Burm. F.) Merr. and *Flacourtia inermis* Roxb. *Food Res. Int.* **62**, 388-396. https://doi.org/10.1016/j.foodres.2014.03.036

Alakolanga AG, Kumar NS, Jayasinghe L, Fujimoto Y. 2015. Antioxidant property and α-glucosidase, α-amylase and lipase inhibiting activities of *Flacourtia inermis* fruits: characterization of malic acid as an inhibitor of the enzymes. *J. Food Sci. Technol*. **52**, 8383. https://doi.org/10.1007/s13197-015-1937-6

Ali AMA, El-Nour MEM, Yagi SM. 2018. Total phenolic and flavonoid contents and antioxidant activity of ginger (*Zingiber officinale* Rosc.) rhizome, callus and callus treated with some elicitors. *J. Genet. Eng. Biotechnol*. **16,** 677-682. https://doi.org/10.1016/j.jgeb.2018.03.003

Annegowda HV, Anwar LN, Mordi MN, Ramanathan S, Mansor SM. 2010. Influence of sonication on the phenolic content and antioxidant activity of *Terminalia catappa* L. leaves. *Pharmacognosy. Res*. **2**, 368-373. https://doi.org/10.4103/0974-8490.75457

AOAC 940.28. 2016. Fatty acids (Free) in crude oil and refined oils. In: Official methods of analysis of AOAC International, 20 th ed. Maryland: AOAC International.

AOAC 965.33. 2016. Peroxide value in oils and fats. In: Official methods of analysis of AOAC International, 20 th ed. Maryland: AOAC International.

Arshad MU, Amjad MU. 2012. Medicinal use of sunflower oil and present status of sunflower in Pakistan: A Review Study. *Sci. Tech. Dev*. **31**, 99-106.

Besbes S, Blecker C, Deroanne C, Lognay G, Drira NE, Attia H. 2004. Quality characteristics and oxidative stability of date seed oil during storage. *Food Sci. Technol. Int*. **10**, 333-338. https://doi.org/10.1177/1082013204047777

Capuano E, Oliviero T, Açar ÖÇ, Gökmen V, Fogliano V. 2010. Lipid oxidation promotes acrylamide formation in fat-rich model systems. *Food Res. Int*. **43**, 1021-1026. https://doi.org/10.1016/j.foodres.2010.01.013

Carelli AA, Franco IC, Crapiste GH. 2005. Effectiveness of added natural antioxidants in sunflower oil. *Grasas Aceites* **56**, 303-310. https://doi.org/10.3989/gya.2005.v56.i4.97

Choe E, Min DB. 2006. Mechanisms and Factors for Edible Oil Oxidation. *Compr. Rev. Food Sci. Food Saf*. **5**, 69-186. https://doi.org/10.1111/j.1541-4337.2006.00009.x

Falowo AB, Fayemi PO, Muchenje V. 2014. Natural antioxidants against lipid–protein oxidative deterioration in meat and meat products: A review. *Food Res. Int.* **64**, 171-181. https://doi.org/10.1016/j.foodres.2014.06.022

Guillén MD, Cabo N. 2002. Fourier transform infrared spectra data versus peroxide and anisidine values to determine oxidative stability of edible oils. *Food Chem*. **77,** 503-510. https://doi.org/10.1021/jf071712c

Guillén MD, Goicoechea E. 2007. Detection of primary and secondary oxidation products by Fourier transform infrared spectroscopy (FTIR) and ^{1}H nuclear magnetic resonance (NMR) in sunflower oil during storage. *J. Agric. Food Chem*. **55**, 10729-10736. https://doi.org/10729-10736.10.1021/jf071712c

Hamed SF, Allam MA. 2006. Application of FTIR spectroscopy in the determination of antioxidant efficiency in sunflower oil. *J. of Appl. Sc. Res*. **2**, 27-33.

ISO 14502-1. 2005. Determination of substances characteristic of green and black tea – Part 1: Content of total polyphenols in tea – Colorimetric method using Folin-Ciocalteu reagent. Geneva: ISO.

Jayasinghe L, Lakdusinghe M, Hara N, Fujimoto Y. 2012. Phenolic constituents from the fruit juice of *Flacourtia inermis*. *Nat. Prod. Res.* **26**, 278-281. https://doi.org/10.1080/14786419.2011.586638

Latha RB. 2009. Storage stability of sunflower oil with added natural antioxidant concentrate from sesame seed oil. *J. Oleo Sci*. **58,** 453-459.

Lercker G, Rodriguez-Estrada MT. 2002. Cholesterol oxidation mechanism, in Guardiola F, Dutta PC, Codony R, Savage GP. (Eds.). *Cholesterol and phytosterol oxidation products: Analysis, occurrence and biological effects*, Champaign, IL: AOCS Press, pp. 1-26.

Liew SS, Ho WY, Yeap SK, Sharifudin SAB. 2018. Phytochemical composition and in vitro antioxidant activities of *Citrus sinensis* peel extracts. *Peer J.* **6**, e5331. https://doi.org/10.7717/peerj.5331. eCollection 2018

Ma JK, Zhang H, Tsuchiya T, Akiyama Y, Chen JY. 2015. Frying stability of rapeseed Kizakinonatane (*Brassica napus*) oil in comparison with canola oil. *Food Sci. Technol. Int.* **21**, 163-174. https://doi.org/10.1177/1082013213520173

Madhavi BR, Devi NKD, Mrudula BS, Babu RN. 2010. The importance of biodegradable bio-oil-Sunflower. *Int. J. Pharm. Tech. Res*. **2**, 1913-1915.

Marina AM, Rosli WI, Noorhidayah M. 2013. Quantitative analysis of peroxide value in virgin coconut oil by ATRFTIR spectroscopy. *Open Conf. Proc. J*. **4**, 53-56. https://doi.org/10.2174/2210289201304020053

Naczk M, Shahidi F. 2004. Extraction and analysis of phenolics in food. J. *Chromatogr. A*. **1054**, 95-111. https://doi.org/10.1016/S0021-9673(04)01409-8

Piyathunga ALI, Mallawaarachchi MALN, Madhujith WMT. 2016. Phenolic Content and Antioxidant Capacity of Selected Underutilized Fruits Grown in Sri Lanka. *Tropl. Agricl. Res.* **27**, 277-286. http://doi.org/10.4038/tar.v27i3.8206

Rohman A, Che Man YB. 2011. Potential use of FT-IR-ATR spectroscopic method for determination of virgin coconut oil and extra virgin olive oil in ternary mixture systems. *Food Anal. Methods* **4**, 155-162. https://doi.org/10.1007/s12161-010-9156-2

Rohman A, Che Man YB. 2013. Application of FTIR spectroscopy for monitoring the stabilities of selected vegetable oils during thermal oxidation. *Int. J. Food Pro*. **16**, 1594-1603. https://doi.org/10.1080/10942912.2011.603874

Rohman A, Che Man YB, Ismail A, Hashim P. 2011. Monitoring the oxidative stability of virgin coconut oil during oven test using chemical indexes and FTIR spectroscopy. *Int. Food Res. J.* **18**, 303-310.

Smith SA, King RE, Min DB. 2005. Oxidative and thermal stabilities of genetically modified high oleic sunflower oil. *Food Chem*. **102**, 1208-1213. https://doi.org/10.1016/j.foodchem.2006.06.058

Szydłowska-Czerniak A, Rabiej D. 2018. Octylsinapate as a new antioxidant to improve oxidative stability and antioxidant activity of rapeseed oil during accelerated storage. *Eur. Food Res. Technol*. **244**, 1397-1406.

Van de Voort FR, Ismail AA, Sedman J, Emo G. 1994. Monitoring the oxidation of edible oils by Fourier transform infrared spectroscopy. *J. Am. Oil Chem. Soc*. **71**, 243-253. https://doi.org/10.1007/BF02638049

Villarino BJ, Dy LM, Lizada M. 2007. Descriptive sensory evaluation of virgin coconut oil and refined, bleached and deodorized coconut oil. *LWT - Food Sci. Technol*. **40**, 193-199. https://doi.org/10.1016/j.lwt.2005.11.007

Wójcicki K, Khmelinskii I, Sikorski M, Sikorska E. 2015. Near and mid infrared spectroscopy and multivariate data analysis in studies of oxidation of edible oils. *Food Chem*. **187**, 416-423. https://doi.org/10.1016/j.foodchem.2015.04.046

GRASAS Y ACEITES 72 (3)
July-September 2021, e417
ISSN-L: 0017-3495
https://doi.org/10.3989/gya.0336201

Improving biodiesel yield from pre-esterified inedible olive oil using microwave-assisted transesterification method

L. Dehghan[a], M.-T. Golmakani[a,✉] and S.M.H. Hosseini[a]

[a]Food Science and Technology Department, School of Agriculture, Shiraz University, Shiraz, Iran.
[✉]Corresponding author: golmakani@shirazu.ac.ir

Submitted: 30 March 2020; Accepted: 08 June 2020; Published online: 14 September 2021

SUMMARY: In the present research, biodiesel production from olive oils with different initial free fatty acid concentrations (2.5, 5.0, and 10.0%) was evaluated. A two-stage acid-catalyzed esterification and alkaline-catalyzed transesterification (ACT) process using the microwave heating method was compared with the traditional heating method. Free fatty acid was reduced to less than 2.0% in the first stage. Although no significant difference was observed between microwave and traditional esterification methods in terms of fatty acid reduction, the microwave treatment significantly decreased reaction time by 92.5%. Comparing microwave ACT results with those of the traditional heating method showed that the microwave can significantly increase methyl ester yield and purity, and simultaneously decrease reaction time. Physical constants of methyl esters were also improved using the microwave heating method. Therefore, the microwave heating method can be regarded as an efficient method instead of the two-stage method for biodiesel production. This method is capable of using inedible olive oil with high concentrations of free fatty acids.

KEYWORDS: *Biodiesel; Esterification; Microwave; Olive oil; Transesterification*

RESUMEN: ***Mejora del rendimiento del biodiesel a partir de aceite de oliva no comestible pre-esterificado mediante transesterificación asistida por microondas.*** En la presente investigación, se evaluó la producción de biodiesel a partir de aceites de oliva con diferentes concentraciones iniciales de ácidos grasos libres (2,5, 5,0 y 10,0%). Se comparó un proceso de esterificación en dos etapas catalizada con ácido y transesterificación catalizada alcalina (ACT) usando microondas con el método de calentamiento tradicional. Los ácidos grasos libres se redujeron a menos del 2,0% en la primera etapa. Aunque no se observaron diferencias significativas entre los métodos de esterificación, por microondas y tradicional, en términos de reducción de ácidos grasos, sin embargo, el microondas disminuyó significativamente el tiempo de reacción en un 92,5%. La comparación de los resultados de ACT de microondas con los del método de calentamiento tradicional mostró que el microondas puede aumentar significativamente el rendimiento y la pureza del éster metílico, y simultáneamente disminuir el tiempo de reacción. Las constantes físicas de los ésteres metílicos también se mejoraron usando el método de calentamiento por microondas. Por lo tanto, el método de calentamiento por microondas puede considerarse como un método eficiente en lugar de la producción de biodiésel en dos etapas. Este método es capaz de usar aceite de oliva no comestible con altas concentraciones de ácidos grasos libres.

PALABRAS CLAVE: *Aceite de oliva; Biodiesel; Esterificación; Microonda; Transesterificación*

Citation/Cómo citar este artículo: Dehghan L, Golmakani M-T, Hosseini SMH. 2021. Improving biodiesel yield from pre-esterified inedible olive oil using microwave-assisted transesterification method. *Grasas Aceites* 72 (3), e417. https://doi.org/10.3989/gya.0336201

1. INTRODUCTION

Biodiesel or fatty acid alkyl ester is produced via transesterification, which is the reaction of triacylglycerol with an alcohol using an appropriate catalyst. Normally, transesterification is an alkaline-catalyzed reaction which is 4000 times faster than an acid-catalyzed reaction (Fukuda *et al.,* 2001). The cost of biodiesel production is one of the main constituents which can be decreased by choosing waste oils as the source of feedstock (Jaliliannosrati *et al.,* 2013). Meher *et al.* (2006) investigated the alkaline-catalyzed transesterification of karanja (*Pongamia pinnata*) oil. They showed that biodiesel yield decreased from 96 to 6.1% by increasing the free fatty acid (FFA) concentration from 0.48 to 5.75%. Therefore, in order to complete the alkaline-catalyzed reaction, a FFA value of lower than 3% is needed. The high amounts of FFAs in biodiesel feedstocks make them unsuitable for alkaline-catalyzed transesterification due to the soap formation between FFAs and the alkaline catalyst (Vicente *et al.,* 2004). Soap decreases the reaction yield and acts as a surfactant between the two final immiscible products (methyl ester and glycerol), making downstream separation more difficult and leading to an increase in biodiesel viscosity and purification costs (Mazubert *et al.,* 2014; Sarantopoulos *et al.,* 2014). A similar explanation has been reported in the study by Thoai *et al.* (2017) on the transesterification of refined palm oil. They showed that by increasing soap concentration from 1.48 to 3.21%, biodiesel purity decreased from 98 to 85%. In addition to soap, water is also another product of saponification. When water is present in the reaction, it generally manifests itself through excessive soap production. Park *et al.* (2016) investigated the transesterification of wet coffee grounds. They noted that by increasing water from 20 to 80%, biodiesel yield decreased from about 98 to less than 40%. Also, soaps of saturated fatty acids tend to solidify at ambient temperatures. Consequently, a reaction mixture with excessive soap may gel and form a semi-solid mass which is very difficult to recover (Van Gerpen *et al.,* 2004).

Olive oil (OO) has been playing an important role in the world market of vegetable oils. The annual worldwide production of virgin OO was 3,050,390 tonnes in 2014, with Spain as its main producer (57% of the global production; 1,738,600 tonnes/year) (FAOSTAT, 2014). In fact, in Spain, edible vegetable oil consumption is approximately 600,000 tonnes/year. Most of this oil (70%) is OO and is primarily used for deep frying. According to the INE (Spanish National Institute of Statistics), about 74,000 tonnes of waste OO is collected per year. In this sense, the transesterification of waste OO for producing biodiesel could decrease the waste disposal problem. Although several approaches have been developed to produce biodiesel from vegetable oils and animal fats, research concerning biodiesel production from waste OO is limited and further research is needed. Due to the presence of moisture and hydrolytic enzymes, the FFA concentration in the waste OO rises rapidly (Shahidi, 2005). Dorado *et al.* (2003) and Yuste and Dorado (2006) investigated the transesterification of waste OO for biodiesel production using a conventional heating method. Waste OO with high FFA is inedible and its refining is costly. Therefore, this high free fatty acid olive oil (HFFAOO) is economically suitable for biodiesel production. Due to undesirable outcomes, HFFAOO needs to be pre-treated before transesterification. Kara *et al.* (2017) applied an acid-catalyzed esterification pre-treatment for reducing high FFA concentrations in waste fish oil from 28 to less than 1.5%. The pre-treated oil is then transformed using alkaline-catalyzed transesterification (Sarantopoulos *et al.,* 2014).

Several heating methods have been investigated for biodiesel production. In conventional heating methods, heat energy is transferred to the raw material by convection and conduction from the hot surface of the reactor, which requires a long time and large amounts of energy (Talebian-Kiakalaieh *et al.,* 2013). Microwave radiation is a novel heating method which can be used for a large number of chemical reactions such as esterification and transesterification (Talebian-Kiakalaieh *et al.,* 2013). Generally, two mechanisms of dipolar rotation and ionic conduction have been introduced for the interaction between microwave energy and raw materials. Polar materials such as methanol can absorb microwave radiation and the ionic molecules, such as KOH, can be divided into positive and negative ions. At the same time, the probability of molecular encounters increases by accelerating the molecular/ionic movement which leads to an increased reaction rate (Sajjadi *et al.,* 2014). Lin and Chen (2017) transesterified Jatropha oil and showed that for obtaining biodiesel purity

higher than 90%, microwave requires just 10 seconds while the conventional hot plate requires 1 hour. Also, energy consumptions of conventional hot plate and microwave heating methods were 2376 and 9.5 kJ, respectively.

Even though some studies have proposed a two-step reaction of acid-catalyzed esterification followed by alkaline-catalyzed transesterification for biodiesel production, none of them is based on comparison between different heating methods in both steps. Therefore, the aim of the present study was to use a microwave heating method for esterification of OO with different initial FFA concentrations followed by its transesterification and to compare it with the conventional magnetic stirrer method. Purity, yield, physical properties, and composition of the fatty acid methyl esters (FAMEs) produced were also compared.

2. MATERIALS AND METHODS

2.1. Materials

All experimental chemicals (solvents, reagents, and standards) were of analytical grade and were purchased from Merck (Darmstadt, Germany) and Sigma–Aldrich (St. Louis, MO). Crude OO mill (three-phase centrifuge) was supplied from Etka Oil Company (Rudbar, Iran).

2.2. Methods

2.2.1. Acid-catalyzed esterification

Microwave-assisted esterification (MAE) was carried out with sulfuric acid (10%, w/w H_2SO_4/FFA) as catalyst. The catalyst was dissolved in methanol (methanol to FFA mole ratio of 40) and was stirred for 5 min to ensure complete mixing. According to the American Oil Chemists' Society (AOCS) Official Method (Ca 5a-40), FFA of OO was 2.36% which increased to 2.5, 5.0, and 10.0% by pure oleic acid (AOCS, 2000). The catalyst–methanol solution was mixed with 100 g high FFA OO. The reaction was carried out for 9 min in a domestic microwave oven (ME3410W, Samsung Malaysia Electronics, Kuala Lumpur, Malaysia) at 500 W with a wave frequency of 2450 MHz, equipped with a condenser (to condense back the methanol escaping from the reaction mixture). Also, the magnetic stirrer operated at 60 ºC for 120 min at 600 rpm as a conventional-assisted esterification (CAE). At the end of the reaction time, the reaction mixture was immediately cooled down to room temperature. The water-soluble components were separated from the product in a separatory funnel. The esterification yield was calculated according to the following equation (Chai *et al.,* 2014):

$$\text{Esterification yield (\%)} = ((\text{initial FFA} - \text{final FFA}) / \text{initial FFA}) \times 100 \quad \text{eq. (1)}$$

2.2.2. Alkaline-catalyzed transesterification

KOH was dissolved in methanol and the mixture was stirred for 10 min to ensure complete mixing. Then, the catalyst-methanol solution was mixed with 100 g esterified HFFAOO. The reaction was carried out using the microwave oven and the conventional magnetic stirrer.

Microwave-assisted transesterification (MAT) of esterified HFFAOO was carried out at 500 W, methanol-to-oil mole ratio of 9, KOH concentration of 1.2%, and reaction time of 9 min. Conventional-assisted transesterification (CAT) was performed using a magnetic stirrer at 60 ºC for 120 min at 600 rpm. To evaluate the effect of esterification pre-treatment on transesterification yield, OO samples (with 2.5, 5.0, and 10.0% FFA) were also transesterified without esterification pre-treatment.

At the end of the reaction time, the reaction mixture was immediately cooled down to room temperature and transferred to a separating funnel where it was left overnight to separate into two phases. The crude methyl ester remained in the upper phase, while the catalyst and unreacted methanol were situated in the lower glycerol phase, meaning that small amounts of catalyst, methanol, and glycerol were present in the upper phase. The excess methanol in the ester phase was distilled off with a magnetic stirrer equipped with a condenser at 70 ºC for 30 min at 450 rpm. Hot distilled water (60 ºC) was sprayed over the surface of ester phase to remove the impurities and catalyst. Washing was performed 5 times to remove all dissolved catalysts and glycerol in the ester phase. The lower phase was discarded and a yellow-colored phase containing FAMEs was finally isolated. FAMEs were then dried using a magnetic stirrer at 80 ºC for 30 min at 250 rpm (Kanitkar *et al.,* 2011; Patil *et al.,* 2011). Margaric acid methyl ester (Methyl margarate; Methyl heptadecanoate) was added to the crude

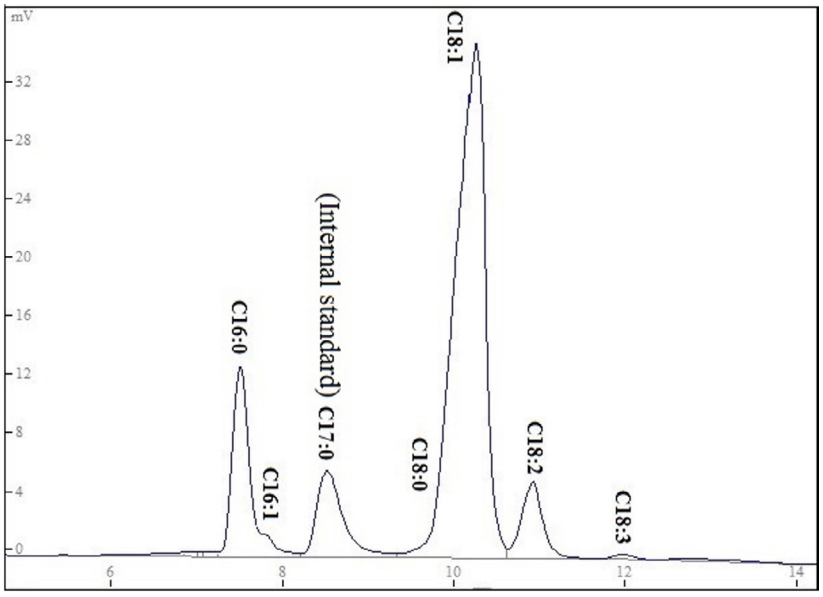

FIGURE 1. Chromatogram of microwave-assisted transesterified inedible olive oil.

FAMEs as an internal standard (Figure 1) (Atapour and Kariminia, 2011). The purity of FAMEs was determined using the GC/FID method according to the method described by Golmakani *et al.,* (2012a; 2012b). The weight of yield, methyl ester purity, and final yield were calculated according to the following equations (Patil *et al.,* 2011; Hsiao *et al.,* 2010):

Weight of yield (%) = ((Weight of final product (g)) / (Weight of olive oil (g)))×100 eq. (2)

Methyl ester purity (%) = ((Area of final product) / (Area of internal standard))×((Weight of internal standard(g)) / (Weight of final product(g)))×100 eq. (3)

Final yield (%) = ((Methyl ester purity (%) × Weight of yield (%)) / 100) eq. (4)

2.2.3. Physical properties of FAME

Kinematic viscosity, refractive index, and density of purified FAMEs were analyzed according to the method of the American Society for Testing Materials (ASTM; D445), AOCS Cc7-25 Official Method, and AOCS 1a-64 Official Method, respectively (AOCS, 2000; ASTM, 2013). The fatty acid composition of FAMEs was determined according to the method described by Golmakani *et al.,* (2012a; 2012b). Color attributes (L*, lightness; a*, greenness to redness; b*, blueness to yellowness) of FAMEs were analyzed using the Habibi *et al.* (2016) method.

2.2.4. Statistical analysis

All experiments were performed in triplicate and the data were reported as mean values of the measurements. Standard deviation values are presented in all tables. A general linear model (GLM) procedure from SAS (Statistical Analysis Software, version 9.1; SAS Institute Inc. Cary, NC) was used for comparison of mean values.

3. RESULTS

3.1. Esterification yield

The effects of initial FFA concentration and esterification method on the esterification yield of HFFAOO are shown in Table 1. The highest esterification yield was obtained for 2.5% initial FFA (i.e. final FFA of lower than 0.5%). Although there were no significant differences between the esterification yield of HFFAOO with 5.0% FFA and that of 10.0%, their esterification yields were lower than that of the sample with 2.5% FFA. Also, despite the fact that there were no significant differences between MAE and CAE methods in terms of final FFA concentration and esterification yield, MAE entailed significantly lower esterification duration and energy consumption. Microwaves heat methanol selectively which may lead to the rapid formation of microzones (hot spots) with temperatures much higher than that of

Table 1. Effect of microwave heating method on esterification yield of high free fatty acid olive oil

Initial free fatty acid concentration	Esterification method	Final free fatty acid concentration	Esterification yield (%)
2.5	Conventional	0.47±0.02c*	81.44±0.79a
2.5	Microwave	0.45±0.01c	82.00±0.36a
5	Conventional	1.01±0.01b	80.10±0.03b
5	Microwave	1.01±0.01b	80.08±0.06b
10	Conventional	2.06±0.08a	79.48±0.50b
10	Microwave	1.98±0.04a	80.27±0.38b

* Mean ± standard deviation; Number of replicates for each analysis: 3; Statistical test: ANOVA and multiple comparison of means using Duncan's test; Degree of significance: $P < 0.05$; In each column, means with different letters are significantly different.

Table 2. Effect of different esterification and transesterification methods on weight of yield, purity, and final yield of olive oil biodiesel

Initial free fatty acid concentration	Esterification method	Transesterification method	Weight of yield (%)	Purity (%)	Final yield (%)
2.5	WEP*	Conventional	82.36±0.03m**	96.03±0.03d	79.09±0.06i
2.5	WEP	Microwave	85.72±0.01l	97.86±0.18c	83.88±0.17f
2.5	Conventional	Conventional	93.15±0.01g	89.33±0.76e	83.21±0.71g
2.5	Conventional	Microwave	98.57±0.05b	99.94±0.03a	98.50±0.08a
2.5	Microwave	Conventional	93.36±0.01f	89.77±0.25e	83.81±0.22fg
2.5	Microwave	Microwave	98.98±0.03a	99.94±0.03a	98.93±0.00a
5	WEP	Conventional	68.32±0.03o	2.92±0.07i	2.00±0.05k
5	WEP	Microwave	76.72±0.01n	3.18±0.08i	2.44±0.06k
5	Conventional	Conventional	92.08±0.04i	87.90±1.08fg	80.94±0.96h
5	Conventional	Microwave	96.51±0.01d	99.82±0.03a	96.33±0.03c
5	Microwave	Conventional	92.27±0.03h	88.24±0.24f	81.42±0.24h
5	Microwave	Microwave	97.60±0.02c	99.90±0.01a	97.50±0.03b
10	WEP	Conventional	44.06±0.01q	0.65±0.02j	0.28±0.01l
10	WEP	Microwave	52.33±0.01p	0.68±0.02j	0.36±0.01l
10	Conventional	Conventional	89.08±0.05k	87.07±0.05h	77.55±0.00j
10	Conventional	Microwave	95.37±0.01e	98.62±0.13b	94.05±0.14e
10	Microwave	Conventional	90.13±0.03j	87.24±0.13hg	78.63±0.15i
10	Microwave	Microwave	96.46±0.04d	98.90±0.01b	95.40±0.05d

* WEP: Without Esterification pre-treatment; ** Mean ± standard deviation; Number of replicates for each analysis: 3; Statistical test: ANOVA and multiple comparison of means using Duncan's test; Degree of significance: $P < 0.05$; In each column, means with different letters are significantly different.

the reaction mixture, thus providing enough energy for increasing the esterification rate (Sajjadi *et al.,* 2014). Unlike microwave, the conventional heating method heats the entire reaction mixture (both methanol and OO), leading to longer reaction time and higher energy consumption (Kumar *et al.,* 2011). These findings are in good agreement with the results of Suppalakpanya *et al.* (2010), who produced ethyl ester from crude palm oil. They showed that MAE and CAE methods reduced FFA concentration from 7.5 to less than 2% after reaction times of 60 and 240 min, respectively.

3.2. Transesterification yield

The effects of different initial FFA concentrations and transesterification methods on weight of yield, purity, and final yield of HFFAOO are shown in

Table 2. The weight of yield, purity, and final yield of transesterified HFFAOOs without esterification were significantly lower than those of esterified ones. The final yield of HFFAOOs with 2.5, 5.0, and 10.0% FFA were 81.48, 2.22, and 0.32%, respectively. There were no significant differences between the final yield of OO with 5.0 and 10.0% FFA. In view of the fact that high initial FFA concentration increases the saponification reaction, esterification pre-treatment plays a key role in increasing transesterification purity and yield. MAT significantly increased the final yield of OO with 2.5% FFA in comparison with that from the CAT method.

In the case of esterified samples (both CAT and MAT methods), the weight of yield, purity, and final yield of FAMEs decreased by increasing the initial FFA concentration. Higher initial FFA concentration leads to increasing soap formation, which resulted in decreasing biodiesel purity and yield.

The highest final yield was obtained using the microwave heating method both in the esterification and transesterification steps. Also, the lowest final yield was obtained using the conventional heating method in both the esterification and transesterification steps. MAT showed higher weight of yield, purity, and final yield in comparison with the CAT method. Microwave radiation can selectively heat polar molecules (alcohols) without significantly heating non-polar molecules (triacylglycerols), which promotes transesterification rate and hence improves the yield and purity of FAMEs. In the conventional heating method, energy is transferred to the reaction mixture through convention and conduction only, which requires a long time and large amounts of energy (Wahidin *et al*., 2014). Similar to our results, Wahidin *et al.* (2014) investigated the effects of MAT on the biodiesel yield of microalgal *Nannochloropsis oculata* oil. They reported that the final yield of MAT (86.41%) was higher than that of the conventional water bath method (71.26%).

3.3. FAME analysis

3.3.1. Fatty acid composition

The effect of different esterification and transesterification methods on the fatty acid composition of the biodiesel produced are shown in Table 3. There were no significant differences among the fatty acid compositions of different initial FFA concentrations or different esterification and transesterification methods. Therefore, transesterification rate is not dependent on the chain length or saturation degree of fatty acids. This phenomenon can be related to the speed and completeness of the transesterification reaction. In contrast to our finding, Stavarache *et al.* (2007) noted that saturated fatty acids, which are commonly located in the 1 and 3 positions of triacylglycerols, had a higher transesterification rate.

3.3.2. Physical properties of transesterified samples

The effect of different esterification and transesterification methods on the physical properties of the biodiesel produced are shown in Table 4. The kinematic viscosity of FAME is one of the most important properties which can affect storage condition, transportation, and biodiesel operation. HFFAOO samples transesterified without esterification had higher kinematic viscosity than those of esterified samples (both CAT and MAT methods). The kinematic viscosity of unesterified samples with 5.0 and 10.0% FFA after transesterification was similar to untreated OO (i.e. without esterification and transesterification; 36.806 mm^2/s). This phenomenon can be related to the fact that although most triacylglycerols participated in the saponification reaction instead of transesterification, transesterification was not affected by saponification in the case of OO with 2.5% FFA. Also, in spite of the fact that the transesterification method had no significant effect on kinematic viscosity, the MAT of OO with 2.5% FFA had significantly higher kinematic viscosity than the CAT method.

According to ASTM D6751 Official Methods, the kinematic viscosity of FAMEs should be 1.9-6 mm^2/s. Except for the FAMEs of OO with 5.0 and 10.0% FFA transesterified without esterification, all the FAMEs fall within the standard range indicated by ASTM.

In the case of esterified samples, MAT samples had lower kinematic viscosity than those of the CAT method. By increasing the initial FFA concentration from 2.5 to 10.0%, the kinematic viscosity of FAMEs increased due to soap formation. There was a significant negative correlation between kinematic viscosity and final yield (R^2 = 0.972; kinematic viscosity = (-0.065 × Final yield) + 10.413). During the transesterification process, triacylglycerols are converted to lower molecular weight FAMEs (Talebian-Kiakalaieh *et al.,* 2013).

TABLE 3. Effect of different esterification and transesterification methods on fatty acid composition of olive oil biodiesel

Initial free fatty acid concentration (%)	Esterification method	Transesterification method	Fatty acid (%)					
			Palmitic acid	Palmitoleic acid	Stearic acid	Oleic acid	Linoleic acid	α-Linolenic acid
2.5	WEP*	Conventional	15.53±0.05**	1.30±0.05	2.19±0.85	71.78±0.85	8.95±0.00	0.25±0.01
2.5	WEP	Microwave	15.97±0.07	1.36±0.08	1.92±0.48	71.55±0.48	8.95±0.00	0.25±0.05
2.5	Conventional	Conventional	14.54±0.00	1.37±0.00	1.94±0.00	72.03±0.00	9.65±0.00	0.47±0.00
2.5	Conventional	Microwave	15.50±0.09	1.36±0.08	1.42±0.11	72.17±0.12	9.08±0.00	0.47±0.02
2.5	Microwave	Conventional	14.65±0.03	1.26±0.03	1.94±0.00	72.03±0.00	9.65±0.00	0.47±0.00
2.5	Microwave	Microwave	15.60±1.02	1.36±0.16	2.40±0.18	71.56±0.96	8.63±0.63	0.45±0.03
5	WEP	Conventional	15.15±0.79	1.50±0.00	2.50±0.00	71.10±0.04	9.35±3.83	0.40±0.00
5	WEP	Microwave	15.13±0.76	1.50±0.00	2.50±0.00	72.33±0.61	8.24±8.37	0.30±0.07
5	Conventional	Conventional	15.64±0.07	1.17±0.07	1.86±0.16	72.30±0.16	8.71±0.00	0.32±0.03
5	Conventional	Microwave	15.54±0.04	1.32±0.04	1.35±0.22	72.24±0.22	9.08±0.00	0.47±0.00
5	Microwave	Conventional	15.55±0.03	1.26±0.03	1.48±0.38	72.68±0.38	8.71±0.00	0.32±0.03
5	Microwave	Microwave	15.41±0.12	1.43±0.15	2.82±0.73	71.06±0.33	8.89±0.26	0.39±0.11
10	WEP	Conventional	15.37±0.36	1.50±0.00	1.95±0.00	71.56±1.54	9.32±2.90	0.30±0.04
10	WEP	Microwave	15.22±4.82	1.20±0.00	2.00±0.00	71.97±1.50	9.21±5.31	0.40±0.02
10	Conventional	Conventional	14.65±0.01	1.26±0.01	1.30±0.46	72.70±0.45	9.62±0.00	0.47±0.08
10	Conventional	Microwave	15.54±0.04	1.32±0.04	1.35±0.22	72.24±0.22	9.08±0.00	0.47±0.00
10	Microwave	Conventional	15.58±0.01	1.44±0.01	2.27±0.92	71.05±0.92	9.37±0.00	0.29±0.03
10	Microwave	Microwave	15.42±0.08	1.44±0.08	2.02±0.40	71.58±0.40	9.07±0.00	0.47±0.06

* WEP: Without esterification pre-treatment; ** Mean ± standard deviation; Number of replicates for each analysis: 3.

TABLE 4. Effect of different esterification and transesterification methods on physical properties of olive oil biodiesel

Initial free fatty acid concentration (%)	Esterification method	Transesterification method	kinematic viscosity (mm2/s)	Density (Kg/m3)	Refractive index	Color attribute		
						L*	a*	b*
2.5	WEP**	Conventional	5.194±0.000c***	881.1685±0.0637g	1.4544±0.0001d	58.50±0.35d	-8.25±0.35cd	44.50±0.71c
2.5	WEP	Microwave	4.159±0.000f	885.1601±0.0920d	1.4531±0.0001de	60.75±0.35ab	-8.60±0.14cd	39.00±0.00de
2.5	Conventional	Conventional	5.126±0.000d	881.9488±0.0495f	1.4544±0.0001d	59.25±0.35cd	-8.60±0.14cd	43.50±0.71c
2.5	Conventional	Microwave	4.019±0.001hi	886.9658±0.0424a	1.4526±0.0001fg	61.50±0.71a	-9.25±0.35e	36.50±0.71f
2.5	Microwave	Conventional	5.018±0.001e	883.1693±0.0637e	1.4544±0.0001d	58.50±0.71d	-8.75±0.07de	42.90±0.14c
2.5	Microwave	Microwave	4.016±0.001i	886.9658±0.2404a	1.4524±0.0001g	61.50±0.71a	-9.25±0.35e	36.50±0.71f
5	WEP	Conventional	36.752±0.033b	874.5209±0.0141h	1.4629±0.0001b	56.50±0.71e	-6.65±0.21b	54.50±0.71b
5	WEP	Microwave	36.760±0.001b	874.8761±0.0212h	1.4627±0.0000b	56.55±0.07e	-6.75±0.07b	54.10±0.14b
5	Conventional	Conventional	5.127±0.000d	881.9288±0.1344g	1.4545±0.0001d	59.24±0.34cd	-8.60±0.14cd	43.50±0.71c
5	Conventional	Microwave	4.035±0.001h	887.0408±0.0212a	1.4525±0.0002g	61.50±0.71a	-9.25±0.35e	36.50±0.71f
5	Microwave	Conventional	5.118±0.000d	881.9338±0.1132f	1.4545±0.0003d	59.25±0.35cd	-8.60±0.14cd	43.50±0.71c
5	Microwave	Microwave	4.018±0.000j	887.0008±0.0071a	1.4526±0.0001fg	61.50±0.71a	-9.25±0.35e	36.50±0.71f
10	WEP	Conventional	36.798±0.000a	874.1603±0.0134i	1.4692±0.0001a	56.49±0.01e	-5.25±0.35a	56.25±0.35a
10	WEP	Microwave	36.798±0.000a	874.1898±0.0014i	1.4691±0.0001a	56.51±0.01e	-5.40±0.14a	55.75±0.35a
10	Conventional	Conventional	5.207±0.001c	881.1685±0.0637g	1.4552±0.0002c	58.50±0.71d	-8.10±0.14c	44.50±0.71c
10	Conventional	Microwave	4.106±0.000g	885.8954±0.3537c	1.4529±0.0001fe	61.05±0.07ab	-8.75±0.35de	37.90±0.14e
10	Microwave	Conventional	5.194±0.000c	881.1885±0.0637g	1.4553±0.0004c	58.50±0.71d	-8.10±0.14c	44.50±0.71c
10	Microwave	Microwave	4.104±0.000g	886.240±0.0071b	1.4529±0.0001fe	61.10±0.14ab	-8.75±0.35de	37.90±0.14e

** WEP: Without esterification pre-treatment; *** Mean ± standard deviation; Number of replicates for each analysis: 3; Statistical test: ANOVA and multiple comparison of means using Duncan's test; Degree of significance: $P < 0.05$; In each column, means with different letters are significantly different.

Hence, by increasing the biodiesel final yield, kinematic viscosity decreased accordingly. The sample with the highest final yield (98.93%) showed the lowest kinematic viscosity (4.02 mm^2/s). In both esterification and transesterification steps, the microwave heating method was more effective than the conventional heating method due to its higher yield of FAME production and accordingly lower kinematic viscosity.

For both CAT and MAT methods, HFFAOO samples transesterified without esterification had lower density in comparison with esterified samples. In the case of unesterified samples, although the transesterification method of OO with 5.0 and 10.0% FFA had no significant effect on density, microwave-assisted transesterified OO with 2.5% FFA had significantly higher density than the CAT method.

In the case of transesterified samples, the MAT of OO showed higher density than that of the CAT method. By increasing the initial FFA concentration, the densities of FAMEs were decreased. There was a significant positive correlation between density and final yield ($R^2 = 0.98$; Density = (0.299 × Final yield) + 857.720). The lower molecular weight of FAMEs in comparison with their corresponding triacylglycerols plays a key role in determining the density of the product (Motasemi and Ani, 2012). Therefore, by increasing final yield (i.e. higher production of lower molecular weight FAMEs), the density of the produced biodiesel increased. Using MAT led to higher final yield and hence density.

The refractive indices of HFFAOO samples transesterified without esterification were higher than those of esterified samples using both CAE and MAE methods. Also, different transesterification methods had no significant effect on refractive indices of OO with 2.5, 5.0, or 10.0% FFA.

In the case of esterified HFFAOOs, microwave-assisted transesterified samples had lower refractive indices. By increasing initial FFA concentration, the refractive indices of FAMEs increased. There was a significant negative correlation between refractive index and final yield ($R^2 = 0.982$; Refractive index = (-0.0001 × Final yield) + 1.465). By increasing final yield, refractive index decreased due to the conversion of triacylglycerols to lower molecular weight FAMEs. Also, microwave-assisted transesterified samples showed lower refractive indices according to their higher final yield.

Color is a qualitative parameter for evaluating the effects of the transesterification process on the biodiesel produced. HFFAOO samples transesterified without esterification had lower L*, a*, and b* values than those of esterified samples using either conventional or microwave methods. Regarding unesterified samples, although different transesterification methods of OO with 5.0 and 10.0% FFA had no significant effect on L*, a*, and b* values, microwave-assisted transesterified OO with 2.5% FFA had significantly higher L* value and lower b* value than those of the CAT method. Also, the a* value for OO with 2.5% FFA was similar in both MAT and CAT methods.

In the case of esterified samples, microwave-assisted transesterified samples had higher L* values and lower a* and b* values than those of conventional-assisted transesterified samples. Although there were no significant differences among different initial FFA concentrations in terms of L* and a* values, microwave-assisted transesterified OO with 10.0% FFA had significantly higher b* values than those of OO with 2.5 and 5.0% FFA. There was a positive correlation between the L* value and final yield ($R^2 = 0.948$; L* value = (0.152 × Final yield) + 46.597). Also, there was a negative correlation between the a* value and final yield ($R^2 = 0.803$; a* value = (-0.044 × Final yield) - 4.889) and between the b* value and final yield ($R^2 = 0.985$; b* value = (-0.4175 × Final yield) + 77.45). Therefore, although the L* value increased by increasing final yield, both a* and b* values decreased. The microwave heating method showed the highest L* value (61.50) and at the same time the lowest a* and b* values (9.25 and 36.50, respectively).

The physical properties of the FAMEs produced are meaningfully related to their transesterification final yield. Therefore, the physical properties of FAMEs can be used as reliable indices for predicting transesterification yield.

4. CONCLUSIONS

In this study, the effects of the microwave heating method on the esterification and transesterification of HFFAOO were evaluated in comparison with the conventional heating method. By increasing the initial FFA concentration, the weight of yield, purity, and final yield of FAMEs decreased significantly. Although there were no significant differences between the

yields of MAE and CAE, the MAE reaction time was significantly lower than CAE. Also, MAT significantly increased FAME yield and simultaneously decreased reaction time in comparison with the CAT method. Therefore, the microwave heating method can be introduced as a suitable alternative method for two-step biodiesel production from different vegetable oils (olive, palm, canola, soybean, safflower, sunflower, etc.). Although the number of studies on the feasibility of novel technologies (such as reactive distillation, membrane reactor, oscillatory baffled reactor, ohmic, ultrasound, etc.) for biodiesel production is significant, detailed analyses of two-step biodiesel production from high free fatty acid waste oils using novel technologies are still needed.

ACKNOWLEDGMENTS

This research project was financially supported by Shiraz University. We would like to thank the Edible Oil Industry Group of Etka Organization for providing the OO. We also thank Seyed Ali Hosseini for editing the English language version of the paper.

REFERENCES

AOCS. 2000. *Official Methods and Recommended Practices of the American Oil Chemists' Society* (5th ed.). USA, AOCS Press, Champaign, Illinois

ASTM. 2013. *Standard Specification for Biodiesel Fuel Blend Stock (B100) for Distillate Fuels*, *ASTM D6751-12*

Atapour M, Kariminia HR. 2011. Characterization and transesterification of Iranian bitter almond oil for biodiesel production. *Appl. Energy* **88**, 2377–2381. https://doi.org/10.1016/j.apenergy.2011.01.014

Chai M, Tu Q, Lu M, Yang YJ. 2014. Esterification pretreatment of free fatty acid in biodiesel production, from laboratory to industry. *Fuel Process Technol*. **125**, 106–113. https://doi.org/10.1016/j.fuproc.2014.03.025

Dorado MP, Ballesteros E, Arnal JM, Gómez J, López FJ. 2003. Exhaust emissions from a Diesel engine fueled with transesterified waste olive oil. *Fuel* **82,** 1311–1315. https://doi.org/10.1016/S0016-2361(03)00034-6

FAOSTAT. 2014. www. fao.org/faostat

Fukuda H, Kondo A, Noda H. 2001. Biodiesel fuel production by transesterification of oils. *J. Biosci. Bioeng.* **92**, 405–416. https://doi.org/10.1016/S1389-1723(01)80288-7

Golmakani M-T, Mendiola JA, Rezaei K, Ibanez E. 2012a. Expanded ethanol with CO_2 and pressurized ethyl lactate to obtain fractions enriched in γ-Linolenic Acid from *Arthrospira platensis* (Spirulina). *J. Supercrit. Fluid* **62**, 109–115. https://doi.org/10.1016/j.supflu.2011.11.026

Golmakani M-T, Rezaei K, Mazidi S, Razavi SH. 2012b. Effect of alternative C2 carbon sources on the growth, lipid, and γ-linolenic acid production of Spirulina (*Arthrospira platensis*). *Food Sci. Biotechnol*. **21**, 355–363. https://doi.org/10.1007/s10068-012-0047-8

Habibi M, Golmakani M-T, Farahnaky A, Mesbahi G, Majzoobi M. 2016. NaOH-free debittering of table olives using power ultrasound. *Food Chem*. **192**, 775–781. https://doi.org/10.1016/j.foodchem.2015.07.086

Hsiao MC, Lin CC, Chang YH, Chen LC. 2010. Ultrasonic mixing and closed microwave irradiation-assisted transesterification of soybean oil. *Fuel* **89**, 3618–3622. https://doi.org/10.1016/j.fuel.2010.07.044

Jaliliannosrati H, Amin NAS, Talebian-Kiakalaieh A, Noshadi I. 2013. Microwave assisted biodiesel production from *Jatropha curcas* L. seed by two-step in situ process: Optimization using response surface methodology. *Bioresour. Technol*. **136**, 565–573. https://doi.org/10.1016/j.biortech.2013.02.078

Kanitkar A, Balasubramanian S, Lima M, Boldor D. 2011. A critical comparison of methyl and ethyl esters production from soybean and rice bran oil in the presence of microwaves. *Bioresour. Technol*. **102**, 7896–7902. https://doi.org/10.1016/j.biortech.2011.05.091

Kara K, Ouanji F, Lotfi EM, Mahi ME, Kacimi M, Ziyad M. 2018. Biodiesel production from waste fish oil with high free fatty acid content from Moroccan fish-processing industries. *Egypt J. Pet.* **27**, 249–255. https://doi.org/10.1016/j.ejpe.2017.07.010

Kumar R, Kumar GR, Chandrashekar N. 2011. Microwave assisted alkali-catalyzed transesterification of *Pongamia pinnata* seed oil for biodiesel production. *Bioresour. Technol*. **102**, 6617–6620. https://doi.org/10.1016/j.biortech.2011.03.024

Lin J, Chen Y. 2017. Production of biodiesel by transesterification of Jatropha oil with microwave heating. *J. Taiwan Inst. Chem. E*. **75**, 43–50. https://doi.org/10.1016/j.jtice.2017.03.034

Mazubert A, Taylor C, Aubin J, Poux M. 2014. Key role of temperature monitoring in interpretation of microwave effect on transesterification and esterification reactions for biodiesel production. *Bioresour. Technol*. **161**, 270–279. https://doi.org/10.1016/j.biortech.2014.03.011

Meher LC, Kulkarni MG, Dalai AK, Na S. 2006. Transesterification of karanja (*Pongamia pinnata*) oil by solid basic catalysts. *Eur. J. Lipid Sci. Tech.* **108**, 389–397. https://doi.org/10.1002/ejlt.200500307

Motasemi F, Ani FN. 2012. A review on microwave-assisted production of biodiesel. *Renew. Sust. Energ. Rev.* **16**, 4719–4733. https://doi.org/10.1016/j.rser.2012.03.069

Park J, Kim B, Lee JW. 2016. In-situ transesterification of wet spent coffee grounds for sustainable biodiesel production. *Bioresour. Technol*. **221**, 55–60. https://doi.org/10.1016/j.biortech.2016.09.001

Patil P, Gude VG, Pinappu S, Deng S. 2011. Transesterification kinetics of *Camelina sativa* oil on metal oxide catalysts under conventional and microwave heating conditions. *Chem. Eng. J.* **168**, 1296–1300. https://doi.org/10.1016/j.cej.2011.02.030

Sajjadi B, Abdul Aziz AR, Ibrahim S. 2014. Investigation, modelling and reviewing the effective parameters in microwave-assisted transesterification. *Renew. Sust. Energ. Rev.* **37**, 762–777. https://doi.org/10.1016/j.rser.2014.05.021

Sarantopoulos I, Chatzisymeon E, Foteinis S, Tsoutsos T. 2014. Optimization of biodiesel production from waste lard by a two-step transesterification process under mild conditions. *Energy Sustain. Dev*. **23**, 110–114. https://doi.org/10.1016/j.esd.2014.08.005

Shahidi F. 2005. *Bailey's Industrial Oil and Fat Products* (6th ed.). New Jersey, USA, John Wiley and Sons Inc.Publication.

Stavarache C, Vinatoru M, Nishimura R, Maeda Y. 2007. Aspects of ultrasonically assisted transesterification of various vegetable oils with methanol. *Ultrason. Sonochem*. **14**, 380–386. https://doi.org/10.1016/j.ultsonch.2006.08.004

Suppalakpanya K, Ratanawilai S, Tongurai C. 2010. Production of ethyl ester from crude palm oil by two-step reaction with a microwave system. *Fuel* **89**, 2140–2144. https://doi.org/10.1016/j.fuel.2010.04.003

Talebian-Kiakalaieh A, Amin NAS, Mazaheri H. 2013. A review on novel processes of biodiesel production from waste cooking oil. *Appl. Energy* **104**, 683–710. https://doi.org/10.1016/j.apenergy.2012.11.061

Thoai DN, Tongurai C, Prasertsit K, Kumar A. 2017. A novel two-step transesterification process catalyzed by homogeneous base catalyst in the first step and heterogeneous acid catalyst in the second step. *Fuel Process Technol*. **168**, 97–104. https://doi.org/10.1016/j.fuproc.2017.08.014

Van Gerpen J, Shanks B, Pruszko R, Clements D, Knothe G. 2004. Biodiesel Production Technology. National Renewable Energy Laboratory. www.nrel.gov

Vicente G, Martinez M, Aracil J. 2004. Integrated biodiesel production: a comparison of different homogeneous catalysts systems. *Bioresour. Technol.* **92**, 297–305. https://doi.org/10.1016/j.biortech.2003.08.014

Wahidin S, Idris A, Muhamad Shaleh SR. 2014. Rapid biodiesel production using wet microalgae via microwave Irradiation. *Energ. Convers. Manage*. **84**, 227–233. https://doi.org/10.1016/j.enconman.2014.04.034

Yuste AJ, Dorado MP.2006. A neural network approach to simulate biodiesel production from waste olive oil. *Energ. Fuel.* **20**, 399-402. https://doi.org/10.1021/ef050226t

GRASAS Y ACEITES 72 (3)
July-September 2021, e418
ISSN-L: 0017-3495
https://doi.org/10.3989/gya.0552201

Chemical and physical properties of fats produced by chemical interesterification of tallow with vegetable oils

A.B. Aktas[a] and B. Ozen[b,] ✉

[a]Cumhuriyet University, Department of Food Engineering, Sivas, Turkey,
[b]Izmir Institute of Technology, Department of Food Engineering, Urla-Izmir, Turkey.
✉Corresponding author: banuozen@iyte.edu.tr

Submitted: 05 May 2020; Accepted: 12 June 2020; Published online: 15 September 2021

SUMMARY: This study aims at manufacturing structured lipids by chemical interesterification (CI) of beef tallow with corn, canola and safflower oils individually at various tallow blend ratios (60, 70, 80%) and catalyst concentrations (0.75, 0.875, 1%). Several physical and chemical properties of interesterified products were determined and data were analyzed using univariate and multivariate statistical techniques. Interesterified lipids were more spreadable and showed plastic behavior due to their lower consistency and solid fat contents. Decreases in melting points to a temperature range of 26.5-45.5 °C regardless of oil type were observed. Interesterified fats displayed mostly β' and β'+β crystal forms. The CI of tallow did not result in the formation of significant amounts of *trans*-fatty acids. Samples interesterified with corn oil had lower free fatty acid contents (1.87-3.9%) and higher oxidation induction times (3.82-12.25h) than other lipids. Therefore, fats containing corn oil-tallow could be used in the baking industry due to their potentially good aeration properties and smooth texture.

KEYWORDS: *Chemical interesterification; Chemical properties; Physical properties; Tallow; Vegetable oils*

RESUMEN: ***Propiedades químicas y físicas de las grasas producidas mediante interesterificación química de sebo con aceites vegetales.*** Este estudio tiene como objetivo la fabricación de lípidos estructurados mediante interesterificación química (IQ) de sebo de res con aceites de maíz, canola y cártamo individualmente en varias relaciones de la mezcla (60% -70% -80%) y concentraciones de catalizador (0,75, 0,875, 1%). Se determinaron varias propiedades físicas y químicas de los productos interesterificados y los datos se analizaron con técnicas estadísticas univariante y multivariantes. Los lípidos interesterificados son más extensibles y tienen un comportamiento plástico debido a su menor consistencia y contenido de grasa sólida. Se observaron disminuciones en los puntos de fusión a un rango de temperatura de 26,5-45,5 °C, independientemente del tipo de aceite. Las grasas interesterificadas muestran principalmente formas cristalinas β 'y β' + β. La IQ de sebo no dio lugar a la formación de cantidades significativas de ácidos grasos *trans*. Las muestras interesterificadas con aceite de maíz tienen un contenido de ácidos grasos libres más bajo (1,87-3,9%) y tiempos de inducción de oxidación más altos (3,82-12,25 h) que otros lípidos. Por lo tanto, las grasas que contienen sebo-aceite de maíz podrían usarse en la industria de la panadería debido a sus posibles buenas propiedades de aireación y textura suave.

PALABRAS CLAVE: *Aceites vegetales; Interesterificación química; Propiedades físicas; Propiedades químicas; Sebo*

Citation/Cómo citar este artículo: Aktas AB, Ozen B. 2021. Chemical and physical properties of fats produced with chemical interesterification of tallow with vegetable oils. *Grasas Aceites* 72 (3), e418. https://doi.org/10.3989/gya.0552201

1. INTRODUCTION

Fats and oils are significant ingredients in food products due to their nutritional and functional properties. The fatty acid compositions, fatty acid distributions, and saturated/unsaturated fatty acids ratio, melting points, crystallization behaviors, storage stabilities, nutritional values, and health-promoting effects of fats and oils vary because of factors such as raw material sources, processing type and conditions and some naturally present fats and oils are not always suitable for food processes due to their properties. Appropriate modifications could be carried out to add desirable characteristics to the lipids so that they can be available to be used in a wider spectrum (Martin *et al.,* 2010; Segura and Jachmanián, 2020). One of these modification techniques is the well-known chemical interesterification method which provides new chemical and physical properties to lipids by altering their triacylglycerol composition, therefore changing the crystal morphology of the lipids (Riberio *et al.,* 2009; Zhu *et al.,* 2019). Chemical interesterification is carried out by the breaking of fatty acid groups from the mixture of fats and a random re-esterification onto the glycerol backbone. The reaction is catalyzed by alkali metals or alkali metal alkylates at high temperatures under vacuum (Zhang *et al.,* 2019). There are various applications for chemical interesterification process in the literature which have been used to improve the properties of several fats (Naeli *et al.,* 2017; Oliveria *et al.,* 2017; Tourchi *et al.,* 2019).

Beef tallow is one of the important by-products of the meat industry. It has limited commercial use due to its hard structure, high melting point and low levels of polyunsaturated fatty acids (PUFA); therefore, modifications are needed to widen its application area. Chemical interesterification can be applied to provide desirable characteristics to the tallow (Kowalska *et al.,* 2005; Zhang *et al.,* 2018). In a study on the chemical interesterification of tallow with sunflower oil, it was observed that the ratio of tallow in the blend, catalyst concentration, and reaction temperature had significant effects on the melting point of the product (Rodriguez *et al.*, 2001). Interesterified fats produced with beef tallow and rapeseed oil have higher free fatty acid, monoacylgycerol and diacylglycerol contents, and shorter oxidation induction times than a non-esterified blend (Kowalska *et al.*, 2007; Kowalski *et al.*, 2004). The solid fat content of the structured lipids produced by the chemical interesterification of beef tallow with canola oil decreased to the desired levels compared to the physical blends and these products consisted mainly of the β' polymorphic form together with a small content of β form (Meng *et al.,* 2010).

As a by-product of the meat indusrty, tallow, having limited usage in food applications due to its properties, could benefit from interesterification by widening its applications in the food industry; however, there are a few studies in the literature about this. To the best of our knowledge, safflower and corn oils have not been used together with tallow to modify the properties of this fat. Depending on compositional factors, different types of fat/oil blends in general result in fats having different physical and chemical properties after chemical interesterification. In this study, beef tallow with high saturated fatty acid content was blended with various vegetable oils with high monounsaturated (canola oil) and polyunsaturated (safflower and corn oils) fatty acids. With this study, it is intended to compare several important properties of fats produced through chemical interesterification of tallow together with three different oils which are easily available and economical. The present study has a purpose to modify several chemical and physical properties of tallow blended with corn, canola and safflower oils individually through the chemical interesterification process. In addition, it is also aimed to evaluate the effects of the oil types, the blend ratios and the catalyst concentrations on the chemical (free fatty acid content, fatty acid composition, mono, di, and triacylglycerol composition, oxidative stability) and the physical properties (solid fat content, consistency, melting point and crystal morphology) of the produced products using both univariate and multivariate statistical analysis techniques.

2. MATERIALS AND METHODS

2.1. Fat samples and reagents

Beef tallow used for chemical interesterification reactions was obtained from two different breeds of 2-year-old calves (Montafon and Holstein) immediately after slaughter and stored at -20 °C. Canola, safflower and corn oils were obtained from the local market. A sodium methoxide (CH_3NaO) catalyst (Solem Kimya, Turkey), was provided by

a local oil processing plant. All other reagents and solvents were of analytical or chromatographic grade and obtained from Sigma (Sigma-Aldrich, Germany).

2.2. Chemical interesterification process

A full factorial design was employed to evaluate the effects of catalyst concentration (0.75-0.875-1%, w/w), oil type (safflower, corn and canola oils), and tallow-to-oil blend ratio (60:40, 70:30 and 80:20, w/w) on the properties of interesterified lipids. Catalyst concentration and blend ratio were chosen according to preliminary trials and studies in the literature (Meng *et al*., 2010, Kowalski *et al*., 2004). A modified procedure from the literature was used for the chemical interesterification process (Kowalski *et al.,* 2004). Thirty different blends were prepared according to an experimental design (Table 1). An oil blend was dried under 185 mPa vacuum in a rotary evaporator (Laborato 4000 Heidolph, Germany) at 90 °C with stirring at 100 rpm for 30 min, then chemical catalyst was added at certain levels provided in the experimental design. The product was washed with 5% phosphoric acid (H_3PO_4) twice in order to inactivate sodium methoxide and re-washed with 10% NaCl to remove impurities. Product, catalyst, NaCl and phosphoric acid were separated from each other with the aid of a separation funnel. The product was then filtered through a vacuum filtration unit with 400 mm pore size filter paper (Macherey-Nagel, Düren, Germany) and washed with hot water three times to remove all residues. The structured lipid and water were also separated from each other by a separation funnel. The traces of water were evaporated under 185 mPa vacuum in the same rotary evaporator at 90 °C with stirring at 100 rpm for 30 min.

2.3. Chemical analyses of interesterified lipids

2.3.1. Free fatty acid (FFA) content

The titrimetric method specified in AOCS method Ca 5a-40 (American Oil Chemists' Society, 2017) was used for the FFA determination of the products. Acidity was expressed as percentage of oleic acid.

2.3.2. Mono- (MAG), -di-(DAG) and triacylglycerol (TAG) content determination

MAG, DAG and TAG contents of the structured lipids were determined according to the AOCS Cd11C-93 (American Oil Chemists' Society, 2017) method by column chromatography. Sample was dissolved in chloroform and transferred to the column by washing with chloroform three times. Then, 250 mL of 10, 25 and 100% (v/v) diethyl ether in petroleum ether were used for the elution of TAG, DAG and MAG fractions, respectively. The fractions were collected separately in a flask and solvents were evaporated in a rotary evaporator (Laborato 4000 Heidolph, Germany) at 50 °C. The flasks were dried until constant weight. Percentages of mass fractions were calculated for each part.

2.3.3. Oxidative stability

The oxidation induction time was determined with Rancimat apparatus (873 Biodiesel, Metrohm, Switzerland). The sample was placed inside the glass reaction vessel for the measurement. The carrier medium was deionized water and the reaction temperature was set to 120 °C for both columns with a constant 20 L/h air flow. Stability was expressed as the oxidation induction time (h).

2.3.4. Fatty acid composition

The fatty acid composition of the samples was determined after converting them into their corresponding fatty acid methyl esters (FAME) according to a procedure provided by IUPAC (1987). Chromatographic analyses were performed with a GC (Agilent 6890) equipped with an auto-sampler, a split/splittless (1:50) injector and an FID detector. An HP 88 capillary column (100 m x 0.25 mm ID x 0.2μm) was used in the analyses. Conditions for GC analysis are described in a previous study (Meng *et al.*, 2010). A 37-component mixture of FAME (Sigma) was used as the standard.

2.4. Physical analyses of interesterified lipids

2.4.1. Crystal morphology

Polymorphic forms of the fat crystals were determined with X-ray diffraction (Philips, Holland) using Cu as anode material (k = 1.54056 Å, voltage = 45 kV, tube current = 40 mA, fixed 1.0, 1.0, and 0.76-mm divergence, anti-scatter and receiving slits). Samples were scanned from 4 to 50° (2θ scale) at a rate of 2.0°/min. The analyses were performed at ambient temperature.

Table 1. Chemical properties of the structured lipids produced

Parameters				Chemical Properties[a]							
Sample	**Oil Type**	**Tallow-oil Blend ratio**	**Catalyst Conc. %**	**OS (h)**	**FFA%**	**TAG%**	**DAG+MAG%**	**MUFA%**	**PUFA%**	**SFA%**	**TFA%**
SA61	Safflower	60-40	0.75	0.71	2.42	79.91	17.55	25.89	30.65	43.46	0.67
SA62	Safflower	60-40	0.875	1.55	1.08	89.76	14.23	28.82	32.54	38.64	0.74
SA63	Safflower	60-40	1	1.12	1.68	82.75	16.59	29.35	33.78	36.87	0.72
SA71	Safflower	70-30	0.75	3.16	2.6	78.53	18.66	33.03	24.22	42.75	0.65
SA72	Safflower	70-30	0.875	2.84	3.25	84.43	15.52	31.96	25.76	42.28	0.92
SA73	Safflower	70-30	1	0.9	3.26	83.34	12.84	29.45	24.94	45.61	0.78
SA81	Safflower	80-20	0.75	1.08	1.6	76.72	16.8	34.06	18.87	47.08	0.82
SA82	Safflower	80-20	0.875	3.09	3.4	84.19	12.82	35.15	18.87	45.98	0.76
SA83	Safflower	80-20	1	2.17	3.23	81.22	17.64	34.80	19.61	45.58	0.82
SA60	Safflower	60-40	0	2.83	0.65	88.3	6.64	29.09	33.04	37.87	0.64
SA70	Safflower	70-30	0	3.17	1.31	82.37	14.4	31.65	25.78	42.57	0.60
SA80	Safflower	80-20	0	4.2	0.46	81.24	5.74	34.84	18.38	46.78	0.68
CO61	Corn	60-40	0.75	7.48	2.74	52.62	22.95	37.21	24.84	37.96	0.76
CO62	Corn	60-40	0.875	7.76	3.11	89.32	8.08	37.65	24.70	37.65	0.72
CO63	Corn	60-40	1	4.78	3.9	82.75	12.82	37.52	24.80	37.68	0.65
CO71	Corn	70-30	0.75	3.82	2.15	89.65	8.23	38.03	20.03	41.94	0.79
CO72	Corn	70-30	0.875	6.77	2.48	81.38	11.92	37.44	20.71	41.86	0.82
CO73	Corn	70-30	1	6.85	3.88	82.89	17.03	38.24	18.83	42.94	0.71
CO81	Corn	80-20	0.75	7.3	2.33	81.62	12.89	38.65	14.18	47.17	0.79
CO82	Corn	80-20	0.875	7.4	3.04	82.02	13.81	39.27	13.74	46.98	0.87
CO83	Corn	80-20	1	5.34	3.85	81.31	15.64	38.95	13.33	47.72	0.89
CO60	Corn	60-40	0	6.73	0.62	85.51	6.17	35.59	29.91	34.50	0.58
CO70	Corn	70-30	0	8.51	0.63	86.84	6.73	37.09	19.90	43.02	0.69
CO80	Corn	80-20	0	10	0.76	85.52	9.05	38.00	13.85	48.15	0.70
CP1	Corn	70-30	0.875	10.92	3.03	77.51	21.33	38.47	19.30	42.23	0.73
CP2	Corn	70-30	0.875	12.25	2.97	82.88	16.97	37.33	19.59	43.08	0.67
CP3	Corn	70-30	0.875	7.98	1.87	74.25	14.57	38.52	18.27	43.21	0.75
CA61	Canola	60-40	0.75	6.43	2.23	79.57	16.48	51.30	11.69	37.20	1.40
CA62	Canola	60-40	0.875	6.37	3.39	83.98	16	50.20	12.36	37.76	1.69
CA63	Canola	60-40	1	2.71	4.12	63.56	18.65	49.41	14.37	36.59	1.69
CA71	Canola	70-30	0.75	8.49	2.7	76.08	17.32	48.74	10.90	40.23	1.66
CA72	Canola	70-30	0.875	7.55	2.9	73.07	15.14	47.60	10.68	41.60	1.88
CA73	Canola	70-30	1	5.55	2.37	70.29	21.23	46.34	11.01	42.56	2.21
CA81	Canola	80-20	0.75	4.72	1.56	64.87	18.25	43.80	8.20	47.93	1.28
CA82	Canola	80-20	0.875	4.25	2.5	84.76	15.16	45.15	8.43	46.79	1.55
CA83	Canola	80-20	1	2.92	2.56	82.3	10.49	43.27	8.59	48.13	1.87
CA60	Canola	60-40	0	5.73	1.03	91.02	8.43	48.45	11.50	40.05	1.52
CA70	Canola	70-30	0	7.74	0.68	94.41	5	48.16	9.93	41.91	1.48
CA80	Canola	80-20	0	9.06	0.77	96.29	3.86	45.81	7.55	46.64	1.55
CA	Canola			4.51	0.09	74.87	6.11	68.21	25.35	6.43	2.53
SA	Safflower			2.04	0.23	90.36	3.72	14.74	75.35	9.91	0.39
CO	Corn			4.98	0.09	92.06	2.36	32.07	54.83	13.10	0.47
T	Tallow			4.81	1.15	97.94	1.4	38.94	3.27	57.79	0.81

[a] OS: oxidative stability, FFA: free fatty acid, TAG: triacylglycerol content, DAG: diacylglycerol content, MAG: monoacylglycerol content, MUFA: monounsaturated fatty acid, PUFA: polyunsaturated fatty acid, SFA: saturated fatty acid, TFA: *trans* fatty acid.
Standard deviations OS:1.78, FFA:0.53, TAG%:3.56, DAG%:3.04, MAG%:1.4, MUFA%:0.55, PUFA%:0.57, SFA%:0.44, TFA%:0.04 (standard deviation for each measurement is calculated from three replicates of central points in the experimental design)

2.4.2. Determination of melting point

The melting points of the structured lipids were measured with a differential scanning calorimeter (DSC, Q10 TA Instruments, Crawley, UK). All samples were conditioned at 4 °C for 24 h prior to measurements. Samples were placed in hermetically sealed aluminum pans and DSC analyses were carried out from 20 to −40 °C and from −40 to 80 °C at a scan rate of 10 °C/min with respect to an empty pan (Rodriguez *et al.,* 2001). Data analysis was performed with DSC TRIOS software (TA Instruments, Crawley, UK).

2.4.3. Consistency measurements

Sample consistency was determined with a penetration test using a 45° acrylic cone fitted to a constant speed texture analyzer (TA.XT plus, UK). Samples were conditioned at 60 °C in an oven for complete melting of the crystals. Tempering was allowed to occur for 24 h in a commercial refrigerator (4 °C), then for 24 h in an oven with controlled temperature (4, 10, 15, 25 °C). Test parameters were penetration depth of 0.4 cm with 0.2 cm/s speed for 5 s testing time (Silva *et al.,* 2009). Consistency was calculated as "yield value" (Haighton, 1959).

2.4.4. Determination of solid fat content (SFC)

The solid fat content of lipids was determined by a nuclear magnetic resonance (NMR) spectrometer (Bruker, USA) according to AOCS Official Method Cd 16b-93 (American Oil Chemists' Society, 2017). Samples were melted at 80 °C and recrystallized at 0 °C for 30 min. Then, they were stabilized for 30 min at various temperatures (10, 20, 30 and 35 °C) before measuring the liquid signal.

2.5. Data Analysis

The data were analyzed according to the univariate (ANOVA) statistical analysis technique to investigate the effects of the oil type, blend ratio and catalyst concentration on the chemical and the physical properties of the structured lipids with software (MODDE 11, MKS Umetrics, Sweeden). To investigate the effects of the same parameters, principal component analysis (PCA) was also used as the multivariate statistical analysis tool (SIMCA 14.1, MKS Umetrics, Sweeden). PCA is generally used to find a relationship between all factors and responses and can extract useful information from multivariate data. Score and loading plots are very helpful in understanding the characteristics of systems or processes. While the score plots show the positioning of the samples in different groups, the loading plot confirms the groupings of these samples by supporting with responses. R^2 and Q^2 values prove degree of fitness and predictability of the constructed models, respectively.

3. RESULTS AND DISCUSSIONS

3.1. Chemical Properties of the Interesterified Lipids

3.1.1. Free fatty acid, mono, di and triacylglycerol contents

The results from the chemical analysis of the produced interesterified samples are listed in Table 1. As can be seen from the table, the FFA content in the tallow is 1.15% while the blends without interesterification have an acidity range of 0.46-1.5%. In general, the FFA percentages of the interesterified lipids (1.08-4.12%) were higher compared to the starting blends. This result is in accordance with previous studies, where an increase in FFA content was observed after chemical interesterification (Hoshino *et al.,* 2004*;* Kowalska *et al.,* 2005). There are some fluctuations among the samples depending on the catalyst concentration; although 1% catalyst concentration led to the formation of structured lipids with higher FFA%, especially for the corn oil-tallow samples. With the increse in catalyst concentration, there would be more FFA released from TAG, DAG and MAG structures. The correlation graphic of DAG + MAG and FFA also supports this result (Figure 1). It was also reported that the higher amount of catalysts in the reaction medium caused the formation of higher amounts of FFA and MAG + DAG, and a lower TAG content (Ledochowska and Wilczynska, 1998). ANOVA was used to investigate the effects of the factors on the chemical parameters of the structured lipids (Table 2). As the ANOVA table indicated, catalyst concentration is the most important factor affecting FFA value and the use of a chemical catalyst at higher concentrations resulted in higher FFA%.

The TAG content in tallow is approximately 98% while the blends without interesterification have lower TAG% (81.24-96.29%) values (Table 1). Both blending and chemical interesterification

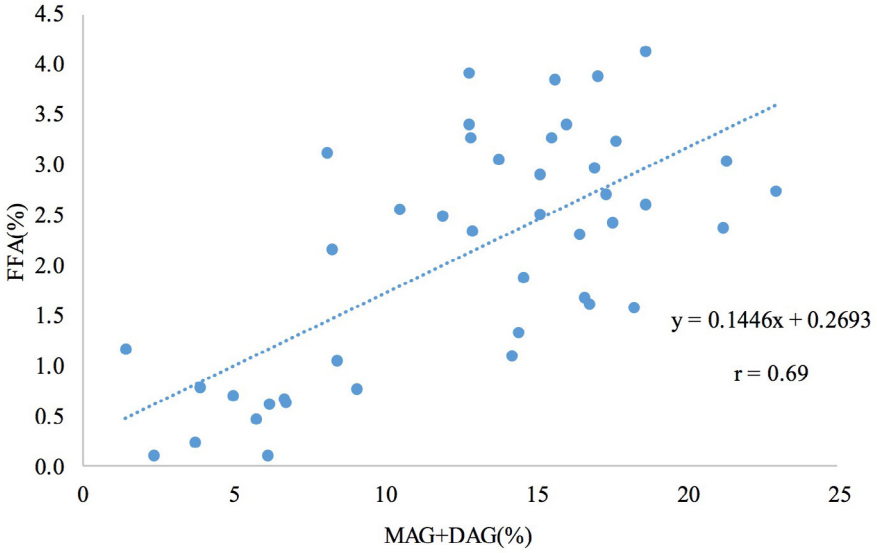

FIGURE 1. Free fatty acid content (FFA) versus monoacylglycerol and diacylglycerol contents (MAG+DAG) of structured lipids

caused an increase in MAG and DAG contents in the samples. The TAG content of the interesterfied lipids varied between 52.62-89.76% and all interesterfied fats containing canola oil had lower TAG contents compared to their starting blends. Fluctuations in TAG contents in the samples exist depending on the catalyst concentrations; although 0.875% CH_3NaO concentration mostly led to the formation of the structured lipids with higher TAG%. As expected, the structured lipids with low TAG contents had higher DAG and MAG values. A correlation between FFA and MAG + DAG contents in the interesterified lipids was evaluated in order to better understand the changes in TAG, DAG and MAG contents after the chemical interesterification reaction (Figure 1) and the 'r' value was calculated as 0.69. Although this value was not especially high, there was still an increasing trend between FFA and MAG + DAG contents in the samples. Generally, samples having higher amounts of MAG + DAG content, also have higher FFA%. Therefore, the increase in both FFA% and MAG + DAG% could be associated with the activity of the chemical catalyst that snatched the fatty acids from their original place and then random distribution of the fatty acids were provided in the TAG backbone of the newly structured lipids. According to ANOVA, models developed for DAG and MAG were significant with non-significant lack of fit at 95% confidence interval (Table 2). Examination of the significance levels of the main factors and their interactions shows that the catalyst concentration, the oil type and the blend ratio did not significantly affect the TAG% of the chemically interesterified lipids (Table 2). The ANOVA table confirms the significance of the oil type (safflower) for the model of DAG%. Generally, the structured lipids interesterified with the safflower oil have lower DAG% values compared to the samples interesterified with the other oil types. Additionally, the interaction between the oil type (safflower) and the blend ratio have some significance ($p \leq 0.05$) for the DAG content model. Oil type, particularly corn and safflower oils, and their interactions with the blend ratio have important effects on the MAG% of structured lipids. Increasing the blend ratio (increasing tallow amount in the blend) resulted in an increase in the MAG contents for corn oil; however, MAG contents decreased slightly with increasing blend ratio for the interesterified lipids with safflower oil according to the interaction plot (not shown).

3.1.2. Oxidative stability

The oxidation induction time of the tallow was 4.81 h while the non-interesterified blends showed a range of induction times from 7.98-12.25 h (Table 1). In general, the oxidation induction times of the interesterified samples decreased compared to their starting blends. Among all the samples, the tallow

interesterified with corn oil had the highest oxidation induction times (3.82-12.25 h). Varying the catalyst concentration resulted in ups and downs in the oxidative stability of the samples. However, 1% CH_3NaO concentration mostly led to the formation of structured lipids with low oxidation induction times regardless of the blend ratio. There was a drastic decrease in the oxidation induction times of the samples produced with safflower oil after the CI process compared to tallow itself. This result is in accordance with the previous studies, which also observed a decrease in oxidative stability after the chemical interesterfication of beef tallow interesterified with rapeseed oil (Hoshino *et al.,* 2004*;* Kowalska *et al.,* 2007; Kowalski *et al.,* 2004). The decrease in oxidative stability could be due to the high linoleic acid and low tocopherol content of safflower oil (240-670 mg/kg) (Codex, 2011). On the other hand, some of the tallow samples interesterified with canola oil had better oxidative stability than tallow itself. The presence of tocopherols in canola oil can be associated with longer induction times. According to the literature, canola oil could contain tocopherols up to in the range of 430-2680 mg/kg, which could have an effect on the improvement in the oxidative stability (Codex, 2011). The ANOVA table reveals that the blend ratio and the catalyst concentration were not significant for oxidative stability, meaning that neither factor affected the oxidative stability of the structured lipids (Table 2). The model showed that oil type was the only significant factor. Generally, corn oil samples have better oxidative stability compared to the other oil types while products which contain safflower oil are the least stable ones against oxidation.

3.1.3. Fatty acid composition

The major fatty acid in safflower and corn oils are linoleic acid (75.12 and 54.59%, respectively) while canola oil is rich in terms of oleic acid (57.82%), a

Table 2. ANOVA table of chemical parameters for chemically interesterified lipids

	Responses[a]								
	FFA%	**OS**	**TAG%**	**DAG%**	**MAG%**	**MUFA%**	**PUFA%**	**SFA%**	**TFA%**
p value-model	***0.02***	***0.00***	0.72	***0.08***	***0.01***	***0.00***	***0.00***	***0.00***	***0.00***
p-value-lack of fit	***0.49***	***0.80***	0.10	***0.50***	***0.86***	***0.25***	***0.97***	***0.14***	***0.11***
R^2	0.57	0.68	0.23	0.48	0.62	0.99	1.00	0.92	0.95
R^2 adj	0.38	0.54	-0.11	0.25	0.45	0.98	0.99	0.89	0.93
Q^2	-0.15	0.35	-1.38	-0.13	0.14	0.96	0.99	0.79	0.87
p value-factors									
BR[b]	0.79	0.94	0.68	0.33	0.70	0.18	***0.00***	***0.00***	0.27
CC[c]	***0.00***	0.22	0.40	0.75	0.89	0.42	***0.04***	0.70	***0.01***
OT[d]									
corn	0.14	***0.00***	0.75	0.11	***0.00***	***0.00***	***0.00***	0.87	***0.00***
canola	0.95	0.32	0.11	0.09	0.29	***0.00***	***0.00***	0.15	***0.00***
safflower	0.18	0.00	0.18	*0.00*	*0.00*	***0.00***	***0.00***	0.11	***0.00***
p-value-interactions									
BR*CC	0.36	0.64	0.87	0.55	0.22	0.69	***0.02***	0.13	0.31
BR*OT(corn)	0.80	0.95	0.37	0.07	***0.01***	0.20	***0.00***	0.42	0.40
BR*OT(canola)	***0.02***	0.41	0.99	0.86	0.62	***0.00***	***0.00***	0.07	0.27
BR*OT(safflower)	***0.01***	0.45	0.38	***0.05***	***0.04***	***0.00***	***0.00***	0.01	0.79
CC*OT(corn)	0.19	0.63	0.46	0.51	0.85	0.33	***0.00***	0.44	0.03
CC*OT(canola)	0.78	0.25	0.40	0.75	0.64	0.07	0.31	0.31	0.00
CC*OT(safflower)	0.30	0.49	0.91	0.73	0.78	0.38	0.04	0.08	0.21

[a] OS: oxidative stability, FFA: free fatty acid, TAG: triacylglycerol content, DAG: diacylglycerol content, MAG: monoacylglycerol content, MUFA: monounsaturated fatty acid, PUFA: polyunsaturated fatty acid, SFA: saturated fatty acid, TFA: *trans* fatty acid.
[b] tallow-oil blend ratio; [c] catalyst concentration; [d] oil type

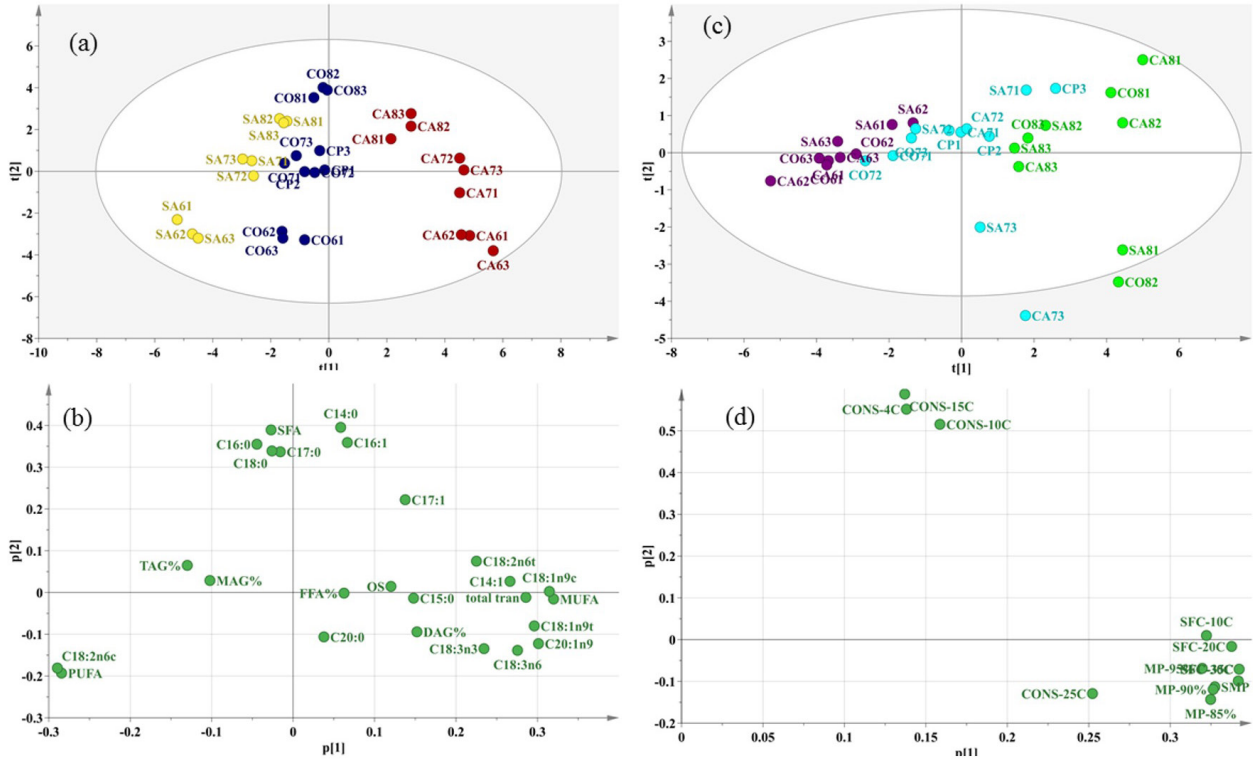

FIGURE 2. (a) Score plot (coloring is done with respect to oil types. Yellow: safflower, dark blue: corn, red: canola oils) and (b) loading plot obtained from principal component analysis for chemical parameters (c) Score plot (coloring is done with respect to tallow to oil blend ratios. Purple: 60:40, light blue: 70:30, green: 80:20) and (d) loading plot obtained with principal component analysis for physical parameters

monounsaturated fatty acid. The main fatty acids in tallow, on the other hand, are palmitic (22.50%), stearic (32.10%) and oleic (36.20%) acids. The MUFA, PUFA and SFA contents in the blends of interesterified products were in the ranges as determined by their blend ratio and intial compositions of tallow and oils without any significant changes as expected and this was also confirmed by ANOVA (Table 1). As in previous studies (Meng *et al*., 2011), the chemical interesterification of of tallow did not result in the formation of significant amounts of *trans* fatty acids. Generally, the amount of fatty acids in the *trans* form is less than 1%, except for samples which contain canola oil (Table 1). Safflower and corn oils themselves have *trans* fatty acid contents of less than 1% and their interesterified forms have slightly higher percentages of *trans* fats. Canola oil used in blending with tallow, on the other hand, has a higher content of *trans* fatty acids (2.5%) compared to the other oils and the interesterified samples containing canola oil have lower *trans*-fat contents compared to the oil itself. Since high temperature treatments are applied during canola oil refining mostly in the deodorization step to eliminate the intense bad odor of this oil, higher amounts of *trans* fatty acids form during this process. The model constructed for the *trans* fatty acids of interesterified fats showed that catalyst concentration and oil type and interaction between oil type and catalyst concentration were the significant factors. Due to higher *trans* fatty acid content in canola oil itself, interesterified products containing canola oil also had higher *trans* fatty acid contents with respect to other samples and this is the reason for the differences between *trans* fatty acid contents in fats containing different oils. In addition, increasing catalyst concentration resulted in an increase in *trans* fatty acid contents in fats which contain canola oil according to statistical analysis. However, most of the products are within acceptable limits.

3.1.4. Combination of chemical parameters

Since many parameters were determined in the study, chemical data were combined and analyzed with a multivariate statistical analysis technique, principal

component analysis (PCA), to obtain a better view of the process. The model was constructed by using all measured chemical parameters with 5 principal components (PC), R^2=0.84, and Q^2=0.42. There was a clear discrimination among the samples with respect to oil type (Figure 2a). While the samples containing canola oil were located at the right part of the ellipse samples with corn oil were placed just right of the center and safflower-containing ones were further to the left. Therefore, a discrimination with respect to the first principal component (PC) was obtained for the oil type. This discrimination mostly resulted from the higher *trans* fatty acid and MUFA contents in canola oil samples as observed in the loading plot (Figure 2b). In addition, the structured lipids containing 40% safflower and corn oils were placed at the bottom part of left quartile due to their higher PUFA contents, especially linoleic acid content. Moreover, groupings among the samples with different blend ratios were observed. The samples with 80% tallow were mostly located at the top of the ellipse regardless of the oil type since they presented higher saturated fatty acid (SFA) contents (Figure 2a). The samples containing 60% tallow were in the lower part of the ellipse and 70% tallow-containing samples were placed in the middle. Therefore, a separation based on the blend ratio was also possible with respect to the second PC. As a result, multivariate analysis of the chemical data indicated that the type of oil and the blend ratio caused differences in the chemical properties of the interesterified products.

3.2. Physical Properties of the Interesterified Lipids

3.2.1. Crystal morphology

The physical properties of the samples are provided in Table 3. As far as the crystal morphology is concerned, tallow contained mixtures of β and β' forms. α forms were not found in either structured lipids nor blends. The non-interesterified blends also contained both β and β' forms together. After the chemical interesterification, β and β' forms were also mostly present together especially for the structured lipids containing safflower and corn oils. Therefore, the interesterification did not cause important changes in the polymorphic structures of the lipids produced from safflower and corn oils. This result was in accordance with previous studies related to beef tallow-palm oil interesterified fats and other similar products (Lee *et al.,* 2008*;* Meng *et al.,* 2010). In general, a lower tallow-oil blend ratio and lower catalyst concentration combination (CA61, CA62, CA71) resulted in the formation of only β crystals while a higher blend tallow-oil ratio and catalyst concentration combination (CA72, CA81, CA82, CA83) caused the formation of β' crystals alone for canola oil-containing samples (Table 3). SA83, along with CA72, CA81, CA82, and CA83 were the samples which contained only the β' polymorphic form and this crystal form is important in the baking industry due to its aeration properties and smooth texture. Therefore, these lipids can be used as alternatives for bakery fats.

3.2.2. Melting point

The melting point range of the tallow was quite high (46.5-49.5 °C) and there were small decreases in the melting points of the samples due to blending the tallow with different oils. However, after the interesterfication sharp decreases in the melting points of the structured lipids were observed regardless of the oil type. These changes in the melting points were in accordance with the results of previous studies (Meng *et al.,* 2011; Morselli Riberio *et al.,* 2017). All samples containing 60% tallow presented lower melting points regardless of the oil type. When the tallow ratio was raised from 60 to 80%, a clear increase was also observed in the melting points. The β' form of crystals has a high melting point between 17–69 °C and the melting point of β form is 32-78 °C depending on the chain length of the fatty acids (Martin *et al.,* 2010). The interesterified fats were more likely to have β and β′ crystal types together and the melting points of the samples were relevant to the melting point of the crystal types. Therefore, it was clear that polymorphic structure of the interesterified lipids was highly related to the melting points of the structured lipids. The ANOVA results for melting point (Table 4) show that the model is significant at $p < 0.05$ with non-significant lack of fit. Blend ratio had the most prominent effect on the melting points of the chemically interesterified lipids. Melting points reached maximum values when the blend ratio of tallow was 80%. Although not to the extent of blend ratio, catalyst concentration had some significance on the melting points of the structured lipids and a slight decrease in melting points was observed with increasing catalyst concentration.

TABLE 3. Physical properties of the structured lipids produced

Parameters						Physical properties							
Sample	Oil type	Tallow-oil Blend ratio	Catalyst conc. (%)	Crystal morphology	Melting point (°C)	Consistency (MPa)				Solid fat content (%)			
						4 °C	10 °C	15 °C	25 °C	10 °C	15 °C	30 °C	35°C
SA61	Safflower	60-40	0.75	β+β'	30.3-39.5	nd	nd	nd	nd	20.7	10.7	4.7	2.1
SA62	Safflower	60-40	0.875	β	26.6-35.3	37.82	3.6	nd	nd	25.3	17.7	7.9	4
SA63	Safflower	60-40	1	β+β'	26.5-35.2	nd	nd	nd	nd	20.8	10.4	4.5	1.9
SA71	Safflower	70-30	0.75	β+β'	38-45.5	48.03	12.04	9.24	nd	27.2	18.7	9.5	5.9
SA72	Safflower	70-30	0.875	β+β'	31.6-38.1	nd	nd	nd	nd	27.1	15.3	7.1	3.8
SA73	Safflower	70-30	1	β+β'	32.0-38.8	411.08	78.05	55.16	nd	29.4	17.2	7.9	4.5
SA81	Safflower	80-20	0.75	β+β'	35.8-44.5	668.9	164.73	103.09	6.79	37.5	24.6	12	7.2
SA82	Safflower	80-20	0.875	β+β'	34.6-42.4	66.57	36.81	29.38	5.8	36.6	24	11.7	6.9
SA83	Safflower	80-20	1	β'	33.8-42.7	136.04	69.51	11.11	nd	34	21.5	9.8	5.7
SA60	Safflower	60-40	0	β+β'	44.9-47.6	116.14	nd	nd	nd	33.5	22.6	12.2	8.2
SA70	Safflower	70-30	0	β+β'	45-48.2	150.92	42.13	14.88	11.63	39.2	26.6	15	9.9
SA80	Safflower	80-20	0	β+β'	39-40.7	140.36	88.02	42.81	26.02	46.6	31.6	18.11	12
CO61	Corn	60-40	0.75	β+β'	26.9-34.6	44.97	12.61	9.3	2.34	20.4	10.7	4.4	1.6
CO62	Corn	60-40	0.875	β+β'	29.8-37.6	33.21	11.97	3.46	nd	22.3	11	4.8	2
CO63	Corn	60-40	1	β	28.8-35.5	19.93	4.22	nd	nd	20.6	9.8	4	1.6
CO71	Corn	70-30	0.75	β+β'	31.2-38.3	76.22	30.23	9.5	6.54	22	12	5.2	2.8
CO72	Corn	70-30	0.875	β+β'	29.8-36.8	76.14	35.27	6.34	2.08	20.8	10.4	4.5	1.9
CO73	Corn	70-30	1	β+β'	31.9-38.2	28.73	14.81	nd	nd	29.2	15.9	7.3	3.6
CO81	Corn	80-20	0.75	β	38.5-42.5	127.13	53.43	10.38	25.01	39.8	26.1	12.6	7.2
CO82	Corn	80-20	0.875	β+β'	35.7-43.2	302.19	339.4	105.96	5.16	38.9	26.1	12.4	7
CO83	Corn	80-20	1	β+β'	34.3-39.7	88.33	72.67	15.6	nd	35.6	23.3	11.4	6.4
CO60	Corn	60-40	0	β+β'	43.3-46.8	54.89	16.62	10.23	9.08	27.8	17.5	9.4	6.2
CO70	Corn	70-30	0	β+β'	44.4-48	97.62	70.13	26.40	9.60	40.1	26.6	15	10.1
CO80	Corn	80-20	0	β+β'	44.7-47.7	164.09	101.37	39.69	20.16	46.8	32.4	18.5	12.6
CP1	Corn	70-30	0.875	β+β'	32.7-38.9	59.44	19.44	5.5	7.03	29.3	17	7.6	4
CP2	Corn	70-30	0.875	β+β'	33.1-39.7	69.37	17.07	29.23	11.37	35.7	20.1	8.4	4.5
CP3	Corn	70-30	0.875	β+β'	37.2-44	52.51	28.23	9.1	8.49	27.7	20.2	10.7	6.5
CA61	Canola	60-40	0.75	β	26.5-34.0	55.94	11.81	3.23	1.52	22.9	11.1	4	1.6
CA62	Canola	60-40	0.875	β	18.2-34.3	17.46	42.18	nd	nd	18.2	8.7	3.1	0.9
CA63	Canola	60-40	1	β+β'	25.7-33.7	40.59	20.45	6.75	3.64	23.1	11.2	3.8	1.4
CA71	Canola	70-30	0.75	β	32.2-40.9	77.16	24.36	3.46	2.22	34.6	18.8	7.4	4
CA72	Canola	70-30	0.875	β'	32.1-39.7	64.13	21.78	4.43	4.23	36.5	19.5	7.6	3.9
CA73	Canola	70-30	1	β+β'	32.7-42	612.49	158.38	153.14	3.34	30.3	17.1	7.3	3.8
CA81	Canola	80-20	0.75	β'	39.1-45.3	68.42	42.75	12.73	16.12	38.1	26.7	14.2	9.3
CA82	Canola	80-20	0.875	β'	37.2-45.1	174.25	51.99	19.6	10.71	43.6	27.7	12.7	7.2
CA83	Canola	80-20	1	β'	33.8-40.1	121.97	71.5	47.15	nd	37.6	23.5	10.6	5.7
CA60	Canola	60-40	0	β+β'	41.1-46.5	61.49	35.31	13.45	10.74	33.9	22.4	12.5	8.4
CA70	Canola	70-30	0	β+β'	42.5-47	78.94	49.03	16.75	14.35	39.5	26.5	14.8	9.8
CA80	Canola	80-20	0	β+β'	44.1-47.9	159.64	91.23	32.69	22.93	47.1	31.7	18.2	12.2
T	Tallow			β+β'	46.6-49.6	385.93	224.52	87.57	69.85	51.1	42.7	24	17.3

Standard deviations Melting point: 2.18, Consistency at 4 °C:6.92, at 10 °C:4.8 at 15 °C:10.44, at 25 °C:1.80, Solid fat content at 10 °C:3.46, at 15 °C:1.49, at 30 °C:1.31, at 35 °C:1.08, nd: could not be determined. (standard deviation for each measurement is calculated from three replicates of central points in the experimental design)

3.2.3. Consistency

The consistency of all the samples decreased clearly as a function of temperature (Table 3). This result can be associated with the gradual melting of the crystals that generated more fragile crystalline networks. The same behavior was observed in previous studies (Bezerra *et al.,* 2017; Oliveria *et al.,* 2017; Silva *et al.,* 2009). The consistency of tallow (69.85-385.93 MPa) was quite higher than both the interesterified lipids and the non-interesterified blends at all temperatures (Table 3). The consistency of the blends in different proportions increased with increasing amounts of tallow in the blends. However, the interesterified lipids presented lower consistency values compared to their physical blends regardless of the oil type and the catalyst concentration. This decrease in the consistency of the interesterified lipids could be attributed to higher amounts of unsaturated fatty acid composition in all positions of (UUU) TAGs produced by interesterification. In addition, differences in polymorphic structure and aggregation behavior which led to the alteration in the structure of the fat crystal network of tallow could change the consistency (Silva *et al.,* 2009). Generally, fats with consistency of 9.8-98 MPa are considered spreadable. If the consistency is between 19.6 and 78.4 MPa products are more suitable for plastic and spreadable purposes and they are classified as very hard at above 147 MPa (Haighton, 1959). Most of the samples interesterified with canola oil could be considered as spreadable and plastic. The consistency values decreased to the levels suitable for spreadability with the increasing temperature. However, the consistency of the samples with canola oil of high blend ratio and high catalyst concentration (CA82 and CA83) were very high at 4 °C, and these lipids could be classified as hard. Moreover, these structured lipids contain β' polymorphic forms which have higher melting points. The consistency of most of the samples interesterified with safflower oil was not measurable at 25 °C; therefore, these structured lipids were viscous at ambient temperature. Moreover, the structured lipids with safflower oil had lower melting points which also explained the lower consistency values of these lipids. Interesterified samples produced with corn oil also resulted in products with mostly spreadable and plastic properties. The statistical analysis results for the consistency at all temperatures indicated that constructed models were insignificant at 4, 10 and 15 °C at $p < 0.05$ (Table 4). Although the models were found insignificant, the ANOVA table reveals that the blend ratio had an important impact on the consistency at these temperatures (Table 4). The model for consistency at 25 ºC was significant with non-significant lack of fit. The blend ratio and the catalyst concentration were the most prominent factors for this model and higher blend ratio meant higher consistency while the opposite effect was true for the catalyst concentration. In addition, oil type, especially safflower oil, highly affected the consistency of the structured lipids at 25 °C since safflower oil-containing interesterified lipids had lower consistency.

3.2.4. Solid fat content

The solid fat contents of both the interesterified lipids and the non-interesterified blends were determined over the temperature range of 10–35 °C (Table 3). As expected, it was observed that raising the temperature caused a marked decrease in solid fat content regardless of the oil type, the blend ratio or the catalyst concentration. The solid fat content profiles of non-interesterified blends in different proportions showed increasing trends with the increasing amounts of tallow in the blends. Interesterified lipids tended to have lower solid fat content values compared to their physical blends. Same trends were also observed in previous studies (Karabulut *et al.,* 2004; Meng *et al.,* 2010). A decrease in the solid fat content of the interesterified lipids could be attributed to the decreased proportion of the high-melting TAGs and médium-chain TAGs in the structured lipids. This decrease in solid fat content with respect to the increase in temperature was expected and has been reported in other studies (Bezerra *et al.,* 2017; Fauzi *et al.,* 2013; Oliveria *et al.,* 2017). In addition, the decrease in solid fat content in tallow and non-esterified blends could be associated with the alteration in the TAG structure caused by the interesesterfication and the melting temperature of crystals. However, a more plastic behavior was observed for both blends and structured lipids above 20 °C. The ANOVA table revealed that the blend ratio is the only effective factor for solid fat content in the temperature range of 10-35 °C. The solid fat content in the samples increased regardless of the oil type when the amount of tallow increased for all temperatures (Table 4).

TABLE 4. ANOVA table of physical parameters for chemically interesterified lipids

	Melting Point	Consistency			Solid Fat Content				
		4 °C	10 °C	15 °C	25 °C	10 °C	20 °C	30 °C	35 °C
p value-model	0.00	0.40	0.272	0.354	0.00	0.00	0.00	0.00	0.00
p-value-lack of fit	0.91	0.00	0.002	0.033	0.759	0.98	0.98	0.99	1.00
R^2	0.80	0.33	0.38	0.35	0.78	0.83	0.85	0.86	0.86
R^2 adj	0.71	0.03	0.10	0.06	0.68	0.75	0.79	0.80	0.80
Q^2	0.58	-0.81	-0.41	-0.64	0.47	0.68	0.73	0.75	0.75
p value-factors									
BR[a]	***0.00***	***0.04***	***0.01***	***0.04***	***0.00***	***0.00***	***0.00***	***0.00***	***0.00***
CC[b]	***0.04***	0.68	0.62	0.41	0.01	0.87	0.42	0.24	0.11
OT[c]									
corn	0.91	0.31	0.74	0.53	***0.04***	0.24	0.28	0.55	0.37
canola	0.35	0.76	0.92	0.59	0.40	***0.05***	0.41	0.73	0.66
safflower	0.41	0.52	0.68	0.96	***0.01***	0.36	0.84	0.37	0.21
p-value-interactions									
BR*CC	0.31	0.41	0.83	0.71	***0.01***	0.50	0.41	0.23	0.13
BR*OT(corn)	0.32	0.81	0.20	0.91	0.29	0.80	0.56	0.70	0.91
BR*OT(canola)	***0.04***	0.45	0.19	0.57	0.88	0.42	0.28	0.13	0.13
BR*OT(safflower)	0.28	0.32	0.99	0.65	0.23	0.30	0.10	0.06	0.11
CC*OT(corn)	0.27	0.53	0.70	0.44	***0.02***	0.58	0.55	0.32	0.25
CC*OT(canola)	0.71	0.16	0.34	0.06	0.45	0.62	0.77	0.63	0.42
CC*OT(safflower)	0.15	0.42	0.57	0.23	0.10	0.96	0.76	0.60	0.72

[a] tallow-oil blend ratio; [b] catalyst concentration; [c] oil type

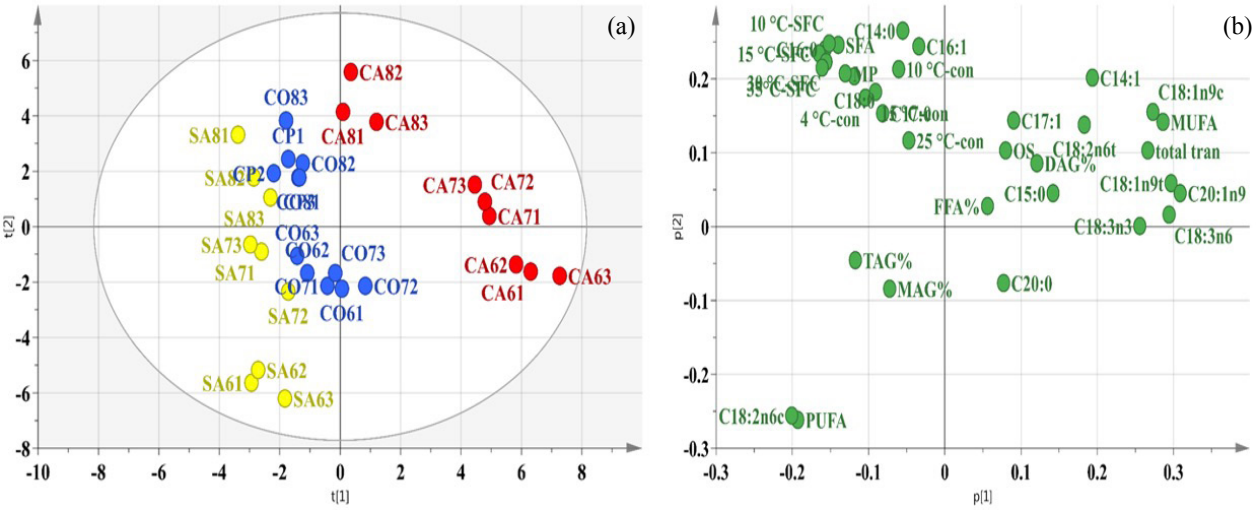

FIGURE 3. (a) Score plot (coloring is done with respect to oil types. Yellow: safflower, dark blue: corn, red: canola oils) and (b) loading plot obtained from principal component analysis for all data

3.2.5. Combination of physical and other parameters

The principal component analysis was also used to investigate the data pertaining to the physical properties of the interesterified lipids. The model was constructed by using all the measured physical parameters with 2 principal components, R^2=0.85, and Q^2=0.69. There is some discrimination among the samples with respect to the blend ratio (Figure 2c). Samples containing 60% tallow were located at the left part of the quartile while the structured lipids with 80% were placed to the right of the quartile. Samples with 70% tallow generally placed between them. Therefore, there was a rough discrimination among the samples depending

on their blend ratio as far as the physical properties are concerned. Discrimination between 60% and 80% tallow-containing samples mostly resulted from the higher solid fat contents and melting points of samples as observed in the loading plot (Figure 2d). Moreover, some of the samples with 80% and 70% tallow were grouped at the bottom of the ellipse regardless of the oil type since they had higher consistency (Figure 2d). The PCA score plot of the physical properties data did not show any separation with respect to the oil type or the catalyst concentration.

In order to better characterize chemically interesterified lipids, a PCA model was also constructed using all data including both chemical and physical properties of the 5 PCs, R^2=0.80, and Q^2=0.45. According to the score plot, there was a clear separation of the samples with respect to oil type (Figure 3a). Samples containing canola oil were located at the right part of ellipse while the interesterified fats with safflower oil were placed at the left part of ellipse. Samples containing corn oil were placed between them. Discrimination of canola oil-containing samples mostly resulted from the higher *trans* fatty acids and MUFA contents and oxidative stability of the samples as observed in the loading plot (Figure 3b). Moreover, canola oil samples were grouped together in between them with respect to their blend ratios since the amount of saturated and unsaturated fatty acids changed by increasing the ratio of tallow (Figure 3b). The interesterified lipids containing safflower oil were separated from other lipids due to their higher PUFA and MAG contents. Corn oil samples were differentiated from the rest since they had higher consistency values as the loading plot confirmed. Groupings in between the interesterified samples according to blend ratio were also observed. The results of the PCA models were in accordance with ANOVA results. Generally, the catalyst concentration did not have a remarkable effect on the chemical and physical properties of the structured lipids while blend ratio and oil type were the significant factors. Among the interesterified fats, samples produced with corn oil were discriminated from the others due to their more desirable physical and chemical properties.

4. CONCLUSIONS

Chemical interesterification served to manufacture new products from tallow in combination with vegetable oils with better spreadable and plastic behaviors. In general, the tallow-oil blend ratio was the most significant factor that affected the end product. The 1% catalyst concentration used in the process had a negative effect on the chemical properties of the structured lipids. As a first study in the literature that uses tallow and corn oil blends in chemical interesterification process, it can be concluded that interesterified lipids produced from corn oil had more desirable properties (higher oxidative stability, lower FFA%, more plastic properties) compared to products containing canola and safflower oils. Consequently, structured tallow and corn oil combinations (60-80% tallow) produced using CI with a catalyst at 0.75-0.875% levels can be particularly suggested as alternative lipid sources for the baking industry due to their possible promising aeration properties and smooth texture.

ACKNOWLEDGMENTS

This study was funded by Izmir Institute of Technology Scientific Research Projects (IYTE SRP) Program (Project No: 2017-IYTE-3)

REFERENCES

American Oil Chemists' Society. 2017. *Official Methods and Recommended Practices of the AOCS*. Urbana, IL, USA.

CODEX, S. 2011. *Codex Standard for Named Vegetable Oils. FAO/WHO, Rome, (Codex Stan 210-1999)*.

Bezerra CV, da Cruz Rodrigues AM, de Oliveira PD, da Silva DA, da Silva LHM. 2017. Technological properties of amazonian oils and fats and their applications in the food industry. *Food Chem.* **221**, 1466-1473. https://doi.org/10.1016/j.foodchem.2016.11.004

Fauzi SHM, Rashid NA, Omar Z. 2013. Effects of chemical interesterification on the physicochemical, microstructural and thermal properties of palm stearin, palm kernel oil and soybean oil blends. *Food Chem*. **137**, 8-17. https://doi.org/10.1016/j.foodchem.2012.09.086

Haighton AJ. 1959. The measurement of the hardness of margarine and fats with cone penetrometers. *J. Am. Oil Chem. Soc.* **36**, 345-348. https://doi.org/10.1007/BF02640051

Hoshina R, Endo Y, Fujimoto K. 2004. Effect of triacylglycerol structures on the thermal oxidative

stability of edible oil. *J. Am. Oil Chem. Soc.* **81**, 461-465. https://doi.org/10.1007/s11746-004-0923-6

IUPAC. 1987. *Standard Methods for Analysis of Oils, Fats and Derivatives*. Oxford, UK. https://doi.org/10.1016/C2013-0-10129-8

Karabulut I, Turan S, Ergin G. 2004. Effects of chemical interesterification on solid fat content and slip melting point of fat/oil blends. *Eur. Food Res. Technol.* **218**, 224-229. https://doi.org/10.1007/s00217-003-0847-4

Kowalska M, Bekas W, Gruczynska E, Kowalski B. 2005. Modification of beef tallow fractions by chemical and enzymatic interesterification with sunflower oil. *J. Food Technol*. **3**, 404-409.

Kowalska M, Bekas W, Kowalska D, Lobacz M, Kowalski B. 2007. Modification of beef tallow stearin by chemical and enzymatic interesterification with rapeseed oil. *Am. J. Food Technol*. **2**, 521. https://doi.org/10.3923/ajft.2007.521.528

Kowalski B, Tarnowska K, Gruczynska E, Bekas W. 2004. Chemical and enzymatic interesterification of a beef tallow and rapeseed oil equal-weight blend. *Eur. J. Lipid Sci. Technol*. **106***,* 655-664. https://doi.org/10.1002/ejlt.200400973

Ledóchowska E, Wilczyńska E. 1998. Comparison of the oxidative stability of chemically and enzymatically interesterified fats. *Lipid/Fett* **100**, 343-348. https://doi.org/10.1002/(SICI)1521-4133(199808)100:8<343::AID-LIPI343>3.0.CO;2-1

Lee JH, Akoh CC, Himmelsbach DS, Lee KT. 2008. Preparation of interesterified plastic fats from fats and oils free of *trans* fatty acid. *J. Agric. Food Chem.* **56**, 4039-4046. https://doi.org/10.1021/jf072936y

Martin D, Reglero G, Señoráns FJ. 2010. Oxidative stability of structured lipids. *Eur. Food Res. Technol.* **231***,* 635-653. https://doi.org/10.1007/s00217-010-1324-5

Meng Z, Liu Y, Shan L, Jin Q, Wang X. 2010. Reduction of graininess formation in beef tallow-based plastic fats by chemical interesterification of beef tallow and canola oil. *JAOCS* **87**, 1435-1442. https://doi.org/10.1007/s11746-010-1627-5

Meng Z, Liu YF, Jin QZ, Huang JH, Song ZH, Wang FY, Wang XG. 2011. Comparative analysis of lipid composition and thermal, polymorphic, and crystallization behaviors of granular crystals formed in beef tallow and palm oil. *J. Agric. Food Chem.* **59**, 1432-1441. https://doi.org/10.1021/jf103875f

Morselli Ribeiro MD, Ming CC, Silvestre IM, Grimaldi R, Ap G, Gonçalves L. 2017. Comparison between enzymatic and chemical interesterification of high oleic sunflower oil and fully hydrogenated soybean oil. *Eur. J. Lipid Sci. Technol.* **119**, 1500473. https://doi.org/10.1002/ejlt.201500473

Naeli MH, Farmani J, Zargaraan A. 2017. Rheological and physicochemical modification of *trans*-free blends of palm stearin and soybean oil by chemical interesterification. *J. Food Process Eng.* **40**, e12409. https://doi.org/10.1111/jfpe.12409

Oliveira PD, Rodrigues AM, Bezerra CV, Silva LH. 2017. Chemical interesterification of blends with palm stearin and patawa oil. *Food Chem.* **215**, 369-376. https://doi.org/10.1016/j.foodchem.2016.07.165

Ribeiro APB, Basso RC, Grimaldi R, Gioielli LA, dos Santos AO, Cardoso LP, Gonçalves LAG. 2009. Influence of chemical interesterification on thermal behavior, microstructure, polymorphism and crystallization properties of canola oil and fully hydrogenated cottonseed oil blends. *Food Res. Int*. **42**, 1153-1162. https://doi.org/10.1016/j.foodres.2009.05.016

Rodríguez A, Castro E, Salinas MC, López R, Miranda M. 2001. Interesterification of tallow and sunflower oil. *J. Am. Oil Chem. Soc.* **78**, 431-436. https://doi.org/10.1007/s11746-001-0280-5

Segura N, Jachmanián I. 2020. Zero-*trans* fats by enzymatic interesterification of blends beef tallow/rice bran oil. *OCL* **27** (4). https://doi.org/10.1051/ocl/2019052

Silva RC, Cotting LN, Poltronieri TP, Balcão VM, de Almeida DB, Goncalves LA, Gioielli LA. 2009. The effects of enzymatic interesterification on the physical-chemical properties of blends of lard and soybean oil. *LWT-Food Sci. Technol.* **42**, 1275-1282. https://doi.org/10.1016/j.lwt.2009.02.015

Tourchi Rudsari M, Najafian L, Shahidi SA. 2019. Effect of chemical interesterification on the physicochemical characteristics of bakery shortening produced from palm stearin and Ardeh oil (*Sesamum indicum*) blends. *J. Food Proc. Pres.* **e14101**, 1-14. https://doi.org/10.1111/jfpp.14101

Zhang Z, Shim YY, Ma X, Huang H, Wang Y. 2018. Solid fat content and bakery characteristics of interesterified beef tallow-palm mid fraction

based margarines. *RSC Adv*. **8**, 12390-12399. https://doi.org/10.1039/C8RA00769A

Zhang Z, Lee WJ, Zhou H, Wang Y. 2019. Effects of chemical interesterification on the triacylglycerols, solid fat contents and crystallization kinetics of palm oil-based fats. *Food Funct.* **10**, 7553-7564. https://doi.org/10.1039/C9FO01648A

GRASAS Y ACEITES 72 (3)
July-September 2021, e419
ISSN-L: 0017-3495
https://doi.org/10.3989/gya.0559201

Chemical parameters and antioxidant activity of turning color natural-style table olives of the Sigoise cultivar

F. Ait Chabane[a], A. Tamendjari[a], P. Rovellini[b], C. Romero[c] and E. Medina[c, ✉]

[a]Laboratoire de Biochimie Appliquée Faculté des sciences de la nature et de la vie - Université de Bejaia, 06000, Bejaia, Algeria.
[b]INNOVHUB – SSI Azienda Speciale della Camera di Commercio di Milano Area SSOG, Via Giuseppe Colombo 79, 20133, Milan, Italy.
[c]Food Biotechnology Department, Instituto de la Grasa, IG-CSIC. Crta. Utrera km 1, Ed. 46, 41013, Seville, Spain.
✉Corresponding author: emedina@ig.csic.es

Submitted: 19 May 2020; Accepted: 24 June 2020; Published online: 15 September 2021

SUMMARY: A chemical characterization of turning color table olives of the Sigoise variety was made through their processing as natural-style. Polyphenols, sugars, tocopherols, fatty acids, and antioxidant activity in the olives were monitored throughout the elaboration process. Oleuropein, salidroside, hydroxytyrosol 4-glucoside, rutin, ligustroside and verbascoside showed a decrease of 16.90–83.34%, while hydroxytyrosol increased during the first months of brining. Glucose was consumed by 90% due to the metabolism of the fermentative microbiota. The tocopherol content remained stable during the process and only the α-tocopherol decreased. The fatty acids were not affected. The loss in antioxidant compounds resulted in a decrease in the percentage of DPPH radical inhibition from 75.91% in the raw fruit to 44.20% after 150 days of brining. Therefore, the turning color natural table olives of the Sigoise variety are a good source of bioactive compounds.

KEYWORDS: *Antioxidant activity; Polyphenols; Sigoise cultivar; Sugars; Tocopherols*

RESUMEN: ***Parámetros químicos y actividad antioxidante de aceitunas de mesa al estilo natural de color cambiante de la variedad Sigoise***. La caracterización química de las aceitunas en salmuera de color cambiante de la variedad Sigoise se ha estudiado durante el proceso de elaboración, en particular la concentración de fenoles, azúcares, tocoferoles, ácidos grasos y la actividad antioxidante. La concentración de oleuropeína, salidrósido, hidroxitirosol 4-glucósido, rutina, ligustrósido y verbascósido disminuyó un 16,90–83,34% durante el primer mes en salmuera. El 90% de la glucosa fue consumida debido al metabolismo de la microbiota fermentativa. El contenido en tocoferoles se mantuvo constante durante el proceso y solo disminuyó el α-tocoferol. Los ácidos grasos no se vieron afectados. La pérdida de actividad antioxidante se tradujo en una disminución del porcentaje de inhibición del radical DPPH de un 75,91% del fruto fresco a 44,20% después de 150 días en salmuera. A pesar de todo, la aceituna color cambiante de la variedad Sigoise en salmuera es una buena fuente de compuestos bioactivos.

PALABRAS CLAVE: *Actividad antioxidante; Azúcares; Polifenoles; Tocoferoles; Variedad Sigoise*

Citation/Cómo citar este artículo: Ait Chabane F, Tamendjari A, Rovellini P, Romero C, Medina E. 2021. Chemical parameters and antioxidant activity of turning color natural-style table olives of Sigoise cultivar. *Grasas Aceites* **72** (3), e419. https://doi.org/10.3989/gya.0559201

1. INTRODUCTION

Table olives are elaborated from the fruit of olive tree (*Olea europaea* L.) and they are considered the most popular fermented vegetable in the Mediterranean countries. The production of table olives in Algeria is estimated at 293000 tons (IOC, 2020) and represents 10% of worldwide production. Olives are mainly composed of water (60-75%) and lipids (12-30%). The fruits also contain a small amount of proteins (1-2%) and sugars (2.6-6%). However, this composition depends on several factors, such as the type of cultivar and the ripening stage (Boskou *et al*., 2014). Among the minor compounds, polyphenols are the most relevant and represent the 1-3% of the fresh pulp weight. Oleuropein is the major phenolic compound and is responsible for the bitter taste, which makes the fresh fruit inedible (Kiai and Hafidi, 2014).

There are three main types of preparations which are widely used worldwide to reduce the bitterness: Spanish-style olives, Californian-style olives and natural olives or Greek-style. The two first use a diluted sodium hydroxide solution to hydrolyze the molecule of the oleuropein into non-bitter compounds and the last process consists of directly brining without using any chemicals.

Recently, there has been a growing interest in the characterization of some bioactive compounds in table olives, in particular polyphenols and tocopherols, and their relationship with the antioxidant activity which acts as a potent radical scavenger against free radicals (Sagratini *et al.*, 2013). The phenolic fraction in table olives can be influenced by many factors such as the olive cultivar (Medina *et al*., 2010), the degree of maturity (Sousa *et al*., 2014) and the de-bittering process applied (Ben Othman *et al*., 2009). Many studies have been carried out to assess the effect of the elaboration processes on these components (Bleve *et al*., 2015; Issaoui *et al*., 2011; Johnson *et al*., 2018; Romero *et al*., 2004a). The Greek-style elaboration process showed higher total phenolic compounds than the Spanish or Californian-style processes and hydroxytyrosol was the predominate compound in all three styles of commercial olives (Johnson *et al*., 2018). Greek-style processing alos better preserved the tocopherol content than the Spanish-style elaboration (Hassapidou *et al*., 1994).

Despite all these studies, only a few works have been focused on turning color table olives. Changes in the polyphenol content in the turning color Sigoise variety during naturally brined olive processing was studied (Mettouchi *et al*., 2016). It was found that turning color Manzanilla olives in brine showed more polyphenol concentration than those elaborated as Spanish-style (Romero *et al*., 2004b). The sugar and polyol compositions in natural olives at the cherry stage of ripening were studied (Marsilio *et al*., 2001), concluding that the determination of these components is important to optimize table olive processing.

According to the "Trade Standard Applying to Table Olives" (IOC, 2004), "natural olives could be "green olives, turning color or black olives placed directly in brine, where they undergo complete or partial fermentation, preserved or not by the addition of acidifying agents". The maturity of the fruit affects the phenolic concentration and may contribute to significant consequences concerning the technology and quality of table olives. The Sigoise variety, which is grown mainly in the north-west of Algeria (Sig region) is the most popular variety used in Algeria as fermented green olives (Kacem and Karem, 2006). In this work, the elaboration of turning color table olives of the Sigoise cv. according to the natural process was studied to characterize the chemical composition and evaluate changes in polyphenols, sugars, tocopherols, fatty acids and antioxidant activity.

2. MATERIALS AND METHODS

2.1. Processing and sampling

Olives of the Algerian Sigoise variety (average weight 3.5 g) were harvested at the turning color stage during the 2015-2016 season and placed in plastic tanks (30 L capacity). The olives were processed according to the natural style elaboration. An initial brine of 11% NaCl was used to cover the fruits, which were then left at ambient temperature to follow spontaneous fermentation for five months. Samples were withdrawn periodically at 60, 120 and 150 days of brining until the brine reached a pH of 4.3. Fresh fruits were also collected at the time of harvesting. Samples were stored frozen at -20 ºC until analysis.

2.2. Determination of physical properties, moisture and oil content in fruits

Fifteen olives from each sample were weighed. Length and diameter were measured using a digital calliper (150 mm (6'')) (Stainless Hardened). The

flesh/stone ratio was estimated to characterize the shape and size of the olives. The pH of the brines was monitored during the elaboration process with a pH meter (Crison Basic 20).

Fruit moisture was determined (Tovar *et al.,* 2002). Five grams of fresh pulp were desiccated at 105 °C until constant e weight.

Oil was extracted from dried olives with hexane in a Soxhlet apparatus for 6 h at 45 ºC (ECC) No 2568/91 of July (1991). The solvent was removed by a rotary evaporator, and the oil was weighed and stored at 4 ºC until further analysis. The results were expressed as percentage of dry weight.

2.3. HPLC analysis of phenolic compounds

The phenolic compounds were extracted from the olive pulp with dimethylsulfoxide (DMSO) as described by Susamci *et al*. (2017). 1.5 g of freeze-dried olive pulp were homogenized with 30 mL of DMSO and centrifuged at 6000g after 30 min of contact. Then, an aliquot of 0.25 mL of supernatant was mixed with 0.5 mL of DMSO and 0.25 mL of 0.2 mM syringic acid in DMSO (internal standard). The mixture was filtered through a 0.22 µm pore size nylon filter, and an aliquot of 20 µL was injected into the chromatograph. The analytical column, mobile phases, gradient and equipment were the same as those used by Susamci *et al.* (2017). The wavelengths selected for phenolic compounds were 280 nm.

2.4. HPLC analysis of sugars

The sugars were extracted from the olive pulp as described elsewhere (Medina *et al*., 2007) with some modifications. One gram of freeze-dried olive flesh was mixed with 20 mL of boiling water and 2 mL of sorbitol (7.5%, w/v) as internal standard, vortexed for 1 min and kept in an ultrasonic bath for 3 min. The mixture was centrifuged at 9000 g for 5 min and filtered through filter paper under vacuum into a 50 mL flask. A second extraction was repeated with another 20 mL of hot water and made up to volume. 2 mL of the filtered solution (0.22 µm pore size nylon filter) were put into contact with 1 g of the acidic resin Amberlite IR-120 plus 1 g of the basic resin Amberlite IRA-93, shaken for 30 min, and centrifuged at 9000 g for 3 min. An aliquot of 20 µL was injected into the chromatograph. The analytical column, mobile phases, gradient and equipment were the same as those used by Medina *et al*. (2007).

2.5. HPLC analysis of tocopherols

After cold extraction of the oil in a laboratory mill (Levi-Dilon-Lerogsame), the tocopherol composition was evaluated using an HPLC system, analytical column, mobile phases, gradient and equipment as described by Rovellini *et al*. (1997). The wavelengths selected for tocopherols were 292 nm. The different isomeric forms were identified by comparing other vegetable oils with typical tocopherol content distribution. The quantification was conducted using an external calibration solution of alpha-tocopherol in acetone (0.01 mg/mL).

2.6. Fatty acid composition

The fatty acid methyl esters (FAME) were prepared in a solution of 2 N methanolic potassium hydroxide according to the method described (Commission Delegated Regulation (EU) 2016/2095 of 26 September 2016 amending Regulation (EEC) No 2568/91) and analyzed by gas chromatography. An Agilent 7890 gas chromatograph (Agilent, Germany) equipped with capillary column HP88 (Agilent, Germany) 112-88177 (100 m, 0.25 mm, 0.20µm), a flame ionization detector (FID) and a split/splitless injector was used. The oven temperature was programmed as follows: from 60 °C (1 min) to 165 °C to 10 °C/min and held for 1 min; then heated to 225 at 2 °C/min and finally an isothermal was used for 25 min. Helium was used as carrier gas.

2.7. Antioxidant activity

2.7.1. Radical scavenging activity of methanolic extracts against DPPH radical

The extraction of phenolic compounds from the pulp was performed according to the method described by McDonald *et al*. (2001). Ten grams of dried pulp were mixed with 50 mL of methanol/water (80:20, v/v) for 20 minutes. The mixture was centrifuged at 3000 rpm for 5 minutes. Then, the residue was extracted twice, and supernatants were combined and washed with hexane to eliminate the oil. The extract was filtered through a 0.45 µm pore size filter. An aliquot of 0.5 mL of methanolic extracts was reacted with 3.9 mL of a methanolic solution of DPPH radical (0.1 mM). The mixture was incubated for 30 min in the dark, and the

absorbance was measured at 515 nm. The radical inhibition was calculated according to the following formula:

% inhibition = [(absorbance of control - absorbance of the sample)/absorbance of control] x100 (Boskou *et al*., 2006).

The antiradical activity was expressed in mg of gallic acid equivalents (GAE)/100g of dry weight (DW). The EC50 value, which represents the concentration of sample required to inhibit 50% 2,2-diphenyl-1-picrylhydrazyl (DPPH) radical was determined for each extract.

2.7.2. Reducing power

The determination of reducing power was carried out (Zhan *et al*., 2006). An aliquot of 2.5 mL of the methanolic extract was mixed with 2.5 mL of phosphate buffer (0.2 M, pH 6.6) and 2.5 mL of potassium ferricyanide (1%). The mixture was incubated at 50 °C for 20 min. Then, 2.5 ml of trichloroacetic acid (10%) were added, and the mixture was centrifuged at 3650 rpm for 10 min. 5 mL of supernatant were mixed with the same volume of distilled water, and 1 mL of ferric chloride (0.1%) and the absorbance was measured at 700 nm. The results were expressed as mg of quercetin equivalents (QE)/100g DW.

2.8. Statistical analysis

Three tests were performed and expressed as mean values (n=3) for each analysis. Statistica software 10.0 (StatSoft, Inc., Tulsa, OK, USA) was used for data analysis. Statistical comparisons of the mean values for each experiment were performed by the least significant difference Newman–Keuls test and significance was defined at $p < 0.05$.

3. RESULTS AND DISCUSSION

3.1. Physical characteristics, moisture and oil content

Table 1 summarizes the main characteristics of olive drupes. The flesh-to-pit ratio is vital to evaluate the mass distribution between the flesh and the stone (Sakouhi *et al*., 2008). A proper appreciation requires drupe with flesh/pit equal to 5 (Rallo *et al*., 2018). Turning color olives of the Sigoise cultivar with a weight of 3.47 g and a flesh/stone ratio of about 5.09 can be considered appropriate for table olive processing. The olives have an oval shape, and the length/diameter ratio is greater than 1.

The evolution of the pH of the brines during the fermentation of table olives showed a significant decrease from 6.65 initially to 4.2 after 150 days. A critical drop was noticed after 60 days of fermentation. This trend is due to the conversion of carbohydrates into organic acids, mainly by LAB metabolism. Also, the hydrolysis of oleuropein, which is decomposed by endogenous and bacterial enzymes in sugars and simple phenols, such as elenolic acid, may contribute to the drop in pH (Kiai and Hafidi, 2014).

The humidity varied between 52.74 and 54.70%; whereas oil content varied between 42.98 and 44.61%. Sigoise turning color table olives recorded a higher rate of oil compared to those reported for the Tunisian table olives (Meski) elaborated according to natural style (Issaoui *et al*., 2011). There was a non-significant effect of processing on all the main characteristics of table olives except for pH.

Table 1. Physicochemical parameters in turning color table olives of the Sigoise variety during natural-style processing.

Time (days)	Weight (g)	Flesh to pit ratio	Length/diameter ratio	pH	Moisture content (%)	Oil content (% Dry weight)
0	3.49 ± 0.49	5.02 ± 0.22	1.32 ± 0.06	6.65 ± 0.05a	55.86 ± 0.53	44.61 ± 1.45
60	3.51 ± 0.74	5.05 ± 0.19	1.34 ± 0.06	5.25 ± 0.05b	52.75 ± 0.67	42.98 ± 2.19
120	3.53 ± 0.63	5.01 ± 0.13	1.34 ± 0.1	4.45 ± 0.05c	54.69 ± 0.33	44.34 ± 1.18
150	3.47 ± 0.34	5.09 ± 0.35	1.35 ± 0.07	4.20 ± 0.05d	53.72 ± 0.04	43.86 ± 1.33

Results are given as mean ± standard deviation of triplicate analyses. No significant differences were found among samples except for the pH, which are indicated by different superscript letters using the Newman–Keuls test ($p < 0.05$).

3.2. Phenolic compounds

Polyphenols are considered to be the most antioxidant substrates in table olives. Still, some of them, in particular the oleuropein, confer a bitter taste which is not accepted by consumers and their removal is necessary (Boskou *et al*., 2006). The phenolic composition in the olives was studied in the raw fruit and throughout processing (Table 2). Hydroxytyrosol 4-glucoside and oleuropein were identified as the major polyphenols in the raw olive fruit with a concentration of 31867.9 and 27730.3 mg/kg DW, respectively, followed by verbascoside, rutin, hydroxytyrosol, ligustroside and salidroside in minor concentrations. These results are in accordance with those found previously (Romero *et al*., 2004b).

Noticeable decreases in oleuropein, hydroxytyrosol 4-glucoside, rutin and ligustroside were observed after 150 days of brining, reaching concentrations of 10891.7, 10860.0, 310.1 and 252.1 mg/kg DW, respectively. Conversely, hydroxytyrosol and salidroside increased after 60 days and decreased at the end of processing to 1617.8 and 303.8 mg/kg respectively. Comselogoside did not show significant differences during processing. The same trend was observed by Sousa *et al*. (2014) which showed a decrease in oleuropein and increase in hydroxytyrosol in samples harvested at different stages of maturation. Moreover, several authors indicated that table olives processed according to the natural style underwent a significant decrease in oleuropein, which is followed by an increase in hydroxytyrosol as the main hydrolysis product during the first days of brining (Issaoui *et al*., 2011; Johnson *et al*., 2018; Ramirez *et al*., 2016).

The total polyphenol content in fresh olives was initially 67335.4 mg/kg. This amount was significantly reduced during processing, reaching 26585.5 mg/kg after 150 days of brining, which corresponds to a decline in total polyphenols of 60.52% (Table 2). Similar total polyphenol concentrations for the Picholine variety in both raw and processed fruit were found (Issaoui *et al*., 2011). Likewise, Sigoise cv. showed a higher content in phenolic compounds compared to Meski and Manzanilla cultivars. The study conducted by Johnson *et al*. (2018) on levels of phenolic compounds in Spanish-style green (SP),

Table 2. Concentration (mg/kg of dry weight) of the phenolic compounds in turning color table olives of the Sigoise variety during natural-style processing.

	Time (days)			
	0	**60**	**120**	**150**
Hydroxytyrosol	1291.8 ± 84.1^{b}	2456.9 ± 178.9^{a}	1679.6 ± 95.8^{b}	1617.8 ± 152.2^{b}
Hydroxytyrosol 4-glucoside	31867.9 ± 1595.4^{a}	28753.7 ± 748.5^{b}	16415.4 ± 99.0^{c}	10860.0 ± 867.2^{d}
Salidroside	684.3 ± 22.7^{b}	916.8 ± 3.0^{a}	429.3 ± 40.8^{c}	303.8 ± 25.1^{d}
Verbascoside	2812.9 ± 170.0^{a}	3854.6 ± 117.8 ^{a}	1952.9 ± 126.0 ^{c}	2337.5 ±168.6 ^{b}
Oleuropein	27730.3 ± 702.9 ^{a}	21128.2 ± 655.1 ^{b}	14049.0 ± 526.5 ^{c}	10891.7 ± 580.2 ^{d}
Comselogoside	20.6 ± 9.5 ^{a}	17.2 ± 4.0 ^{a}	19.8 ± 4.8 ^{a}	12.3 ± 8.3 ^{a}
Rutin	1861.1 ± 82.1 ^{a}	771.2 ± 69.1 ^{a}	389.3 ± 60.9 ^{c}	310.1 ± 60.4 ^{c}
Ligustroside	1066.5 ± 126.4 ^{a}	531.4 ± 20.3 ^{b}	402.6 ± 17.4 ^{c}	252.1 ± 35.5 ^{d}
Sum of polyphenols	67335.4 ± 2233.4 ^{a}	58430.2 ± 1082.1 ^{b}	35338.6 ± 765.5 ^{c}	26585.5 ± 1106.0 ^{d}

Results are given as mean ± standard deviation of triplicate analyses. Significant differences in the same row are marked with different superscript letters using the Newman–Keuls test ($p < 0.05$).

Californian-style black ripe (CA), and Greek-style natural fermentation, showed that olives in brine had the highest concentrations; whereas CA olives had the lowest level.

It is well-known that the diffusion of polyphenols between fruits and the water phase takes place when olives are directly brined and soluble components move from olive to the surrounding solution (Poiana and Romeo, 2006). This diffusion can occur more rapidly if the cellular structure of the fruit becomes naturally soft. It was reported that the de-bittering process occurs by the breakdown of the oleuropein into non-bitter products by the action of the activity of endogenous enzymes, esterase and β-glucosidase during the first month of brining followed by slow chemical hydrolysis throughout the rest of the storage (Ramirez *et al*., 2016). The acidic conditions of the brine can also favor the chemical hydrolysis of oleuropein (Medina *et al*., 2008). Also, an oleuropeinolytic activity has been reported for different yeast and lactic acid bacteria strains, which are responsible for fermentation in natural table olives (Bonatsou *et al*., 2015; Ramírez *et al*., 2017).

3.3. Sugars

The sugar content in olives is the most important fermentative substrate for the growth of the microorganisms which are responsible for fermentation during the natural style elaboration. The soluble sugars are transformed by microorganisms into organic acids as the product of the fermentation and second metabolites responsible for the desirable organoleptic characteristics in the final product. As shown in Figure 1, the main sugars in the raw olive fruits are glucose, mannitol, fructose and sucrose with concentrations of 29.2, 10.5, 5.2 and 1.5 g/kg, respectively. The sugar content registered a significant decrease after 150 days of brining with a glucose degradation rate of 91.05% and lower for the mannitol and fructose (74.57 and 74.76%, respectively). Sucrose was consumed in the first 60 days of brining. A decrease in sugar content has also been noted for different cultivars elaborated in the natural style (Bianchi, 2003; Issaoui *et al*., 2011). Likewise, these results are in agreement with those noted (Bleve *et al*., 2015) for Taggiasca natural table olives but with a higher degradation rate for fructose (92.28%) than for glucose (83.55%).

3.4. Tocopherols

The study on tocopherols contributes to empowering the nutritional value and the biological properties like the antioxidant capacity of table olives (Sakouhi *et al*., 2008). The main tocopherol present in the oil fraction of raw olives was α-tocopherol with 133.8 mg/kg. β, γ, and δ-tocopherol were present at in small amounts of 0.4, 4.2, and 1.5 mg/kg, respectively (Table 3). A significant decrease was observed for α-tocopherol throughout processing and a loss of

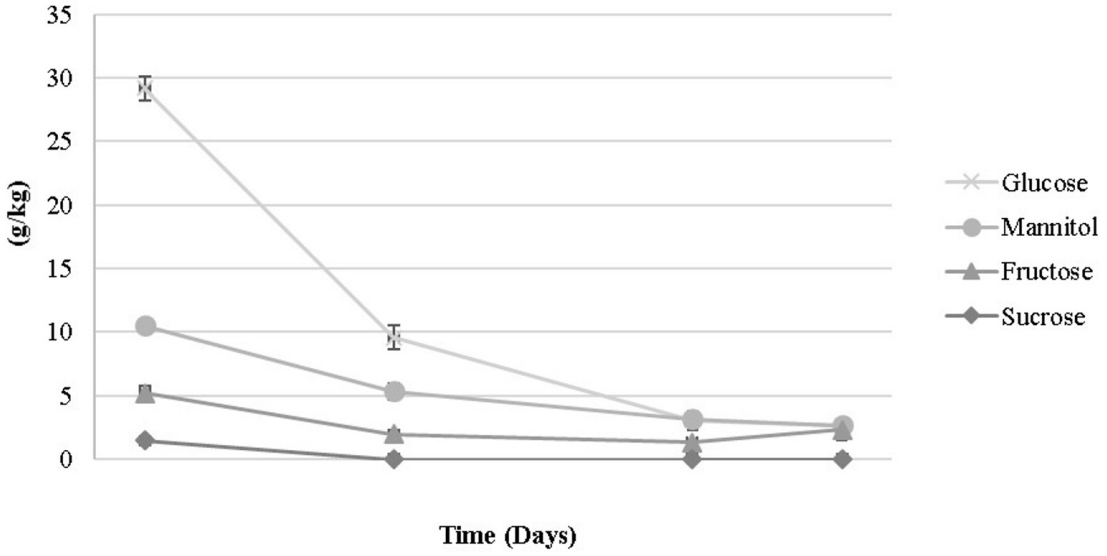

FIGURE 1. Concentration of sugars (g/kg) in turning color table olive pulp of the Sigoise variety during natural-style processing. Results are given as the mean of triplicate analyses. Bars indicate standard deviation.

TABLE 3. Concentration of tocopherols (mg/kg) and fatty acids (%) in turning color table olives of the Sigoise variety during natural-style processing.

	Time (days)			
	0	**60**	**120**	**150**
α-tocopherol	133.8 ± 3.9[a]	131.8 ± 3.5[ab]	122.8 ± 0.5[b]	122.4 ± 0.6[b]
β-tocopherol	1.5 ± 0.1[a]	1.5 ± 0.1[a]	1.4 ± 0.1[a]	1.4 ± 0.1[a]
γ-tocopherol	4.2 ± 0.4[a]	4.3 ± 0.4[a]	4.5 ± 0.2[a]	4.5 ± 0.1[a]
δ-tocopherol	0.4 ± 0.0[a]	0.5 ± 0.1[a]	0.3 ± 0.0[a]	0.4 ± 0.1[a]
Sum of tocopherols	139.8 ± 4.5[a]	138.1 ± 3.7[a]	128.9 ± 0.4[b]	128.8 ± 0.7[b]
C14:0	0.02 ± 0.00	0.02 ± 0.00	0.02 ± 0.00	0.02 ± 0.00
C16:0	9.09 ± 0.04	9.16 ± 0.02	9.12 ± 0.01	9.30 ± 0.20
C16:1	0.64 ± 0.00	0.64 ± 0.01	0.64 ± 0.00	0.66 ± 0.02
C17:0	0.05 ± 0.00	0.05 ± 0.00	0.05 ± 0.01	0.06 ± 0.00
C17:1	0.07 ± 0.00	0.07 ± 0.00	0.07 ± 0.00	0.08 ± 0.00
C18:0	2.84 ± 0.00	2.87 ± 0.03	2.84 ± 0.02	2.87 ± 0.01
C18:1	75.90 ± 0.04	75.72 ± 0.04	75.94 ± 0.03	75.67 ± 0.18
C18:2	9.89 ± 0.04	9.98 ± 0.03	9.86 ± 0.04	9.86 ± 0.04
C18:3	0.75 ± 0.00	0.76 ± 0.00	0.75 ± 0.00	0.76 ± 0.00
C20:0	0.32 ± 0.01	0.32 ± 0.00	0.31 ± 0.01	0.31 ± 0.01
C20:1	0.33 ± 0.00	0.33 ± 0.00	0.32 ± 0.00	0.32 ± 0.01
C22:0	0.07 ± 0.00	0.07 ± 0.00	0.07 ± 0.01	0.07 ± 0.01
C24:0	003 ± 0.00	0.03 ± 0.00	0.03 ± 0.00	0.04 ± 0.01
trans C18:1	0.02 ± 0.01	0.01 ± 0.00	0.02 ± 0.01	0.02 ± 0.01
trans C18:2	0.00 ± 0.00	0.00 ± 0.00	0.00 ± 0.00	0.00 ± 0.00
trans C18:3	0.00 ± 0.00	0.00 ± 0.00	0.00 ±0.00	0.00 ± 0.00
Sum of *trans*	0.02 ± 0.01	0.01 ± 0.00	0.02 ± 0.01	0.02 ± 0.01

Results are given as mean ± standard deviation. Significant differences in the same row are marked with different superscript letters ($p < 0.05$). No significant differences were found for fatty acids among samples using the Newman–Keuls test ($p < 0.05$). ND means not detected.

7.88% was recorded after 150 days of brining, while the other isomers did not show significant changes.

The turning-color table olives of the Sigoise cv. registered higher tocopherol content than those found for Italian varieties (Sagratini *et al*., 2013) with maximum concentrations of 90 mg/kg in several samples of table olives elaborated by different processing methods. Similarly, Sakouhi *et al*. (2008) recorded higher tocopherol levels in three cultivars (Meski, Sayali and Picholine) at a cherry stage of ripeness than green ones, but still lower than the Sigoise variety. Hassapidou *et al*. (1994) reported that the natural-style elaboration did not affect the α-tocopherol contents in Conservolea or Kalamata black olives; however, the lye treatment used in the Spanish-style processing caused a reduction in α-tocopherols (Boskou *et al*., 2014).

3.5. Fatty acids

The fatty acid composition (Table 3) showed that oleic acid (C18:1) was the major fatty acid in the olive flesh (75.90% of the total). Linoleic (C18:2) and palmitic (C16:0) acids were present in similar amounts

of 9.89 and 9.09%, respectively. The variations related to processing were insignificant, which is in agreement with the results of many authors (Issaoui *et al*., 2011; Sakouhi *et al*., 2008). The stability of the fatty acids in processed olives could be related to their nature and the protective action of antioxidants. Oleic acid and tocopherols were present in considerable amounts in our variety. The *trans* forms of linoleic and linolenic acids were not detected, whereas *trans*-oleic acid (C18:1t) had a value (0.02%) which was below the limit values requested by the Commission Regulation (EU); ≤ 0.05 (Commission Delegated Regulation (EU) 2016/2095 of 26 September 2016 amending Regulation (EEC) No 2568/91). The preservation of essential fatty acids can also be explained by the firmness of olives and the non-use of alkaline treatment (Rallo *et al*., 2018; Jiménez *et al.,* 1997).

3.6. Antioxidant activity

In this study, antioxidant activity was evaluated by two different chemical assays, the scavenging effect on DPPH free radicals and the reducing power (Figure 2). The raw fruit recorded high values for antioxidant scavenging activity (40654.13 mg GAE/kg) and reducing power (12296.79 mg QE/kg). The inhibition rate of the DPPH radical and EC50 was 75.81% and 3.36 mg/mL, respectively. The antioxidant activity

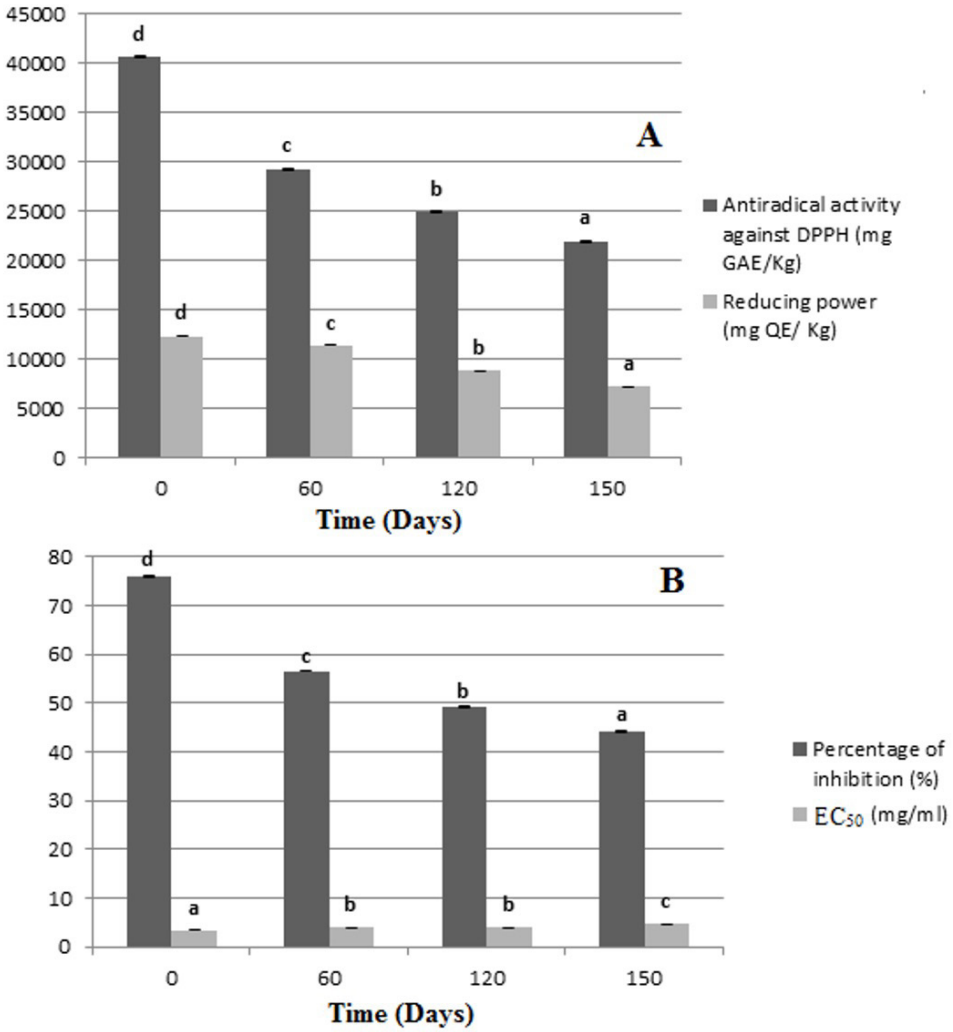

FIGURE 2. Antioxidant activity, reducing power (Panel A), percentage of inhibition and EC50 (Panel B) in turning color table olives of the Sigoise variety during natural-style processing. Results are given as mean of triplicate analyses. Significant differences are marked with different superscript letters using the Newman–Keuls test ($p < 0.05$). Bars indicate standard deviation. GAE means gallic acid equivalents. QE means quercetin equivalents.

decreased significantly throughout processing. The DPPH radical scavenging and reducing power decreased to 21917.71 mg GAE/kg and 7176.09 mg QE/kg, respectively, with an inhibition rate of 44.20%. The antioxidant activity showed a highly significant correlation with phenolic compounds (r = 0.99); whereas the effective concentration EC50 of the extracts was negatively correlated (r = -0.91). According to several authors, there is a linear correlation between the total polyphenol content in table olives and their antioxidant activity (Ben Othman *et al*., 2009; Romero *et al*., 2004b; Sousa *et al*., 2014). Mettouchi *et al*. (2016) reported a similar behavior for the loss in reducing power but with the influence of environmental conditions for the same variety. Indeed, Sigoise from the Sig region exhibited a low reducing power compared to Sigoise from the Tazmalt region. The differences could be explained by the effectiveness of each phenolic component in the fruit composition. So far, the antioxidant activity depends on the concentration of the polyphenol profile. Furthermore, Ben Othman *et al*. (2009) monitored the evolution of phenolic compounds during the natural table olive elaboration of the Chétoui cultivar at three degrees of ripeness (green, turning color and black) and they found a decrease in the antioxidant activity by 60–72%, with the turning color olives presenting an intermediate value. The Sigoise cultivar showed a lower reduction in the antioxidant capacity (46.09%) due to a more moderate loss in phenolic compounds.

4. CONCLUSIONS

This study has characterized the main compounds, in particular, polyphenols, sugars, fatty acids and tocopherols, in the turning color table olives elaborated as natural-style of the Sigoise cultivar. The total polyphenol content decreased as the process progressed, except for the hydroxytyrosol, which increased at the beginning of brining and then decreased. There was also a consumption of sugars, especially glucose, which is typical of the fermentation process. The concentration of fatty acids was not affected by the elaboration process without significant differences throughout the process. The tocopherol concentration remained constant during the processing, and a decrease was only observed for α-tocopherols after 150 days of brining. The losses in the latter and other phenolic compounds came as a consequent reduction in the antioxidant activity. Therefore, the turning color natural table olives of the Sigoise variety have an outstanding nutritional value and constitute an excellent source of antioxidant compounds that can exert beneficial properties to consumers.

ACKNOWLEDGEMENTS

We want to thank the Algerian Ministry of Higher Education and Scientific Research for sponsoring this work. The authors are grateful to the staff of the company KHODJA & CO Seddouk (Bejaia, Algeria) for providing the samples. This work was also supported by the Spanish Government (Project RTI2018-093994-J-I00, AEI/FEDER, UE and Ramón y Cajal Programme RyC2018-024752-I).

REFERENCES

Ben Othman N, Roblain D, Chammen N, Thonart P, Hamdi M. 2009. Antioxidant phenolic compounds loss during the fermentation of Chétoui olives. *Food Chem.* **116**, 662-669. https://doi.org/10.1016/j.foodchem.2009.02.084

Bleve G, Tufariello M, Durante M, Grieco F, Ramires FA, Mita G, Tasioula-Margari M, Logrieco AF. 2015. Physico-chemical characterization of natural fermentation process of Conservolea and Kalamata table olives and development of a protocol for the pre-selection of fermentation starters. *Food Microbiol.* **46**, 368-382. https://doi.org/10.1016/j.fm.2014.08.021

Bonatsou S, Benitez A, Rodríguez-Gómez F, Panagou EZ, Arroyo-López FN. 2015. Selection of yeasts with multifunctional features for application as starters in natural black table olive processing. *Food Microbiol.* **46**, 66-73. https://doi.org/10.1016/j.fm.2014.07.011

Boskou D, Campasio S, Clodoveo ML. 2014. Table olives as source of bioactive compounds, in: Boskou D (Ed.) Olive and olive oil bioactive constituents, 1st edition. AOCS press, Urbana, IL, USA.

Boskou G, Salta FN, Chrysostomou S, Mylona A, Chiou A, Andrikopoulos NK. 2006. Antioxidant capacity and phenolic profile of table olives from the Greek market. *Food Chem.* **94**, 558-564. https://doi.org/10.1016/j.foodchem.2004.12.005

European Commission regulation (ECC) No 2568/91 of July (1991) on the characteristics of olive oil and olive-residue oil and on the relevant methods of analysis, Official Journal of the European Communities 1991, *OJ L* **248**, 5.9, 1-110.

Commission Delegated Regulation (EU) 2016/2095 of 26 September 2016 amending Regulation (EEC) No 2568/91 of July (1991) on the characteristics of olive oil and olive-residue oil and on the relevant methods of analysis. *Official Journal of the European Union* 326/1-6.

Hassapidou MN, Balatsouras GD, Manoukas AG. 1994. Effect of processing upon the tocopherol and tocotrienol composition of table olives. *Food Chem.* **50**, 111-114. https://doi.org/10.1016/0308-8146(94)90105-8

International Olive Oil Council (IOC). 2004. Trade Standard Applying to Table Olives, COI/OT/NC No. 1, Resolution No. RES-2/91-IV/04.

International Olive Oil Council (IOC). 2020. Updates Series of World Statistics on Production, Imports, Exports and Consumption. Internet: http://www.internationaloliveoil.org/estaticos/view/132-world-table-olive-figures. Accessed 19 May 2020

Issaoui M, Dabbou S, Mechri B, Nakbi M, Chehab H, Hammami M. 2011. Fatty acid profile, sugar composition, and antioxidant compounds of table olives as affected by different treatments. *Eur. J. Lipid Sci. Tech.* **232**, 867-876. https://doi.org/10.1007/s00217-011-1455-3

Jimenez A, Guillen R, Fernandez-Bolaños J, Heredia A. 1997. Factors Affecting the "Spanish Green Olive" Process: Their Influence on Final Texture and Industrial Losses. *J. Agric. Food Chem*. **45**, 4065-4070. https://doi.org/10.1021/jf970161v

Johnson R, Melliou E, Zweigenbaum J, Mitchell AE. 2018. Quantitation of oleuropein and related phenolics in cured Spanish-style green, California-style black ripe and Greek-style natural fermentation olives. *J. Agric. Food Chem.* **66**, 2121-2128. https://doi.org/10.1021/acs.jafc.7b06025

Kacem M, Karam NE. 2006. Microbiological study of naturally fermented Algerian green olives: isolation and identification of lactic acid bacteria and yeasts along with the effects of brine solutions obtained at the end of olive fermentation on Lactobacillus plantarum growth. *Grasas Aceites* **57**, 292-300. https://doi.org/10.3989/gya.2006.v57.i3.51

Kiai H, Hafidi A. 2014. Chemical composition changes in four green olive cultivars during spontaneous fermentation. *LWT – Food Sci. Technol.* **57**, 663-670. https://doi.org/10.1016/j.lwt.2014.02.011

McDonald S, Prenzler PD, Antolovich M, Robards K. 2001. Phenolic content and antioxidant activity of olive extracts. *Food Chem*. **73**, 73-87. https://doi.org/10.1016/S0308-8146(00)00288-0

Marsilio V, Campestre C, Lanza B, De Angelis M. 2001. Sugar and polyol compositions of some European olive fruit varieties (*Olea europaea* L.) suitable for table olive purposes. *Food Chem* **72**, 485-490. https://doi.org/10.1016/S0308-8146(00)00268-5

Medina E, Brenes M, Romero C, Garcia A, Castro A. 2007. Main antimicrobial compounds in table olives. *J. Agr. Food Chem.* **55**, 9817-9823. https://doi.org/10.1021/jf0719757

Medina E, Gori C, Servili M, de Castro A, Romero C, Brenes M. 2010. Main variables affecting the lactic acid fermentation of table olives. *Int. J. Food Sci. Tech.* **45**, 1291-1296. https://doi.org/10.1111/j.1365-2621.2010.02274.x

Medina E, Romero C, Brenes M, García P, de Castro A, García A. 2008. Profile of anti-lactic acid bacteria compounds during the storage of olives which are not treated with alkali. *Eur. J. Lipid Sci. Tech.* **228**, 133-138. https://doi.org/10.1007/s00217-008-0916-9

Mettouchi S, Bachir Bey M, Tamendjari A, Louaileche H. 2016. Antioxidant activity of table olives as influenced by processing method. *International Journal of Chemical and Biomolecular Science* **2**, 8-14. http://www.aiscience.org/journal/ijcbs

Poiana M, Romeo FV. 2006. Changes in chemical and microbiological parameters of some varieties of Sicily olives during natural fermentation. *Grasas Aceites* **57**, 402-408. https://doi.org/10.3989/gya.2006.v57.i4.66

Ramírez E, Brenes M, de Castro A, Romero C, Medina E. 2017. Oleuropein hydrolysis by lactic acid bacteria in natural green olives. *LWT – Food Sci. Technol.* **78**, 165-171. https://doi.org/10.1016/j.lwt.2016.12.040

Ramirez E, Brenes M, Garcia P, Medina E, Romero C. 2016. Oleuropein hydrolysis in natural green olives: importance of endogenous enzymes. *Food Chem.* **206**, 204-209. https://doi.org/10.1016/j.foodchem.2016.03.061

Rallo P, Morales Sillero A, Brenes M, Jimenez MR, Sanchez AH, Suarez MP, Casanova L, Romero C. 2018. Elaboration of table olives: assessment of new olive genotypes. *Eur. J. Lipid Sci. Tech.* **120**, 1800008. https://doi.org/10.1002/ejlt.201800008

Romero C, Brenes M, Garcia P, Garcia A, Garrido A. 2004a. Polyphenol changes during fermentation of naturally black olives. *J. Agr. Food Chem.* **52**, 1973-1979. https://doi.org/10.1021/jf030726p

Romero C, Brenes M, Garcia P, Garcia A, Garrido, A. 2004b. Effect of cultivar and processing method on the contents of polyphenols in table olives. *J. Agr. Food Chem.* **52**, 479-484. https://doi.org/10.1021/jf030525l

Rovellini P, Azzolini M, Cortesi N. 1997. Tocoferoli e tocotrienoli in oli e grassi vegetali. *Riv. Ital. Sostanze Gr.* **74**, 1-5.

Sagratini G, Allegrini M, Caprioli G, Cristalli G, Giardina D, Maggi F. 2013. Simultaneous determination of squalene, α-tocopherol and β-carotene in table olives by solid phase extraction and high performance liquid chromatography with diode array detection. *Food Anal. Methods* **6**, 5-60. https://doi.org/10.1007/s12161-012-9422-6

Sakouhi F, Harrabi S, Absalon C, Sbei K, Boukhchina S, Kallel H. 2008. α-Tocopherol and fatty acids contents of some Tunisian table olives (*Olea europea* L.): Changes in their composition during ripening and processing. *Food Chem.* **108**, 833-839. https://doi.org/10.1016/j.foodchem.2007.11.043

Sousa A, Malheiro R, Casal S, Bento A, Pereira JA. 2014. Antioxidant activity and phenolic composition of Cv. Cobrançosa olives affected through the maturation process. *J. Funct. Foods* **11**, 20-29. https://doi.org/10.1016/j.jff.2014.08.024

Susamci E, Romero C, Tuncay O, Brenes M. 2017. An explanation for the natural debittering of Hurma olives during ripenning on the tree. *Grasas Aceites* **68**, 182-189. https://doi.org/10.3989/gya.1161162

Tovar MJ, Romero M P, Girona J, Motilva MJ. 2002. L-Phenylalanine ammonia-lyase activity and concentration of phenolics in developing olive (*Olea europaea* L cv Arbequina) fruit grown under different irrigation regimes. *J. Sci. Food Agric.* **82,** 892-898. https://doi.org/10.1002/jsfa.1122

Zhan Y, Hong-Dong C, Yao YJ. 2006. Antioxidant activities of aqueous extract from cultivated fruit-bodies of *Cordyceps militaris* (L.) Link in vitro. *J. Integr. Plant Biol.* **48**, 1365-1370. https://doi.org/10.1111/j.1744-7909.2006.00345.x

GRASAS Y ACEITES 72 (3)
July-September 2021, e420
ISSN-L: 0017-3495
https://doi.org/10.3989/gya.0325201

Thermal and chemical characterization of fractions from *Syagrus romanzoffiana* kernel oil

T.S. Tavares[a], K.T. Magalhães[a], N.D. Lorenzo[a] and C.A. Nunes[b, ✉]

[a]Department of Chemistry, Federal University of Lavras, University Campus, Post Office Box 3037, 37200-000 Lavras, Minas Gerais, Brazil
[b]Department of Food Science, Federal University of Lavras, University Campus, Post Office Box 3037, 37200-000 Lavras, Minas Gerais, Brazil
✉Corresponding author: cleiton.nunes@ufla.br

Submitted: 02 March 2020; Accepted: 29 June 2020; Published online:15 September 2021

SUMMARY: The Jerivá (*Syagrus romanzoffiana*) kernel oil (JKO) has a pleasant coconut-like smell, with about 33% lauric acid and 28% oleic acid. The oil also contains bioactive compounds, such as phenolics, carotenoids, and tocopherols. JKO has a solid consistency at low temperatures, but has a low melting point and low solid content at room temperature. Thus, this work aimed to evaluate the thermal properties related to crystallization and fusion, as well as the chemical and oxidative characteristics of JKO fractions, olein and stearin, obtained from dry and solvent fractionation. In general, stearins had higher crystallization and melting temperatures, and higher solid fat content, unlike oleins, which may be associated with the concentration of high melting triglycerides in the stearins. No statistically significant difference was found for fatty acid profile or oxidative stability of the fractions. The type of fractionation influenced the chemical and thermal properties of JKO fractions. The solvent process promoted the most relevant differentiation of fractions. An olein was obtained with 7% less solid fat at 25 °C which remained visually liquid at 2 °C below the oil, as well as a stearin with 17% more solid fat at 25 °C which remained visually solid at 3 °C above the oil.

KEYWORDS: *Crystallization; Fractionation; Melting; Olein; Stearin*

RESUMEN: ***Caracterización térmica y química de fracciones de aceite de semilla de*** **Syagrus romanzoffiana.** El aceite de semilla de Jerivá (*Syagrus romanzoffiana*) (ASJ) tiene un agradable olor a coco, con aproximadamente un 33% de ácido láurico y un 28% de ácido oleico. Este aceite también contiene compuestos bioactivos, como fenólicos, carotenoides y tocoferoles. El ASJ tiene una consistencia sólida a baja temperatura, pero tiene un punto de fusión bajo y un contenido de sólidos bajo a temperatura ambiente. Este trabajo tuvo como objetivo evaluar las propiedades térmicas relacionadas con la cristalización y fusión, así como las características químicas y oxidativas de las fracciones de ASJ, oleína y estearina, obtenidas mediante fraccionamiento en seco y con solvente. En general, las estearinas tuvieron temperaturas de cristalización y fusión más altas y un mayor contenido de grasa sólida, a diferencia de las oleínas, esto puede estar asociado con la concentración de triglicéridos de alto punto de fusión en las estearinas. No se encontraron diferencias estadísticamente significativas para el perfil de ácidos grasos ni en la estabilidad oxidativa de las fracciones. El tipo de fraccionamiento influyó en las propiedades químicas y térmicas de las fracciones de ASJK. El proceso mediante solvente favoreció la diferenciación de fracciones más relevantes. Se obtuvo una oleína con 7% menos de grasa sólida a 25 °C que permaneció visualmente líquida a 2 °C por debajo del aceite, así como una estearina con 17% más de grasa sólida a 25 °C y que permaneció visualmente sólida a 3 °C por encima del aceite.

PALABRAS CLAVE: *Cristalización; Estearina; Fusión; Fraccionamiento; Oleina*

Citation/Cómo citar este artículo: Tavares TS, Magalhães KT, Lorenzo ND, Nunes CA. 2021. Thermal and chemical characterization of fractions from *Syagrus romanzoffiana* kernel oil. *Grasas Aceites* **72** (3), e420. https://doi.org/10.3989/gya.0325201

1. INTRODUCTION

Lauric oils are obtained from various palm species and are characterized mainly by high contents in lauric acid (C12:0) and small amounts of other medium and short-chain fatty acids. Lauric oils can be found mainly in coconut and palm kernels, Jarivá, and Macaúba, which have a solid consistency at low room temperatures but still melt below 30 °C (Coimbra and Jorge, 2011; Gunstone, 2010). Therefore, these natural fats have a short melting range, which makes them suitable for the manufacture of a variety of fatty foods. In this respect, the low melting points and the low solid contents at room temperature are favorable for the production of some products, such as confectionery coatings and couvertures; although it is a drawback that can be alleviated by the fractional crystallization and separation of harder and softer fractions (Gunstone, 2010; Magalhães *et al*., 2020b; Rossell, 1985). In this sense, fractional crystallization, or simply fractionation, refers to a separation process in which fatty material is crystallized at a suitable temperature, after which a low melting phase (olein) is separated from a high melting phase (stearin) (Kellens *et al*., 2007; Sonwai *et al*., 2017). Nowadays, where *trans* fatty acids in food are questioned, fractionation oil modification stands out as an alternative for the industry because it is a physical process that does not promote changes in fat at the molecular level (Kellens *et al*., 2007; Magalhães *et al*., 2020b; Sonwai *et al*., 2017).

Lauric oils are widely modified by fractionation. Olein and stearin are obtained in this process in order to increase the applicability of the oils in different food processes. They are used in the food industry to produce spreads, specialty fats, ice cream, chocolate, and others, where most of them are specially derived from palm kernel oil. In addition, the increasing use of cocoa butter substitutes by the chocolate industry drives a growing demand for lauric oils (Calliauw *et al*., 2007; Chaleepa *et al*., 2010; Kellens *et al*., 2007; Magalhães *et al*., 2020b; Rossell 1985; Sonwai *et al*., 2017). Therefore, there is still room to explore other lauric oils, as well as their fractions, to obtain products with distinct characteristics from or equivalent to those derived from palm or coconut oil.

In this context, the *Syagrus romanzoffiana* palm is an interesting alternative resource in the production of lauric oil. This plant, commonly known as Jerivá, queen palm or coconut palm, is a native palm tree from South America and was introduced around the world as a popular ornamental garden tree used in urban landscaping (Pittenger *et al*., 2009). The Jerivá palm fruit is an oval drupe, yellowish or orange, with a rigid endocarp involving an almond with about 50% oil. The almond (kernel) oil has a pleasant coconut-like smell, with about 33% lauric acid and 28% oleic acid. The oil also contains bioactive compounds, such as phenolics, carotenoids, and tocopherols (Coimbra and Jorge, 2011; Coimbra and Jorge, 2012; Pierezan *et al*., 2015; Magalhães *et al*., 2020b). Jerivá kernel oil has interesting characteristics for biofuel production, such as low acidity, a high oxidative stability and transesterification reaction with an ester conversion rate above the minimum percentage required (Falasca *et al*., 2012; Moreira *et al*., 2013), but also has potential for human consumption (Lescano *et al*., 2018; Magalhães *et al*., 2020a). Nevertheless, research aiming to explore food applications of JKO is scarce.

Thus, this work aimed to evaluate the thermal properties related to crystallization and fusion, as well as the chemical and oxidative characteristics of JKO fractions obtained from dry and solvent fractionation. Possible changes in the fatty acid profile and oxidative stability of the fractions were evaluated by gas chromatography and Rancimat, respectively. Differential Scanning Calorimetry was used to assess the solid fat content, and the crystallization and melting behavior of the fractions. Changes in the physical state were determined by visual inspection.

2. MATERIALS AND METHODS

2.1. Oil extraction

The jerivá fruits (Figure 1) were collected from the south-east region of Brazil (Lavras, Minas Gerais state) directly from the ground in the mature stage, broken in a hydraulic press (MPH-15, Marcon) and the kernels were manually separated. The JKO was obtained using an expeller press (Home Up Yoda), with an oil yield of 42.6%, and centrifuged for 5 minutes at 4000 rpm (relative centrifugal force of 2150 g) to remove fine particles. Figure 1 illustrates the treatment process of treatment and characterization of the samples.

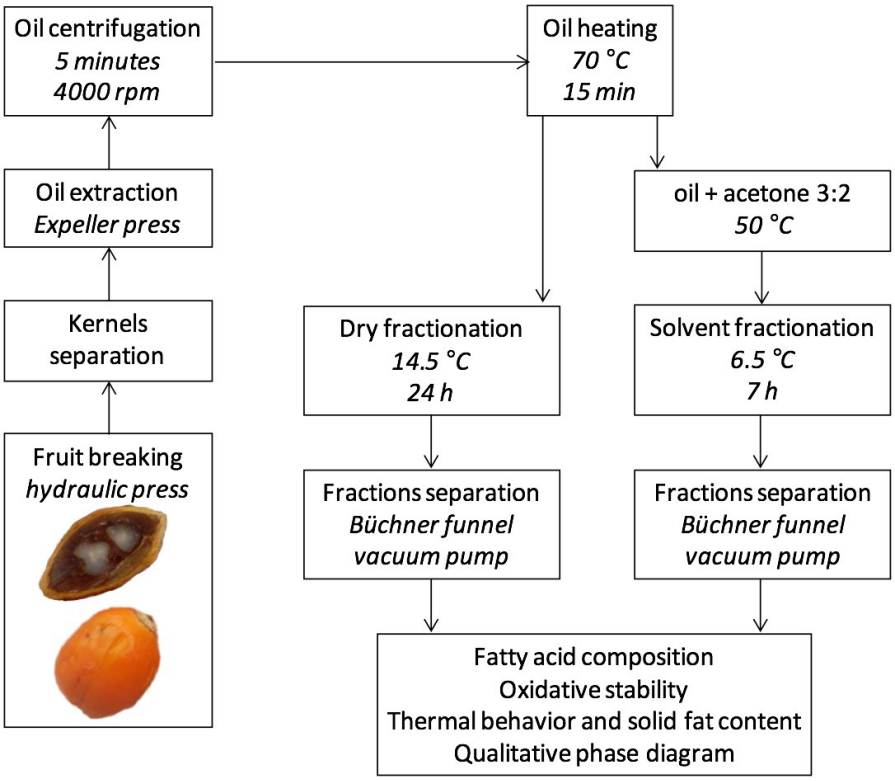

FIGURE 1. Process of extraction, fractionation and characterization of Jerivá kernel oil (JKO) and its fractions.

2.2. Fractionation

2.2.1. Dry fractionation

JKO (30 g) was heated in a water bath (HH-S3-Warmnest) at 70 °C for 15 min to remove any previous structure. The oil was cooled in BOD (T-34-THELGA) at 14.5 °C for 24 h. The fractions were separated by centrifugation (K14-4000-Kasvi) for 2 minutes at 4000 rpm. Olein and stearin were weighed to evaluate yield.

2.2.2. Solvent fractionation

The fractionation was carried out in a 100 mL jacketed glass reactor, connected to an ultratermostatic bath (Q214M-Quimis) with water circulation. The fractionation conditions established by Sonwai (2017) for coconut oil were used, with modifications defined through previous tests. Tests were carried out at different temperatures between 10 and 6 °C using a mass of 30 g of oil previously heated at 70 °C in a water bath (HH-S3-Warmnest) for 15 minutes and then cooled to 50 °C before being mixed with 20 mL of hot acetone (50 °C).

The temperature at which the crystals formed in significant amounts and remained stable was at 6.5 °C, in which two fractions were carried out: one for 5 hours with agitation at 20 rpm and another for 7 hours without agitation. After the crystals were formed, the fractions were separated by sieving (72 mesh) and the acetone was evaporated. Oleins and stearins were weighed to evaluate yield.

2.3. Fatty acid composition

A fatty acid composition analysis was performed according to the AOCS Ce 2-66 method (AOCS, 1993). Samples were transesterified in methyl esters with potassium hydroxide in methanol and n-hexane. All reagents and solvents (analytical grade) were from Vetec. The methyl esters were analyzed by gas chromatography (GC-2010 - Shimadzu) equipped with a flame ionization detector and an SPTM-2330 capillary column (30 m x 0.25 mm x 0.20 µm). Chromatographic conditions were split ratio 1:100, initial column temperature 140 °C, heating from 140 °C to 250 °C for 3 min at a rate of 5 °C/min for 25 min. Helium was used as carrier gas at a flow rate of 1 mL/

min and detector/injector at a temperature of 260 °C. For identification of the peaks, the retention times of the fatty acid methyl ester (Supelco 37 Component FAME Mix) standards were compared with the observed peak retention times using the Openchrom software. Quantification was done by normalizing the peak area and expressed in percentage. The saturated and unsaturated percentages were compared by the Tukey test ($p < 0.05$) using the online tool available at https://statpages.info.

2.4. Oxidative stability

Oxidative stability was expressed with the induction period in hours and was determined using 3 g of sample in a Rancimat apparatus (873 - Biodiesel Rancimat) at 110 °C with airflow of 10 L/h and 50 mL of distilled water in vials containing electrodes, according to the AOCS Cd 12b-92 method (AOCS, 1993). The oxidative stability indices were compared by the Tukey test ($p < 0.05$) using the online tool available at https://statpages.info.

2.5. Thermal behavior and solid fat content

Previously established conditions (Márquez *et al*., 2013) were used with modifications. Samples were heated at 60 °C for 15 min and left at 4 °C for 24 h. The thermograms of crystallization and melting were obtained using a Differential Scanning Calorimeter (DSC-60A - Shimadzu) coupled to the flow controller (FC-60A). The samples (5 mg) were placed in capped aluminum crucibles and cooled to -50 °C at 10 °C/min, maintaining this temperature for 10 min. The samples were then heated to 80 °C at 5 °C/min using a modulation amplitude of 1 °C every 60 s.

The solid fat content (SFC) was determined based on the area percentages of the integrated melting thermogram at 10, 15, 20, 25, 30, 35, and 40 C° (Cobo *et al*., 2017; Gunstone *et al*., 1994). Measurements for onset, peak, and final temperatures for crystallization and melting, as well as enthalpies, were obtained using the SciDAVis program. The deconvolution peak and integration were determined using the MagicPlot software.

2.6. Qualitative phase diagram

Experimental phase diagrams were obtained by storing the samples in capped 5-ml glass tubes and kept inverted at temperatures of 10, 11, 12, 13, 14, 15, 16, 17, 18, 19, and 20 °C for 24 hours. The phase change described as solid, thick liquid, or liquid was visually evaluated. Non-flowing materials were named as solids, slowly-flowing materials were named as thick liquid, and immediately-flowing materials were named as liquids (Rocha *et al*., 2013).

3. RESULTS AND DISCUSSION

3.1. Fractionation process

The dry fractionation yielded 63.2% olein and 36.8% stearin, while the solvent fractionation yielded 71.8% olein and 28.2% stearin. In dry fractionation, crystals grew agglomerated on the vessel wall, unlike solvent fractionation, in which crystals grew dispersed in the medium. This higher amount of stearin in dry fractionation may be due to entrapment of the liquid fraction in the crystals. Slowly cooling at high temperatures typically results in larger crystals that can become trapped within the liquid fraction, while rapid cooling at low temperatures forms smaller crystals in larger quantities (Chaleepa *et al*., 2010; Rodrigues-Ract *et al*., 2010; Silva *et al*., 2008).

In solvent fractionation, there is a lower viscosity medium due to the presence of solvent and better heat transfer compared to the dry process, which results in a high nucleation rate and a rapid crystal growth which facilitate dispersion of the crystals. These effects were evaluated by Grall and Hartell (1992), who reported that the rate of nucleation and crystal growth increased when crystallization times decreased when using agitation. By increasing the agitation, the crystal mass increased, but with a greater effect on solid fractions at lower temperatures and less effect at elevated temperatures. Thus, with the use of solvents, crystals can grow more stable and faster than in the dry process, which could contribute to better phase separation (Kellens *et al*., 2007; Rossell, 1985).

3.2. Fatty acid composition and oxidative stability

Nine fatty acids were identified, including seven saturated (caproic; caprylic; capric; lauric; myristic; palmitic and stearic) one monounsaturated (oleic), and one polyunsaturated (linoleic) (Table 1). JKO had 73.4% saturated fatty acids and 26.6% unsaturated fatty acids, mainly lauric acid (37.4%), myristic acid (10.0%) and oleic acid (21.3%), which

Table 1. Fatty acid composition and oxidative stability of JKO and its fractions obtained by dry and solvent fractionation.

Fatty acid		JKO	Ed	Es	Od	Os
Caproic	C6:0	0.5±0.2	0.6±0.1	1.2±0.1	0.5±0.1	0.7±0.1
Caprylic	C8:0	9.1±0.1	9.3±0.3	9.8±0.3	9.1±0.2	9.3±0.4
Capric	C10:0	7.0±0.3	7.2±0.3	6.6±0.4	7.0±0.2	7.3±0.5
Lauric	C12:0	37.4±1.3	39.0±0.5	38.0±1.1	37.2±1.1	37.7±1.7
Myristic	C14:0	10.0±0.7	10.0±0.3	9.4±0.8	9.8±1.1	9.5±1.0
Palmitic	C16:0	7.8±1.0	7.6±0.6	7.6±0.6	7.8±0.8	7.2±0.5
Stearic	C18:0	1.6±0.5	1.7±0.4	2.9±0.6	1.7±0.3	2.1±0.3
Oleic	C18:1	21.3±1.1	20.0±1.3	20.0±0.9	21.5±1.4	20.4±1.6
Linoleic	C18:2	5.3±0.7	4.8±0.6	4.5±0.6	5.3±0.6	4.8±0.6
ΣSaturated		73.4±0.3	73.3±0.1	75.3±1.6	75.4±1.2	72.9±2.8
ΣUnsaturated		26.6±0.4	26.6±0.7	24.8±1.6	24.4±0.8	26.8±1.1
Oxidative stability (h)		19.4±1.1	19.4±1.3	22.0±1.2	19.6±1.3	17.3±1.5

JKO: Jerivá kernel oil, Ed: dry fractionation stearin, Es: solvent fractionation stearin, Od: dry fractionation olein, Os: solvent fractionation olein. The mean ± standard deviation (n = 2).

is in agreement with what is reported in the literature (Coimbra and Jorge, 2011; Moreira *et al*., 2013).

In general, there was a slight numerical increase in saturated fatty acids in stearin (Es), with a consequent decrease in unsaturated ones, as opposed to olein (Os) fractions, although without statistically significant differences. Olein compositions were more similar to oil than stearins, which may indicate the presence of crystals in the oleins. However, it should be considered that the melting (or crystallizing) temperature of an oil or fat depends on the triacylglycerol (TAG) configuration, not just on the fatty acid composition. Previous work reported slight significant variations in the fatty acid compositions of coconut oil fractions (Marikkar *et al*., 2013) and palm oil fractions (Mo *et al*., 2016), but these fractions still had very distinct characteristics for the composition of TAG and thermal properties.

JKO presented oxidative stability of 19.4 h, similar to that previously reported (Moreira *et al*., 2013). Despite the fact that stearins showed numerically greater oxidative stability than oleins, no statistically significant difference was found. In general, the oxidative stability of oils is related to their composition and distribution of the fatty acids in TAG, as well as the presence of constituents with antioxidant properties. As previously reported (Ullah *et al*., 2016), approximately 70% of the oxidative stability of chia oil fractions depended on the fatty acid profile, but 30% depended on antioxidant substances such as chlorogenic and caffeic acids, quercetin, and phenolic glycoside. Thus, the similarities in the fatty acid composition of the fractions may explain the similarities in their oxidative stabilities.

3.3. Crystallization profile

The analysis of DSC peaks serves to determine the transition temperature of a fat or oil (Tan and Che Man, 2002). The stearins obtained started and ended crystallization at higher temperatures than oleins (Table 2, Figure 2), *i.e.*, stearins should be more abundant in high melting TAGs than oleins. The olein obtained from dry fractionation started crystallization before oil, presenting higher T_{onset}. This may indicate that this olein dragged a reasonable amount of high melting (crystalline phase) TAGs into the liquid matrix during the fractionation process. Crystals are known to tend

TABLE 2. Crystallization and melting temperatures of JKO and its fractions obtained by dry and solvent fractionation.

	Crystallization (ºC)				Melting (ºC)		
	T_{onsetc}	T_{pc1}	T_{pc2}	T_{fc}	T_{onsetm}	T_{pm}	T_{fm}
JKO	15.8±0.3	8.3±0.4	-	-0.6±0.1	17.2±0.9	30.9±2.1	36.0±1.9
Ed	16.3±0.9	13.4±0.5	6.4±0.4	1.9±0.1	16.4±0.8	31.9±1.8	36.6±1.8
Es	19.0±1.0	16.7±0.8	9.9±0.5	1.0±0.0	17.5±0.7	33.4±1.2	37.6±2.3
Od	16.1±0.8	8.0±0.6	-	0.1±0.0	16.7±0.7	30.3±2.0	35.2±2.4
Os	14.5±0.8	10.6±0.2	3.4±0.2	-2.1±0.2	13.7±0.8	30.1±1.5	35.4±2.0

T_{onsetc}: crystallization onset temperature, T_{pc}: crystallization peak temperature, T_{fc}: final crystallization temperature, T_{onsetm}: melting onset temperature, T_{pm}: melting peak temperature, T_{fm}: melting final temperature. JKO: Jerivá kernel oil, Ed: dry fractionation stearin, Es: solvent fractionati$_o$n stearin, Od: dry fractionation olein, Os: solvent fractionation olein. The mean ± standard deviation (n = 2).

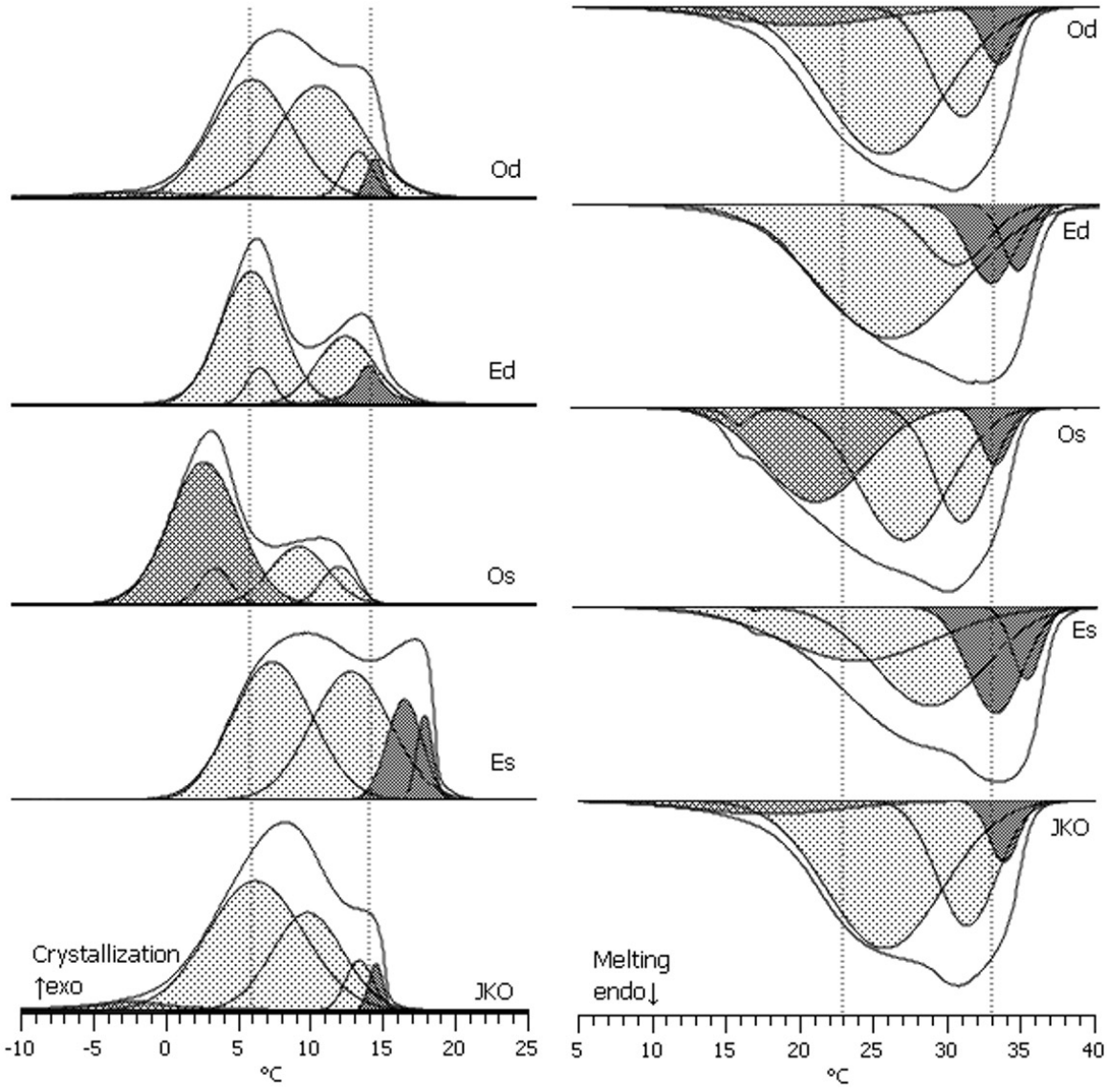

FIGURE 2. DSC crystallization and melting curves for JKO and its fractions obtained by dry and solvent fractionation. JKO: Jerivá kernel oil, Ed: dry fractionation stearin, Es: solvent fractionation stearin, Od: dry fractionation olein, Os: solvent fractionation olein. n = 2.

to form clusters due to attractive interactions between them, which can drag the olein into the crystals, decreasing the efficiency of separation (Kellens *et al*., 2007). The largest crystals that can be observed during crystallization are often composed of small crystals held together by weak interactions. Thus, this agglomeration may lead to lower separation efficiency due to a high drag of liquid in the agglomerates.

The crystallization curves (Figure 2) presented different profiles in different temperature ranges. After deconvolution, the curves revealed some sub-events associated with the crystallization of different TAG species. The thermograms were divided into three temperature ranges that were associated with the sub-events involving high, medium and low melting temperature TAGs. A first sub-event was associated with TAGs with crystallization temperature above 14 °C; a second sub-event was associated with TAGs with crystallization temperatures between 6 and 14 °C; and a third TAG-associated sub-event with crystallization temperatures below 6 °C. The enthalpies associated with these sub-events were calculated and are presented in Table 3.

When the temperature was reduced and the JKO started to crystallize (Figure 2), a small crystallization peak was observed near 15 °C with 0.8 J/g enthalpy (7.4% total enthalpy) associated with high melting TAGs, overlapping the larger enthalpy of crystallization peaks of 9.5 J/g (88% total enthalpy) associated with medium melting TAGs (Table 3). This peak overlap, as well as the presence of a broad peak, is due to the crystallization of more than one TAG species in the same temperature range due to the complexity of the structures of these compounds. The sharpness of a DSC peak indicates the cooperative nature of the transition from TAG composition. If the transition occurs in a narrow temperature range, it is highly cooperative. Therefore, the crystallization (or melting) of two or more TAG structures could take place simultaneously in a certain temperature range, resulting in a broad or overlapping DSC peak (Tan and Che Man, 2002).

The olein crystallization curve from dry fractionation was similar to the JKO curve, but with slight differences in the enthalpies in each temperature range, *i.e.*, a decrease in the enthalpy fraction associated with high melting TAGs (0.2 J/g, 2.6% total enthalpy) and an increase associated to medium melting TAGs (7.3 J/g, 93.6% total enthalpy) (Table 3). The crystallization olein peaks of the solvent fractionation occurred at lower temperatures compared to JKO and stearins. A relevant increase in enthalpy associated with low melting TAGs (5.5 J/g, 70.5% total enthalpy) was also observed, as well as a decrease in enthalpy associated with medium melting TAGs (2.3 J/g, 29.5% total enthalpy) and absence of those with a high melting point (Table 3).

Table 3. Absolute and relative enthalpy for crystallization and melting of JKO and its fractions obtained by dry and solvent fractionation.

			JKO	Ed	Es	Od	Os
Crystallization	Enthalpy (J/g)	<6 °C	0.5±0.1	0.0±0.0	0.0±0.0	0.3±0.0	5.5±0.5
		6-14 °C	9.5±0.3	4.0±0.4	4.4±0.5	7.3±0.4	2.3±0.4
		>14 °C	0.8±0.2	0.5±0.1	1.0±0.3	0.2±0.1	0.0±0.0
	Enthalpy (%)	<6 °C	4.6	0.0	0.0	3.8	70.5
		6-14 °C	88.0	88.9	81.5	93.6	29.5
		>14 °C	7.4	11.1	18.5	2.6	0.0
Melting	Enthalpy (J/g)	<23 °C	0.5±0.0	0.0±0.0	0.0±0.0	0.8±0.2	2.5±0.3
		23-33 °C	6.4±0.6	5.5±0.6	5.1±0.5	6.5±0.4	4.4±0.6
		>33 °C	0.5±0.1	1.4±0.3	2.1±0.4	0.5±0.1	0.4±0.1
	Enthalpy (%)	<23 °C	6.8	0.0	0.0	10.3	34.2
		23-33 °C	86.5	79.7	70.8	83.3	60.3
		>33 °C	6.8	20.3	29.2	6.4	5.5

JKO: Jerivá kernel oil, Ed: dry fractionation stearin, Es: solvent fractionation stearin, Od: dry fractionation olein, Os: solvent fractionation olein. The mean ± standard deviation (n = 2).

The stearins began to crystallize at higher temperatures compared to oil and oleins, with an increase in the enthalpy fraction associated with high melting TAGs. A slighter variation was observed for dry fraction stearin, with a relative area of 11.1% (0.5 J/g) associated with high melting TAGs, while in solvent fractionation this variation was more relevant, yielding an 18.5% enthalpy stearin associated with high melting TAGs, as well as a decrease in the enthalpy fraction associated with medium melting TAGs (Table 3).

The solvent fractionation revealed a greater ability to modify the crystallization characteristics of JKO when compared to dry fractionation. Moreover, even with the similarity in fatty acid composition (Table 1), differences in oil thermograms and fractions were observed. This reinforces the notion that the thermal characteristics of the fractions depend not only on the fatty acid composition, but also on the disposition of these fatty acids in the TAGs, as well observed for the solvent fractionation of coconut oil (Sonwai *et al*., 2017).

3.4. Melting profile

The JKO melting process started at 17.2 °C (T_{onset}) and continued at 36.0 °C (T_f), with only one broad endothermic peak at 30.9 °C (Table 2). The presence of only one endothermic transition can be characteristic of the constitution of the JKO, which should have TAGs with a less diversified structure when compared to other oils, such as palm oil, cocoa butter and some hydrogenated fats, which have fusion thermograms with a higher number of endothermic events (Tan and Che Man, 2002; Zaliha *et al*., 2004; Hinrichsen, 2016). The melting curve profile of the fractions was similar to that of oil, but with differences in initial, final and peak melt temperatures (Table 2). Similar results were found by Yantya *et al*. (2013).

After deconvolutions, the melting curves (Figure 2) also presented distinct sub-events which were divided into three temperature ranges associated with TAGs with different melting temperatures. In a first temperature range, low melting TAGs melted at temperatures below 23 °C, predominantly in oleins; in a second range, medium melting TAGs melted at temperatures between approximately 23 and 33 °C; and in a temperature range above 33 °C, high melting TAGs were melted, predominantly in stearins. The enthalpies associated with these sub-events were calculated and are presented in Table 3.

All olein melting curves changed to lower temperatures compared to JKO (Figure 2); while stearin melting curves changed to higher temperatures. The main differences were related to the concentration of high melting TAGs in stearins and of low melting TAGs in oleins. This effect was most relevant in solvent fractionation, where enthalpy associated with the melting of high melting TAGs represented 29.2% of total enthalpy, compared to 20.3% in dry fraction stearin and 6.8% in JKO, similar to Macaúba kernel oil fractions (Magalhães *et al*., 2020a). In addition, fusion enthalpy associated with low melting TAGs represented 34.2% of total enthalpy in solvent fractionation olein, compared to 10.3% and 6.8% in dry fractionation olein and JKO, respectively.

3.5. Solid fat content

The SFC curves for the JKO and their fractions (Figure 3) revealed a substantial reduction in solid fat content with increasing temperature, especially in a narrow range between 25 and 35 °C, which should be the melting temperature range of the major TAGs of these products.

The SFC curves of the fractions showed that JKO's stearins and oleins had different melting profiles, despite similar fatty acid profiles (Table 1). It is known that TAGs can pack tightly together, which influences their melting. TAGs with larger amounts of unsaturated fatty acids cannot pack as tightly together because of kinks in the fatty acid chain, leading to a lower melting point. However, it has been reported that the SFC profile does not only depend on the level of saturation or unsaturation of fatty acids in the TAG. In a study on the thermal behavior of vegetable oils with changes in fatty acids in the TAGs, the authors observed that the solid contents tended to increase when saturated fatty acids were more symmetrically distributed between the external positions of the TAGs. They concluded that the physical properties of the oils studied depended on the fatty acid distribution in the TAGs, as well as on the composition of the fatty acids themselves (Bootello *et al*., 2016). Marikkar *et al*. (2013) and Mo *et al*. (2016) also reported distinct thermal properties for oleins and stearins from coconut oil and palm oil, even with slight variations in the fatty acid compositions of the fractions.

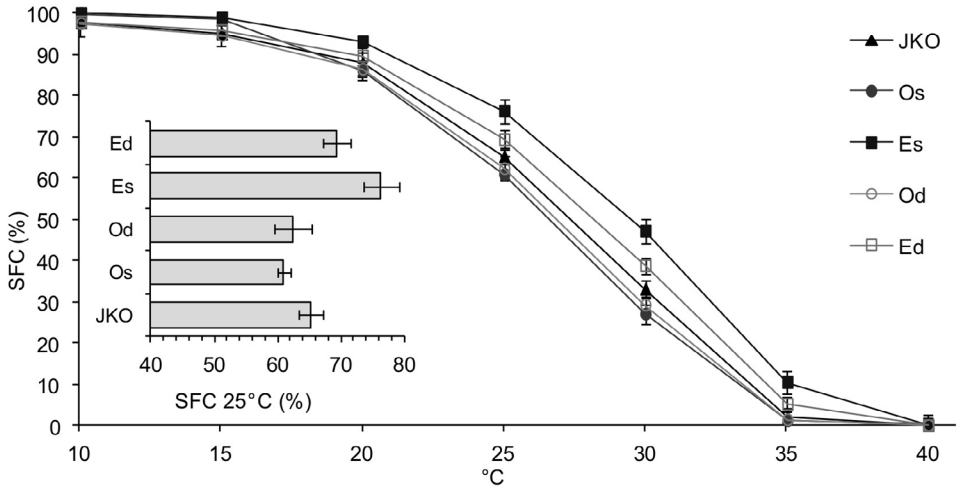

FIGURE 3. Solid Fat Content in JKO and its fractions obtained by dry and solvent fractionation. JKO: Jerivá kernel oil, Ed: dry fractionation stearin, Es: solvent fractionation stearin, Od: dry fractionation olein, Os: solvent fractionation olein. n = 2.

The oleins were completely melted at 35 °C, while stearins SFC were about 10% at this temperature. In most of the temperature ranges, oleins had lower SFC than JKO, while stearins had higher SFC, which was to be expected considering the enthalpy percentages associated with the lowest, medium and high melting TAGs previously presented (Table 3). This can be highlighted at the temperature of 25 °C (bars, Figure 3), especially for the solvent fractionation of stearin, which presented SFC above the other products throughout the temperature range, corroborating the enthalpy percentages associated with high and low melting TAGs (Table 3). The SFC at 25 °C of the solvent stearin was 17% higher than that of MKO, whereas the SFC at 25 °C of the solvent olein decreased by 7%.

The increase and decrease in SFC is expected in the stearin and olein fractions, respectively, compared with JKO after fractional crystallization. It was reported that the SFC of stearins from a dry fractionation of palm oil was higher than that of the oil and melted completely above 45 °C; while the SFC of oleins was lower than oil and entirely melted at 20 °C (Zaliha *et al*., 2004). This is because the olein fraction generally contains a higher content in low melting TAGs than oil and stearin.

The SFC curves of the fractions obtained in this work reveal that stearins and oleins have different profiles, making it possible to obtain fractions that cover varying ranges of solid fat as a function of temperature. With the increase in the solid fat content, the lipids tend to have a firmer texture, which is relevant to some applications in food formulation, mainly with higher contents close to 25 °C, which contributes to the fraction having greater resistance to melting in ambient conditions when compared to unfractionated oil (Sonwai *et al*., 2017).

3.6. Qualitative phase diagram

An experimental phase diagram (Figure 4) was obtained for the JKO and its fractions, where three phases were identified according to the visual appearance of the samples: solid, thick liquid and liquid. The phase diagram revealed that the stearins remained visually solid until higher temperatures (16 and 18 °C) when compared to the oleins (13 to 15 °C). This behavior again corroborates the distribution of the lowest and highest melting TAGs in the fractions, as well as their solid fat content.

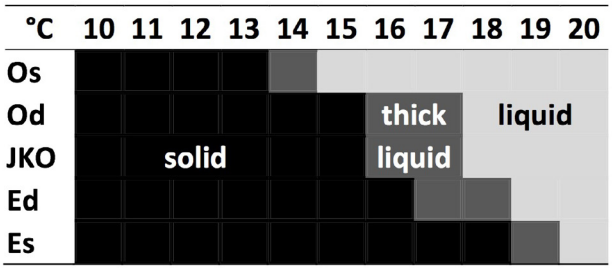

FIGURE 4. Experimental phase diagram of JKO and its fractions obtained by dry and solvent fractionation. JKO: Jerivá kernel oil, Ed: dry fractionation stearin, Es: solvent fractionation stearin, Od: dry fractionation olein, Os: solvent fractionation olein. n = 2.

The olein obtained from dry fractionation had a visual appearance similar to that of the oil, which is in agreement with the crystallization and melting thermal profiles obtained by DSC (Figures 2 and 3), indicating that the crystals may have dragged in the liquid phase. On the other hand, solvent fractionation resulted in more distinct fractions compared to JKO, with smaller liquid phase dragged in the clusters at the end of the fractionation, allowing for more effective separation and resulting in fractions with more distinct compositions. As reported by Kellens *et al*. (2007), the main advantage of solvent fractionation is the high separation efficiency and higher purity of the finished products. The solvent fractionation olein and stearin differed most from the oil in the phase diagram, with the olein visually solidified at 14 °C and the stearin at 18 °C.

4. CONCLUSIONS

This work presented a new approach which showed that the thermal characteristics of Jerivá kernel oil can be modified by fractionation, but without statistically significant differences in fatty acid profile or oxidative stability. In general, stearins had higher crystallization and melting temperatures in addition to higher SFC, unlike oleins, which may be associated with the concentration of high melting TAGs in stearins. The type of fractionation (dry or solvent) influenced the chemical and thermal properties of Jerivá kernel oil fractions, and the solvent process promoted a more relevant differentiation of the fractions in relation to the oil. Thus, it was possible to obtain an olein with 7% less solid fat at 25 °C which remained visually liquid at a temperature 2 °C below that of the oil, as well as a stearin with 17% more solid fat at 25 °C which remained visually solid at 3 °C above the oil. With these results, JKO oil can be an outstanding raw material and has the possibility of using its fractions, olein and stearin, in the food industry to produce spreads, specialty fats, ice cream, chocolate, and others products. These preliminary results may support future studies.

ACKNOWLEDGMENTS

The authors would like to thank the Central of Analysis and Chemical Prospecting of the Federal University of Lavras, Finep and Capes for supplying the equipment and technical support for experiments. This study was supported by Conselho Nacional de Desenvolvimento Científico e Tecnológico (CNPq, Brazil) and Fundação de Amparo à Pesquisa de Minas Gerais (FAPEMIG, Brazil, APQ-00638-14 and PPM-00498-16).

REFERENCES

AOCS (1993). Official Methods and Recommended Practices of the American Oil Chemists Society. Champaing.

Bootello MA, Garcés R, Martínez-Force E, Salas JJ. 2016. Effect of the distribution of saturated fatty acids in the melting and crystallization profiles of high-oleic high-stearic oils. *Grasas Aceites* **67**, e149. https://doi.org/10.3989/gya.0441161

Calliauw GH, Gibon V, De Greyt WFJ. 2007. Principles of palm olein fractionation: a bit of science behind the technology. *Lipid Technol.* **19**, 152–155. https://doi.org/10.1002/lite.200700050

Chaleepa K, Szepes A, Ulrich J. 2010. Effect of additives on isothermal crystallization kinetics and physical characteristics of coconut oil. *Chem. Phys. Lipids* **163**, 390–396. https://doi.org/10.1016/j.chemphyslip.2010.03.005

Cobo M, Deublein E, Haber A, Kwamen R, Nimbalkar M, Decker F. 2017. TD-NMR in Quality Control: Standard Applications, in Webb G (Ed.) *Modern Magnetic Resonance*. Springer, Cham, pp. 1819-1836. https://doi.org/10.1007/978-3-319-28388-3_12.

Coimbra MC, Jorge N. 2011. Characterization of the Pulp and Kernel Oils from *Syagrus oleracea*, *Syagrus romanzoffiana*, and *Acrocomia aculeata*. *J. Food Sci.* **76**, 1156–1161. https://doi.org/10.1111/j.1750-3841.2011.02358.x

Coimbra MC, Jorge N. 2012. Fatty acids and bioactive compounds of the pulps and kernels of Brazilian palm species, guariroba (*Syagrus oleraces*), jerivá (*Syagrus romanzoffiana*) and macaúba (*Acrocomia aculeata*). *J. Sci. Food Agric.* **92**, 679–684. https://doi.org/10.1002/jsfa.4630

Falasca SL, Miranda del Fresno C, Ulberich A. 2012. Possibilities for growing queen palm (*Syagrus romanzoffiana*) in Argentina as a biodiesel producer under semi-arid climate conditions. *Int. J. Hydrogen Energy* **37**, 14843–14848. https://doi.org/10.1016/j.ijhydene.2011.12.092

Gunstone FD. 2010. Lauric oils. *Lipid Technol.* **22**, 168–168. https://doi.org/10.1002/lite.201000035

Gunstone FD, Harwood JL, Padley FB. 1994. *The Lipid Handbook*. 2nd ed, CRC Press, London, UK.

Grall DS, Hartel RW. 1992. Kinetics of butterfat crystallization. *J. Am. Oil Chem. Soc*. **69** (8), 741–747. https://doi.org/10.1007/BF02635909

Hinrichsen N. 2016. Commercially available alternatives to palm oil. *Lipid Technol*. **28** (3), 65-67. https://doi.org/10.1002/lite.201600018

Kellens M, Gibon V, Hendrix M, De Greyt W. 2007. Palm oil fractionation. *Eur. J. Lipid Sci. Technol.* **109**, 336–349. https://doi.org/10.1002/ejlt.200600309

Lescano CH, de Oliveira IP, Freitas de Lima F, Baldivia DS, Justi PN, Cardoso CAL, Raposo Júnior JL, Sanjinez-Argandoña EJ. 2018. Nutritional and chemical characterizations of fruits obtained from *Syagrus romanzoffiana*, *Attalea dubia*, *Attalea phalerata* and *Mauritia flexuosa*. *J. Food Meas. Charact.* **12**, 1284–1294. https://doi.org/10.1007/s11694-018-9742-3

Magalhães KT, Tavares TS, Gomes TMC, Nunes CA. 2020b. Effect of process variables on the yield and quality of jeriva (*Syagrus romanzoffiana*) kernel oil from aqueous extraction. *Grasas y Aceites* **71**, 339. https://doi.org/10.3989/gya.1063182

Magalhães KT, Tavares TS, Nunes CA. 2020a. The chemical, thermal and textural characterization of fractions from Macauba kernel oil. *Food Res. Int.* **130**, 108925. https://doi.org/10.1016/j.foodres.2019.108925

Marikkar JMN, Saraf D, Dzulkifly MH. 2013. Effect of Fractional Crystallyzation on Composition and Thermal Behavior of Coconut Oil. *Int. J. Food Prop.* **16**, 1284–1292. https://doi.org/10.1080/10942912.2011.585728

Márquez AL, Pérez MP, Wagner JR. 2013. Solid fat content estimation by differential scanning calorimetry: Prior treatment and proposed correction. *J. Am. Oil Chem. Soc.* **90**, 467–473. https://doi.org/10.1007/s11746-012-2190-z

Mo S-Y, Teng K-T, Nesaretnam K, Lai O-M. 2016. Similar physical characteristics but distinguishable sn-2 palmitic acid content and reduced solid fat content of chemically interesterified palm olein compared with native palm olein by dry fractionation: A lab-scale study. *Eur. J. Lipid Sci. Technol.* **118**, 1389–1398. https://doi.org/10.1002/ejlt.201500305

Moreira MAC, Payret Arrúa ME, Antunes AC, Fiuza TER, Costa BJ, Weirich Neto PH, Antunes SRM. 2013. Characterization of *Syagrus romanzoffiana* oil aiming at biodiesel production. *Ind. Crops Prod.* **48**, 57–60. https://doi.org/10.1016/j.indcrop.2013.04.006

Pierezan L, Cabral MRP, Martins Neto D, Stropa JM, Oliveira, LCS, Scharf DR, Simionatto EL, Silva RCL, Simionatto E. 2015. Chemical composition and crystallization temperatures of esters obtained from four vegetable oils extracted from seeds of Brazilian cerrado plants. *Quim. Nova* **38**, 328–332. https://doi.org/10.5935/0100-4042.20150018

Pittenger DR, James Downer A, Hodel DR, Mochizuki M. 2009. Estimating water needs of landscape palms in mediterranean climates. *Horttechnology* **19**, 700–704. https://doi.org/10.21273/HORTSCI.19.4.700

Rocha JCB, Lopes JD, Mascarenhas MCN, Arallano DB, Guerreiro LMR, Cunha RL. 2013. Thermal and rheological properties of organogels formed by sugarcane or candelilla wax in soybean oil. *Food Res. Int.* **50**, 318–323. https://doi.org/10.1016/j.foodres.2012.10.043

Rodrigues-Ract JN, Cotting LN, Poltronieri TP, Silva RC, Gioielli LA. 2010. Crystallization behavior of structured lipids by chemical interesterification of milkfat and sunflower oil. *Food Sci. Technol.* **30**, 258–267. https://doi.org/10.1590/S0101-20612010000100038

Rossell JB. 1985. Fractionation of lauric oils. *J. Am. Oil Chem. Soc.* **62**, 385–390. https://doi.org/10.1007/BF02541409

Silva RC da, Escobedo JP, Gioielli LA. 2008. Crystallization behavior of structured lipids by chemical interesterification of milkfat and sunflower oil. *Quim. Nova* **31**, 330–335. https://doi.org/10.1590/S0101-20612010000100038

Sonwai S, Rungprasertphol P, Nantipipat N, Tungvongcharoan S, Laiyangkoon N. 2017. Characterization of Coconut Oil Fractions Obtained from Solvent Fractionation Using Acetone. *J. Oleo Sci.* **66**, 951–961. https://doi.org/10.5650/jos.ess16224

Tan CP, Che Man YB. 2002. Differential scanning calorimetric analysis of palm oil, palm oil based products and coconut oil: effects of scanning rate variation. *Food Chem.* **76**, 89–102. https://doi.org/10.1016/S0308-8146(01)00241-2

Ullah R, Nadeem M, Ayaz M, Muhammad I, Muhammad T. 2016. Fractionation of chia oil for enrichment of omega 3 and 6 fatty acids and oxidative stability of fractions. *Food Sci. Biotechnol.* **25**, 41–47. https://doi.org/10.1007/s10068-016-0006-x

Yantya NAM, Marikkar JMN, Shuhaimia M. 2013. Effect of fractional crystallization on the composition and thermal properties of engkabang (*Shorea macrophylla*) seed fat and cocoa butter. *Grasas Aceites* **64** (5), 546-553. https://doi.org/10.3989/gya.023213

Zaliha O, Chong C, Cheow C, Norizzah AR, Kellens MJ. 2004. Crystallization properties of palm oil by dry fractionation. *Food Chem.* **86**, 245–250. https://doi.org/10.1016/j.foodchem.2003.09.032

GRASAS Y ACEITES 72 (3)
July-September 2021, e421
ISSN-L: 0017-3495
https://doi.org/10.3989/gya.0449201

Selection criteria for yield in safflower (*Charthamus tinctorius* L.) genotypes under rainfed conditions

H. Koç ✉

Bahri Dagdas International Agricultural Research Institute, Konya, Turkey
✉Correspondence: koc175@hotmail.com

Submitted: 21 April 2020; Accepted: 30 June 2020; Published online: 17 September 2021

SUMMARY: This research was conducted on 20 safflower genotypes and lasted 3 years (2014-2016) in the Central Anatolia Region of Turkey. The experiments were conducted in randomized block design with four replications. The relationships among yield 9 other traits in safflower genotypes were investigated. As the average of three years, the greatest seed yield (SY) was obtained from genotype G5 (PI 451952) with 3156.3 kg·ha^{-1}. It was followed by genotypes G4 (PI 525458) and G9 (PI 306686) with 3013.2 and 2977.1 kg·ha^{-1}, respectively. Among the standard cultivars, the greatest seed yield (2750.4 kg·ha^{-1}) was obtained from the Dinçer cultivar. The greatest oil content (OC) was obtained from the genotype G11 (PI 537665) with 36.5%. It was followed by the genotypes G9 (PI 306686) (35.4%), G6 (PI 537598) (35.4%) and G14 (PI 560169) (35.3%). Oil contents varied between 29.1-36.5%. Yield-trait relationships were assessed through both correlation analysis and GT (Genotype by Trait) biplot analysis. Based on the results of the two approaches, plant height (PH), number of branches (NB), number of heads (NH) and thousand-seed weight (TSW) were identified as the most significant selection criteria for yield from safflower. The combined use of correlation and biplot analysis in the assessment of relationships among the traits improved the chance for success.

KEY WORDS: *Correlation; GT (Genotype by Trait)-biplot; Safflower; Selection; Yield*

RESUMEN: ***Criterios de selección para el rendimiento en genotipos de cártamo (*Charthamus tinctorius *L.) en condiciones de secano*.** Esta investigación se realizó con 20 genotipos de cártamo durante 3 años (2014-2016) en la región de Anatolia central de Turquía. Los experimentos se realizaron en bloques de diseño aleatorio con cuatro repeticiones. Se investigaron las relaciones de rendimiento con los otros rasgos y las relaciones genotipo-rasgo en plantas de cártamo. Como promedio de tres años, el mayor rendimiento de semillas (SY) se obtuvo del genotipo G5 (PI 451952) con 3156,3 kg·ha^{-1}. Le siguieron los genotipos G4 (PI 525458) y G9 (PI 306686) con 3013,2 y 2977,1 kg·ha^{-1} respectivamente. Entre los cultivares estándar, el mayor rendimiento de semilla (2750,4 kg·ha^{-1}) se obtuvo del cultivar Dinçer. El mayor contenido de aceite (OC) se obtuvo del genotipo G11 (PI 537665) con 36,5%. El contenido de aceite varió entre 29,1 - 36,5%. Las relaciones rendimiento-rasgo se evaluaron mediante análisis de correlación y análisis biplot GT (Genotipo por rasgo). Con base en los resultados de dos enfoques, la altura de la planta (PH), el número de ramas (NB), el número de cabezas (NH) y el peso de miles de semillas (TSW) se identificaron como los criterios de selección más importantes para el rendimiento en el cártamo. El uso combinado de análisis de correlación y biplot en la evaluación de las relaciones entre los rasgos mejoró la posibilidad de éxito.

***PALABRAS CLAVE*:** *Cártamo; Correlación; GT (genotipo por rasgo)-biplot; Rendimiento; Selección*

Citation/Cómo citar este artículo: Koç H. 2021. Selection criteria for yield in safflower (*Charthamus tinctorius* L.) genotypes under rainfed conditions. *Grasas Aceites* **72** (3), e421. https://doi.org/10.3989/gya.0449201

1. INTRODUCTION

Safflower (*Charthamus tinctorius* L.) requires less water than other oil crops such as rapeseed (*Brassica napus ssp. oleifera* L.), sunflower (*Helianthus annuus* L.) and soybean *(Glycine max* L. Merr.*)* and it is quite well adapted to dry conditions. Thus, it had become a salient crop in the midst of present climate change and global warming trends. Safflower is an important oil crop both for cooking oil and biodiesel production. High drought resistance provides significant advantages to safflower over other oil crops in cropping patterns (Kose, 2017).

Low yield and decreased percentage are the basic limitation in safflower production. Therefore, plant improvement studies mostly focused on the development of new safflower lines with high seed yield and more oil content so as to meet the demands of growers and the industry (Koç *et al.,* 2010).

Success of a breeding program is directly related to the proper selection of yield components at every stage of the program, efficient interpretation and use of resultant data (Flores *et al.,* 1998; Rubio *et al.,* 2004; Baljani *et al.,* 2015).

In breeding programs for high yield cultivars, the assessment of yield and highly-heritable characteristics may improve the chance for success. Therefore, while generating breeding programs, it is useful to know the relationships among the characteristics. The ultimate target in safflower breeding is to develop new and superior cultivars with high seed yield and oil content. Breeders search for reliable selection criteria and then select the characteristics which are directly or indirectly related to yield. Especially in the early stages (F2-F5) with insufficient seed quantity for yield experiments, yield-related parameters play an important role.

Genotype selection brings a new dimension to the complexity and difficulty of plant breeding programs. Multiple breeding targets should be taken into consideration when selecting genotypes and recommending cultivars. In fact, plant breeding not only improves the yield of a plant, but also integrates high yield with the desired parameters like quality and performance (Yan *et al*., 2019a).

Despite reasonable values for the other parameters, genotypes with a value for a certain trait below the minimum requirements are hard to register. For instance, high quality is a valuable trait only when it is related to high yield; a high-quality genotype with a low yield will not be registered as a cultivar. Therefore, it is quite significant to take entire key traits into consideration when selecting genotypes and/or agronomic methods (Yan *et al*., 2019b).

The genotype – trait (GT) biplot procedure of GGE biplot method is used to assess the different traits of the genotypes. GT biplot allows the user to make visual assessments of genotype-trait data. Compared to conventional methods, the GT biplot approach has some advantages: 1. Graphical presentation of the data improves comprehension of data patterns; 2. It is easy to interpret, facilitate the comparison of genotypes or traits and efficiently presents the relationships among the investigated traits; 3. It is easy to see which genotype is winning or losing in which trait; 4. It can be used in multi-trait-based selections and in the comparison of selection strategies (Yan *et al*., 2007). While correlation analysis identifies the level of relationship between the traits, the GT biplot is able to put forth both the relationships among the traits and genotype – trait relationships (Yan and Reid, 2008).

In this study, the GT (Genotype by Trait) biplot technique and correlation analysis were used together to investigate the Genotype-Trait relationships and the relations among the traits.

The aim of this study is for the findings to be useful for safflower breeders and safflower producers who are concerned with increasing seed yield with the data obtained.

2. MATERIALS AND METHODS

This research was carried out with 20 genotypes (Table 1) over 3 years (2014-2016) in the Central Anatolia Region of Turkey. The experiments were conducted in randomized block design with 4 replications. The plot size was 6 m^2 (1.2 x 5 m) and seeds were sown with an experimental sowing machine. Sowing was performed in the last week of March so as to have 125 seed per m^2. Harvest was carried out in the second week of August with a plot combine harvester.

The experimental soils were of a clay texture with a moderate organic material level (2.3%) and high lime content (29%). The soils were slightly alkaline (pH 7.8), rich in phosphorus and potassium and deficient in zinc. There were no salinity problems at the research site.

Monthly average temperatures during the experimental years were close to long-term averages

TABLE 1. Name and origin of the studied safflower genotypes

Entry	Genotip	Code	Accession number	Origin
1	28-2	G1	PI 537110	Mexico
2	11-1	G2	PI 560172	United States
3	77-2-a	G3	PI 537606	United States
4	82-3	G4	PI 525458	United States
5	25-4-b	G5	PI 451952	India
6	106-2	G6	PI 537598	United States
7	Göktürk	Göktürk	BDYAS-4	Turkey
8	63-2-b	G7	PI 537702	United States
9	Dinçer	Dinçer	GKTAE	Turkey
10	64-3-b	G8	PI 537703	United States
11	91-2	G9	PI 306686	Israel
12	Linas	Linas	TTAE	Turkey
13	Balcı	Balcı	EGKTAE	Turkey
14	77-1-d	G10	PI 537607	United States
15	89-1-c	G11	PI 537665	United States
16	13-2-c	G12	PI 537607	United States
17	96-3	G13	PI 544059	China
18	56-2-c	G14	PI 560169	United States
19	52-1	G15	PI 307056	Mexico
20	83-1-a	G16	PI 537694	United States

(Table 2). On the other hand, total temperatures throughout the vegetation period (March - August) were 5.8 °C greater in 2014 and 2016 than the long-term averages (104.8 °C).

Total precipitation was measured as 366 mm in 2014 (44 mm greater than the long-term average), as 309 mm in 2015 (close to long-term average of 322 mm) and as 201 mm in 2016 (121 mm lower than long-term average) (Table 2).

Observations and measurements: Seed yield (kg·ha^{-1}), oil content (%), oil yield, plant height (cm), number of days to 50% flowering, number of branches, number of heads, head diameter (cm), thousand-seed weight (g).

Variance analyses were run on the data obtained from 20 safflower genotypes. A linear correlation analysis was applied pairwise to all the parameters studied, yield (SY) and other traits (OC, OY, PH, NDF, NB, NH, HD, and TSW). The experimental data were subjected to variance and correlation analyses with the aid of JMP 5.0 software. Significant means were compared with the aid of the LSD test. A GT biplot analysis for the visual assessment of Genotype – Trait relationships and the relationships among the traits was conducted with the use of XLSTAT software. The GT biplot analysis was employed to display the two-way relationship between genotype and trait. It was based on the following formula:

$$\frac{Tij - \beta j}{Sj} = \sum_{n=1}^{2} \lambda n \xi in \eta jn + \varepsilon ij = \sum_{n=1}^{2} \xi * in\eta * jn + \varepsilon ij$$

where T_{ij} is the average value for genotype i for trait j; β_j is the average value for all genotypes in trait j; S_j is the standard deviation of trait j among the genotype averages; λ_n is the singular value for principal component PC_n; ξ_{in} and η_{jn} are scores for genotype I and trait j on PC_n, respectively; and ϵ_{ij} is the residual associated with genotype i in trait j. To achieve symmetric scaling between the genotype

TABLE 2. Monthly precipitation (mm) and monthly temperature averages (C0) for years and during years (1929-2016) of the experiment

		Months												
	Years	**Jan.**	**Feb.**	**Mar**	**Apr**	**May**	**June**	**July**	**Aug.**	**Sept**	**Oct**	**Nov.**	**Dec.**	**TOT**
Prep.	**2014**	58.8	17.4	20.4	19.2	26	31.4	3	4.6	31.4	89.6	32.2	32.1	366
	2015	24.6	23.5	55.9	7.6	53.2	39.6	8.6	17.2	31.4	39.0	5.8	2.6	309
	2016	42.4	2.8	37.8	9.4	35.2	18.4	0.2	0.0	23	0.0	16.0	16.4	201
	Long years	38	29	28	32	43	24	6	5	13	30	32	42	322
Temp.	**2014**	2.4	6.4	7.2	12.3	15.5	19.7	25.1	25.0	22.6	15.8	5.8	5.5	163
	2015	0.7	4.8	5.9	8.1	15.7	18.7	24.0	24.6	21.8	14.6	7.9	-0.8	146
	2016	0.1	6.8	7.7	14.5	15.9	22.2	24.9	19.6	17.9	12.8	7	2	151
	Long years	-0.3	1	5.7	11	15.8	20.4	23.6	23.2	18.7	12.6	5.9	1.5	139

TOT: Total, Prep: Precipitation, Temp: Temperature

scores and the trait scores the singular value λ_n had to be absorbed by the singular vector for genotypes ξ_{in} and that for traits η_{jn}. That is, $\xi^{in} = \lambda^{n.5}\ \xi_{in}$ and $\eta^{jn} = \lambda^{n.5}\ \eta_{jn}$. Only PC1 and PC2 were retained in the model because such a model tends to be the best for extracting pattern and rejecting noise from the data. The GT biplot was generated by plotting ξ^{i1} and ξ^{i2} against η^{j1} and η^{j2}, respectively, so that each genotype or trait was represented by a marker in the biplot. In the GT biplot, a vector was drawn from the biplot origin to each marker of the traits to facilitate visualization of the relationships between and among the traits (Yan and Rajcan, 2002; Akçura, 2011).

3. RESULTS AND DISCUSSION

The variance analysis revealed that there were significant differences among all the traits of the genotypes ($P < 0.01$). Year x genotype interaction was also found to be significant for all traits, except for head diameter (HD) (Table 3).

For the average of the three years, genotype G5 had the greatest seed yield (SY) with 3156.3 kg·ha^{-1}. It was followed by genotypes G4 and G9 (with 3013.2 and 2977.1 kg·ha^{-1}) (Table 4). Among the standard cultivars, the greatest seed yield (2750.4 kg·ha^{-1}) was obtained from the Dinçer cultivar. The greatest oil content (36.5%) was observed in genotype G11 and it was followed by genotypes G9 (35.4%), G6 (35.4%) and G14 (35.3%). The oil contents in the genotypes varied from 29.1 - 36.5%. The oil yield (OY) values, calculated by multiplying seed yield by oil content, varied from 717.9 - 1058.6 kg·ha^{-1}.

Plant height (PH) values varied from 67.8 - 81.5 cm. Ideal safflower plant heights for machine harvest should be between 60 - 80 cm (Weiss, 2000). All the present genotypes yielded plant heights within this range. The number of days to flowering (NDF) values varied from 68 - 76 days; the number of branches

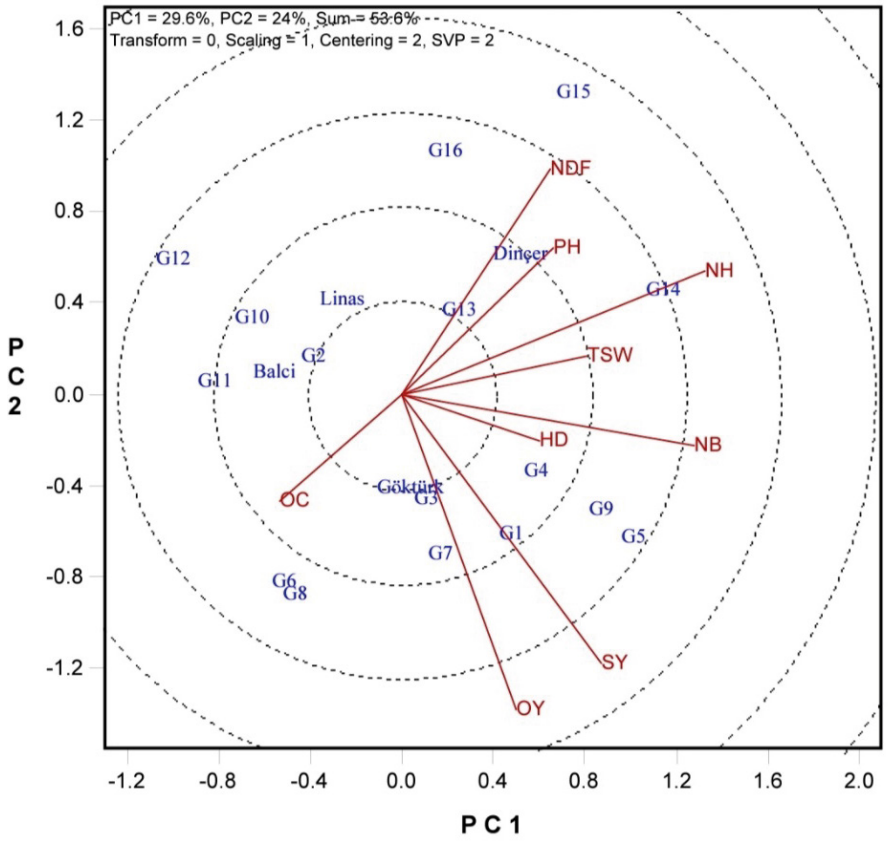

FIGURE 1. Vector view of genotype by trait biplot, showing the interrelationship among all measured traits for 20 different safflower genotypes. Traits: SY: Seed Yield, OC: Oil Content, OY: Oil Yield, PH: Plant Height, NDF: Number of Days to %50 Flowering, NB: Number of Branches, NH: Number of Heads, HD: Head Diameter, TSW: Thousand-Seed Weight

Table 3. Analysis of the combined variance of the properties studied

SV	DF	SY	OC	OY	PH	NDF	NB	NH	HD	TSW
		MS	MS	MS	MS	MS	MS	MS	MS	MS
Replication	3	3541**	0.9	383**	98	4.6*	0.7	3*	0.06	0.3
Year	2	278845**	43**	30859**	10194**	3222**	18**	89**	0.01	81**
Genotyp	19	7674**	42**	1021**	138**	48**	7.4**	13**	0.06*	58**
Year x Genotyp	38	6179**	9**	870**	97**	34**	1.2*	5.8**	0.04	30**
Error	177	575	0.4	65	38	1.6	0.7	1.0	0.04	0.8
Total	239	4396**	5.5**	530**	141**	37**	1.5**	3.4**	0.04	11**

SV: Source of Variance, **DF**: Degrees of Freedom, MS: Mean Square, **P<0.01 significant, *P<0.05 significant
SY: Seed Yield, **OC**: Oil Content, **OY**: Oil Yield, **PH**: Plant Height, **NDF**: Number of Days to %50 Flowering, NB: Number of Branches, **NH**: Number of Heads, **HD**: Head Diameter, **TSW**: Thousand Seed Weight**(g)**

Table 4. Mean yield and yield components (4 replications) of 20 safflower genotypes tested over 3 (2014-2016) years

Code	SY	OC	OY	PH	NDF	NB	NH	HD	TSW
G5	3156.3 a	32.34 g	1024.2 ab	76.9 abc	71.3 fg	6.2 ab	6.7 bc	2.30a-d	41.5def
G4	3013.2 ab	32.89 ef	978.7 bcd	76.4 bcd	73.0cde	5.5 bcd	6.0 cde	2.35 ab	39.1 k
G9	2977.1 abc	35.46 b	1058.6 a	77.2 abc	72.5cde	6.4 a	6.6 bc	2.25a-d	41.2 fg
G7	2975.4 abc	32.05 g	947.0 cde	69.9 fg	70.7 g	5.2 cde	5.6 def	2.37 a	40.2 hı
G3	2955.2 bc	32.91 ef	968.9 bcd	71.5 d-g	71.4 fg	5.0 def	5.9 cd	2.17 d	42.1cde
G1	2892.9 bcd	33.24 de	967.3 bcd	73.8 b-f	69.5 h	5.5 bcd	6.0 cde	2.33abc	43.7 b
G8	2854.1 bcd	33.68 cd	967.6 bcd	67.8 g	69.2 h	4.7 efg	4.9 fg	2.26a-d	40.0hıj
G6	2819.5 cde	35.45 b	1009 abc	70.2 efg	69.2 h	4.3 fgh	5.0 fg	2.18 cd	42.3 cd
Dinçer	2750.4 def	29.11 h	803.6 ıj	78.4 ab	71.4 fg	5.8 abc	6.3 bcd	2.16 d	41.3 fg
G2	2640.9 efg	32.08 g	849.5 ghi	71.7 d-g	73.2bcd	4.4 fgh	4.9 fg	2.35 ab	37.5 m
Göktürk	2635.7 e-h	34.19 c	897.1 efg	71.6 d-g	68 hı	6.4 a	6.1 cde	2.18 cd	39.8ıjk
G14	2634.7 e-h	35.33 b	935.2 def	78.4 ab	74.0 b	5.7 a-d	8.5 a	2.37 a	42.7 c
G13	2582.7 f-ı	33.23 de	858.1 ghı	75.4 bcd	72.0 ef	4.6 efg	5.8 cde	2.32a-d	45.5 a
Linas	2557.6 f-ı	35.02 b	895.5 efg	81.5 a	72.5 de	4.1 gh	5.3 efg	2.19bcd	40.6 gh
Balcı	2497.4 g-j	35.00 b	873.2 fgh	72.5 e-g	71.3 fg	4.7 efg	5.3 efg	2.16 d	39.9hıj
G10	2442.7 h-k	33.39 de	816.5 hıj	74.3 b-f	70.5 g	4.2 gh	4.8 fg	2.20bcd	41.7def
G15	2421.6 ı-k	29.51 h	717.9 k	73.0 c-f	73.5 bc	6.0 ab	7.9 a	2.18 cd	45.2 a
G16	2401.1 ı-k	32.48 fg	779.1 jk	73.8 b-f	76.2 a	5.0 def	6.9 b	2.31a-d	39.3 jk
G11	2336.0 jk	36.46 a	853.4 ghı	71.8 d-g	68.9 hı	4.7 efg	5.5 def	2.23a-d	37.7 lm
G12	2297.6 k	33.67 c	779.3 jk	75.2 b-e	71.1 fg	3.8 h	4.5 g	2.24a-d	38.2 l
LSD (%5)	187.2	0.51	64.9	4.9	1.0	0.3	0.8	0.15	0.7
CV (%)	8.5	1.8	8.7	8.0	1.8	15	16	8	2.2

SY: Seed Yield (kg·ha^{-1}), OC: Oil Content (%), OY: Oil Yield (kg·ha^{-1}), PH: Plant Height (cm), NDF: Number of Days to %50 Flowering, NB: Number of Branches, NH: Number of Heads, HD: Head Diameter (cm), TSW: Thousand-Seed Weight (g)

Table 5. Correlation coefficients among characteristics of safflower genotypes

	SY	OC	OY	PH	NDF	NB	NH	HD	TSW
SY	1.00								
OC	0.03NS	1.00							
OY	0.96**	0.30**	1.00						
PH	0.56**	-0.07 NS	0.51**	1.00					
NDF	0.15*	0.13*	0.17**	0.009 NS	1.00				
NB	0.16*	-0.20**	0.09 NS	0.24**	-0.16*	1.00			
NH	0.44**	-0.05 NS	0.40**	0.47**	0.34**	0.48**	1.00		
HD	0.06 NS	0.002 NS	0.06 NS	0.14*	0.02 NS	0.13*	0.20**	1.00	
TSW	0.18**	-0.08 NS	0.15 *	0.04 NS	0.19**	0.07 NS	0.26**	0.09 NS	1.00

**Significant at P < 0.01, * Significant at P < 0.05and NS: not significant.
SY: Seed Yield, **OC**: Oil Content, **OY**: Oil Yield, **PH**: Plant Height, **NDF**: Number of Days to 50% Flowering, NB: Number of Branches, **NH**: Number of Heads, **HD**: Head Diameter, **TSW**: Thousand-Seed Weight.

(NB) varied from 3.8 - 6.4; the number of heads per plant (NH) varied from 4.5 - 8.5; head diameters (HD) varied from 2.16 - 2.37 cm; and thousand-seed weights (TSW) varied from 37.5 - 45.5 g.

Correlation coefficients among the investigated traits are provided in Table 5 and the genotype – trait (GT) biplot graph is presented in Figure 1.

Seed yield (SY) showed significant positive correlations with oil yield (OY), plant height (PH), number of days to flowering (NDF), number of branches (NB), number of heads (NH) and thousand-seed weight (TSW). Seed yield (SY) had insignificant correlations with oil content (OC) and head diameter (HD).

Safflower breeding programs are implemented to obtain seed yield components, to determine the relationships among these components and to identify proper selection criteria. Similar to the present study, Mozaffari and Asadi (2006), Camas *et al.* (2007), Hussein *et al*. (2018) and Ali *et al*. (2020) reported the number of heads per plant as the most significant yield component and indicated significant correlations between seed yield and number of heads per plant.

Koç *et al.* (2010) conducted studies on safflower genotypes and reported significant positive correlations between number of days to flowering and seed yield. In the present study, a significant positive correlation (r = 0.15*) was observed between seed yield and number of days to flowering at the 5% level (Table 5). The lower level of significance in the present study compared to previous studies was mainly attributed to the effects of environmental factors on the number of days to flowering. Especially under water stress conditions, plants pass into the generative stage faster. The levels of relationships between seed yield and number of days to flowering is higher and positive under normal climate conditions, but weaker under stress conditions. Plant height is also used as a selection criterion for safflower. Alizadeh (2005), Arslan (2007), Coşge and Kaya (2008), Nabloussi *et al*. (2008), Eslam *et al*. (2010) and Koç *et al.* (2010) conducted research on safflower genotypes and reported significant positive correlations between seed yield and plant height. Similar to those studies, a significant positive correlation (r = 0.56**) was observed between seed yield and plant height in this study (Table 5).

Branching is an important parameter for the number of heads per plant. Thus, the number of branches increases seed yield. Similar to the present study, Camas *et al*. (2007), Golkar *et al*. (2012), Ali *et al*. (2020) also reported significant positive correlations between seed yield and number of branches.

Head diameter is an important morphological trait of safflower. However, the correlations between seed yield and head diameter were not found to be significant (r = 0.06) (Table 5). Akbar and Kamran (2006), Baljani *et al*. (2015), Hussein *et al*. (2018) and Ali *et al*. (2020) reported significant positive correlations between seed yield and head diameter. There were significant positive correlations between thousand-seed weight and seed yield in the present study. Head diameter alone does not influence seed yield, but becomes significant with the number of

heads. High seed yields are achieved with both greater number of heads and greater head diameters and head diameter alone is not significant for seed yield.

Oil content (OC) showed significant positive correlations with oil yield (OY), number of days to flowering (NDF) and number of branches (NB). While seed yields are mainly influenced by environmental conditions, plant genetics play a key role in oil content (Kaya *et al*., 2009). Therefore, it is not efficient to select genotypes for oil content based on morphological traits.

Oil yield (OY) had insignificant correlations with number of days to flowering (NDF) and head diameter (HD), but had significant positive correlations with the other traits (Table 5).

The crude oil yield of safflower is calculated from the crude oil ratio and seed yield values. Therefore, the factors influencing oil content and seed yield also influence oil yield. Therefore, it is possible to state that all factors influencing seed yield also influence crude oil yield (Oztürk *et al*., 2009).

The GT biplot graph showed two principle components (PC1 and PC2) and explained 53.6% of total variation (PCI 29.6% and PC2 24%) (Figure 1). High explanation ratios are desired in GT biplot graphs since such graphs allow researchers to better and more reliably assess experimental data (Yan *et al*., 2007).

Provided that the biplot graph sufficiently explains total variation (≥ 50%), the correlation coefficient is almost equal to the *cosine* of the angle between the vectors of two traits (Kroonenberg, 1995).

A correlation coefficient (r) is positive when the angle between the vectors of two traits is < 90°, negative when the angle is > 90° and independent (0) when the angle is 90°. The traits with longer vector lengths are more susceptible to genotype combinations; the traits with shorter vector lengths are less susceptible to genotype combinations (Rad *et al*., 2013). According to the present biplot graph, the angle of seed yield (SY) vector with oil yield (OY), head diameter (HD), number of branches (NB), thousand-seed weight (TSW), number of heads (NH) and plant height (PH) vectors was < 90o (Figure 1). Seed yield had significant positive correlations with these traits. The angle of seed yield (SY) vector with number of days to flowering (NDF) and oil content (OC) was about 90o (Figure 1). Therefore, seed yield had insignificant correlations with these traits (r = cos 90 = 0). The angle between the oil content (OC) and oil yield (OY) vectors was < 90o and there was a positive correlation between these traits (r = cos 0 = +1 and r = cos 60 = 0.5). The angle of oil content (OC) vector with seed yield (SY) and head diameter (HD) vectors was about 90º, thus the correlation coefficient was almost zero (0), indicating insignificant correlations (r = cos 90= 0). The angle of oil content (OC) vector with number of days to flowering (NDF), number of heads (NH), thousand-seed weight (TSW) and number of branches (NB) vectors was >90, thus oil content had negative correlations with these traits (r = cos 120 = -0.5 and r = cos 180= -1). Since oil yield was calculated from seed yield and oil content values, it yielded similar outcomes with these traits. Although the biplot analysis was developed for the analysis of genotype x environment interactions on seed yield, such as quantitative traits, it is also used to assess the relationships between the agronomic traits of the genotype (Yan and Kang, 2003).

With regard to genotype-trait relationships, it was observed that the genotypes G5, G4, G9 and G1 were prominent for seed yield (SY); G6, G11, Linas, Balcı and Göktürk genotypes were prominent for oil content (OC); G7, G3, G1, Göktürk, G4, G5, G9 genotypes were prominent for oil yield (OY). The genotypes Dinçer, G14 and G13 generated a difference for plant height (PH) and the genotypes G16, G13 and G15 generated a difference for number of days to flowering (NDF). The genotypes G5, G9, G4 and G1 were superior for head diameter (HD) and the genotypes G13, G15 and G14 were superior for thousand-seed weight (TSW) over the other genotypes.

The outcomes from the biplot graph (Fig.1) and correlation table (Table 5) mostly supported each other. Slight differences were attributed to normalized values for the biplot analysis and 53.6% rate of explanation of total variance by the biplot graph (PC1 and PC 2: 53.6%).

Since the GGE Biplot analysis allowed visual assessment of several traits simultaneously and thus influenced the success of selection, it was considered as an innovative approach to be used in plant breeding programs (Yau, 1995; Yan *et al*., 2007).

4. CONCLUSIONS

This study is significant in that it presented the relationships between traits through both correlation

analysis and biplot analysis. Based on the results of the two approaches, plant height (PH), number of branches (NB), number of heads (NH) and thousand-seed weight (TSW) were identified as the most significant selection criteria for yield in safflower. On the other hand, while there were significant positive correlations between seed yield (SY) and head diameter (HD) in the biplot graph, the relationships between these traits were not found to be significant in the correlation analysis.

Seed yield had insignificant correlations with number of days to flowering (NDF) in the biplot analysis, but significant correlations at 5% level in the correlation analysis. Combined use of different approaches in the assessment of relationships between the traits will improve the chance for success.

The data obtained from this study could be useful for safflower breeders and safflower producers concerned with increasing seed yield. The main traits determined in this study which affected seed yield in safflower were plant height (PH), number of branches (NB), number of heads (NH) and thousand-seed weight (TSW) and this can be used as selection criteria during safflower breeding programs.

The GT biplot graph put forth the relationships among the investigated traits of the genotypes and provided significant advantages for the selection of genotypes and cultivars to be used as parent materials in breeding programs. The method also offered practical and efficient assessment of the strong and weak points of the genotypes.

REFERENCES

Akbar AA, Kamran M. 2006. Relationship among yield components and selection criteria for yield improvement in safflower (*Cathamus tinctorious* L.). *J. Appl. Sci*. **6**, 2853-2855.

Akçura M. 2011. The relationships of some traits in Turkish winter bread wheat landraces. *Turk. J. Agric. Forestry* **35** (2), 115-125. https://doi.org/10.3923/jas.2006.2853.2855

Ali F, Yilmaz A, Chaudhary HJ, Nadeem MA, Rabbani MA, Arslan Y, Nawaz MA, Habyarımanas E, Baloch FS. 2020. Investigation of morphoagronomic performance and selection indices in the international safflower panel for breeding perspectives. *Turk. J. Agric. Forestry.* **44** (2), 103-120. https://doi.org/10.3906/tar-1902-49

Alizadeh K. 2005. Safflower as a new crop in the cold drylands of Iran. Sesame and Safflower *Newslatter* **20**, 92-94.

Arslan B. 2007. The path analysis of yield and its components in safflower (*Carthamus tinctorius* L.). *J. Biologic. Sci*. **7**, 668-672. https://doi.org/10.3923/jbs.2007.668.672

Baljani R, Shekari F, Sabaghnia N. 2015. Biplot analysis of trait relations of some safflower (*Carthamus tinctorius* L.) genotypes in Iran. *Crop Res*. **50**, 63-73.

Camas N, Cirak C, Esendal E. 2007. Seed yield, oil content and fatty composition of safflower (*Carthamus tinctorius* L.) grown in northern Turkey conditions. *J. Agric. Fac. Ondokuz Mayıs University* **22**, 98-104.

Coşge B, Kaya D. 2008. Performance of some safflower (*Carthamus tinctorius* L.) varieties sown in late-autumn and late-spring. *SDU J. Nat. Appl. Sci*. **12**, 13-18.

Eslam BP, Monirifar H, Ghassemi MT. 2010. Evaluation of late season drought effects on seed and oil yields in spring safflower genotypes. *Turk. J. Agric. Forestry* **34**, 373-380.

Flores F, Moreno MT, Cubero JI. 1998. A comparison of univariate and multivariate methods to analyze G× E interaction. *Field Crops Res*. **56**, 271-286. https://doi.org/10.1016/S0378-4290(97)00095-6

Golkar P, Arzani A, Rezai AM. 2012. Genetic analysis of agronomic traits in safflower (*Carthamus tinctorious* L.). *Notulae Botanicae Horti Agrobotanici Cluj-Napoca* **40** (1), 276-281. https://doi.org/10.15835/nbha4017209

Hussein A, Ibrahim AE, Hussein I, Idris S. 2018. Assessment of genotype x environment interactions and stability for seed yield of selected safflower (*Carthamus tinctorius* L.) genotypes in central and northern Sudan. *Gezira J. Agric. Sci*. **16.**

Kaya Y, Evci G, Pekcan V, Gucer T, Yilmaz Mİ. 2009. The Determination Relationships between Oil Yield and Some Yield Traits in Sunflower. *J. Agric. Sci*. **15**, 310-318.

Koç H, Keles R, Ulker R, Gumuscü G, Ercan B, Akcacik AG, Gunes A, Ozdemir F, Ozer E, Uludag E. 2010. Determination of yield, yield components and quality properties of some safflower (*Carthamus tinctorius* L.) lines and relations between these properties. *J. Crop Res.* **2,** 1–7.

Kose A. 2017. Agricultural performances of some safflower (*Carthamus tinctorius* L.) varieties under Eskisehir vonditions. *Selcuk J. Agric. Food Sci.* **31**, 1-7. https://doi.org/10.15316/SJAFS.2018.55

Kroonenberg PM. 1995. Introduction to biplots for G × E tables. Department of Mathematics. Research Report 51. University of Queensland, Australia. [Online] Available: http://three-mode.leidenuniv.nl/document/biplot.pdf.

Mozaffari K, Asadi A. 2006. Relationships among traits using correlation principal components and path analysis in safflower mutants sown in irrigated and drought stress condition. *Asian J. Plant Sci.* **5**, 977-983. https://doi.org/10.3923/ajps.2006.977.983

Nabloussi A, Fechtali ME, Lyagoubi S. 2008. Agronomic and technological evaluation of a world safflower collection in Moroccan Conditions. VII. International Safflower Conference. Wagga -Australia.

Ozturk O, Ada R, Akinerdem F. 2009. Determınatıon of yield and yield components of some safflower cultivars under irrigated and dry condıtıons. *Selcuk J. Agric. Food Sci.* **23**,16-27.

Rad MN, Kadir MA, Rafii MY, Jaafar HZ, Naghavi MR, Ahmadi F. 2013. Genotype environment interaction by AMMI and GGE biplot analysis in three consecutive generations of wheat (*Triticum aestivum*) under normal and drought stress conditions. *Australian J. Crop Sci*. **7**, 956.

Rubio J, Cubero JI, Martin LM, Suso MJ, Flores F. 2004. Biplot analysis of trait relations of white lupin in Spain. *Euphytica* **135**, 217–224. https://doi.org/10.1023/B:EUPH.0000014911.70355.c9

Weiss EA. 2000. Oilseed Crops. Blackwell Publishing Limited, London, UK.

Yan W, Kang MS, Manjit B, Woods CS, Corneliusd PL. 2007. GGE Biplot vs. AMMI Analysis of Genotypeby-Environment Data. *Crop Sci.* **47**, 643-653. https://doi.org/10.2135/cropsci2006.06.0374

Yan W, Kang MS. 2003. GGE biplot analysis. A graphical tool for breeders, geneticists and agronomists. CRC press. https://doi.org/10.1201/9781420040371

Yan W, Rajcan I. 2002. Biplot analysis of test sites and trait relations of soybean in Ontario. *Crop Sci.* **42**, 11-20. https://doi.org/10.2135/cropsci2002.1100

Yan W, Frégeau-Reid J. 2008. Breeding line selection based on multiple traits. *Crop Sci*. **48**, 417-423. https://doi.org/10.2135/cropsci2007.05.0254

Yan W, Tinker NA, Bekele WA, Mitchell-Fetch J, Fregeau-Reid J. 2019a. Theoretical unification and practical Integration of conventional methods and genomic selection in plant breeding. *Crop breed. Genetics and Genomics* **1** (2).

Yan W, Frégeau-Reid J, Mountain N, Kobler J. 2019b. Genotype and management evaluation based on genotype by yield* trait (GYT) analysis. *Crop Breed Genetics and Genomics* **1** (2).

Yau SK. 1995. Regression and AMMI analyses of genotype x environment interactions, an empirical comparison. *Agronomy J.* **87**, 121-126. https://doi.org/10.2134/agronj1995.00021962008700010021x

GRASAS Y ACEITES 72 (3)
July-September 2021, e422
ISSN-L: 0017-3495
https://doi.org/10.3989/gya.0664201

Phenomenological model for the prediction of *Moringa oleifera* extracted oil using a laboratory Soxhlet apparatus

Y. Díaz[a, ✉], D. Tabio[a], M. Rondón[a], R. Piloto-Rodríguez[b] and E. Fernández[a]

[a]Faculty of Chemical Engineering, Universidad Tecnológica de La Habana José A. Echeverría, Cujae, 19390, La Habana, Cuba.
[b]Center of Studies for Renewable Energies, Universidad Tecnológica de La Habana José A. Echeverría, Cujae, 19390, La Habana, Cuba.
✉Corresponding author: ydiaz@quimica.cujae.edu.cu

Submitted: 14 June 2020; Accepted: 15 July 2020; Published online: 20 September 2021

SUMMARY: *Moringa oleifera* is an oilseed crop with potential for biodiesel production. The second step in this process is the extraction of oil. Extraction in hot water, with a Soxhlet apparatus and the ultrasound technique are the most commonly used methods. The aim of the present work was to obtain a phenomenological model for the *Moringa oleifera* oil extraction process using Soxhlet. Effective diffusivity for Moringa oil through the kernels is obtained, using the kinetics of the extraction process (experimentally determined) and the Fick's diffusion second law for non-steady state. The value of $0.685 \cdot 10^{-12}$ m^2/s fully matched reports on effective diffusion coefficient for other solids. It was also verified from the statistical analysis and a linear fit for experimental data that the model can be used to describe the oil extraction process of *Moringa oleifera* in the Soxhlet extractor, responding to the diffusive phenomenon (process controlled by internal resistance).

KEYWORDS: *ANOVA; Effective diffusivity; Kinetics; Moringa oleifera seed oil; Phenomenological model; Soxhlet extraction*

RESUMEN: ***Modelo fenomenológico para la predicción del aceite extraído de Moringa oleífera utilizando un equipo de laboratorio Soxhlet.*** *Moringa oleífera* es un cultivo oleaginoso con potencial para producir biodiesel. La segunda etapa del proceso es la extracción de aceite. Los métodos más utilizados son la extracción en agua caliente, con Soxhlet y la técnica de ultrasonidos. El objetivo del trabajo fue obtener un modelo fenomenológico para el proceso de extracción de aceite de *Moringa oleífera* en Soxhlet. Utilizando la cinética del proceso extractivo (determinada experimentalmente) y la segunda ley de difusión de Fick en estado no estacionario, se obtuvo la difusividad efectiva del aceite de Moringa a través de los cotiledones. El valor de $0.685 \cdot 10^{-12}$ m^2/s, se corresponde con reportes del coeficiente de difusión efectiva para otros sólidos. Se verificó a partir del análisis estadístico y ajuste lineal de los datos experimentales, que el modelo describe el proceso de extracción de aceite de *Moringa oleífera* en Soxhlet, respondiendo al fenómeno difusivo (proceso controlado por la resistencia interna).

PALABRAS CLAVE: *Aceite de semillas de Moringa oleífera; Análisis de varianza; Cinética; Difusividad efectiva; Extracción con Soxhlet; Modelo fenomenológico*

Citation/Cómo citar este artículo: Díaz Y, Tabio D, Rondón M, Piloto-Rodríguez R, Fernández E. 2021. Phenomenological model for the prediction of *Moringa oleifera* extracted oil using a laboratory Soxhlet apparatus. *Grasas Aceites* **72** (3), e422. https://doi.org/10.3989/gya.0664201

1. INTRODUCTION

According to several reports, *Moringa oleifera* Lam. is an oilseed crop with potential for biodiesel production (Rahid *et al*., 2008; Rashid *et al*., 2011). The Moringaceae plant family consists of 12-14 species belonging to only one genus, Moringa (Díaz *et al*., 2019). *Moringa oleifera* is native to Asia, Africa and Arabia. The height of the tree can reach 10 m. It can grow well in the humid tropical or hot dry lands; it can survive in very poor soils and is hardly affected by drought (Anwar and Bhanger, 2003; Díaz *et al*., 2017). Seeds are fleshy, and covered by a fine husk of coffee color. They have three wings, or winged seeds from 2.5 to 3 mm in length. The kernel-to-husk percentage ratio of the whole seed is approximately 75:25 (Salaheldeen *et al*., 2014).

The seed kernels contain a significant amount of oil, commercially known as "Ben oil" or "Behen oil" (Anwar and Bhanger, 2003). The oil content and its properties widely vary depending mainly on the species and environmental conditions (Adegbe *et al*., 2016). The oil produced from the seed kernel of *Moringa oleifera* is golden yellow and contains high amounts of oleic acid, with approximately 75%. The ester profile of *Moringa oleifera* oil differs from other common vegetable oils used as biodiesel feedstocks, and influences fuel properties. It may also be noted that oils with high oleic acid contents could have a positive influence on fuel properties (Díaz *et al*., 2019).

Moringa oleifera seeds have also been used as an effective coagulant and antimicrobial agent to remove hardness, undesirable chemicals and biological contaminants from water (Falowo *et al*., 2018; Kayode and Kabir, 2018). The active agents of coagulation are dimeric cationic proteins of molecular weight of approximately 13 kilodaltons (kDa) (Prasad, 2009).

The second step in biodiesel production from oilseeds is the extraction of oil. The husk and remaining cake are generated as by-products. Extraction of vegetable oil is commonly based on mechanical pressing and solvent extraction (Reverchon *et al*., 1999). It is well-known that oil extraction efficiency by mechanical pressing is significantly lower than chemical extraction. Nevertheless, by solvent extraction, chemical residues could remain, which can be quite harmful to human health and to the environment (Zhao and Zhang, 2013). Due to this fact, after solvent extraction, a step of solvent-removal by vacuum evaporation is applied (Stamenković *et al.*, 2018). Extraction in hot water with Soxhlet apparatus and the ultrasound technique are the most commonly used methods.

The solvent extraction of vegetable oil is usually carried out with hexane (Kostic *et al.*, 2014). For the extraction process, vegetable oils can be referred to as a simple component, since all glycerides are soluble in hexane. The other components that are extracted with some difficulty are phosphatides, since they have limited solubility.

Solvent extraction modeling. During solvent extraction, oil seeds are put in contact with the pure solvent or a solvent mix to transfer the oil from the solid matrix to the fluid medium. This is developed following a complex mechanism, especially for oil materials because of the cell structure of vegetable lipidic thickness. For that reason, it is difficult to explain all phenomena which take place during the solvent extraction through a single theory (Carrin and Craspite, 2008). Different authors have considered the mathematic modeling of vegetable oil extraction (Thomas *et al*., 2005).

Diffusive transport. The success of an industrial extraction process is a function of how fast a compound dissolves. Different phenomena are involved in the passage of the solute from the solid to the solvent. The oil diffuses through the internal structure to the surface of the solid and then passes into the liquid by a convective mechanism (external transport) (Treybal, 2001). Therefore, the convective transport of oil into the liquid phase and the diffusive transport produced within the solid must be evaluated in order to characterize the transfer of matter.

The traditional Fickian approach uses the concentration gradient between the raw material particles and the solution as the driving force of the extraction (Doulia and Gekas, 2001). This development can be used (considering that there are no changes in the effective diffusivities with the solute concentration and that external resistance to mass transfer is negligible) using a distribution coefficient between two phases and with diluted extracts. Thus, the extraction rate increases with increasing concentration gradient. It can also be increased by increasing the diffusion coefficient or by reducing the particle size (Cacace and Mazza, 2003). The diffusion coefficient is frequently

reported as the effective diffusion coefficient.

From the above, it is important to know the phenomenological characterization of the oil extraction process. Numerical modeling and simulation are important substitutes of the experiments. The advantages of modeling and simulation are cost and time saving. The best type of model is phenomenological. It is based on physical and/or chemical principles. Nevertheless, a model requires empirical validation (Muharam *et al*., 2019). Numerical modeling and simulation research on *Moringa oleifera* oil production through solvent extraction are not reported.

The aim of the present work was to obtain a phenomenological model for the *Moringa oleifera* oil extraction process using Soxhlet apparatus.

2. MATERIALS AND METHODS

2.1. Seed origin

The seeds of *Moringa oleifera* were harvested at a facility located at (23° 7′ 0″ N, 82° 23′ 0″ W) in Havana, Cuba. They were globular, three-winged seeds and covered with a thick blackish seed coat. The weight of 100 seeds of *Moringa oleifera* was found to be 23.90 g ± 0.38. The seed contained 72.74% ± 1.26 kernels and 27.26% ± 1.21 husks. According to literature reports (Salaheldeen *et al*., 2014; Díaz *et al*., 2017), the contents and properties of Moringa seeds depend on species and environmental conditions. After removing the husk, the kernels were milled and dried.

2.2. Particle size

The size-reduced particles were analyzed using the Cuban standard (NC, 2008). A representative sample of 14 g of milled kernels was taken, according to the standard report. The average diameter of the particle conglomerate (Dp) in m was determined from Equation 1 (Rosabal and Garcel, 2006).

$$Dp = \frac{1}{\sum \frac{\Delta xi}{Dpi}} \quad (1)$$

Where Δxi is the retained fraction in the bottom sieve of each pair and Dpi the average size of the particles retained in the bottom sieve of each pair.

2.3. Drying of milled kernels

The milled kernels were dried at 55 °C in a stove (model DHG 9146A, Shanghai Huitai Instrument Manufacturing CO., LTD, Shanghai, China). Removing water during this operation made the oil extraction more efficient, since drying favored the breakdown of the water-oil emulsions, guaranteeing the oil easily dissolved in the organic solvent. The moisture determination was carried out by weighing the difference using an analytical balance, model SARTORIUS BS 124S. The drying curve was obtained to define the operation time. Weighing was carried out every half hour until reaching constant weight.

2.4. Oil extraction

A lab scale Soxhlet apparatus fitted with a 1-L round-bottom flask and a condenser was used to extract the oil from the kernels. About 10 g of dried sample were used for each extraction. Hexane (purity > 98%, specific gravity: 0.659, refractive index: 1.375) was added as solvent according to a solvent-kernels ratio (6:1) (mass: volume ratio) in accordance with previous studies (Díaz *et al*., 2017; Tabio *et al*., 2018). An evaporation process was applied to the mixture of oil and solvent in order to remove one from the other. The process was developed in a rotary evaporator (IKA-WERK HB 4 basic, Germany). The extracted oil yield was expressed in mass percentage, which is defined as the weight of the oil extracted over the weight of the sample.

2.5. Kinetics of the process

The extraction kinetics of the Moringa oil were studied in the Soxhlet using hexane at 69 °C (boiling temperature) as solvent. During the experimental runs, the change in time of the extracted oil percentage was obtained. The measurements were carried out in triplicate.

2.6. Diffusion model and effective diffusivity coefficient determination

The calculation method to apply the solution to Fick´s diffusion second law, using natural logarithms was followed by a simple regression analysis of the solute's adimensional concentration with respect to time.

Oilseeds have a cellular structure. Therefore, the internal diffusion within the solid structure is the determining mechanism of the extraction rate. Therefore, this type of phenomenon is represented

by Fick's diffusion second law for a non-steady state (Varzakas *et al*., 2005). To obtain the effective diffusivity coefficient, the kinetics of the extractive process must be experimentally determined and the aforementioned law must be used. Fick's diffusion second law for non-steady state was used to assess whether the extraction of *Moringa oleifera* oil using Soxhlet was controlled by internal resistance (diffusive transport). To mathematically model the diffusion according to this law, the following conditions must be taken into account:

- The diffusion coefficient must be an independent constant of the solid particle radius
- The solid structure must be homogeneous and isotropic
- The oil distribution in the cell must be uniform
- In the case of spheres, the solid particle radius must be uniform and the same for all particles
- Mass transfer from solid to liquid phase is considered to be dominated by internal resistance (diffusive transport)

The effective diffusivity of the solid is constant throughout the sphere and the differential equation that describes the diffusion process in spherical coordinates can be obtained according to Hinnes *et al*. (1987) (Equation 2).

$$\frac{\partial c}{\partial t} = D_{ef} \cdot \left(\frac{\partial^2 c}{\partial r^2} + \frac{2\partial c}{r\partial r}\right) \quad (2)$$

Where $\frac{\partial c}{\partial t}$ is the cumulative term, $\frac{\partial^2 c}{\partial r^2} + \frac{2\partial c}{r\partial r}$ the diffusive term, r the sphere radius in m, t is the time of diffusion in s and Def are the effective diffusivity coefficients of solute in m^2/s.

To model the mass transfer, an initial and boundary conditions are required:

For $t = 0$ $c = c_0$ (c_0: initial solute concentration (g/mL))

For $t > 0$ $c = 0$ at $r = a$, a: Radius on the surface of the sphere

The differential equation mathematics solution can be determined from Equation 3:

$$\frac{c}{c_0} = \frac{2a}{\pi} \sum_{n=1}^{\infty} \frac{(-1)^n}{n} \cdot e^{-\frac{D_{ef} n^2 \pi^2 t}{a^2}} \cdot \text{sen}\, \frac{n\pi r}{a} \quad (3)$$

Because triglycerides have different molecular structures and masses, it is better to measure the amount of oil with respect to the solid mass. Therefore, the concentration ratio $\frac{c}{c_0}$ is transformed into the relationship between the remaining oil mass (q) and the initial mass of oil (q_0), obtaining the $\frac{q}{q_0}$ ratio.

For longer times, series converge and, consequently, for most practical calculations, a few points are sufficient. Indeed, all the series points, except the first one, are negligible. The solution of Fick's diffusion second law is reduced to Equation 4, where the amount of solute remaining in the solid at time t with respect to the initial amount is:

$$\frac{q}{q_0} = \frac{6}{\pi^2} \cdot e^{-\pi^2 \cdot \frac{D_{ef}}{r^2}} \cdot t \quad (4)$$

Where $\frac{q}{q_0}$ is the relationship between the remaining and initial quantity of oil, q the amount of remaining oil in g at time t, q_0 the initial amount of oil in g and π is the mathematical constant 3.1418.

Equation 4 was linearized by applying natural logarithms to obtain Equation 5. The fit models were tested for fit quality. For simple regression analysis, the Statgraphics Centurion statistical program, version XV was used. The slope of the line was used to estimate the effective diffusion coefficient. An initial oil content (c_0) of 45% was considered since it is the maximum reported by Abdulkareem *et al*. (2011); Ayerza (2011) and Efeovbokhan *et al*. (2015) for *Moringa oleifera*. The equivalent radius of the sphere was taken as the average radius of the particle conglomerate obtained by the sieving operation.

$$\ln \frac{q}{q_0} = -0.498 - \frac{9.87 D_{ef}}{r^2} \cdot t \quad (5)$$

3. RESULTS AND DISCUSSION

3.1. Sieving analysis

The sieving analysis served to obtain the distribution of the present size of particles in the *Moringa oleifera* seeds kernels after the milling process (Table 1 and Figure 1).

A varied distribution of particle sizes can be observed in Figure 1. The largest amount of milled seeds kernels (56.09%) began to cluster in smaller diameter sieves (between $1.0 \cdot 10^{-3}$ and $0.5 \cdot 10^{-3}$ m).

TABLE 1. Sieving analysis data of *Moringa oleifera* milled kernels

Sieves breach relationship	Retained mass (g)	Δxi	Dpi·10³
2.000	1.57	0.107	2.000
2.000/1.600	0.74	0.051	1.800
1.600/1.400	0.80	0.055	1.500
1.400/1.000	2.35	0.161	1.200
1.000/0.800	1.22	0.084	0.900
0.800/0.630	2.16	0.148	0.715
0.630/0.500	2.46	0.168	0.565
0.500/0.400	0.35	0.024	0.450
0.400/0.315	0.93	0.064	0.357
0.315/0.200	1.69	0.116	0.257
0.200/0.160	0.27	0.018	0.180
0.160/0.125	0.06	0.004	0.142
0.125	0.00	-	0.125

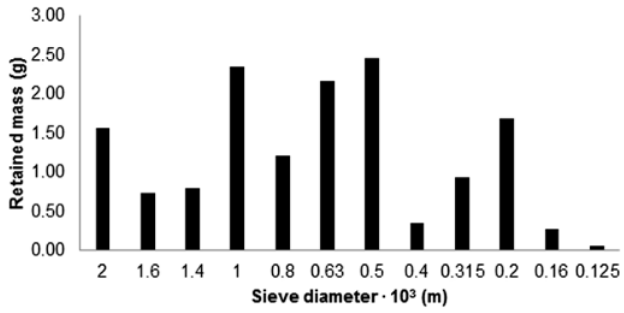

FIGURE 1. Particle size distribution of *Moringa oleifera* milled kernels.

The average diameter of the particle conglomerate (determined by Equation 1) was $0.602 \cdot 10^{-3}$ m. This result corroborates the fact that with this milling method it was possible to further decrease the particle size and therefore the oil extraction process was expected to be favored.

It has been reported (Abdulkareem *et al*., 2011) that particle size can directly affect the rate and yield of the extraction process. Generally, at smaller particle sizes the contact area between the solvent and the solid increases, which caused the oil transfer rate to increase (Abdulkareem *et al*., 2011).

Abdulkareen *et al*. (2011), recommend a small size range (between $0.7 \cdot 10^{-3}$ and $0.5 \cdot 10^{-3}$ m) so that each particle required approximately the same extraction time. The results obtained in the present work are in agreement with this aspect, the average diameter of the milled seeds kernels being included in the aforementioned interval. The diffusion coefficient for internal mass transport depends of the solid structure. To reduce the particle size of oilseeds the cellular wall is broken, thus increasing the access to the lipid content. It means that oil could be extracted with a higher extraction rate.

3.2. Moisture content of the seed kernels

The initial moisture content of *Moringa oleifera* seeds kernels was 4.61%. This result was found to be lower than that of *Moringa oleifera* from Pakistan (5.70%) and Yucatan (5.84%) (Anwar and Bhanger, 2003; Ortiz *et al*., 2012). However, the above-mentioned moisture reports are related to the whole seed (husk and kernel). For this reason, the husk moisture content of *Moringa oleifera* from Cuba should be taken into account to make a precise comparison. Recently a husk moisture content of 6.25% was reported for *Moringa oleifera* grown in Cuba (Pfeil *et al*., 2020). Therefore, a seed moisture content of 5.05% could be obtained by mass balance using this last value.

The drying curve serves to determine the moisture content of the kernels at any instant in time. The results are shown in Figure 2.

The moisture content of *Moringa oleifera* seed kernels decreased from 4.61 to 0.22% during the drying process as can be seen in Figure 2. From the aforementioned, a drying time of two hours was established because the moisture decreased to percentages lower than 0.3%.

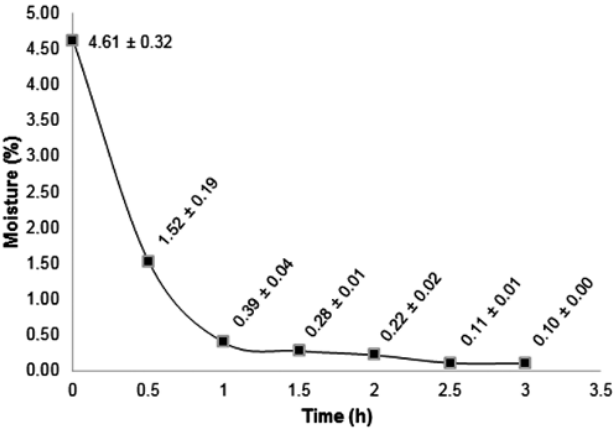

FIGURE 2. Drying curve of *Moringa oleifera* kernels at 55 °C. Each moisture percentage is an average of three determinations, mean ± SD.

3.3. Kinetics of extractive process

The results for kinetic extraction are shown in Figure 3.

An oil extraction behavior over time is observed in Figure 3, which indicated, as expected, that oil yield is time dependent. The amount of extracted oil is practically constant for extraction times of six hours and longer, which was demonstrated with the asymptotic behavior of the curve. The high rate of extraction observed at the early stages may be due to the high solubility of the oil in the freshly charged solvent and the high concentration of the oil at the solid surface. The freshly charged solvents (lean oil) created a positive gradient or the needed driving force that resulted in a higher mass transfer rate of oil in to the extracting solvents. After the optimum point had been reached, the extracting solvents (oil rich) gave rise to lower driving force or slower extraction rates (Efeovbokhan *et al*., 2015). The experimental kinetics of the extractive process were required to determine the effective diffusivity coefficient.

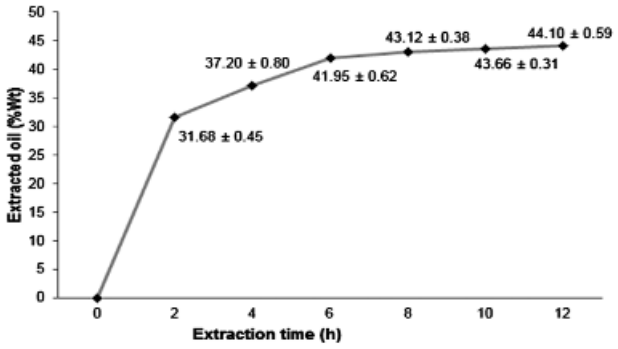

FIGURE 3. Extraction kinetic curve of *Moringa oleifera* seed oil using hexane. The extracted oil percentages are expressed as means ± SD of triplicate experiments.

3.4. Phenomenological model of extraction

It should be expected that internal mass transport will be the controlling phase during the extraction process of *Moringa oleifera* oil using Soxhlet apparatus because of the cellular structure of abovementioned oilseed. This phenomenon was verified through Fick's diffusion second law in a non-steady state, taking into account the kinetics of the extraction process as shown in Figure 3. Fick's mathematic solution was linearized by applying the natural logarithms in Equation 5.

The established initial oil content of *Moringa oleifera* kernels and sample mass were 45% and 10 g, respectively. The remaining oil content was calculated as a mass fraction per unit of initial oil mass ($\frac{q}{q_0}$). Table 2 shows the experimental remaining oil masses determined from kinetics extraction with hexane.

A linear fit was corroborated for the experimental data when $\ln (q / q_0)$ is plotted against time (Figure 4).

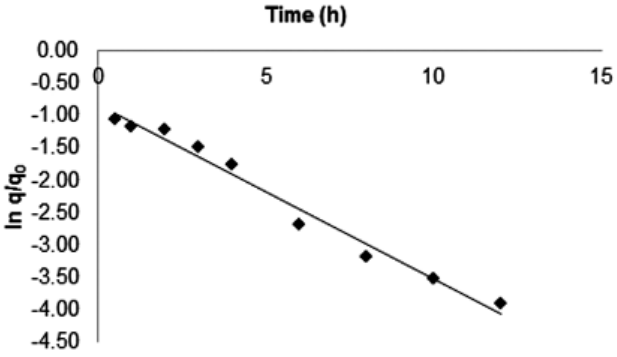

FIGURE 4. Experimental data fitting to the Fick's diffusion second law for non-steady state

The model obtained is represented by Equation (6):

$$\ln \frac{q}{q_0} = -0.2689 \cdot t - 0.8302 \quad (6)$$

TABLE 2. Experimental values for *Moringa oleifera* remaining oil from kinetic study with hexane at 69 °C (q_0 = 4.5 g)

Time (h)	Extracted oil fraction from the kernels (Mean ± SD)*	Remaining oil [q] (g)	Remaining oil/initial oil ratio [q/q₀]	ln(q/q₀)
0.5	0.2942 ± 0.0074	1.558	0.346	-1.0607
1.0	0.3096 ± 0.0092	1.404	0.312	-1.1648
2.0	0.3168 ± 0.0045	1.332	0.296	-1.2174
3.0	0.3483 ± 0.0051	1.017	0.226	-1.4872
4.0	0.3720 ± 0.0080	0.780	0.173	-1.7527
6.0	0.4195 ± 0.0062	0.305	0.068	-2.6927
8.0	0.4312 ± 0.0038	0.188	0.042	-3.1756
10.0	0.4366 ± 0.0031	0.134	0.030	-3.5166
12.0	0.4410 ± 0.0059	0.090	0.020	-3.9120

*Values are expressed as means ± standard deviation (SD) of triplicate experiments.

Table 3. ANOVA of the phenomenological model for *Moringa oleifera* oil extraction process using Soxhlet

Source	Sum of Squares	DF	Mean Square	F-Ratio	P-Value
Model	9.69578	1	9.69578	334.56	0.0000
Residual	0.202865	7	0.0289808		
Total (corr.)	9.89865	8			
Correlation coefficient	-0.9897				
R^2	97.95%				
R^2 (adjusted for DF)	97.66%				
Standard Error of Est.	0.170237				
Mean absolute Error	0.134161				
Durbin-Watson statistic	1.33855 (P=0.0560)				
Lag1 residual autocorrelation	0.255402				

Table 4. Statistical significance of the phenomenological model coefficients

Parameter	Least Squares	Standard Error	t statistic	P-Value
Intercept	-0.830176	0.09483	-8.7540	0.0001
Slope	-0.268992	0.01470	-18.2910	0.0000

The tests of model fit were verified to validate the quality. The analysis of variance (ANOVA) of the model and the statistical significance of its parameters are presented in Tables 3 and 4.

Since the P-value in the ANOVA table is less than 0.05, there is a statistically significant relationship between ln (q/q_0) and time at the 95.0% confidence level. The R-Squared statistic indicates that the model as fitted explains 97.9506% of the variability in ln (q/q_0). The correlation coefficient equals -0.9897, indicating a relatively strong relationship between the variables.

The adjusted R^2 statistic, which is more suitable for comparing models with different numbers of independent variables, was 97.65%. The high value of the determination coefficient R^2 justified a good correlation between the parameter and for this reason, the model is suitable for a satisfactory representation of the real process.

The Durbin-Watson (DW) statistic tests the residuals to determine if there is any significant correlation based on the order in which they occur in the data. Since the P-value (0.0560) is greater than 5.0%, there is no indication of serial autocorrelation in the residuals at the 5.0% significance level. The residuals, which are the difference between the observed values and the predicted values, should lie on a straight line in the normal probability plot.

Therefore, these three suppositions imply that the suggested model (Equation 6) is adequate and can be used to describe the oil extraction process of *Moringa oleifera* in the Soxhlet extractor, responding to the diffusive phenomenon according to Fick's diffusion second law in a non-steady state.

3.5. Comparative analysis of oil extraction percentages determined from the phenomenological model and laboratory experiments

Three oil extraction experiments were developed according to the description in the materials and methods section. For any extraction process, it is possible to obtain a high quantity of the product in the first hours, with a time from which the effectiveness of the extraction is very low. The difference between the overall maximum at 12 h and the value at 6 h, as obtained from the respective seed samples, extracting solvent and times was only nominal (see Figure 3). That is the main reason for fixing six hours as the extraction time for the experiments. This would not affect the oil extraction percentage and will be related to the energy consumption during the operation with the Soxhlet apparatus. This means that if the cost of solvent extraction is considered, the optimum conditions must be used. The nominal oil yield after this optimum point bears a negative

cost on the overall extraction cost (Efeovbokhan *et al*., 2015).

The experimental extraction oil percentages of *Moringa oleifera* from Cuba were 40.12, 40.56 and 42.48%. These results were higher than those reported for *Moringa oleifera* Wild (NWFP, Pakistan) 34.80% and *Moringa oleifera* variety Mbololo (Kenya) 35.70%. However, the extracted oil content was comparable to *Moringa oleifera* Sindh (Pakistan) 40.39% (Anwar and Rashid, 2007). The differences found might be attributed to the diversity of natural habitats and agroclimatic constraints (Efeovbokhan *et al*., 2015).

In addition, the extraction percentage obtained from the phenomenological model (41.09%) was compared to the experimental results. The relative error was lower than 5% in all cases, which validated the degree of accuracy of the phenomenological model to predict the extraction percentage of *Moringa oleifera* oil in Soxhlet.

3.6. Effective diffusivity estimation of *Moringa oleifera* oil through the kernels

The effective diffusivity (Def) was obtained from the slope of the fitted model (Equation 6). The equivalent sphere radius was $0.301 \cdot 10^{-3}$ m as calculated from the average diameter of the particle conglomerate ($0.602 \cdot 10^{-3}$ m). The effective diffusivity for *Moringa oleifera* oil through the kernels was obtained for the first time. The value of $0.685 \cdot 10^{-12}$ m^2/s, fully matched with reports of effective diffusion coefficient (between 10^{-12} to 10^{-10} m^2/s) for other solids (Doulia and Gekas, 2001; Cacace and Mazza, 2003; Varzakas *et al*., 2005). Diffusion within a solid structure is a more complex phenomenon than inside liquids and gases. For this reason, lower diffusion coefficient and slower mass transfer are to be expected.

4. CONCLUSIONS

A phenomenological model to describe the oil extraction process using Soxhlet was obtained. The validity of the model was demonstrated when Fick's diffusion second law in a non-steady state was applied to the oil extraction from *Moringa oleifera* kernels with hexane. The extraction percentage determined from the phenomenological model (41.09%) was compared to the experimental results. The relative error was lower than 5% in all cases, which indicated the degree of accuracy of the model. The effective diffusivity for *Moringa oleifera* oil through the kernels at 69 °C was determined for the first time. The value of $0.685 \cdot 10^{-12}$ m^2/s fully matched reports of effective diffusion coefficient for other solids.

REFERENCES

Abdulkareem A, Uthman H, Afolabi AS, Awenebe OL. 2011. Extraction and Optimization of Oil from *Moringa Oleifera* Seed as an Alternative feedstock for the Production of Biodiesel, in *Sustainable Growth and Applications in Renewable Energy Sources*. In Tech, Rijeka, pp. 244-268. https:/doi.org/10.5772/2433

Adegbe A, Larayetan R, Omojuwa T. 2016. Proximate Analysis, Physicochemical Properties and Chemical Constituents Characterization of *Moringa Oleifera* (Moringaceae) Seed Oil Using GC-MS Analysis. *Am. J. Chem*. **6**, 23-28. https://doi.org/10.5923/j.chemistry.20160602.01

Anwar F, Bhanger M. 2003. Analytical characterization of *Moringa oleifera* seed oil grown in temperate regions of Pakistan. *J. Agric. Food Chem.* **51**, 6558-6563. https://doi.org/10.1021/jf0209894

Anwar F, Rashid U. 2007. Physico-chemical characteristics of *Moringa oleifera* seeds and seed oil from a wild provenance of Pakistan. *Pak. J. Bot*. **39**, 1443-1453.

Ayerza R. 2011. Seed yield components, oil content, and fatty acid composition of two cultivars of moringa (*Moringa oleifera* Lam.) growing in the Arid Chaco of Argentina. *Industrial Crops Prod*. **33**, 389-394. https://doi.org/10.1016/j.indcrop.2010.11.003

Cacace J, Mazza G. 2003. Mass transfer process during extraction of phenolic compounds from milled berries. *J. Food Eng*. **59**, 379-389. https://doi.org/10.1016/S0260-8774(02)00497-1

Carrín ME, Capriste GH. 2008. Mathematical modeling of vegetable oil-solvent extraction in a multistage horizontal extractor. *J. Food Eng*. **85**, 418. https://doi.org/10.1016/j.jfoodeng.2007.08.003

Díaz Y, Tabio D, Goyos L, Fernández E, Muñoz S, Piloto R, Verhelst S. 2017. Extraction and characterization of oil from *Moringa oleifera* for energy purpuses. *Wulfenia* **24**, 86-103.

Díaz Y, Tabio D, Goyos L, Fernández E, Rondón M, Fischer T, Piloto R. 2019. Rheological behavior and properties of biodiesel and vegetable oil from *Moringa oleifera* Lam. *Afinidad* **587**, 83–90.

Doulia D, Gekas V. 2001. A knowledge base for the apparent mass diffusion coefficient (D_{EFF}) of foods. *Int. J. Food Prop*. **3**, 1-14. https://doi.org/10.1080/10942910009524613

Efeovbokhan VE, Hymore FK, Raji D, Sanni SE. 2015. Alternative solvents for *Moringa oleifera* seeds extraction. *J. Applied Sci.* **15**, 1073-1082. https://doi.org/10.3923/jas.2015.1073.1082

Falowo AB, Makumbo FE, Idamokoro EM, Lorenzo JM, Afolayan AJ, Muchenje V. 2018. Multi-functional application of *Moringa oleifera* Lam. in nutrition and animal food products: A review. *Int. Food Res. J*. **106**, 317-334. https://doi.org/10.1016/j.foodres.2017.12.079

Hines AL, Maddox RN, Rodríguez JL. 1987. *Mass Transfer-Fundamentals and Applications*. Prentice-Hall Hispanoamericana, Mexico.

Kayode O, Kabir A. 2018. Optimization of shelling efficiency of a *Moringa oleifera* seed shelling machine based on seed sizes. *Industrial Crops Prod*. **112**, 775-782. https://doi.org/10.1016/j.indcrop.2018.01.011

Kostic MD, Jokovic NM, Stamenkovic OS, Rajkovic KM, Milic PS, Veljkovic VB. 2014. The kinetics and thermodynamics of hempseed oil extraction byn-hexane. *Industrial Crops Prod*. **52**, 679-686. https://doi.org/10.1016/j.indcrop.2013.11.045

Muharam Y, Putri AD, Hamzah A. 2019. Phenomenological model for prediction of the performance of a slurry bubble column reactor for green diesel production. *J. Phys.: Conf. Ser.* **1349**, 1-8. https://doi.org/10.1088/1742-6596/1349/1/012057

NC (Norma Cubana). 2008. Minerales-Análisis granulométrico por tamizado-Requisitos generales. Oficina Nacional de Normalización. La Habana.

Ortiz J, Navarrete A, Sacramento JC, Rubio C, Acereto P, Rocha JA. 2012. Extraction and Characterization of Oil from *Moringa oleifera* Using Supercritical CO_2 and Traditional Solvents. *Am. J. Anal. Chem*. **3**, 946-949. https://doi.org/10.4236/ajac.2012.312A125

Pfeil M, Piloto R, Díaz Y, Sánchez Y, Melo EA, Denfeld D, Pohl S. 2020. Data on the thermochemical potential of six Cuban biomasses as bioenergy sources. *Data brief*. **29**, 105207. https://doi.org/10.1016/j.dib.2020.105207

Prasad RK. 2009. Color removal from distillery spent wash through coagulation using *Moringa oleifera* seeds: Use of optimum response surface methodology. *J. Hazard. Mater*. **165**, 804-811. https://doi.org/10.1016/j.jhazmat.2008.10.068

Rashid U, Anwar F, Ashraf M, Saleem M, Yusup S. 2011. Application of response surface methodology for optimizing transesterification of *Moringa oleifera* oil: biodiesel production. *Energy Convers. Manage*. **52**, 3034-3042. https://doi.org/10.1016/j.enconman.2011.04.018

Rashid U, Anwar F, Moser BR, Knothe G. 2008. *Moringa oleifera* oil: A possible source of biodiesel. *Bioresour. Technol*. **99**, 8175-8179. https://doi.org/10.1016/j.biortech.2008.03.066

Reverchon E, Daghero J, Marrone C, Mattea M, Poletto M.1999. Supercritical fractional extraction of fennel seed oil and essential oil: experiments and mathematical modeling. *Ind. Eng. Chem. Res.* **38**, 3069–3075. https://doi.org/10.1021/ie990015+

Rosabal J, Garcel L. 2006. *Hidrodinámica y Separaciones Mecánicas*. Editorial Félix Varela, Cuba.

Salaheldeen M, Aroua MK, Mariod AA, Cheng SF, Abdelrahman. 2014. An evaluation of *Moringa peregrina* seeds as a source for bio-fuel. *Industrial Crops Prod*. **61**, 49-61. https://doi.org/10.1016/j.indcrop.2014.06.027

Stamenkovic OS, Djalovic IG, Kostic MD, Mitrovic PM, Veljkovic VB. 2018. Optimization and kinetic modeling of oil extraction from white mustard (*Sinapis alba* L.) seeds. *Industrial Crops Prod*. **121**, 132-141. https://doi.org/10.1016/j.indcrop.2018.05.001

Tabio D, Espinosa C, Díaz Y, Rondón M, Fernández E, Piloto R. 2018. Extracción etanólica de aceite de semillas de *Moringa oleífera*. *Revista Investig. y Cienc. la Univ. Autónoma Aguascalientes* **74**, 32-38.

Thomas GC, Krioukov VG, Vielmo HA. 2005. Simulation of vegetable oil extraction in counter-current crossed flows using the artificial neural network. *Chem. Eng. Processing*. **44**, 581. https://doi.org/10.1016/j.cep.2004.06.013

Treybal R. 2001. *Operaciones con transferencia de masa*. McGraw-Hill, United States.

Varzakas TH, Leach GC, Israilides CJ, Arapoglou D. 2005. Theoretical and experimental approaches towards the determination of solute effective diffusivities in foods. *Enzyme Microb. Tech.* **37**, 29-41. https://doi.org/10.1016/j.enzmictec.2004.06.015

Zhao S, Zhang D. 2013. A parametric study of supercritical carbon dioxide extraction of oil from *Moringa oleifera* seeds using a response surface methodology. *Sep. Purif. Technol*. **113**, 9–17. https://doi.org/10.1016/j.seppur.2013.03.041

GRASAS Y ACEITES 72 (3)
July-September 2021, e423
ISSN-L: 0017-3495
https://doi.org/10.3989/gya.0554201

Kinetic modeling of oxidation parameters and activities of lipase-lipoxygenase in wheat germ oil

Y. Erim Köse ✉

Van Yüzüncü Yıl University, Faculty of Engineering, Department of Food Engineering, Van-Turkey
✉Corresponding author: yagmurerim@yyu.edu.tr

Submitted: 07 May 2020; Accepted: 20 July 2020; Published online:24 September 2021

SUMMARY: This study aimed to investigate the oxidation profile of wheat germ oil extracted from raw germ during the stabilization with microwave (MW) treatment, and the kinetics of the oxidation parameters (free fatty acids (FFA), peroxide value (PV), thiobarbituric acid (TBA), α-tocopherol, lipase (LA) and lipoxygenase (LOX) enzymes activities) under different storage conditions. For stabilizing raw germ, the MW was treated at 700 W for three minutes. The oxidation parameters for the kinetic modeling were analyzed at different storage times (0, 15, 30, 45, 60,75, 90, and 105. days) and storage temperatures (-18, 0, 4, and 25 °C). The parameters were mathematically modelled and the PV and LA fitted well to the zero-order kinetic model, while FFA with α-tocopherol and TBA followed the first and second-order kinetics, respectively. The kinetic constant (k) was described by an Arrhenius equation and the activation energy ranged from 5.72 to 18.5 kJ/mol for the stabilized germ.

KEYWORDS: *Activation energy; Kinetic parameters; Lipase enzyme; Oxidative stability*

RESUMEN: ***Modelo cinético de los parámetros de oxidación y actividades de la lipasa-lipoxigenasa en aceite de germen de trigo.*** Este estudio tuvo como objetivo investigar el perfil de la oxidación del aceite crudo extraído del germen de trigo durante tratamientos de estabilización con microondas (MW), y la cinética de los parámetros de oxidación (ácidos grasos libres (FFA), índice de peróxido (PV), ácido tiobarbitúrico (TBA), actividades de enzimas α-tocoferol, lipasa (LA) y lipoxigenasa (LOX), en diferentes condiciones de almacenamiento. Para estabilizar el germen crudo en MW, se trató a 700 W durante tres minutos. Los parámetros de oxidación para el modelo cinético se analizaron a diferentes tiempos de almacenamiento (0, 15, 30, 45, 60, 75, 90 y 105 días) y temperaturas de almacenamiento (-18, 0, 4 y 25 °C). Los parámetros fueron tratados matemáticamente y el PV y LA se ajustaron bien al modelo cinético de orden cero, mientras que FFA con α-tocoferol y TBA siguieron una cinética de primer y segundo orden, respectivamente. La constante cinética (k) se describió mediante una ecuación de Arrhenius y la energía de activación varió de 5,72 a 18,5 kJ/mol para los gérmenes estabilizados.

PALABRAS CLAVE: *Energía de activación; Enzimas lipasa; Estabilidad oxidativa; Parámetros cinéticos*

Citation/Cómo citar este artículo: Erim Köse Y. 2021. Kinetic modeling of oxidation parameters and activities of lipase-lipoxygenase in wheat germ oil. *Grasas Aceites* **72** (3), e423. https://doi.org/10.3989/gya.0554201

1. INTRODUCTION

Wheat germ is the most valuable part of wheat with important nutritional components, such as essential amino acids (lysine, methionine, threonine), vitamins E and B, dietary fiber, sugars, minerals and fat (Ali *et al.,* 2013; Zhu *et al.,* 2010). Germ also contains valuable antioxidant components such as phenolic acids, flavonoids and carotenoids, especially tocopherols, which have protective effects against free radicals. Wheat germ oil is the richest source of α-tocopherol and is more unsaturated than other cereal oils. The highly unsaturated fatty acids and the activity of hydrolytic and oxidative enzymes (LA and LOX) in raw wheat germ are factors that accelerate the development of rancidity. LA is the primary enzyme that is responsible for the hydrolysis of triglycerides into glycerol and free fatty acids. LOX and peroxidase also play key roles in the deterioration of raw germ (Orthoefer, 2005). As a result, rancid-flavor, bitterness taste, and off-odor develop and finally, raw germ becomes completely inedible. Therefore, raw germ is mostly blended with wheat bran in the milling process and generally used as an animal feed all over the world (Ge *et al.,* 2000). Several stabilization techniques have been used for inactivating LA activity, preventing rancidity and so improving the shelf-life of germ. Recently, the most popular stabilization method is a heat treatment which includes baking (Megahed, 2011; Attia and Abou-Gharbia, 2011; Meriles *et al.,* 2019), roasting (Krings *et al.,* 2000; Zou *et al.,* 2018), toasting (Ali *et al.,* 2013), MW drying (Srivastava *et al.,* 2007; Zhang *et al.,* 2008, Xu *et al.,* 2013, Xu *et al.,* 2016), drying in a fluidized bed dryer (Marti *et al.,* 2014, Yöndem-Makascıoğlu *et al.,* 2005), infrared drying (Jha *et al.,* 2013; Li *et al.,* 2016, Gili *et al.,* 2017), extrusion cooking (Gomez *et al.,* 2012), and moist heat treatment (Sudha *et al.,* 2007; Srivastava *et al.,* 2007).

Among these methods, MW treatment has a minimum effect on the nutrient loss from germ and also decreases the Maillard reaction rate because of its mechanism. Moreover, it provides rapid and uniform heating. Reports on wheat germ stabilization by MW generally deal with nutritional changes after stabilization. For example, Sjöwall *et al.* (2000) stabilized raw wheat germ by MW oven at 45-55 ˚C and stored it for seven weeks at room temperature. Rancid odor and flavor changes were observed in the untreated wheat germ after three weeks, whereas no difference was observed in the MW-heated wheat germ after seven weeks of storage. A study by Zhang *et al.* (2008) revealed that MW could effectively destroy LOX enzyme in raw germ and improve shelf-life quality as well. Xu *et al.* (2016) measured LA and LOX activities as a result of the stabilization of raw germ in MW and convection ovens. These treatments inactivated enzymes completely with increasing temperature and time. Their study also showed that LA was more heat-stable than LOX. Xu *et al*. (2013) reported that there was a significant decrease in LA activity, and LOX became completely inactive in MW-treatment germ samples. In addition, it was reported that an increase in acidity was not high at the end of 60 days in the stabilized germs, which were subjected to a rapid oxidation test, and MW treatment could cause the death of harmful microorganisms. Previous studies have demonstrated that different stabilization and storage conditions of wheat germ have changed the physical, chemical or microbiological parameters of the germ drastically. Kinetic modeling is a good way to predict these changes in quality parameters during stabilization and also long-term storage conditions. Therefore, this study aimed to investigate the oxidation aspect parameters of raw germ during the stabilization of MW treatment and different storage conditions. In this study, valuable results were achieved regarding processing quality thanks to the calculated kinetic parameters.

2. MATERIALS AND METHODS

2.1. Materials

The raw wheat germ used in this study was obtained from the Sağlık Flour Company in Konya, Turkey. The samples were collected directly after milling in polyethylene bags and stored at a temperature of -36 °C in a freezer until they were used. All chemicals were of analytical-reagent grade (Sigma-Aldrich, Oakville, Canada).

2.2. Stabilization method and oil extraction

Two hundred grams per batch of raw sample were heated in a MW oven (Arçelik, MD554) at 700 W for three min. The samples were spread out evenly to a thickness of 0.4 cm and heated at 100% power. The inner temperature of the sample was about 120 ± 5 °C

after heating. The stabilized samples were kept at -18, 0, + 4 and, + 25 °C for 105 days in polyethylene bags after cooling to room temperature.

The oils of the germ samples were extracted using the cold extraction method. Wheat germ and hexane (10-fold hexane of wheat germ oil content) were homogenized with a homogenizer (Heidolph, Germany) for 90 s at 12500 rpm. The mixture was placed in the glass flask and shaken with a circular shaker for two hours at 200 rpm and then filtered to the extraction flask. The above procedure was repeated twice and pooled filtrates were removed by a rotary vacuum evaporator at 40 °C at 150 rpm (Heidolph, Germany) (Bakkalbaşı *et al.,* 2012).

The wheat germ oil was extracted from stabilized and stored germ samples on days 0, 15, 30, 45, 60, 75, 90, and 105. FFA, PV, TBA, and α-tocopherol in germ oil samples were analyzed. LA and LOX activities were measured.

2.2.1. Determination of oxidation parameters and enzyme activities

The oxidative parameters of raw and stabilized germ oil samples were evaluated by the measurement of FFA, PV (AOCS 1994), TBA (Tarladgis *et al*., 1960), α-tocopherol (AOCS 1994) and calculated LA (Xu *et al.,* 2013) and LOX (Xu *et al.,* 2016) activities.

2.2.2. Kinetic modeling

Zero-order (Eq. 1), first-order (Eq. 2) and second-order (Eq. 3) kinetic models were used to describe the oxidation aspects and enzyme activity changes during storage with different storage temperatures of the MW-stabilized germ oil samples.

$$C = C_0 \pm kt \quad (1)$$

$$C = C_0 \exp(\pm kt) \quad (2)$$

$$1/C = 1/C_0 \pm kt \quad (3)$$

In these equations, C is quality parameter, C_0 is the value of this quality parameter at its initial state, t is storage time (day) and k is kinetic constant (day^{-1}). Where (+) and (-) indicated formation and degradation of the quality parameters, respectively.

3. RESULTS AND DISCUSSION

The oxidation parameters and activity of LA and LOX values of wheat germ oils extracted from raw, as well as MW-treated samples at the beginning of storage are given in Table 1. As the microwaves penetrate into the raw germ and target water molecules (Wray and Ramaswamy, 2015), the water activity decreases rapidly and reduces the rate of oxidative reactions by limiting both LA and LOX activities (Xu *et al.,* 2013). Therefore, significant decreases ($p < 0.05$) were observed in the primary and secondary oxidation products of the germ oils after exposure to MW heating. The FFA and PV of raw germ oil decreased from 4.65 to 2.44% oleic acid and 3.60 to 1.66 $meqO_2$/kg after stabilization using MW treatment, respectively. These results are comparable to previous stabilization studies conducted by Attia and Abou-Gharbia, 2011, Suresh Kumar *et al.,* 2014 and Zou *et al.,* 2018. However, Yöndem-Makascıoğlu *et al.,* 2005 and Xu *et al.,* 2013 reported an increase in FFA and PV in MW-treated germ samples. In these studies, the water, which is the essential reactant for hydrolysis reaction may not be reduced due to an inadequate heat and time combination of the MW oven. Therefore, the hydrolysis reaction rate may not be decreased in these studies. The secondary products from the lipid oxidation of unsaturated fatty acids are generally measured by TBA value and stated as mg malondialdehyde/kg (mgMA/kg) (Sorensen and Jorgensen, 1996; Ercoşkun and Özkal, 2011). Its value decreased from 0.278 to 0.187 mg MA/kg product during MW treatment. The LA of raw germ oil was 4.77 U/g, while the MW-treated germ remained at 0.32 U/g. All of the MW-treated samples (stored with different conditions for 105 days) retained some residual LA activity. However, MW-treated samples lost LOX activity completely

Table 1. Parameters of raw and microwave-treated germ samples at the beginning of the storage

Parameters	Raw Mean ± SD	Microwave-treated Mean ± SD
FFA (%)	4.65±0.07	2.44±0.17
Peroxide ($meqO_2$/kg)	3.60±0.22	1.66±0.20
TBA (mg MA/kg)	0.278±0.02	0.187±0.02
α-tocopherols (mg/kg)	1750±1.41	1676±1.21
Lipase (U/g)	4.77±0.04	0.32±0.09
Lipoxygenase (U/mg)	4.020±0.04	nd

Data are expressed as mean ± SD (standard deviation) (n= 3).
FFA: Free fatty acids, TBA: thiobarbituric acid, nd: not detected.

Table 2. Kinetic parameters of microwave-treated germ samples after 105 days of storage.

Parameter	Storage Temperature	Model	C_0 Mean ± SD	k (day^{-1}) Mean ± SD	R^2	E_a (kj/mol)
FFA	-18 °C	First-order kinetic	2.408±1.42	0.0110±0.22	0.988	6.98
	0 °C		2.519±0.97	0.0134±0.66	0.995	
	4 °C		2.593±1.07	0.0156±0.34	0.993	
	25 °C		2.785±1.02	0.0175±0.22	0.994	
PV	-18 °C	Zero-order kinetic	0.828±0.65	0.0999±0.25	0.972	5.95
	0 °C		1.457±1.12	0.1080±0.84	0.994	
	4 °C		1.569±1.27	0.1275±0.13	0.991	
	25 °C		1.582±1.03	0.1483±0.21	0.961	
TBA	-18 °C	Second-order kinetic	0.197±0.19	-0.0095±0.04	0.718	6.54
	0 °C		0.193±0.58	-0.0113±0.05	0.611	
	4 °C		0.205±0.30	-0.0138±0.04	0.789	
	25 °C		0.220±0.66	-0.0146±0.02	0.742	
α-tocopherol	-18 °C	First-order kinetic	1667.532±2.82	-0.0004±0.00	0.925	18.5
	0 °C		1680.253±2.12	-0.001±0.00	0.967	
	4 °C		1679.580±2.44	-0.0012±0.01	0.997	
	25 °C		1656.065±2.21	-0.0014±0.01	0.927	
LA	-18 °C	Zero-order kinetic	0.0133±0.24	0.0349±0.00	0.976	5.72
	0 °C		0.2783±0.41	0.0365±0.08	0.988	
	4 °C		0.3900±0.38	0.039±0.02	0.993	
	25 °C		0.477±1.05	0.0514±0.08	0.972	
LOX	nd					

Data are expressed as mean ± SD (standard deviation) (n= 3). FFA: Free fatty acids, PV: peroxide value, TBA: thiobarbituric acid, LA: lipase activity, LOX: lipoxygenase activity, nd: not detected.

(Table 1). From this research, it was evident that LA is tolerable to heat in low moisture systems like MW-oven, and also LOX is more thermally sensitive under the same conditions of LA. This phenomenon is supported by previous studies on heat-stabilized wheat germ (Sudha *et al.,* 2007; Attia and Abou-Gharbia, 2011, Xu *et al.,* 2013; Li *et al.,* 2016). The content in vitamin E (α-tocopherol) changed drastically in MW-treated wheat germ compared to raw samples because of the low thermal stability of α-tocopherol (Srivastava *et al.,* 2007; Yılmaz *et al.,* 2014).

Table 2 shows the estimated kinetic parameters of oxidation and enzyme activity values for wheat germ oils which were extracted from MW-treated samples under different storage conditions. The high determination coefficient of R^2 value was confirmed as the most accurate fit. Only the models with the highest R^2 values are presented in Table 2. The reaction rate constant (k) and the initial quality value (C_0) were also calculated for all the oxidation quality parameters.

Changes in FFA during the storage of MW-treated germ samples with different storage temperatures are given in Figure 1. As expected, the amounts of FFA increased with increasing storage temperature and time. It was best represented by the first-order kinetic model with high R^2 (0.994-0.988). The highest FFA value (16.32%) was observed in the sample, which was stored at 25 °C on day 105. Hydrolytic and oxidative rancidity in wheat germ oil during long-term storage is responsible for this increase. Similar results were found for wheat germ oil by (Attia and Abou-Gharbia, 2011; Megahed, 2011; Mahmoud

et al., 2015). Generally, the first products of lipid oxidation appear within a certain storage period in foods and as can be seen in Figure 2, the PV increased during long-term storage. The initial and final PV increased from 1.66 to 11.76 and 18.44 meq O_2/kg. This increase may be due to the hydrolytic rancidity of germ oil by residual LA activity. (As was previously reported, the enzyme inactivation process is not enough in a MW-oven because of the thermal-stability of LA). The results obtained were in agreement with the studies published in the literature that the PV of germ oil was increased under long-term storage conditions (Hygreeva, 2013; Li *et al.,* 2016; Zou *et al.,* 2018). For the mathematical modeling of PV, a zero-order kinetic model was used (Figure 2). The kinetic rate constant (k) of FFA and PV increased from 0.011 to 0.0175 and 0.0999 to 0.1483 day^{-1}, respectively. This suggests that the degradation rate of primary products of lipid oxidation becomes faster as a result of high storage

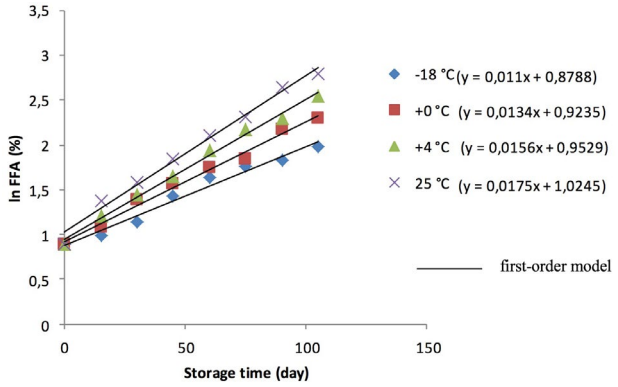

FIGURE 1. Kinetic changes in the free fatty acids (FFA) of the MW-stabilized wheat germ oil during storage. Three replicates were performed for each kinetic experiment (n=3).

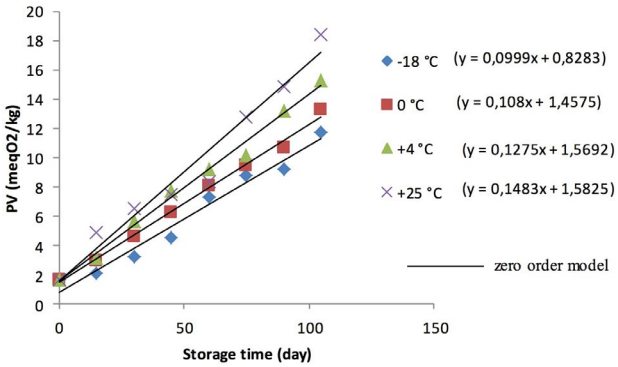

FIGURE 2. Kinetic changes in the peroxide value (PV) of the MW-stabilized wheat germ oil during storage. Three replicates were performed for each kinetic experiment (n=3).

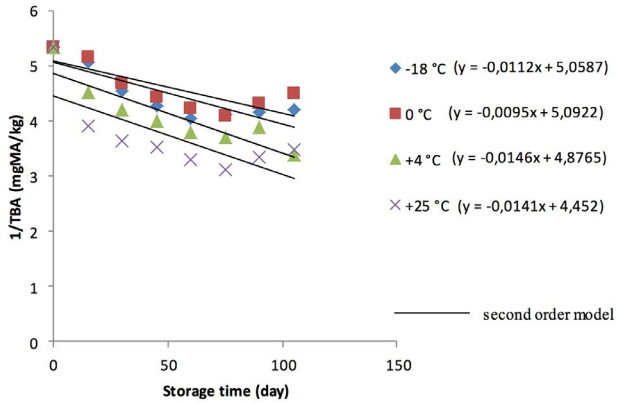

FIGURE 3. Kinetic changes in the thiobarbituric acid (TBA) of the MW-stabilized wheat germ oil during storage. Three replicates were performed for each kinetic experiment (n=3).

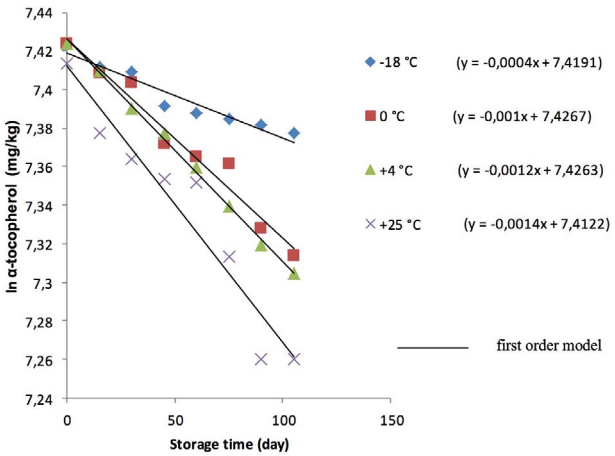

FIGURE 4. Kinetic changes in the α-tocopherol of the MW-stabilized wheat germ oil during storage. Three replicates were performed for each kinetic experiment (n=3).

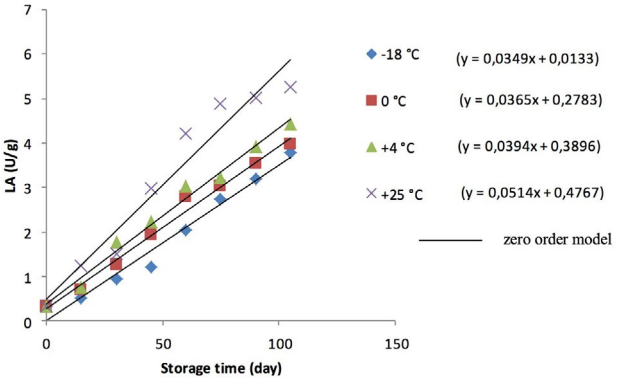

FIGURE 5. Kinetic changes in the lipase activity (LA) of the MW-stabilized wheat germ oil during storage. Three replicates were performed for each kinetic experiment (n=3).

temperature. A linear increase was observed in the TBA values of all samples in the first 60 days of storage, but a small decrease was determined from day 75. The increase in TBA indicates the formation of secondary products due to more intense lipid oxidation in the first 60 days, while the decrease in TBA may be indicative of the degradation of these components to volatile compounds at later stages of storage (Ercoşkun and Özkal, 2011). At the end of the storage period, the highest value for TBA (0.333 mg MA/kg) was determined in the sample stored at 25 °C on day 60. Changes in TBA value were best represented by the second-order kinetic model with negative k values being changed from -0.0095 to -0.0146 (Figure 3). The α-tocopherol content decreased during the storage period (Figure 4). Although this decrease was fast in the samples stored at 25 °C, it was slow at lower temperatures. It was also observed that increased storage time accelerated a loss in tocopherol. The change in α-tocopherol content was determined by Capitani *et al.* (2011), and was dependent on the storage conditions of the germ. The reported values were in agreement with the data in this study. a 35% reduction has been reported in the α-tocopherol content in the germ with increasing storage time and storage temperature. The decrease in α-tocopherol content was best represented by the first-order kinetic model with the negative k-value changing from -0.0004 to -0.0014 (Table 2). Figure 5 shows that a linear increase was determined for the LA activity value, and this enzyme process can be described by the zero-order kinetic model. On the other hand, LOX activity completely disappeared immediately after MW treatment, so no modeling was done. As mentioned above, under the same conditions, LA is more tolerable to heat than LOX.

The Arrhenius model described the temperature dependence of the reaction rate constant for all the oxidation parameters, and the estimated activation energies, which had the highest R^2 values are also shown in Table 2.

Arrhenius relationship:

$$lnk = lnA - \left(\frac{E_a}{Rt}\right)$$

where k is the reaction rate constant; A—pre-exponential factor; Ea is the activation energy (kJ/mol); R is the universal gas constant (kJ/molK), and T is the absolute temperature (K).

4. CONCLUSIONS

Many studies on the stabilization of raw wheat germ have focused on traditional heating methods. Recently, MW treatment has been widely used to prevent wheat germ from oxidation with inactivation of enzymes and minimum effects on the nutritional value. In this study, a MW-stabilization technique for wheat germ and wheat germ oil was investigated using experimental and analytical methods for quality parameters of the oxidation. Findings in the kinetic evaluation of MW conditions showed that the acid value of raw wheat germ oil decreased by 47.5% after MW treatment. The same trend was observed for other oxidation parameters. As expected, decreasing the storage temperature slowed down the oxidation rate and ideal storage temperature was -18 °C in all samples. MW treatment inactivated LOX completely, while LA was reduced to 93.2% and the zero-order kinetic equation fit the LA inactivation curve quite well. These results reveal that LOX is more thermally sensitive under the same conditions of LA. The kinetic models used in this study adequately described the MW process and gave oxidation values that were in good agreement with the experimental results. For the process, the activation energy was also calculated, assuming an Arrhenius-type temperature reliance. Thanks to this study, the effects of different stabilization methods on the quality of different cereal wastes like germ can be investigated following the same parameters and models.

REFERENCES

Ali S, Usman S, Nasreen Z, Zahra N, Nazir S, Yasmeen A, Yaseen T. 2013. Nutritional evaluation and stabilization studies of wheat germ. *Pak. J. Food Sci.* **23**, 148-152.

AOCS 1994. *Official Methods and Recommended Practices of the American Oil Chemists' Society*, 4th Edition. AOCS Press, Illinois.

Attia RS, Abou-Gharbia HA. 2011. Evaluation and stabilization of wheat germ and its oil characteristics. *Alex J. Fd. Sci. Technol.* **8**, 31-39.

Bakkalbaşı E, Yılmaz ÖM, Javidipour I, Artık N. 2012. Effects of packaging materials, storage conditions and variety on oxidative stability of shelled walnuts. *LWT-Food Sci Technol.* **46**, 203-209. https://doi.org/10.1016/j.lwt.2011.10.006

Capitani M, Mateo CM, Nolasco SM. 2011. Effect of temperature and storage time of wheat germ on the oil tocopherol concentration. *Braz. J. Chem. Eng.* **28**, 243-250. https://doi.org/10.1590/S0104-66322011000200008

Ercoşkun H, Özkal SG. 2011. Kinetics of traditional Turkish sausage quality aspects during fermentation. *Food Control* **22** (2), 165-172. https://doi.org/10.1016/j.foodcont.2010.06.015

Ge Y, Sun A, Ni Y, Cai T. 2000. Some nutritional and functional properties of defatted wheat germ protein. *J. Agric. Food. Chem.* **48**, 6215-6218. https://doi.org/10.1021/jf000478m

Gili RD, Palavecino PM, Penci MC, Martinez ML, Ribotta PD. 2017. Wheat germ stabilization by infrared radiation. *J. Food Sci. Technol.* **54**, 71-81. DOI:10.1007/s13197-016-2437-z

Gomez M, Gonzalez J, Oliete B. 2012. Effect of extruded wheat germ on dough rheology and bread quality. *Food Bioprocess Technol.* **5**, 2409-2418. https://doi.org/ 10.1007/s11947-011-0519-5.

Hygreeva D, Pandey MC, Radhakrishna K. 2012. A preliminary study on evaluation of antioxidant activity and oxidative stability of wheat germ oil in poultry and mutton meat systems. *IJFANS* **2**, 40-46.

Jha PK, Kudachikar VB, Kumar S. 2013. Lipase inactivation in wheat germ by gamma irradiation. *Radiat. Phys. Chem.* **86**, 136-139. https://doi.org/ 10.1016/j.radphyschem.2013.01.018

Krings U, El-Saharty YS, El-Zeany BA, Pabel B, Berger RG. 2000. Antioxidant activity of extracts from roasted wheat germ. *Food Chem.* **71**, 91-95. https://doi.org/ 10.1016/S0308-8146(00)00148-5

Li B, Zhao L, Chen H, Sun D, Deng B, Li J, Liu Y, Wang F. 2016. Inactivation of lipase and lipoxygenase of wheat germ with temperature-controlled short wave infrared radiation and its effect on storage stability and quality of wheat germ oil. *Plos One* **11**, 1-13. https://doi.org/10.1371/journal.pone.0167330

Marti A, Torri L, Casiraghi MC, Franzetti L, Limbo S, Morandin F, Pagani MA. 2014. Wheat germ stabilization by heat-treatment or sourdough fermentation: Effects on dough rheology and bread properties. *LWT-Food Sci. Technol.* **59**, 1100-1106. https://doi.org/10.1016/j.lwt.2014.06.039

Mahmoud AA, Mohdaly AA, Elneairy NA. 2015. Wheat germ: an overview on nutritional value, antioxidant potential and antibacterial characteristics. *Food Nutr. Sci.* **6**, 265-277. https://doi.org/10.4236/fns.2015.62027

Megahed MG. 2011. Study on stability of wheat germ oil and lipase activity of wheat germ during periodical storage. *Agric. Biol. J. N. Am.* **2**, 163-168. https://doi.org/10.5251/abjna.2011.2.1.163.168

Meriles SP, Steffolani ME, León AE, Penci MC, Ribotta PD. 2019. Physico-chemical characterization of protein fraction from stabilized wheat germ. *Food Sci. Biotechnol.* **28**, 1327-1335. https://doi.org/10.1007/s10068-019-00594-9

Orthoefer FT. 2005. Rice bran oil. *Bailey's industrial oil and fat products*. https://doi.org/10.1002/047167849X.bio015

Sjövall O, Virtalaine T, Lapveteläinen A, Kallio H. 2000. Development of rancidity in wheat germ analyzed by headspace gas chromatography and sensory analysis. *J. Agric. Food Chem.* 48, 3522–3527. https://doi.org/10.1021/jf981309t

Sudha ML, Srivastava AK, Leelavathi K. 2007. Studies on pasting and structural characteristics of thermally treated wheat germ. *Eur. Food Res. Technol.* **225**, 351-357. https://doi.org/10.1007/s00217-006-0422-x

Srivastava AK, Sudha ML, Baskaran V, Leelavathi K. 2007. Studies on heat stabilized wheat germ and its influence on rheological characteristics of dough. *Eur. Food Res. Technol.* **224**, 365-372. https://doi.org/10.1007/s00217-006-0317-x

Suresh Kumar G, Swathi R, Gopala Krishna AG. 2014. Fat-soluble nutraceuticals and their composition in heat-processed wheat germ and wheat bran. *Int. J. Food Sci. Nutr.* **65**, 327-334. https://doi.org/10.3109/09637486.2013.866640

Sørensen G, Jørgensen SS. 1996. A critical examination of some experimental variables in the 2-thiobarbituric acid (TBA) test for lipid oxidation in meat products. *Z. Lebensm. Unters Forsch*. **202**, 205-210. https://doi.org/10.1007/BF01263541

Tarladgis BG, Watts BM, Younathan MT, Dugan L. 1960. A distillation method for the quantitative determination of malonaldehyde in rancid foods. *J. Am. Oil Chem. Soc*. **37** 44-48. https://doi.org/10.1007/BF02630824

Xu B, Zhou SL, Miao WJ, Gao C, Cai MJ, Dong Y. 2013. Study on the stabilization effect of continuous microwave on wheat germ. *J. Food Eng.* **117**, 1-7. https://doi.org/ 10.1016/j.jfoodeng.2013.01.031

Xu B, Wang LK, Miao WJ, Wu QF, Liu YX, Sun Y, Gao C. 2016. Thermal versus microwave inactivation kinetics of lipase and lipoxygenase from wheat germ. *J. Food Process Eng.* **39**, 247-255. https://doi.org/ 10.1111/jfpe.12216

Yöndem-Makascıoğlu F, Gürün B, Dik T, Suzan Kıncal N. 2005. Use of a spouted bed to improve the storage stability of wheat germ followed in paper and polyethlyene packages. *J. Sci. Food Agric.* **85***,* 1329-1336. https://doi.org/ 10.1002/jsfa.2102

Wray Derek, Ramaswamy HS. 2015. Novel concepts in microwave drying of foods. *Drying Technol.* **33** (7), 769-783. https://doi.org/10.1080/07373937.2014.985793

Yılmaz N, Tuncel NB, Kocabıyık H. 2014. Infrared stabilization of rice bran and its effects on *γ*-oryzanol content, tocopherols and fatty acid composition. *J. Sci. Food Agric.* **94**, 1568-1576. https://doi.org/10.1002/jsfa.6459

Zhu KX, Sun XH, Chen ZC, Peng W, Qian HF, Zhou HM. 2010. Comparison of functional properties and secondary structures of defatted wheat germ proteins separated by reverse micelles and alkaline extraction and isoelectric precipitation. *Food Chem.* **123**, 1163-1169. https://doi.org/10.1016/j.foodchem.2010.05.081

Zou Y, Gao Y, He H, Yang T. 2018. Effect of roasting on physico-chemical properties, antioxidant capacity, and oxidative stability of wheat germ oil. *LWT-Food Sci. Technol.* **90**, 246-253. https://doi.org/10.1016/j.lwt.2017.12.038

Zhang YR, Zhou XQ, Guo Y R. 2008. Study on the technologıcal parameters of de actıvatıng enzyme ın wheat germ by mıcrowave. *Journal of Henan University of Technol. (Natural Sci. Edt.)* **2**, 7-10.

GRASAS Y ACEITES 72 (3)
July-September 2021, e424
ISSN-L: 0017-3495
https://doi.org/10.3989/gya.0334201

Improving the oxidative stability of breadsticks with ginkgo (*Ginkgo biloba*) and ginseng (*Panax ginseng*) dried extracts

K.S.M. Hammad, N.F.S. Morsy✉ and E.A. Abd El-Salam

Food Science Dep., Faculty of Agriculture, Cairo University, Egypt
✉Corresponding author: nanafsm@yahoo.com

Submitted: 29 March 2020; Accepted: 27 July 2020; Published online: 17 September 2021

SUMMARY: Recently, there has been a growing interest in the use of natural antioxidants instead of synthetic ones. The aim of this work was to determine the effect of ginkgo and ginseng dried extracts as natural antioxidants on the stability of lipids in breadsticks over 55 days of storage at room temperature compared to butylated hydroxytoluene. Ginkgo and ginseng dried extracts were incorporated individually into breadstick formulae at levels of 0.5 and 1% to enhance its oxidative stability in storage. The increases in peroxide, *p*-anisidine and Totox values in the oil phase of the samples during storage were monitored. The changes in hydroperoxide, trans fatty acid and aldehyde contents were investigated by Fourier transform infrared spectroscopy. The sensory analysis was performed to evaluate the perceptible changes occurring during storage. The results indicated that the oxidation of oil in breadstick samples can be retarded by enriching the breadstick formula with dried ginseng extract at a 1% level.

KEYWORDS: *Antioxidant; Breadstick; Ginkgo; Ginseng; Oxidative stability; Shelf-life*

RESUMEN: ***Mejora de la estabilidad oxidativa de la barra de pan con extractos secos* de *ginkgo (*Ginkgo biloba*) y ginseng (*Panax ginseng*).*** En la actualidad existe un creciente interés por el uso de antioxidantes naturales en lugar de sintéticos. El objetivo de este trabajo fue determinar el efecto de extractos secos de ginkgo y ginseng como antioxidantes naturales sobre la estabilidad de los lípidos en barras de pan durante 55 días de almacenamiento a temperatura ambiente, en comparación con el butilhidroxitolueno. Los extractos secos de ginkgo y ginseng se incorporaron individualmente en la formulación de barra de pan a niveles de 0,5% y 1% para mejorar su estabilidad oxidativa durante el almacenamiento. Se siguió el aumento de los valores de peróxido, *p*-anisidina y Totox de la fase oleosa de las muestras durante el almacenamiento. Los cambios en los contenidos de hidroperóxido, ácidos grasos *trans* y aldehídos se investigaron mediante espectroscopía infrarroja por transformada de Fourier. El análisis sensorial se realizó para evaluar los cambios perceptibles ocurridos durante el almacenamiento. Los resultados indican que la oxidación del aceite en las muestras de barra de pan se puede retardar enriqueciendo la fórmula de barra de pan con extracto de ginseng seco al 1%.

PALABRAS CLAVE: *Antioxidante; Barra de pan; Estabilidad oxidativa; Gingko; Ginseng; Vida media*

Citation/Cómo citar este artículo: Hammad KSM, Morsy NFS, Abd El-Salam EA. 2021. Improving the oxidative stability of breadsticks with ginkgo (*Ginkgo biloba*) and ginseng (*Panax ginseng*) dried extracts. *Grasas Aceites* **72** (3), e424. https://doi.org/10.3989/gya.0334201

1. INTRODUCTION

A breadstick is a rolled-shaped crispy texture bakery product with a low moisture content, which is widely consumed all over the world. Maintaining the quality of bakery products, stored at room temperature, for a specific time is important from an economic point of view (Thanushree *et al*., 2017). Lipid oxidation and loss in crunchiness are the main causes of deterioration of the bakery products with low moisture and high fat contents, such as cookies and breadsticks (Calligaris *et al*., 2008; Caruso *et al*., 2017).

Unsaturated vegetable oils are used at different levels in the production of breadsticks (Difonzo *et al*., 2018). Extra virgin olive oil is used at 25% to prepare breadsticks. The type and level of fat in breadsticks are responsible for accelerated quality depletion. Increases in the degrees of fatty acids' unsaturation accelerates the rate of lipid oxidation. Antioxidants can be added into the formulae of food items to retard lipid oxidation and extend their shelf-life (Alamprese *et al*., 2017).

Ginkgo (*Ginkgo biloba*, Family: Ginkgoaceae) is an ancient plant. Ginkgo leaves have been used as food and in traditional remedies for centuries (Wang and Zhang, 2019). The ginkgo leaf extract contains high amounts of flavonoids (24%) and terpene lactones (6%) (Wang *et al*., 2015). The antioxidant activity of ginkgo extract is attributed to its phenolic and flavonoid compounds (Sati *et al*., 2019). Kobus-Cisowska *et al*. (2014) inhibited the lipid oxidation of pork meatballs during 21 days of refrigerated storage by the addition of ginkgo lyophilized leaf extract to the meat batter at 500 mg/kg. Dipping silver pomfret (*Pampus argenteus*) fillets in ginkgo leaf extract at 2.5 mg/mL extended its shelf-life from 8 to 15 days during refrigerated storage in ice at 4 ºC by suppressing lipid oxidation (Lan *et al*., 2018).

The roots of ginseng (*Panax ginseng*, Family: Araliaceae) are well known for their high contents in saponins, ginsenosides, phenolic compounds, and carotenoids (Riaz *et al*., 2019). Ginseng products including ginseng extract have been approved for use as a food or food ingredient, according to the Codex Standard (321-2015). Supplementing milk or yogurt with ginseng extract at 2% significantly increased the DPPH radical scavenging activity of the product (Park *et al*., 2018).

There are only a few studies available concerning the shelf-life of breadsticks (Calligaris *et al*., 2008; Alamprese *et al*., 2017; Barbieri *et al*., 2018). To date, no study using ginkgo or ginseng dried extracts as natural antioxidants to extend the shelf-life of bakery products has been reported. Thus, the aim of this study was to investigate the effectiveness of ginkgo and ginseng dried extracts on the oxidative stability of breadsticks during storage at room temperature.

2. MATERIALS AND METHODS

2.1. Materials

Refined sunflower oil (without added antioxidants) was obtained from Ajwa for Food Industries Co., Egypt. *Ginkgo biloba* dried leaf extract powder was procured from Changsha Huakang Biotechnology Development Co., LTD (Changsha, Hunan, China). Asian *Panax ginseng*, dried root extract was provided by Dalian Tianshan Industrial Co., LTD (Dalian, China). Ginsenoside standards (Rb1, Rb2, Rc, Rd, Re, Rf, and Rg1) were obtained from Extrasynthese (Lyon, France). Butylated hydroxy toluene (BHT), Gallic acid and Folin Ciocalteu reagent were procured from Sigma Aldrich, USA. Wheat flour, type 55 (72% extraction rate), Five Star Flour Mills Company, Suez, Egypt, and instant dry yeast (Lesaffre, Egypt) were purchased from a local market (Cairo, Egypt).

2.2. Preparation of breadsticks

Six breadstick formulae were prepared using 500 g wheat flour, 208.5 mL water, 50 g sugar, 3.5 g salt, 13.5 g yeast and 100 mL sunflower oil. Based on the wheat flour weight, the investigated formulae were: (1) without antioxidant (control), (2) BHT (0.02%), (3) Ginkgo extract (0.5%), (4) Ginkgo extract (1%), (5) Ginseng extract (0.5%), and (6) Ginseng extract (1%). Investigated extracts and BHT were completely dissolved in the oil phase using a vortex mixer for 5 min. All of the previous ingredients were mixed at slow speed for 2 min, then at medium speed for 10 min using a kitchen mixer (Moulinex, Supermix 150, France). The dough was left to rest for 10 min. After that, the dough was hand-rolled to form long cylindrical strips. The fermentation was performed at 35 °C and 80% relative humidity for 40 min. Baking was carried out at 170 °C for 35 min in a rotary oven fitted with a fermentation room (SHOF, Jeddah, Saudi Arabia). The breadstick samples were

allowed to cool for 2 h. Breadstick samples made from each formula were packed (200 g each pack) in plastic bags before storage at 25 °C.

2.3. Extraction of oil from breadstick samples

A breadstick sample (20 g) was ground into a fine powder using a laboratory blender. The oil fraction of the ground breadstick sample was extracted using diethyl ether at a ratio of 1:10 (w/v) with magnetic stirring for 1 h at room temperature followed by filtration through filter paper (Whatman No. 1). The solvent was evaporated under vacuum at 30 °C by a rotary evaporator. The extracted oil was stored at 5 °C. Analyses were carried out after processing (0, 10 days of storage) and periodically every 15 days. The experiment was terminated when the peroxide value of the oil phase of either ginkgo or ginseng breadstick samples in both concentrations reached or exceeded 10 meq O_2/kg oil (limit of acceptability as reported by Calligaris *et al*., 2008).

2.4. Determination of total phenolic contents in the ginkgo and ginseng extracts

The total phenolic contents (TPC) in the ginkgo and ginseng extracts were determined by Folin Ciocalteu's colorimetric method (Arnous *et al.,* 2002). An aliquot of sample (10 µL) was mixed with 50 µL of Folin-Ciocalteu reagent and 790 µL of distilled water using a vortex mixer. The mixture was allowed to stand for 1 min for reaction. Afterwards, the mixture was neutralized by 150 µL sodium carbonate (20%) and left to stand in the dark for 2 h. The absorbance of the samples was determined using a Shimadzu UV-2450 Spectrophotometer, Japan, at 750 nm. Gallic acid was used as a standard. Results were expressed as mg gallic acid equivalents (GAE)/g dry extract.

2.5. Determination of total phenolic content in prepared breadsticks

The determination of TPC in the freshly prepared breadstick samples was carried out according to Bhat *et al*. (2019). Crushed breadsticks (0.5 g) were suspended in 25 mL of acidified methanol (HCl/methanol/water, 1:80:10, v/v/v) for 2 h. After centrifugation at 2000 g for 10 min, 200 µL of the supernatant were mixed with 1.5 mL of the diluted (10 fold) Folin-Ciocalteu reagent using a vortex mixer. The mixture was allowed to equilibrate for 5 min and neutralized with 1.5 mL of sodium carbonate solution (60 g/L). The samples were incubated for 90 min at room temperature (25 °C). The absorbance of the samples was determined as above mentioned.

2.6. High performance liquid chromatography (HPLC) analysis of phenolic compounds in ginkgo extract and ginsenosides in ginseng extract

The determination of phenolic compounds in the ginkgo extract was performed by Agilent 1260 series HPLC (Agilent Technologies Co., CA, USA). The separation was carried out using an Agilent Zorbax Eclipse XDB-C18 column (4.6 mm x 250 mm, 5 µm particle size). The mobile phase consisted of water containing 1% acetic acid (A) and acetonitrile (B) and the flow rate was maintained at 1 mL/min. The mobile phase was programmed consecutively in a linear gradient as follows: 0-5 min (80% A); 5-8 min (40% A); 8-12 min (50% A); 12-25 min (80% A). The detector was monitored at 284 nm. The injection volume was 10 µL. The column temperature was maintained at 35 ºC. The peaks were identified by retention time after matching with authentic standards. The linear calibration curve of the standards was used for quantification.

The ginsenosides in the ginseng extract were analyzed using a Shimadzu LC-20 (Prominence) connected to an ultraviolet detector (Hitachi, Tokyo, Japan) at 203 nm. The ginseng extract sample was dissolved in 30% methanol by sonication and filtered (0.45 µm, Acrodisk). The separation was performed on an Altima HP C_{18} HL column (150 mm x 4.6 mm i.d., 3 µm). The analysis was carried out with a binary gradient elution using (A) water and (B) acetonitrile as the mobile phase, according to the method of Li and Fitzloff (2002). The gradient elution program was as follows: 0-33 min, 19-35% B; 33-33.6 min, 35-80% B; 33.6-37 min, 80-19% B. The flow rate was 1.5 mL/min. The temperature of the analytical column was 30 °C. The identification of ginsenosides was carried out using the reference standards. The quantification was performed according to the area normalization method.

2.7. Quality characteristics of oil samples extracted from prepared breadsticks

2.7.1. Peroxide value

The peroxide value (PV) of the samples was determined according to AOCS (2009) methods.

The results were expressed as the average of three measurements in meq O_2/kg oil. The analysis was carried out in triplicate. Samples with PV over 10 meq O_2/kg oil were excluded and not subjected to further analysis.

2.7.2. p-Anisidine value

The *p*-anisidine value (*p*-AnV) was determined according to the AOCS (2009) method using a Shimadzu UV-2450 Spectrophotometer, Japan at 350 nm against a blank of isooctane. *p*-AnV was calculated by the following formula:

$$p - \text{AnV} = 25(1.2As - Ab)/m$$

where: Ab is the absorbance for sample dissolved in isooctane, As is the absorbance for the oil solution after reaction with *p*-AnV, and m is the mass of oil in 25 mL isooctane. The analysis was done in triplicate.

2.7.3. Totox value

The level of total oxidation was calculated from the following equation according to AOCS (2009) method:

$$\text{Totox} = 2\text{PV} + p - \text{AnV}$$

2.8. Spectral characteristics of oil extracted from breadsticks

2.8.1. IR spectroscopy

Infrared absorption spectra were recorded in the mid IR region of 4000-400 cm^{-1} for potassium bromide (KBr) disks of oil extracted from breadstick samples (~2 μL) to monitor changes related to the oxidative process with an FTIR spectrometer (JASCO 6100, Japan). The spectrometer was connected to a computer using Windows XP Professional software to manipulate the spectra.

2.9. Sensory evaluation

The sensory assessment was carried out on breadstick samples prepared with and without different levels of ginkgo leaf or ginseng root extracts compared to those formulated with BHT. Ten staff members of the Food Science Department (six females and four males), aged between 25 and 35 years, were selected for sensory evaluation. The sensory attributes (odor, taste and texture) were evaluated. The scores for each parameter ranged from one to a maximum of nine, where one indicated poor quality, and nine represented the best quality.

2.10. Statistical analyses

The chemical and sensory analyses were carried out in triplicate and the results presented are the average of the obtained values ± standard deviation. The data were submitted to analysis of variance (ANOVA) and the Tukey's test. A bivariate analysis of the data was carried out by Pearson's correlation test. A value of $P < 0.05$ was considered statistically significant. Analyses were performed using XLSTAT software.

3. RESULTS AND DISCUSSION

3.1. Chemical composition of ginkgo and ginseng extracts

The total polyphenol content of the dried ginkgo ethanol extract was 92.3 ± 0.3 mg GAE/g. Pereira *et al*. (2013) reported that the phenolic contents of aqueous and methanol extracts of the *G. biloba* dry leaves were 61.58 and 129.5 mg GAE/g, respectively. The HPLC profile of the dried ginkgo extract (Figure 1a) contained ellagic acid (490.46 μg/g), gallic acid (223.31 μg/g), resveratrol (181.24 μg/g), *p*-hydroxy benzoic acid (112.56 μg/g) followed by myricetin (58.74 μg/g), quercetin (27.55 μg/g) and o-coumaric acid (23.99 μg/g). The other components were quinol (15.71 μg/g), kampherol (12.14 μg/g), syringic acid (8.2 μg/g) and vanillic acid (7.13 μg/g).

According to HPLC analysis, Re (38.03%), Rd (23.12%) and Rg1 (10.69%) represented the major identified ginsenosides of the investigated ginseng extract (Figure 1b). The other identified ginsenosides were Rb1 (9.47%), Rb2 (6.90%), Rf (6.43%) and Rc (5.37%). Ginsenosides are considered the main active components of *Panax ginseng* extract (Chen *et al*., 2017). A quantitative analysis was carried out on 45 Asian and American ginseng samples by HPLC. The aim was to correlate ginsenoside contents with morphological features of the ginseng plant roots to provide a scientific basis for evaluating the quality of Asian and American ginsengs through morphological features. The analysis indicated that many of the Asian ginseng samples contained ginsenoside profiles similar to the one found in this study.

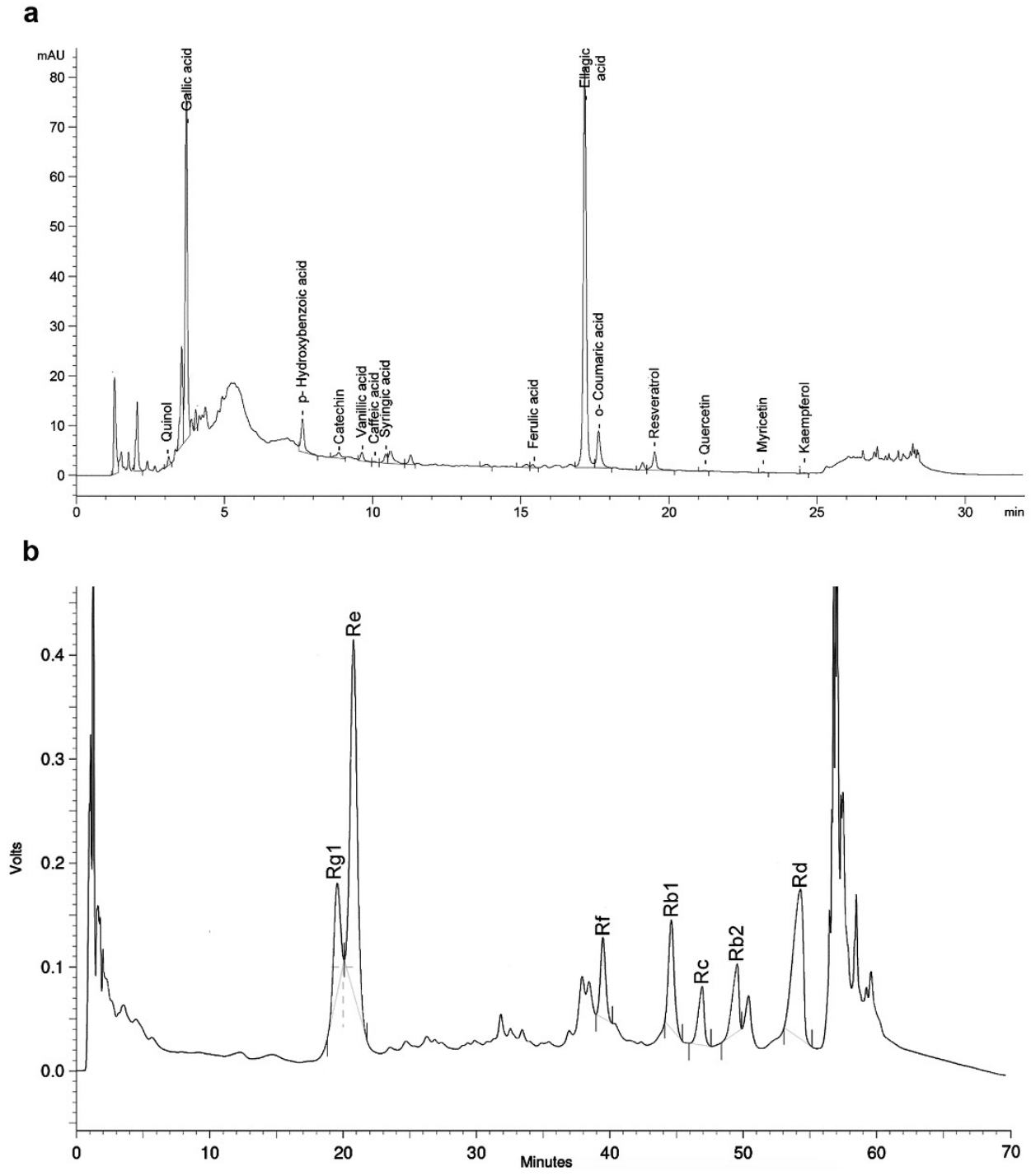

FIGURE 1. HPLC chromatograms of polyphenols of gingko extract (a) and ginsenosides of ginseng extract (b). The values refer to a single determination

In addition, the TPC of the dried ginseng extract was found to be 0.225 ± 0.01 mg GAE/g. Hwang *et al*. (2014) found that the TPC of the ginseng root extract was 0.43 mg GAE/g.

Results indicated that the polyphenol content of ginkgo 1% breadstick samples (0.412 ± 0.018 mg GAE/g) was significantly ($P < 0.05$) higher than other samples. Ginkgo 0.5%, ginseng 1% and ginseng 0.5%

breadstick samples contained 0.351 ± 0.019, 0.338 ± 0.02 and 0.316 ± 0.02 mg GAE/g, respectively. They were not significantly ($P > 0.05$) different from each other. The lowest TPC was recorded for the control (0.288 ± 0.007 mg GAE/g) and BHT (0.291 ± 0.018 mg GAE/g) breadstick samples. No significant ($P > 0.05$) difference was observed between the TPC of the control, BHT and ginseng 0.5% breadstick samples. Reis and Abu-Ghannam (2014) found that TPC of breadsticks (control sample) was about 0.1 mg GAE/g. On the other hand, the TPC of "crostini" reached 2.3 mg GAE/g. This type of dried bakery food was prepared with extra virgin olive oil at a level of 10% (Niccolai *et al*., 2019). The effect of baking on the TPC of the baked products is dependent on the type of phenolic compounds and baking conditions (Abdel-Aal and Rabalski, 2013). They reported that baking caused an apparent increase in free phenolic acids in bread due to the degradation of conjugated polyphenolic compounds.

3.2. Evaluation of the chemical oxidation indices of oil extracted from breadstick

The peroxide value (PV) was used as an indicator to follow up the oxidation state of the oil in prepared breadsticks. Calligaris *et al*., (2008) reported that peroxide value is a good index of the quality decay of breadsticks during their shelf-life. Figure 2 shows the PV of the oil extracted from the breadsticks after baking and during storage.

Immediately after baking, the investigated samples showed a PV of between 4.07 ± 0.23 and 7.37 ± 0.15 meq O_2/kg oil. The samples with ginseng extract at a 1% level or BHT showed the lowest content of peroxides at zero storage time. The baking process initiated the oxidation process, which was very fast in the control sample. After 25 days of storage at room temperature (25 °C), the PV exceeded 10 meq O_2/kg oil in the control sample (14.93 meq O_2/kg oil), and in the sample prepared with 0.5% ginkgo extract (11.9 meq O_2/kg oil).

Breadstick samples with ginseng extract at the 1% level, showed PV lower than the BHT ones throughout the storage period. The incorporation of ginkgo or ginseng extracts at 1% extended the shelf-life of the breadsticks from < 25 days to 55 days. This indicated the protective effect of ginkgo and ginseng extracts against oil oxidation in breadsticks. Alamprese *et al*., (2017) found that the PV of the breadstick samples

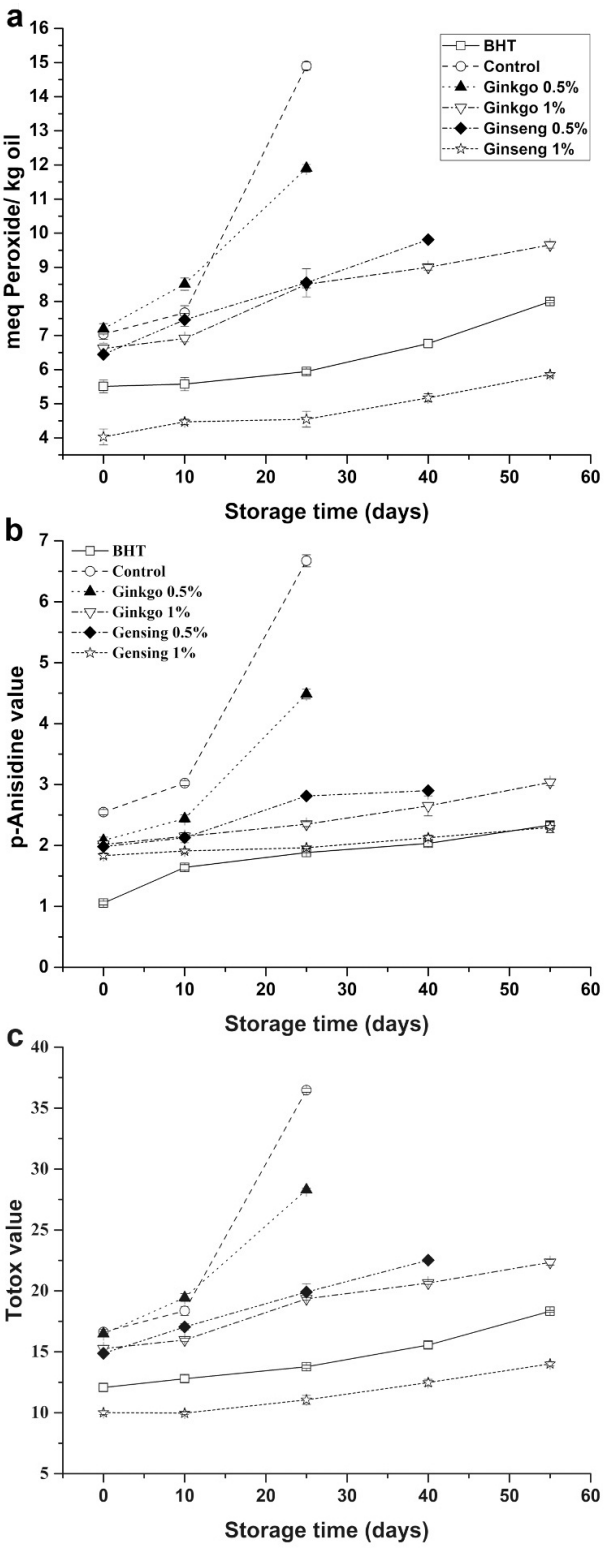

FIGURE 2. Progression of oil oxidation during the storage of the breadstick samples at 25 °C. Peroxide value (a), *p*-anisidine value (b) and Totox value (c). Values are expressed as means ± standard deviation (n = 3). Data were analyzed using one-way analysis of variance (ANOVA) and Tukey's test. Samples with peroxide values higher than 10 meq O_2/Kg were rejected and excluded from analysis

prepared with only 3.2% olive oil exceeded 10 meq O_2/kg oil after 60 days of storage at 27 °C. Calligaris *et al*., (2008) found that the consumer acceptability of the breadsticks progressively decreased with the increase in PV value to higher than 10 meq O_2/kg oil. Hydroperoxides decomposed to secondary oxidation products that could be detected by the *p*-anisidine test (Barbieri *et al*., 2018).

Peroxide and *p*-AnV values help to assess the oxidative degradation of lipids in lipid-containing food (Kozłowska *et al*., 2019). Mustac *et al*. (2020) reported that a product is considered acceptable if the *p*-AnV value is less than 10. The *p*-Anisidine value of the control and 0.5% ginkgo breadstick samples reached high levels (> 4) after 25 days of storage at room temperature. On the other hand, the *p*-AnV value of breadstick samples prepared with ginkgo or ginseng extracts at 1% or 0.02% BHT did not exceed 2.5 at the end of storage. Caruso *et al*. (2017) reported that the *p*-AnV value of freshly prepared breadstick samples with 13.3% olive oil was 5.89.

The combination of PV with *p*-AnV indicates the oxidation state (total oxidation value, Totox value) of oils. The Totox value must be equal or below 19.5 meq/kg (Esfarjani *et al*., 2019). The totox value of the investigated samples showed the same trend as those of the PV and *p*-AnV values. The Totox value of the control and 0.5% ginkgo breadstick samples was the highest (~20 meq/kg) after 10 days of storage.

Among all the investigated breadstick samples, 1% ginseng and 0.02% BHT samples had the lowest Totox value (< 17 meq/kg) after 55 days of storage at room temperature.

The progressive increase in PV in the stored breadstick samples due to lipid oxidation is associated with the development of an increase in *p*-AnV and Totox values. From the results, the ginseng extract at a concentration of 1% has a greater antioxidant effect than that of 0.02% BHT. Phenolics are responsible for the antioxidant activity of ginkgo extract (Pereira *et al*., 2013) while the antioxidant activity of ginseng extract is attributed to the identified ginsenosides (Rb1, Rg1, Rc, Rb2, and Rd) as reported by Chien *et al*., (2016).

3.3. Evaluation of the FTIR spectrum of breadstick oil

The FTIR spectra of the oil extracted from the fresh and stored breadstick samples were recorded in the range of 4000–400 cm^{-1} and illustrated in Figure 3.

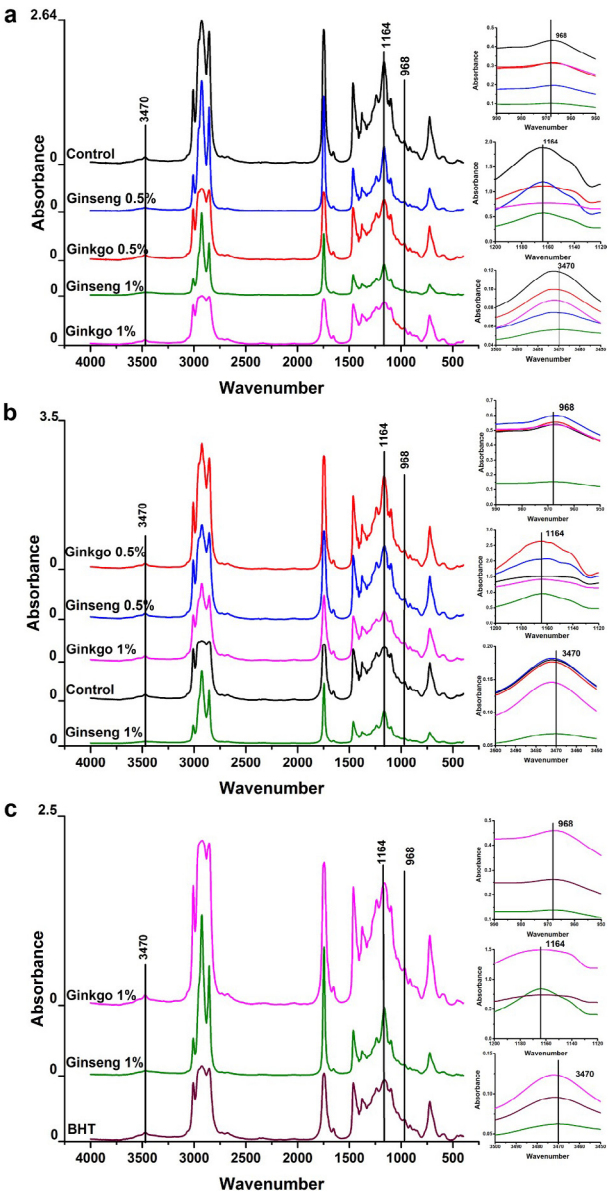

FIGURE 3. Time-course spectra of sunflower oil in breadsticks during storage on IR, illustrating the development of hydroperoxides (3470 cm^{-1}), aldehydes (1164 cm^{-1}) and trans double bonds (968 cm^{-1}) over time (0, 25 and 55 days, correspond to labels a, b and c, respectively). Samples with peroxide values higher than 10 meq O_2/Kg were rejected and excluded from analysis. The values refer to a single determination

These spectra appear to be similar and show the typical characteristic of absorption peaks for triglycerides (wave number 1746 cm^{-1} represented the ester functional group of the triglycerides) as shown by Klaypradit *et al*. (2011). In terms of oxidation analysis, the IR spectral bands of the functional groups hydroperoxide (3470 cm^{-1}), carbonyl group

(1164 cm^{-1}) and trans double bond (968 cm^{-1}) were used to assess the quality of the oil as reported by Daoud *et al*., (2019). The absorption peak at 3470 cm^{-1} increased progressively in the control samples and in the samples prepared with ginkgo or ginseng extracts at 0.5% during the first 25 days of storage at room temperature. The addition of ginkgo or ginseng extracts at 1% or 0.02% BHT in the formula of the breadsticks kept the band at 3470 cm^{-1} after 55 days, which is similar to the pattern of the control sample at zero storage time.

As the oxidation processes proceed, the formation of the aldehyde functional group is represented by an increase of the absorbance at 1164 cm^{-1} according to Daoud *et al*., (2019). The control sample recorded the highest absorbance at 1164 cm^{-1} at the beginning of storage. The level of aldehydes in samples prepared with ginkgo or ginseng extracts at the 0.5% level was similar at zero time storage and progressively increased after 25 days of storage. The lowest absorbance at this wavenumber was recorded for the samples containing 1% ginseng during storage.

The absorbance at the wavenumber 968 cm^{-1} appears as a weak band. An increase in the absorbance at this band is associated with the formation of trans double bonds that arose in the course of oxidation as reported by Daoud *et al*. (2019). At zero storage time, the highest absorbance at this wavenumber was observed for the control sample. The oil in the breadstick sample prepared with ginseng extract at 1% recorded the lowest peak intensity at this band compared to other samples throughout the storage period.

The oil in the breadsticks prepared with 1% ginseng showed the lowest absorbance in all the investigated spectral bands in comparison to all other samples throughout the storage period.

3.4. Sensory characteristics of breadsticks

The shelf-life of a food item depends mainly on its sensory characteristics and marketability (Alamprese *et al*., 2017). Lipid oxidation exerts rancidity and deteriorative changes in its odor and taste. Figure 4 shows the results of the sensory analysis of the tested samples.

No significant differences ($P>0.05$) were found in the sensory attributes of the breadstick samples at zero storage time (Figure 4a). The addition of ginkgo or ginseng extracts at the 1% level did not significantly ($P > 0.05$) affect the perception of baked odor or taste and texture attributes. The odor, taste and texture scores for the samples prepared with ginkgo or ginseng extracts at the 1% level and stored for 10 and 25 days were not significantly different ($P > 0.05$) from those of the BHT samples (Figure 4b and 4c). The perceived odor and taste of the samples prepared with a low level (0.5%) of ginkgo, ginseng or extracts were recognized as significantly less desirable ($P < 0.05$) than those prepared with the same extract at a higher level (1%) after 25 days of storage (Figure 4c). The same trend was also noticed in the ginseng samples stored for 40 and 55 days. The sensory characteristics of the control and 0.5% ginkgo samples were not significantly different ($P > 0.05$) after 25 days of storage. Moreover, both samples recorded significantly ($P<0.05$) the lowest scores compared to those of the other samples (Figure 4 c). On the other hand, the odor and taste sensory attributes of the 1% ginseng and BHT samples were not significantly different ($P > 0.05$) after 40 and 55 days of storage (Figure 4d and 4e). Meanwhile, the odor and taste scores for both breadstick samples were significantly higher ($P < 0.05$) than those of the 1% ginkgo and 0.5% ginseng samples.

The crispiness of the breadstick samples prepared with ginseng extract at 0.5% or 1% of either ginkgo or ginseng extracts was not significantly different ($P > 0.05$) from that of the BHT sample after 40 and 55 days of storage (Figure 4d and 4e). It could be noticed that the preparation of breadsticks with 1% ginseng extract extended their shelf-life to 55 days at room temperature.

The correlation between oxidative indices and the sensory attributes (odor, taste and texture) using Pearson's correlation is shown in Table 1.

The results in Table 1 show an inverse correlation ($r < -0.74$, $P < 0.01$) between the oxidative chemical indices and the good odor, taste and texture scores. Loss in crispness is negatively correlated with the oxidation products in the oil phase of the breadstick samples. This result is consistent with that reported by Caruso *et al*. (2017). The results revealed significant ($P < 0.01$) positive ($r > 0.89$) correlations among the oxidative chemical indices. The same statistical trend ($r > 0.93$) was found between odor and taste sensory attributes.

In addition, it has previously been shown by Barbieri *et al*. (2018) that the secondary products

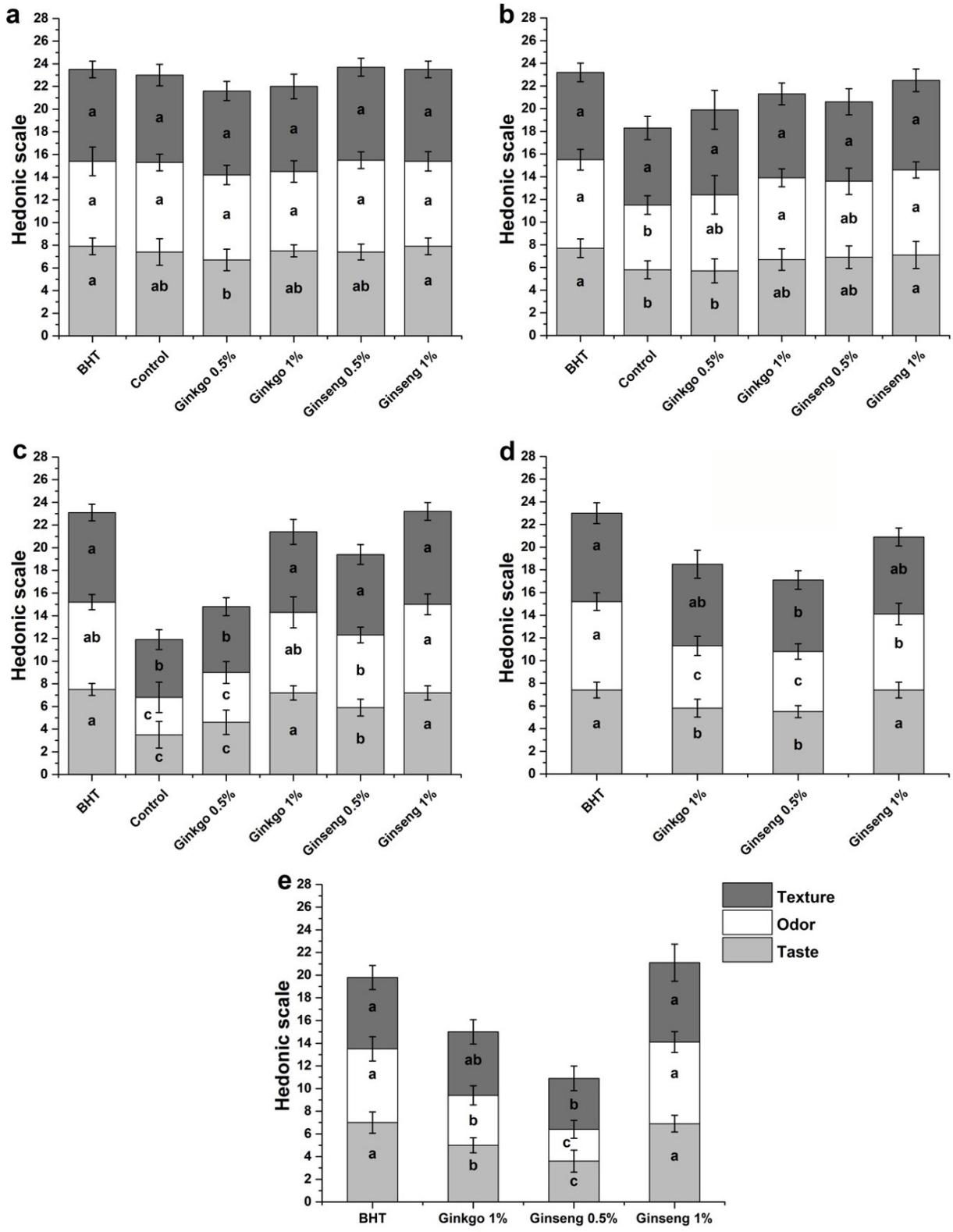

FIGURE 4. Averages of sensory attribute consumer´ acceptance (9 point hedonic scale, 1=poor quality, 9=best quality) of fresh breadstick samples (a) and after storage at room temperature for 10 days (b), 25 days (c), 40 days (d) and 55 days (e). Significant differences among the means (n=3) were determined by analysis of variance and Tukey's test. Sensory attribute scores sharing the same letter are not significantly different ($P > 0.05$). The error bars show ± standard deviation values. Samples with peroxide values higher than 10 meq O_2/Kg were rejected and excluded from analysis

Table 1. Pearson's correlation analyses between oxidation indices, taste, odor and texture of breadstick samples

Variables	Correlation coefficient (r)					
	Taste	Odor	Texture	Peroxide value	*ρ*-Anisidine value	Totox
Taste	1	0.9352**	0.7804**	-0.9504**	-0.8403**	-0.9443**
Odor	0.9352**	1	0.6246**	-0.8950**	-0.7893**	-0.8904**
Texture	0.7804**	0.6246**	1	-0.7741**	-0.7432**	-0.7761**
Peroxide value	-0.9504**	-0.8950**	-0.7741**	1	0.8945**	0.9967**
ρ-Anisidine value	-0.8403**	-0.7893**	-0.7432**	0.8945**	1	0.9253**
Totox value	-0.9443**	-0.8904**	-0.7761**	0.9967**	0.9253**	1

**Values are different from 0 with a significance level alpha (P=0.01). The number of replicates performed to determine the values of each variable was 3 (n=3)

of lipid oxidation which are responsible for the rancid odor and taste of the Italian Taralli (ring-shape, breadsticks contained 20% vegetable oil) are the same products that are evaluated with the *p*-anisidine test.

4. CONCLUSIONS

Ginseng extract significantly increased the oxidative stability of breadsticks up to 55 days at room temperature. Breadstick samples prepared with 1% ginseng extract were significantly well accepted ($P < 0.05$) in terms of odor, taste and texture compared to BHT samples.

ACKNOWLEDGMENT

The authors wish to thank Prof. Samy Mohamed Galal, Professor in the Food Science Department, Faculty of Agriculture, Cairo University for his advice and support during the investigation.

REFERENCES

Abdel-Aal EM, Rabalski I. 2013. Effect of baking on free and bound phenolic acids in wholegrain bakery products. *J. Cereal Sci*. **57**, 312–318. https://doi.org/10.1016/j.jcs.2012.12.001

Alamprese C, Cappa C, Ratti S, Limbo S, Signorelli M, Fessas D, Lucisano M. 2017. Shelf life extension of whole-wheat breadsticks: Formulation and packaging strategies. *Food Chem.* **230**, 532–539. https://doi.org/10.1016/j.foodchem.2017.03.092

AOCS. 2009. Official Methods and Recommended Practices of the American Oil Chemists' Society, 6th edn. AOCS Press, Champaign, IL.

Arnous A, Makris DP, Kefalas P. 2002. Correlation of pigment and flavanol content with antioxidant properties in selected aged regional wines from Greece. *J. Food Compos. Anal*. **15**, 655–665. https://doi.org/10.1006/jfca.2002.1070

Barbieri S, Bendini A, Balestra F, Palagano R, Rocculi P, Gallina Toschi T. 2018. Sensory and instrumental study of Taralli, a typical Italian bakery product. *Euro. Food Res. Technol.* **244**, 73–82. https://doi.org/10.1007/s00217-017-2937-8

Bhat NA, Wani IA, Hamdani AM, Gani A. 2019. Effect of extrusion on the physicochemical and antioxidant properties of value added snacks from whole wheat (*Triticum aestivum* L.) flour. *Food Chem*. **276**, 22-32. https://doi.org/10.1016/j.foodchem.2018.09.170

Calligaris S, Pieve SD, Kravina G, Manzocco L, Nicoli CM. 2008. Shelf life prediction of bread sticks using oxidation indices: A validation study. *J. Food Sci*. **73**, E51–E56. https://doi.org/10.1016/j.foodres.2018.03.034

Caruso MC, Galgano F, Colangelo MA, Condelli N, Scarpa T, Tolve R, Favati F. 2017. Evaluation of the oxidative stability of bakery products by OXITEST method and sensory analysis. *Eur. Food Res. Technol.* **243**, 1183–1191. https://doi.org/10.1007/s00217-016-2831-9

Chen Y, Zhao Z, Chen H, Brand E, Yi T, Qin M, Liang Z. 2017. Determination of ginsenosides in Asian and American ginsengs by liquid chromatography-quadrupole/time-of-flight MS: assessing variations based on morphological characteristics. *J. Ginseng Res.* **41**, 10–22. https://doi.org/10.1016/j.jgr.2015.12.004

Chien YS, Yu ZR, Koo M, Wang BJ. 2016. Supercritical fluid extractive fractionation: Study of the antioxidant activities of *Panax ginseng*. *Sep. Sci. Technol.* **51**, 954–960. https://doi.org/10.1080/01496395.2016.1140202

CODEX STAN. 321-2015. 2015. Standard for ginseng products.

Daoud S, Bou-maroun E, Dujourdy L, Waschatko G, Billecke N, Cayot P. 2019. Fast and direct analysis of oxidation levels of oil-in-water emulsions using ATR-FTIR. *Food Chem.* **293**, 307–314. https://doi.org/10.1016/j.foodchem.2019.05.005

Difonzo G, Pasqualone A, Silletti R, Cosmai L, Summo C, Paradiso VM, Caponio F. 2018. Use of olive leaf extract to reduce lipid oxidation of baked snacks. *Food Res. Int.* **108**, 48–56. https://doi.org/10.1016/j.foodres.2018.03.034

Esfarjani F, Khoshtinat K, Zargaraan A, Mohammadi-Nasrabadi F, Salmani Y, Saghafi Z, Hosseini H, Bahmaei M. 2019. Evaluating the rancidity and quality of discarded oils in fast food restaurants. *Food Sci. Nutr.* **7**, 2302–2311. https://doi.org/10.1002/fsn3.1072

Hwang CR, Lee SH, Jang GY, Hwang IG, Kim HY, Woo KS, Lee J, Jeong HS. 2014. Changes in ginsenoside compositions and antioxidant activities of hydroponic-cultured ginseng roots and leaves with heating temperature. *J. Ginseng Res.* **38**, 180–186. https://doi.org/10.1016/j.jgr.2014.02.002

Klaypradit W, Kerdpiboon S, Singh RK. 2011. Application of artificial neural networks to predict the oxidation of menhaden fish oil obtained from Fourier transform infrared spectroscopy method. *Food Bioproc. Tech.* **4**, 475–480. https://doi.org/10.1007/s11947-010-0386-5

Kobus-Cisowska J, Flaczyk E, Rudzińska M, Kmiecik D. 2014. Antioxidant properties of extracts from *Ginkgo biloba* leaves in meatballs. *Meat Sci.* **97**, 174–180. https://doi 10.1016/j.meatsci.2014.01.011

Kozłowska M, Zbikowska A, Szpicer A, Połtorak A. 2019. Oxidative stability of lipid fractions of sponge-fat cakes after green tea extracts application. *J. Food Sci. Technol*. **56**, 2628–2638. https://doi.org/10.1007/s13197-019-03750-5

Lan W, Che X, Xu Q, Wang T, Du R, Xie J, Hou M, Lei H. 2018. Sensory and chemical assessment of silver pomfret (*Pampus argenteus*) treated with *Ginkgo biloba* leaf extract treatment during storage in ice. *Aquaculture Fisheries* **3**, 30–37. https://doi.org/10.1016/j.aaf.2017.09.003

Li W, Fitzloff JF. 2002. HPLC determination of ginsenosides content in ginseng dietary supplements using ultraviolet detection. *J. Liq. Chromatogr. Relat. Technol.* **25**, 2485–2500. https://doi.org/10.1081/JLC-120014269

Mustac NC, Novotni D, Habu M, Drakula S, Nanjara L, Voucko B, Benkovic M, Curic D. 2020. Storage stability, micronisation, and application of nutrient-dense fraction of proso millet bran in gluten-free bread. *J. Cereal Sci.* **91**, 102864. https://doi.org/10.1016/j.jcs.2019.102864

Niccolai A, Venturi M, Galli V, Pini N, Rodolfi L, Biondi N, D'Ottavio M, Batista AP, Raymundo A, Granchi L, Tredici MR. 2019. Development of new microalgae based sourdough "crostini": functional effects of *Arthrospira platensis* (spirulina) addition. *Sci. Rep*. **9**, 19433. https://doi.org/10.1038/s41598-019-55840-1

Park H, Lee M, Kim KT, Park E, Paik HD. 2018. Antioxidant and antigenotoxic effect of dairy products supplemented with red ginseng extract. *J. Dairy Sci.* **101**, 8702–8710. https://doi.org/10.3168/jds.2018-14690

Pereira E, Barros L, Ferreira ICFR. 2013. Chemical characterization of *Ginkgo biloba* L. and antioxidant properties of its extracts and dietary supplements. *Ind. Crops Prod*. **51**, 244–248. https://doi.org/10.1016/j.indcrop.2013.09.011

Reis SF, Abu-Ghannam N. 2014. Antioxidant capacity, arabinoxylans content and in vitro glycaemic index of cereal-based snacks incorporated with brewer's spent grain. *LWT-Food Sci. Technol.* **55**, 269–277.

Riaz M, Rahman NU, Zia-Ul-Haq M, Jaffar HZE, Manea R. 2019. Ginseng: A dietary supplement as immune-modulator in various diseases. *Trends Food Sci. Technol*. **83**, 12–30. https://doi.org/10.1016/j.tifs.2018.11.008

Sati P, Dhyani P, Bhatt ID, Pandey A. 2019. *Ginkgo biloba* flavonoid glycosides in antimicrobial perspective with reference to extraction method. *J. Tradit. Complement. Med.* **9**, 15–23. https://doi.org/10.1016/j.jtcme.2017.10.003

Thanushree MP, Sudha ML, Crassina K. 2017. Lotus (*Nelumbo nucifera*) rhizome powder as a novel

ingredient in bread sticks: rheological characteristics and nutrient composition. *J. Food Meas. Charact.* **11**, 1795–1803. https://doi.org/10.1007/s11694-017-9561-y

Wang HY, Zhang YQ. 2019. The main active constituents and detoxification process of *Ginkgo biloba* seeds and their potential use in functional health foods. *J. Food Compost. Anal.* **83**, 103247. https://doi.org/10.1016/j.jfca.2019.103247

Wang X, Xie K, Zhuang H, Ye R, Fang Z, Feng T. 2015. Volatile flavor compounds, total polyphenolic contents and antioxidant activities of a China Ginkgo wine. *Food Chem.* **182**, 41–46. https://doi.org/10.1016/j.foodchem.2015.02.120

GRASAS Y ACEITES 72 (3)
July-September 2021, e425
ISSN-L: 0017-3495
https://doi.org/10.3989/gya.0335201

Changes in fatty acid profile of *Holothuria forskali* muscle following acute mercury exposure

I. Rabeh[a, ✉], K. Telahigue[a], T. Hajji[b], C. Fouzai[a], M. El Cafsi[a] and N. Soudani[a]

[a]Laboratory of Ecology, Biology and Physiology of Aquatic organisms, Faculty of Sciences of Tunis, Univ. Tunis El Manar, 2092 Tunis, Tunisia.
[b]BVBGR-LR11ES31, Higher Institute of Biotechnology - Sidi Thabet, Biotechpole Sidi Thabet, Univ. Manouba, 2020 Ariana, Tunisia.
✉Corresponding author: rabehimen@yahoo.fr

Submitted: 30 March 2020; Accepted: 10 August 2020; Published online: 21 September 2021

SUMMARY: The present study aimed to document the interaction between mercury (Hg), as a model chemical stressor to an aquatic organism, and Fatty acid (FA) profile in the longitudinal muscle of the sea cucumber *Holothuria forskali*. To assess the sensitivity of this species to the toxic effects of Hg, young *H. forskali* were exposed to gradual doses of Hg (40, 80 and160 µg·L^{-1}) for 96 h. The results showed that following Hg exposure, the FA profile of *H. forskali* corresponded to an increase in the level of saturated fatty acids, and the decrease in the level of monounsaturated and polyunsaturated fatty acids. The most prominent changes in the FA composition were recorded at the lowest dose with noticeable decreases in linoleic, arachidonic and eicosapentaenoic acid levels and an increase of docosahexaenoic acid. The occurrence of a state of oxidative stress induced by Hg contamination was evidenced by the enhanced levels of malondialdehyde, hydrogen peroxide and lipid hydroperoxide. Overall, the low concentration of mercury exerted the most obvious effects on lipid metabolism, suggesting that changes in fatty acid composition may be act as an early biomarker to assess mercury toxicity in this ecologically and economically important species.

KEYWORDS: *Acute exposure; Fatty acid composition; Holothuria forskali; Indices of lipid peroxidation; Mercuric chloride ($HgCl_2$); Sea cucumber*

RESUMEN: ***Cambios en el perfil de ácidos grasos del músculo de* Holothuria forskali *tras una exposición aguda a mercurio*.** El presente estudio tuvo como objetivo demostrar la interacción entre el mercurio (Hg), como modelo de estresor químico para el organismo acuático, y el perfil de ácidos grasos (FA) en el músculo longitudinal del pepino de mar *Holothuria forskali*. Para evaluar la sensibilidad de esta especie a los efectos tóxicos del Hg, los juveniles de *H. forskali* fueron expuestos a dosis graduales de Hg (40, 80 y 160 µg·L^{-1}) durante 96 h. Los resultados mostraron que después de la exposición al Hg, el perfil de FA de *H. forskali* respondió con una tendencia direccional anclada por el aumento en el nivel de ácidos grasos saturados y la disminución en el nivel de ácidos grasos monoinsaturados y poliinsaturados. Los cambios más prominentes en la composición de AG se registraron a la dosis más baja con una disminución notable en los niveles de ácido linoleico, araquidónico y eicosapentaenoico frente a un aumento de ácido docosahexaenoico. La aparición de un estado de estrés oxidativo inducido por la contaminación con Hg se puso de manifiesto por el aumento en los niveles de malondialdehído, peróxido de hidrógeno e hidroperóxido de lípidos. En general, la concentración más baja de mercurio ejerció efectos más obvios sobre el metabolismo de los lípidos, lo que sugiere que los cambios en la composición de los ácidos grasos pueden actuar como un biomarcador anterior para evaluar la toxicidad del mercurio en esta especie de importancia ecológica y económica.

PALABRAS CLAVE: *Cloruro de mercurio ($HgCl_2$); Composición de ácidos grasos; Exposición aguda; Holothuria forskali; Índices de peroxidación lipídica; Pepino de mar*

Citation/Cómo citar este artículo: Rabeh I, Telahigue K, Hajji T, Fouzai C, El Cafsi M, Soudani N. 2021. Changes in fatty acid profile of *Holothuria forskali* muscle following acute mercury exposure. *Grasas Aceites* **72** (3), e425. https://doi.org/10.3989/gya.0335201

1. INTRODUCTION

Over the last centuries, the environmental impacts of heavy metal pollution have increased in the coastal areas, causing a major threat to the ecosystems and the biota they support (Ruiz *et al*., 2014). Among these xenobiotics, mercury (Hg) is listed as one of the most toxic elements due to its tendency to bioaccumulate and biomagnify through the food chain (Balshaw *et al*., 2007). The sources of mercury contamination in aquatic ecosystems include natural and anthropogenic emissions (Verlecar *et al.,* 2008). The later generally come from incineration, fungicides, paints and industrial processes. One of the established mechanisms of Hg toxicity is its ability to induce cellular oxidative stress through the generation of reactive oxygen species (ROS) which react with macromolecules such as lipids, proteins and DNA (Uttara *et al.,* 2009). As the cell membrane is tightly linked to cellular physiology, several authors have reported that the membrane is the primary detector of stress stimuli and activator of the cellular stress response (Dindia *et al.,* 2013; Vígh *et al.,* 2007). According to several authors, changes in the membrane biophysical properties as a primary response to stress, mainly trigger changes in lipid and fatty acid compositions (Los *et al.,* 2004; Thyrring *et al.,* 2015). Indeed, FAs, as the main constituent of the cell membrane, play crucial roles in several physiological functions as well as in the maintenance of membrane structures (Neves *et al*., 2015). It therefore appears that lipids and their constitutional components could be closely involved in cellular responses to pollutants such as Hg in aquatic organisms (Ferrain *et al.,* 2018). In this context, it has been proven that the susceptibility of individual FA to peroxidation increases exponentially with an increasing number of double bonds on the carbon chain (Holman, 1954). Thus, polyunsaturated fatty acids (PUFAs) like eicosapentaenoic acid (20:5n-3, EPA) and docosahexaenoic acid (22:6n-3, DHA) are not only targets that are damaged by ROS, but also play a key role in enhancing an organism's adaptation to environmental stress (Munro *et al*., 2016). Given this, FAs were recently argued to be promising bio-indicators to assess stress exposure and ecosystem health in a marine environment (Silva *et al.,* 2017).

Nowadays, most of the available data regarding the use of FA as biomarkers for marine pollution monitoring refers to bivalves, micro and macroalgae and fish (Filimonova *et al.,* 2016; Gonçalves *et al.,* 2016); however, little is known about other marine organisms such as holothurians. Our previous study (Telahigue *et al.,* 2019) investigated for the first time, the impact of acute mercury exposure on several biochemical parameters including fatty acid profile in the *Holothuria forskali* body wall. Holothurians, commonly known as sea cucumbers, represent an important marine resource due to their numerous nutraceutical and pharmaceutical proprieties (Bordbar *et al.,* 2011). The sea cucumber fishery and aquaculture trade have been an active industry in Asia for a long time. In recent years, the sea cucumber trade has also flourished in some Mediterranean sea and NE Atlantic Ocean countries (Sicuro and Levine, 2011). The black sea cucumber or cotton-spinner *Holothuria forskali,* which is one of the most common sea cucumber species in the Mediterranean sea, is listed as a new target resource for future farming industries. (Sicuro and Levine, 2011). Like most of other sea cucumbers species, *H. forskali* is a deposit feeder and may ingest a large amount of sediment (Navarro *et al*., 2014) which make it particularly prone to heavy metal pollution. Several authors have reported that sea cucumbers could be considered as a potential bioindicator for heavy metal pollution (Turk Culha *et al.*, 2016). Indeed, it is well established that mercury tends to accumulates in tissue in a specific manner depending on the organ's physiological role and its regulatory ability. Generally, some tissues/organs such as body wall and respiratory tree have received particular attention to evaluate the impact of noxious stimuli in holothurians. Nonetheless, little information is available on the longitudinal muscles. In fact, muscle constitutes an interesting organ to analyze owing to the energy supply function and to its major role in locomotion and contraction movements in response to environmental stimuli and to its being a target tissue for bioaccumulation of merury (as confirmed by unpublished data obtained in our laboratory). The current study was mainly designed to evaluate the impact of Hg contamination on the fatty acid composition of *H. forskali* muscle. The results may provide valuable data concerning the underlying toxicity mechanism of Hg in lipid metabolism and to verify the validity of the FA profile as a biomarker of mercury intoxication in sea cucumber. Other

parameters such as levels of H_2O_2 and LOOH were also assessed in order to verify the induction of an oxidative stress state in *H. forskali* muscle tissue following acute Hg exposure.

2. MATERIALS AND METHODS

2.1. Chemicals

Mercury chloride ($HgCl_2$ > 99.5% purity) was obtained from Sigma–Aldrich (St. Louis, MO, USA). It was dissolved in pure water for stock concentrations, and the desired test solutions used in the present study were prepared by diluting the stock solution with double-distilled water. Reduced glutathione (GSH), 5,5-dithiobis-2-nitrobenzoic acid (DTNB), and thiobarbituric acid (TBA) were purchased from Sigma Chemical Co. (St. Louis, MO, USA). All other chemicals were purchased from standard commercial suppliers.

2.2. Experimental design

Young *H. forskali*, with an average body length of 20.25 ± 2.75 cm, were collected by hand during scuba diving off the Bizerte coast (North east of Tunisia), a relatively clean sea shore. The sea cucumbers were transported to the laboratory in cooler boxes with water from the collection site. Once in the laboratory, the specimens were kept in tanks filled with aerated seawater (18 °C ± 1; photoperiod of 12:12 h) for three days prior to experimentation. The animals were acclimated and then randomly divided into 4 groups of 12 specimens each (triplicate design) in order to ensure the reproducibility of the results. As we proceeded in our previously published research (Rabeh et *al.,* 2018), the animals were exposed to a range of mercury chloride ($HgCl_2$) concentrations as follows: (controls (0), D1 (40 μg·L^{-1}), D2 (80 μg·L^{-1}) and D3 (160 μg·L^{-1}). Tested doses were chosen based on studies that investigated the effects of the acute exposure of marine invertebrates to mercury, using similar concentrations (Bhamre *et al.,* 2010; Oliveira *et al.,* 2015). The lowest concentration (40 μg·L^{-1}) was in the range of concentrations that can be found in some heavily contaminated water bodies near industrialized areas (Alinnor, 2005; Guilherme *et al.,* 2008); while the highest tested concentrations (60 and 80 μg·L^{-1}), were selected to guarantee the observable effects of Hg and to elucidate the responsiveness of sea cucumber to the worst-case-scenario of mercury contamination. To ensure water quality, 50% of the water was replaced every 24 h and the concentrations of mercuric chloride were re-established. The changed volume of water was replaced by an equal amount of water containing the initial concentration of $HgCl_2$. During the exposure period, sea cucumbers were not fed to avoid prandial effects and to prevent the deposition of feces. No mortalities were observed throughout the experimental period in any group. At the end of experiments, nine animals from each treatment were removed from the tanks by dip-net and weighed. Muscle was carefully dissected and immediately frozen in liquid nitrogen and then stored at −80 °C until the biochemical assays were carried out.

2.3. Hydrogen peroxide generation assay

The amount of hydrogen peroxide (H_2O_2) generation in tissues was monitored by the ferrous ion oxidation xylenol orange method of Ou and Wolff (1996). The amount of H_2O_2 produced was determined using the extinction coefficient of 2.67×105 $cm^{-1}M^{-1}$ and results were expressed as nmol per gram of tissue.

2.4. Lipid hydroperoxide assay

Lipid hydroperoxide levels were estimated using the ferrous oxidation in xylenol orange assay (FOX assay) described by Jiang *et al.,* (1992). The amount of hydroperoxides produced was calculated using the molar extinction coefficient of 4.6 × 9 × 104 M^{-1} cm^{-1}, and the results were expressed as nanomoles per milligram of protein.

2.5. Lipid extraction

Total lipids in each sample were extracted according to the Folch, Lees, and Sloane-Stanley (1957) method with the solvent mixture chloroform–methanol (2:1, v/v). Following solvent evaporation under nitrogen, lipids were transferred to pre-weighed 2ml vials. The solvent mixture was again evaporated under nitrogen, and the extracts were further dried overnight at ambient temperature (18 °C) in a vacuum desiccator. Once weighed, the lipids were re-dissolved in chloroform–methanol (2:1, v/v) with 0.01% butylated hydroxy toluene (BHT, Sigma-Aldrich) added as an antioxidant to minimize the risk of lipid oxidation.

2.6. Fatty acid analysis

Fatty acids from total lipid extracts were transesterified according to the Cecchi *et al*., (1985) method. Methyl nonadecanoate C19:0 (Sigma) was added as internal standard. The resulting fatty acid methyl esters (FAME) were extracted using sodium methylate ($NaOCH_3$) in the presence of hexane and sulfuric acid (H_2SO_4). Separation of FAMEs was carried out on a HP 6890 gas chromatograph (Agilent Technologies, Sacramento,CA, USA) with a split/splitless injector equipped with a flame ionization detector at 275 °C, and a 30m HP. Innowax capillary column with an internal diameter of 250 µm and a 0.25 µm film thickness. The injector temperature was held at 250 °C. The oven was programmed to rise from 50 to 180 °C at a rate of 4 ºC·min^{-1}, from 180 to 220 °C at 1.33 ºC·min^{-1} and to stabilize at 220 °C for 7 min. The carrier gas was nitrogen. Identification of FAMEs was based on the comparison of their retention times with those of a mixture of methyl esters (Supelco 47085U PUFA No: 3 and Supelco 37 component FAME mix 47885-U). Fatty acid peaks were integrated and analyzed using Hewlett-Packard ChemStation software. All fatty acid data are reported as percentage of total fatty acids.

2.7. Calculation of indices and statistical analysis

The indices of desaturase activities were estimated as the product/precursor ratios of individual fatty acids according to the following formulas:

D9D: Δ9-desaturase = stearoyl-CoA-desaturase = (C18:1n-9)/C18:0); D5D: Δ5-desaturase = C20:5n3/ C20:4n3, D6D: Δ6-desaturase =22:6n-3/ C20:5n-3 (Da costa *et al.,* 2015; Rabei *et al.*, 2018).

The indices of the elongase (Elovl 6) activity were calculated using the C18:0/C16:0 ratio (Kotronen *et al.*, 2010).

Mercuric chloride effects on fatty acid composition were analyzed by one way ANOVA of variance (ANOVA) followed by the Tukey's test in order to compare results between doses. Results were expressed as mean ± SD and differences were considered significant at $p < 0.05$. First the data for each variable was checked for normality and homogeneity of variance by Kolmogorov–Smirnov and Levene's tests, respectively. Raw values were arcsine-transformed or log_{10}-transformed (if necessary) to meet the requirements for normal distribution and homogeneity of the variances. Student unpaired t-test was also used when comparison between two groups was required. All statistical analyses were run by the statistical software program R version 3.0.2 (R Core Team2017).

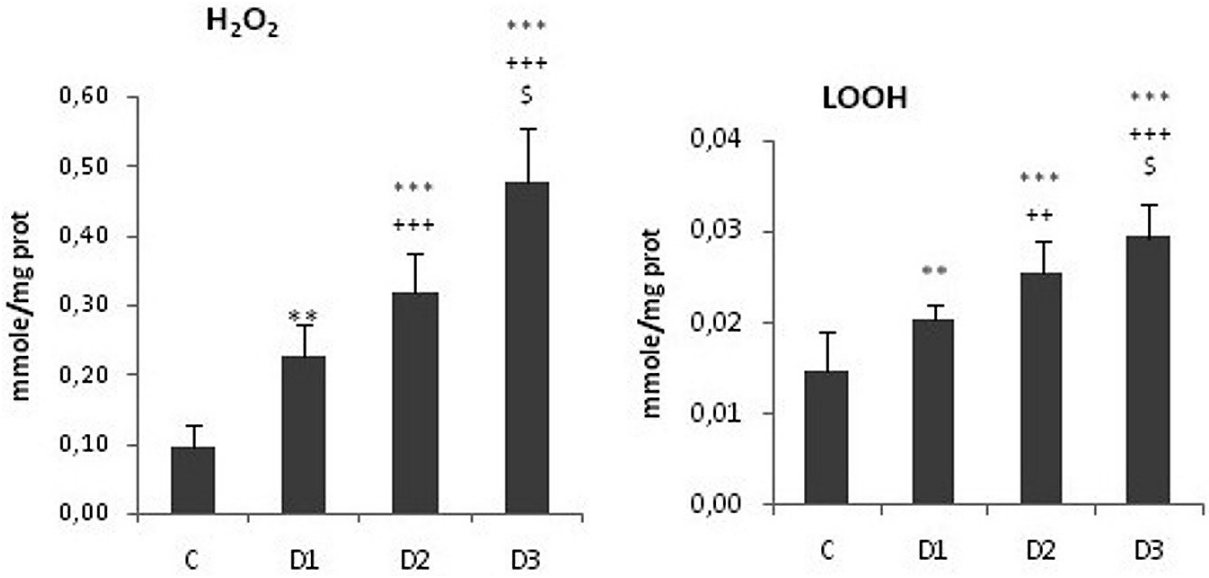

FIGURE 1. Levels of oxidative damage measured as hydrogen peroxide generation (H_2O_2) and in the muscle of unexposed (C) and exposed *Holothuria forskali* to different doses of $HgCl_2$ for 96 h. Data were expressed as means ± SD (n=9). * $p < 0.01$; * * $p < 0.001$: D1, D2 and D3 groups vs. control group. + $p < 0.01$; ++ $p < 0.001$: D2 and D3 groups vs. D1 group. $ $p < 0.001$: D3 group vs. D2 group

TABLE1. Fatty acid profile (%) of *Holothuria forskali* muscle of the control and $HgCl_2$-treated *groups* (D1 (40 µg·L^{-1}), D2 (80 µg·L^{-1}) and D3 (160 µg·L^{-1})) for 4 days.

Fatty acids	Control	Hg (D1)	Hg (D2)	Hg (D3)
C14:0	5.46 ± 0.4 [a]	3.61 ± 0.05 [b]	4.93 ± 0.86 [d]	4.61±0.51 [c]
C15:0	1.15 ± 0.15 [a]	4.77 ± 0.22 [b]	3.93 ± 0.01 [c]	2.08±0.20 [b]
C14:1	0.22 ± 0.23 [a]	0.52 ± 0.08 [b]	1.00 ± 0.50 [c]	1.31±0.35 [c]
C15:1	1.40 ± 0.14 [a]	5.75 ± 0.12 [b]	1.87 ± 0.08 [a]	0.88±0.54 [c]
C16:0	4.86 ± 1.4 [a]	9.74 ± 0.34 [b]	5.35 ± 0.75 [c]	5.02±0.13 [c]
C16:1n-9	4.37 ± 0.17 [a]	3.67 ± 0.17 [b]	3.74 ± 1.63 [a]	7.29 ± 1.32 [b]
C16:1n-7	8.72 ±1.42 [a]	3.97 ± 0.29 [b]	8.60 ±0.32 [a]	4.83±1.16 [c]
C16:2n-4	2.42 ± 0.13 [a]	1.50 ± 0.05 [b]	2.89 ± 0.28 [c]	1.82±0.31 [a]
C17:0	0.4 ± 0.15 [a]	1.56± 0.27 [b]	1.20±0.08 [b]	2.70±0.44 [c]
C16:4	2.81 ± 0.30 [a]	1.78 ± 0.36 [b]	1.51 ± 0.05 [b]	2.46±0.15 [a]
C16:3n-4	3.35 ± 0.5 [a]	6.37 ± 0.80 [b]	2.25 ± 0.30 [b]	2.24±0.26 [b]
C18:0	5.62 ± 0.49 [a]	6.83 ± 0.13 [b]	5.12±1.06 [c]	4.55±0.52 [c]
C18:1n-9	2.38 ± 0.01 [a]	1,15 ± 0.10 [b]	1.06 ± 0.03 [b]	2.04±0.25 [c]
C18:1n-7	1.92 ± 0.2 [a]	0.62 ± 0.18 [b]	1.36 ± 0.09 [c]	2.46±0.57 [d]
C18:2n-6	11.6± 1.23 [a]	4.42 ± 0.65 [b]	11.48 ±0.40 [a]	13.79 ± 1.90 [d]
C18:4n-3	2.05 ± 0.29 [a]	6.93 ± 0.51 [b]	4.25 ± 0.08 [c]	1.35 ± 0.10 [a]
C18:3n-3	2.08 ± 0.05 [a]	4.85 ± 0.42 [b]	2.46 ± 0.42 [a]	1.92 ± 0.15 [c]
C20:0	3.73 ± 0.45 [a]	3.19 ± 0.40 [b]	4.19 ± 0.06 [a]	2.60 ± 0.28 [b]
C20:1n-9	6.69 ± 0.8 [a]	3.04 ± 0.04 [b]	7.87 ± 0.34 [a]	7.74 ± 0.35 [c]
C20:3n-6	4.94 ± 0.09 [a]	1.97 ± 0.06 [b]	6.16 ±0.12 [a]	7.70 ± 0.53 [c]
C20:2n-6	5.91 ± 0.24 [a]	9.07 ± 0.05 [b]	5. 87 ± 0.13 [c]	4.25 ± 0.84 [d]
C20:4n-6	4.68 ± 0.03 [a]	0.57 ± 0.06 [b]	2.35 ± 0.12 [c]	6.06 ± 0.93 [d]
C20:3n-3	3.31 ± 0.01 [a]	2.25 ± 0.20 [b]	3.89 ± 0.28 [a]	2.41 ± 0.12 [c]
C20:5n-3	3.13 ± 0.43 [a]	1.30 ± 0.06 [b]	1.27 ± 0.11 [b]	3.17 ± 0.41 [a]
C22:0	0.38 ± 0.08 [a]	1.01 ± 0.07 [b]	0.62 ± 0.05 [b]	0.69 ± 0.08 [b]
C22:1	0.36 ± 0.02 [a]	0.11 ± 0.01 [b]	0.16 ± 0.04 [b]	0.09 ± 0.01 [b]
C22:5n-6	2.46 ± 0.08 [a]	1.14 ± 0,20 [b]	0.99 ± 0.07 [b]	2.02 ± 0.47 [a]
C22:6n-3	3.62 ± 0.02 [a]	7.05 ± 1.18 [b]	1.72 ± 0.17 [c]	2.79 ± 0.38 [a]
∑SFA	21.85±0.89 [a]	31.72±0.94 [b]	24.23±0.77 [a]	22.09±5.55 [c]
∑MUFA	25.79±0.72 [a]	19.11±0.42 [b]	27.70±3.08 [a]	27.02±5.90 [a]
∑PUFA	52.36±3.26 [a]	49.17±1.38 [b]	48.07±3.03 [b]	51.15±11.45 [a]
∑PUFA (n-3)	14.20±1.21 [a]	22.38±1.94 [b]	13.59±2.29 [a]	11.63±0.09 [c]
∑PUFA (n-6)	23.67±1.20 [a]	13.57±0.3 [b]	26.85±0.24 [c]	34.15±13.08 [d]
n-3/n-6	0.59±0.05 [a]	1.67±0.01 [b]	0.5±0.08 [a]	0.34±0.03 [c]
Total lipid (mg/g ww)	5.64±0.16 [a]	0.99±0.03 [b]	7.5±0.41 [c]	10.19±1.02 [d]

Data are expressed as percentage of major fatty acids (mean ± standard deviation; n=9); Means followed by different letters in the same line are significantly different ($p < 0.05$) by Tukey's test.
SFAs: saturated fatty acids, MUFAs: monounsaturated fatty acids, PUFAs: polyunsaturated fatty acids

Principal Component Analysis (PCA) was applied to evaluate the relationship between mercury treatments and fatty acid composition in the muscle of the control and the exposed groups of *H. forskali*.

3. RESULTS

3.1. Lipid hydroperoxide (LOOHs), and hydrogen peroxide (H_2O_2) levels

Significant increases ($p < 0.05$) in H_2O_2 and LOOH levels were recorded in the treated *H. forskali*, respectively, compared to the controls (Figure 1).

3.2. Fatty acids composition

As shown in Table 1, a significant decrease in lipid content was recorded in D1 however, in D2 and D3 a substantial increase was noticed compared to the control. The Fatty acid profiles of the muscle in the control and $HgCl_2$-treated *H. forskali* are presented in Table 1. The untreated sea cucumber group showed a significantly higher proportion of polyunsaturated fatty acids (PUFA) (52.36% of total FA) followed by monounsaturated fatty acids (MUFA) and saturated fatty acids (SFA) with 25.79 and 21.84%, respectively. Over all, we noticed that exposure to the nominal dose of Hg (D1, 40 $\mu g \cdot L^{-1}$) substantially changed the main fatty acid groups. In fact, significant increases in SFA levels with a decrease in unsaturated fatty acid levels (MUFA and PUFA) were observed compared to the controls. A closer examination of data showed that the recorded increase in the SFA group, which almost doubled under D1 treatment, was mainly due to the increased levels of C15:0 and C16:0. As for unsaturated fatty acids, we recorded that C18:1n-7 and C20:1n-9 were the most affected FAs by the Hg treatments and to a lesser extent in D2 and D3. In the PUFA group, the primary source of variation was due to the decrease in the n-6 group level in D1. In fact, the levels of C18:2n-6 and C20:4n-6 dropped by 70 and 90%, respectively, compared to the control group. Regarding the n-3 group, significant decreases of 70 and 40% were recorded for the EPA (C20: 5n-3) levels in D1 and D2 groups, respectively. The EPA level remained statistically unchanged in the D3 group in comparison to the control. Significant changes were also observed for DHA (C22:6 n3) in all treatments. This fatty acid tended to rise in D1 and diminish at higher doses.

3.3. Estimated activity of fatty acid desaturases and elongases

Desaturase and elongase activities were determined in the muscle of *H. forskali* exposed to gradual doses of mercury (Table 2). The obtained results showed that D9D (C18:1n9/C18:0), D5D (C20:4n6/C20:3n-6) and Elongase 6 (C18:0/C16:0) activities decreased significantly at the lower doses (40 and 80 $\mu g \cdot L^{-1}$) but remained unaffected at the highest dose (Table 2). The activity of the D6D:Δ6-desaturase (C22:6n-3/C20:5n-3) was significantly influenced by Hg exposure, expressing much higher values at D1 when compared to the control group.

3.4. Principal component analysis

The PCA carried out on the fatty acid composition data matrix produced a two-dimensional pattern which explained 77.7% of total variance (Figure 2). Those two components explained 56.7 (PC1) and 21.0% (PC2) of the total variance. The PCA plot showed a considerable distinction between control and treated groups along the PC2 axis. In addition, we noticed that the group exposed to the lowest dose (D1) was separated from all other groups along the PC1 axis. The most highly-sensitive fatty acids were C18:4n.3 and C14:1 for the PC1 axis and C17:0 and C20:0 for the PC2 axis.

4. DISCUSSION

Heavy metals such as mercury are potential stressors that exert toxic effects through redox cycling which results in the uncontrolled production of ROS and a failure in antioxidant defense systems (Lushchak, 2011). In the current study, an over production of ROS was confirmed by the increase in the H_2O_2 level in all Hg-treated groups. Our results are consistent with several studies which reported a close correlation between the generation of intracellular ROS and the toxicity exerted by the inorganic Hg in several marine organisms (Verlecar *et al.,* 2008; Wang *et al.,* 2016). In this context, Patrick (2002) reported that exposure to Hg promotes the synthesis of H_2O_2, which could be converted into a reactive hydroxyl radical and lipid peroxidation (LPO) products in mitochondrial membranes. Furthermore, Hg ions are able to increase the action potential in the inner membrane of the mitochondria which regulates HO^-, O_2^- and H_2O_2, and negatively

TABLE 2. Estimated fatty acid desaturase and elongase activities of *Holothuria forskali* muscle of control and $HgCl_2$-treated *groups* (D1(40 µg·L^{-1}), D2 (80 µg·L^{-1}) and D3(160 µg·L^{-1})) for 4 days.

Treatments and parameters	Control	D1	D2	D3
D9D(18:1n9/18:0)	0.4±0.07	0.18±0.14**	0.30 ±0.03*	0.45±0.02
D5D(20:4n6/20:3n6)	0.79±0.05	0.27±0.049**	0.38±0.05**	1.183±0.2**
D6D(22:6n3/20:5n3)	1.15±0.01	5.4±1.04***	1.39±0.06	0.87±0.08*
Elovl6(18:0/C16:0)	1.23.16±0.04	0.7±0.08**	1.14±0.03	0.62±0.08*

Results are given in means ± standard deviation of nine replicates in each group.
D1, D2, and D3 vs control: *p < 0.05; **p < 0.01; ***p < 0.001 (using Tukey's test)
D9D: Δ9-desaturase (stearoyl-CoA-desaturase=18:1n9/18:0);
D5D: Δ5-desaturase (20:4n6/20:3n-6);
D6D: Δ6-desaturase (22:6n-3/20:5n-3);
Elovl 6: Elongase 2 (18:0/C16:0).

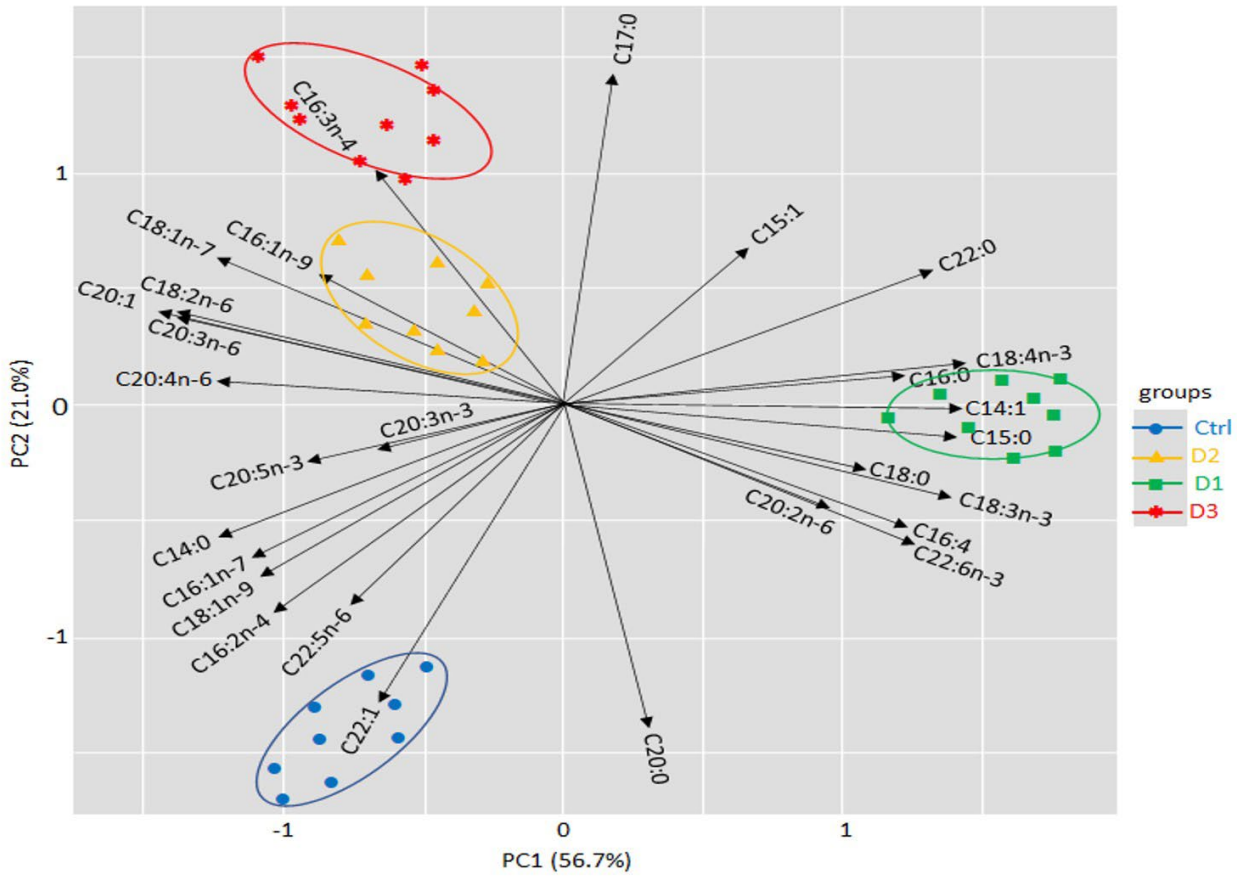

FIGURE 2. Principal component analysis (PCA) represented by two factors (F1=56.7% and F2=21.0%) and produced by fatty acid composition of *Holothuria forskali* muscle of control and $HgCl_2$-treated groups (D1(40 µg·L^{-1}), D2 (80 µg·L^{-1}) and D3 (160 µg·L^{-1})) for 4 days.

adjusts the defense enzymes SOD, CAT, GPx, as well as GSH (Flores *et al.,* 2019).

Besides biomarker analysis, the determination of the fatty acid composition has proven to be a good indicator of stress and ecosystem health, due to their high sensitivity to stress factors and environmental changes (Gonçalves *et al.,* 2016). Indeed, changes in lipid metabolism are known to be a common biochemical response to pollutant exposure and accumulation in marine organisms (Dailianis *et al.,* 2011). Our results showed significant changes in the FA composition of treated sea cucumbers indicating an evident harmful impact of Hg on lipid metabolism. Thereby, after exposure to Hg, the FA profile of sea cucumber showed directional tendency anchored by an increase in SFAs, and the decrease in MUFAs and PUFAs levels. The observed changes are thought to be a compensatory process to defend the integrity of biological membranes and reduce cytotoxicity (Signa *et al.,* 2015). It should also be noted that the most prominent changes in the FA composition of the Hg-treated *H. forskali* were mostly recorded at the lowest tested dose as confirmed further by the PCA analysis. Such findings can be attributed to a hormeosis response and suggest that low Hg dose response may be considered as a manifestation of the plasticity of biological systems. In fact, hormeosis, which is a dose–response phenomenon characterized by a low-dose stimulation and a high-dose inhibition, was observed for Algae exposed to silver ions and nanoparticles (Tayemeh *et al.,* 2020). The increased proportions of SFA mostly resulted from the increment in palmitic acid (C16:0) and may reflect an inflammation response to Hg intoxication. Indeed, the last cited FA is particularly known as a potent agent involved in the activation of proinflammatory signaling pathways (Ma *et al.,* 2018). Another interesting finding recorded in the current study is the decrease in the MUFA group mainly due to the diminution of the oleic acid (C18:1n-9, OA) level. The latter is a nonessential FA which derives from the desaturation of stearic acid (C18:0) by the stearoyl-CoA desaturase (Scd). The recorded decline in the OA level is probably due to the inhibition of the Δ9-desaturase activity by Hg ions as reflected by the product-to-precursor ratio used in the current study. Furthermore, OA was probably used for energy production through β-oxidation and/or in modulation of membrane fluidity (Funari *et al.,* 2003) and/or in detoxification related mechanisms as suggested by Ruiz-Gutiérrez *et al.*, (1999). Also worthy of note, a significant depletion of the n-6 group and particularly ARA (C20:4n-6) and its precursor LA (C18:2n-6), which are presumably required for activation of eicosanoid synthesis through the arachidonic cascade. In fact, ARA is largely reported in the literature to be an important mediator involved in inflammation, immune response, and adaptation to stress through eicosanoid pathways (Calder, 2015). Likewise, we note the expenditure of EPA, another precursor to eicosanoids, which may reflect a compensatory mechanism to maintain membrane fluidity and to promote the adaptive response of the organism to stress (Delaporte *et al.,* 2006). Another PUFA, docosahexaenoic acid (DHA), which is a main component of membrane phospholipids, was found to increase in Hg-treated animals. Such findings might reflect the ability of *H. forskali* to cope with Hg injuries through the induction of Δ6-desaturase activity as reflected by the enhanced 22:6n-3/22:5n-3 ratio. Indeed, it has been proven that the DHA may act as an antioxidant to reduce lipid peroxidation (Mayurasakorn *et al.,* 2016). Furthermore, Vanse *et al.* (2002) reported that DHA could be involved in modulating the inflammatory response and regulating membrane homeoviscous to protect the cell from oxidative disruption caused by Hg intrusion. Similar pictures were observed for other marine organisms following exposure to metals and organic pollutants (Telahigue *et al.,* 2019; Silva *et al.,* 2017).

To further explore the impact of Hg on lipid metabolism, LOOH levels, primary breakdown products of long-chain fatty acid peroxidation, were determined. The increased LOOH levels recorded in all Hg-treated groups clearly reflected the dysfunction of the mitochondrial respiratory chain. Indeed, being rich in polyunsaturated fatty acids (PUFA) as other marine organisms (Liu *et al.,* 2017), sea cucumber seemed to be vulnerable to lipid peroxidation. The continued oxidation of fatty acid, and the fragmentation of peroxides to produce aldehydes may eventually lead to losses in membrane integrity by alteration of its fluidity.

5. CONCLUSIONS

In the current study, the acute exposure to Hg promoted a state of oxidative stress as denoted by

increased hydrogen peroxide and lipid hydroperoxide levels. The changes in the FA profiles of treated sea cucumber clearly indicated an evident toxic effect of Hg on the longitudinal muscle. The palette of acids, including SFA, MUFA and PUFA, determined in the muscle tissue, can be used in ecotoxicological research as an efficient test of the effect of mercury exposure. Furthermore, the prominent effects observed at the lowest dose, which is probably due to a hormeosis response, must be interpreted with caution since no information is available concerning the mechanistic difference between the toxicity and inhibitory effects of mercury to fatty acid pathways in holothurians. Lastly, our findings extend the understanding of the adaptive mechanisms of sea cucumbers and the usefulness of the FA analysis as a biomarker for Hg contamination.

ACKNOWLEDGEMENTS

The authors are indebted to the editor and the anonymous reviewers for their acceptance to review this work and their valuable comments and suggestions for improving the quality of the manuscript.

REFERENCES

Balshaw S, Edwards JW, Ross KE, Daughtry BJ. 2008. Mercury distribution in the muscular tissue of farmed southern bluefin tuna (*Thunnus maccoyii*) is inversely related to the lipid content of tissues. *Food Chem.* **111**, 616- 621. https://doi.org/10.1016/j.foodchem.2008.04.041

Bhamre PR, Thorat SP, Desai AE. 2010. Evaluation of acute toxicity of mercury, cadmium and zinc to a freshwater mussel *Lamellidens consobrinus*. *Our Nat.* **8**, 180–184.

Bordbar S, Anwar F, Saari N. 2011. High-value components and bioactives from sea cucumbers for functional foods-A Review. *Mar. Drugs* **9** (10), 1761–1805. https://doi.org/10.3390/md9101761

Calder PC. 2015. Marine omega-3 fatty acids and inflammatory processes: effects, mechanisms and clinical relevance. *Biochim. Biophys. Acta Mol. Cell Biol Lipids* **1851**, 469–484. https://doi.org/10.1016/j.bbalip.2014.08.010

Cecchi G, Basini S, Castano C. 1985. Méthanolyse rapide des huiles en solvant. *Rev. Franc. Corps Gras* **4**, 63–164.

Da Costa F, Robert R, Quéré C, Wikfors GH, Soudant P. 2015. Essential fatty acid assimilation and synthesis in larvae of the bivalve *Crassostrea gigas*. *Lipids* **50** (5), 503–511. https://doi.org/10.1007/s11745-015-4006-z

Dailianis S. 2011. Environnemental impact of anthropogenic activities: the use of mussels as a reliable tool for monitoring marine pollution. In: McGevin, L.E. (Ed.), Mussels: Anatomy. Habitat and Environmental Impact. *Nova Science Publishers. Inc*. pp. 1–30.

Dindia LA, Faught EL, Leonenko Z, Thomas RH, Vijayan MM. 2013. Rapid cortisol signaling in response to acute stress involves changes in plasma membrane order in rainbow trout liver. *Am. J. Physiol. Endoc. M.* **304**, E1157–E1166

Delaporte M, Soudant P, Moal J, Kraffe E, Marty Y, Samain J.F .2005. Incorporation and modification of dietary fatty acids in gill polar lipids by two bivalve species *Crassostrea gigas* and *Ruditapes philippinarum*. *Comp. Biochem. Phys. A* **140**, 460–470.

Folch J, Lees M, Sloane-Stanley GA. 1957. A simple method for the isolation and purification of total lipids from animal tissues. *J. Biol. Chem.* **226** (1) 497–509.

Flores JS, Torres-Jasso JH, Rojas-Bravo D, Reyna-Villela ZM, Erandis D, Torres-Sánchez ED. 2019. Effects of Mercury, Lead, Arsenic and Zinc to Human Renal Oxidative Stress and Functions: A Review. *J. Heavy Met. Toxicity Dis.* **4,** 1-2. https://doi.org/10.21767/2473-6457.10027

Filimonova V, Gonçalves F, Marques JC, De Troch M, Gonçalves ANN. 2016. Fatty acid profiling as bioindicator of chemical stress in marine organisms: A review. *Ecol. Indic.* **67**, 657–672. https://doi.org/10.1016/j.ecolind.2016.03.044

Ferain A, Bonnineau C, Neefs I, Das K, Larondelle Y, Rees JF, Debier C, Lemaire B. 2018. Transcriptional effects of phospholipid fatty acid profile on rainbow trout liver cells exposed to methylmercury. *Aquat. Toxicol.* **199**, 174-187.

Funari SS, Barceló F, Escribá PV. 2003. Effects of oleic acid and its congeners, elaidic and stearic acids, on the structural properties of phosphatidylethanolamine membranes. *J. Lipid R.* **44**, 567-575. https://doi.org/10.1194/jlr.M200356-JLR200

Gonçalves A, Mesquita A, Verdelhos T, Coutinho J, Marques J, Gonçalves F. 2016. Fatty acids pro-

files as indicator of stress induced by of a common herbicide on two marine bivalves species: *Cerastoderma edule* (Linnaeus, 1758) and *Scrobicularia plana* (da Costa, 1778). *Ecol. Indic.* **63**, 209–218. https://doi.org/10.1016/j.ecolind.2015.12.006

Holman TR. 1954. Autoxidation of fats and related substances. In Progress in the Chemistry of Fats and Other Lipids. *Academic Press*, *New York*. 2, 491–514.

Jiang ZY, Hunt JV, Wolf SP. 1992. Detection of lipid hydroperoxides using Fox method. *Anal. Biochem.* **202**, 384-389.

Kotronen A, Seppanen-Laakso T, Westerbacka J, Arola J, Ruskeepaa AL, Yki-Jarvinen H, Oresic M. 2011. Comparison of lipid and fatty acid composition of the liver, subcutaneous and intra-abdominal adipose tissue, and serum. *Obesity* **18**, 937–944

Lushchak VI. 2011. Environmentally induced oxidative stress in aquatic animals. *Aquatic Toxicol.* **719** (101), 13-30.

Liu X, Wang L, Feng Z, Song X, Zhu X. 2017b. Molecular cloning and functional characterization of the fatty acid delta 6 desaturase (FAD6) gene in the sea cucumber *Apostichopus japonicus*. *Aquac. Res.* **48**, 4991–5003.

Los DA, Murata N. 2004. Membrane fluidity and its roles in the perception of environmental signals. *Biochim. Biophys. Acta* **1666**, 142–157. https://doi.org/10.1016/j.bbamem.2004.08.002

Munro D, Banh S, Sotiri, Tamanna N, Treberg J. 2016. The thioredoxin and glutathione□dependent H_2O_2 consumption pathways in muscle mitochondria: Involvement in H_2O_2 metabolism and consequence to H_2O_2 efflux assays. *Free Radic. Biol. Med.* **96**, 334–346. https://doi.org/10.1016/j.free radbiomed.2016.04.014

Ma XZ, Pang ZD, Wang JH, Song Z, Zhao LM, Du XJ, Deng XL. 2018. The role and mechanism of $K_{Ca}3.1$ channels in human monocyte migration induced by palmitic acid. *Exp. Cell Res.* **369**, 208–217. https://doi.org/10.1016/j.yexcr.2018.05.020

Mayurasakorn K, Niatsetskaya ZV, Sosunov SA, Williams JJ, Zirpoli H, Vlasakov I, Ten VS. 2016. DHA but not EPA emulsions preserve neurological and mitochondrial function after brain hypoxia-ischemia in neonatal mice. *PLOS One* **11**. https://doi.org/10.1371/journal.pone.0160870

Navarro PG, García-Sanz S, Tuya F. 2014. Contrasting displacement of the sea cucumber *Holothuria arguinensis* between adjacent nearshore habitats. *J. Exp. Mar. Biol. Ecol.* **453**, 123–130. https://doi.org/10.1016/j.jembe.2014.01.008

Neves M, Castro BB, Vidal T, Vieira R, Marques JC, Coutinho JAP, Gonçalves F. 2015. Biochemical and populational responses of an aquatic bioindicator species, *Daphnia longispina*, to a commercial formulation of an herbicide (primextraç gold TZ) and its active ingredient (S-metolachlor). *Ecol. Indic.* **53**, 220–230. https://doi.org/10.1016/j.ecolind.2015.01.031

Oliveira P, Lopes-Lima M, Machado J, Guilhermino L. 2015. Comparative sensitivity of European native (*Anodonta anatina*) and exotic (*Corbicula fluminea*) bivalves to mercury. *Estuar. Coast. Shelf Sci*. **167**, 191–198. https://doi.org/10.1016/j.ecss.2015.06.014

Ou P, Wolff SP. 1996. A discontinuous method for catalase determination at near physiological concentrations of H_2O_2 and its application to the study of H_2O_2 fluxes within cells. *J. Biochem. Biophys. Meth.* **31** (1–2), 59–67

Patrick L. 2002. Mercury toxicity mercury toxicity and antioxidants: Part 1: role of glutathione and alpha-lipoic acid in the treatment of mercury toxicity. *Altern. Med. Rev.* **7** (6), 456-471.

Rabeh, Telahigue K, Bejaoui S, Hajji T, Nechi S, Chelbi E, EL Cafsi M, Soudani N. 2019. Effects of mercury graded doses on redox status, metallothione in levels and genotoxicity in the intestine of sea cucumber *Holothuria forskali*. *Chem. Ecol.* **35** (3), 204-218. https://doi.org/10.1080/02757540.2018.1546292

Rabei A, Hichami A, Beldi H, Bellenger S, Khan NA, Soltani N. 2018. Fatty acid composition, enzyme activities and metallothioneins in *Donax trunculus* (Mollusca, Bivalvia) from polluted and reference sites in the Gulf of Annaba (Algeria): pattern of recovery during transplantation. *Environ. Pollut.* **237**, 900–907. https://doi.org/10.1016/j.envpol.2018.01.041

Ruiz-Gutierrez V, Muriana FJ, Guerrero A, Cert AM, Villar J. 1996**.** Plasma lipids, erythrocyte membrane lipids and blood pressure of hypertensive women after ingestion of dietary oleic acid from two different sources. *J. Hypertens* **14**, 1483–1490.

Ruiz F, González-Regalado ML, Muñoz JM, Abad M, Toscano A, Prudencio MI, Dias MI. 2014. Distribution of heavy metals and pollution pathways in a shallow marine shelf: assessment for a future management. *J. Environ. Sci. Technol.* **11**, 1249. https://doi.org/10.1007/s13762-014-0576-1

Silva CO, Simões T, Novais SC, Pimparel I, Granada L, Soares AM, Barata C, Lemos MF. 2017. Fatty acid profile of the sea snail *Gibbula umbilicalis* as a biomarker for coastal metal pollution. *Sci. Total Environ.* **15** (586), 542–550. https://doi.org/10.1016/j.scitotenv.2017.02.015

Signa G, Di Leonardo R, Vaccaro A, Tramati CD, Mazzola A, Vizzini S. 2015. Lipid and fatty acid biomarkers as proxies for environmental contamination in caged mussels *Mytilus galloprovincialis*. *Ecol. Indic.* **57**, 384-394.

Sicuro B, Levine J. 2011**.** Sea cucumber in the Mediterranean: a potential species for aquaculture in the Mediterranean. *Rev. Fish. Sci.* **19**, 299-304. https://doi.org/10.1080/10641262.2011.598249

Tayemeh MB, Esmailbeigi M, Shirdel I, Joo HS, Johari SA, Banan A, Nourani H, Mashhadi H, Jami MJ, Tabarrok M. 2020. Perturbation of fatty acid composition, pigments, and growth indices of *Chlorella vulgaris* in response to silver ions and nanoparticles: A new holistic understanding of hidden ecotoxicological aspect of pollutants. *Chemosphere* **238**, 124576. https://doi.org/10.1016/j.chemosphere.2019.124576

Thyrring J, Juhl BK, Holmstrup M, Blicher ME, Sejr M. 2015. Does acute lead (Pb) contamination influence membrane fatty acid composition and freeze tolerance in intertidal blue mussels in arctic Greenland? *Ecotel.* **24**, 2036–2042. https://doi.org/10.1007/s10646-015-1539-0

Turk Culha S, Dereli H, Karaduman FR, Culha M. 2016. Assessment of trace metal contamination in the sea cucumber (*Holothuria tubulosa*) and sediments from the Dardanelles Strait (Turkey). *Environ. Sci. Pollut. R.* **23** (12), 11584–11597.

Telahigue K, Rabeh I, Bejaoui S, Hajji T, Nechi S, Chelbi E, El Cafsi M, Soudani N. 2018. Mercury disrupts redox status, up-regulates metallothionein and induces genotoxicity in respiratory tree of sea cucumber (*Holothuria forskali*). *Drug. Chem. Toxicol.* **43** (3), 287-297. https://doi.org/10.1080/01480545.2018.1524475

Telahigue K, Rabeh I, Hajji T, Trabelsi W, Bejaoui S, Chouba L, El Cafsi M, Soudani N. 2019. Effects of acute mercury exposure on fatty acid composition and oxidative stress biomarkers in *Holothuria forskali* body wall. *Ecotox. Environ. Safe.* **169**, 516–522. https://doi.org/10.1016/j.ecoenv.2018.11.051

Uttara B, Singh AV, Zamboni P, Mahajan RT. 2009. Oxidative stress and neurodegenerative diseases: a review of upstream and downstream antioxidant therapeutic options. *Curr. Neuropharmacol.* **7**, 65-74. https://doi.org/10.2174/157015909787602823

Verlecar XN, Jena KB, Chainy GBN. 2008. Modulation of antioxidant defences in digestive gland of *Pernaviridis* (L.), on mercury exposures. *Chemosphere* **71**, 1977–1985. https://doi.org/10.1016/j.*Chemosphere*.2007.12.014

Vigh L, Nakamoto H, Landry J, Gomez-Muñoz A, Harwood DJL, Horvath I. 2007. Membrane regulation of the stress response from prokaryotic models to mammalian cells. *Ann. N. Y. Acad. Sci.* **1113**, 40–51. https://doi.org/10.1196/annals.1391.027

Wang P, Wang R, Wang C, Qian J, Hou J. 2016. Exposure-dose-response relationships of the freshwater bivalve *Corbicula fluminea* to inorganic mercury in sediments. *J. Comput. Theor. Nanosci.* **13**, 5714–5723. https://doi.org/10.1166/jctn.2016.5476

GRASAS Y ACEITES 72 (3)
July-September 2021, e426
ISSN-L: 0017-3495
https://doi.org/10.3989/gya.0662201

Quality detection of tea oil by ^{19}F NMR and ^{1}H NMR

T. Liu[a], T.M. Olajide[a], W. Wang[c], Z. Cheng[d], Q. Cheng[c] and X.C. Weng[a,b,✉]

[a]School of Environmental and Chemical Engineering, Shanghai University, 351, Nanchen Road, Shanghai, 200444, People's Republic of China
[b]School of Life Sciences, Shanghai University, 351, Nanchen Road, Shanghai, 200444, People's Republic of China
[c]Anhui Xueyan Tea Oil Co., Ltd, Standardized Factory Building, Jintongtong Pioneer Park, Jinzhai County Modern Industrial Park, Lu'an City, Anhui Province, 237000, People's Republic of China
[d]Xuhui District Donger Primary School, 2, Wanping South Road, Shanghai, 200030, People's Republic of China
✉Corresponding author: wxch@staff.shu.edu.cn

Submitted: 06 June 2020; Accepted: 26 August 2020; Published online: 24 September 2021

SUMMARY: The nuclear magnetic resonance (NMR) technique was applied to monitor the quality of tea oil herein. The adulteration of virgin tea oil was monitored by ^{19}F NMR and ^{1}H NMR. The ^{19}F NMR technique was used as a new method to detect the changes in quality and hydroperoxide value of tea oil. The research demonstrates that ^{19}F NMR and ^{1}H NMR can quickly detect adulteration in tea oil. High temperature caused a decrease in the ratio D and increase in the total diglyceride content. Some new peaks belonging to the derivatives of hydroperoxides appeared at δ-108.21 and δ-109.05 ppm on the ^{19}F NMR spectrum when the oil was autoxidized and became larger when the hydroperoxide value increased. These results have great significance in monitoring the moisture content, freshness and oxidation status of oils and in detecting adulteration in high priced edible oils by mixing with cheap oils.

KEYWORDS: *^{1}H NMR; ^{19}F NMR; Hydroperoxides; Quality detection; Tea oil*

RESUMEN: ***Determinación de la calidad del aceite de té mediante ^{19}F RMN y ^{1}H RMN***. En este trabajo se utiliza la técnica de resonancia magnética nuclear (RMN) para controlar la calidad del aceite de té. La adulteración del aceite de té virgen se controló mediante las técnicas de ^{19}F RMN y ^{1}H RMN. La técnica de ^{19}F RMN se utilizó como un nuevo método para detectar los cambios en la calidad y el índice de hidroperóxido del aceite de té. La investigación demuestra que las técnicas ^{19}F RMN y ^{1}H RMN pueden detectar rápidamente la adulteración del aceite de té. La alta temperatura provoca una disminución en la proporción D y un aumento en el contenido total de diglicéridos. Algunos picos nuevos, pertenecientes a derivados de hidroperóxidos, aparecieron a δ-108,21 y δ-109,05 ppm en el espectro de ^{19}F RMN cuando el aceite se autoxidaba e incrementaban cuando aumentaba el índice de hidroperóxido. Estos resultados tienen gran importancia en el seguimiento del contenido de humedad, de la frescura y del estado de oxidación de los aceites y en la detección de la adulteración de aceites comestibles de alto valor con aceites baratos mediante el uso de ^{19}F RMN y ^{1}H RMN.

PALABRAS CLAVE: *^{1}H RMN; ^{19}F RMN; Aceite de té; Detección de calidad; Hidroperóxidos*

Citation/Cómo citar este artículo: Liu T, Olajide TM, Wang WJ, Cheng ZJ, Cheng Q, Weng XC. 2021. Quality detection of tea oil by ^{19}F NMR and ^{1}H NMR. *Grasas Aceites* **72** (3), e426. https://doi.org/10.3989/gya.0662201

1. INTRODUCTION

Camellia oleifera, commonly called oil tea tree, belongs to the Theaceae family and has been widely cultivated in China for a long time (Qin *et al*., 2018). Camellia oil is widely referred to as tea oil and is commonly utilized for cooking in China (Tu *et al.*, 2017). It is rich in unsaturated fatty acids such as linolenic, linoleic and oleic acids (Weng *et al*., 2018). Its oleic acid content is similar to that found in olive oil, reaching up to 70%. In addition, there are also some unsaponifiable compounds such as tocopherols, squalene, phytosterols, and flavonoids present in tea oil (Memon, 2011; Xiao *et al*., 2016). These nutrients can easily be digested and absorbed by the human body, and are beneficial to lowering cholesterol, preventing and treating hypertension, and cardiovascular diseases (Wang *et al.,* 2012; Lee and Yen, 2006). Tea oil has been reported to exhibit antioxidant activity (Zhou *et al.,* 2018), and is also known as "Oriental Olive Oil", which has been very much preferred by consumers in China. Among plant oils, the low-temperature and cold-pressed tea oil has a higher price than others because it retains nutrients as much as possible. Thus, some unscrupulous merchants adulterate tea oil with other low-price plant oils in order to make higher profits.

The adulteration of tea oil by other low-cost oils damages consumer interest. There are some certain analytical methods for detecting the adulteration and quality of oils, such as GC-MS, ultraviolet spectroscopy, infrared spectroscopy and nuclear magnetic resonance (NMR) spectroscopy (Li *et al.,* 2016; Gurdeniz and Ozen, 2009; Zhou *et al.,* 2015). However, the NMR technique, especially ^{1}H NMR (Sacchi *et al.,* 1997), has become a favorable choice (Santos *et al*., 2018), owing to its fast and effective approach over the traditional methods like GC-MS. Andrade *et al.* (2012) analyzed the degree of unsaturation of combined and free fatty acids in several plant oils (soybean, corn, sunflower, canola, linseed, cottonseed and jatropha) using ^{1}H NMR, which was found to be satisfactory when compared to other conventional methods. Jiang *et al.* (2018a) used ^{1}H NMR as a fast method to determine soybean oil deterioration during deep frying and discovered that it is similar to the conventional gas chromatography method for analyzing secondary oxidation products. ^{1}H NMR can be also used to determine the chemometric characteristics of extra-virgin olive oil (EVOO) in order to identify the specific compounds responsible for olive oil characteristics (Ingallina *et al*., 2019). Shi *et al.* (2018) used ^{1}H NMR combined with chemometrics for the rapid detection of adulteration in tea oil, and also confirmed the efficacy of this method in terms of speed and accuracy.

Our laboratory has previously established a new technique for monitoring the quality and adulteration of olive oil by ^{19}F NMR (Zhou *et al.,* 2015). Jiang et al. (2018b) used this method combined with ^{1}H NMR to detect EVOO adulteration successfully. As far as we know, no study based on a ^{19}F NMR approach for the detection of the quality of tea oil according to temperature and time changes has been reported. In this work, the quality and adulteration of tea oil using ^{19}F NMR was studied and specifically, the determination of moisture content and the detection of oxidation with temperature were conducted in order to expand the application of NMR techniques for the assessment of plant oil quality.

2. MATERIALS AND METHODS

2.1. Chemicals

All solvents were of reagent or analytical grade. Hexafluorobenzene (99%), 4-tert-butylphenol, pyridine and chloroform-d were purchased from Shanghai Macklin Biochemical Co., Ltd. (Shanghai, China). The deriving fluorine reagent (4-fluorobenzoyl chloride, purity: 98%) was purchased from Sigma-Aldrich (Shanghai, China). The rest of the reagents used in the experiment were from Sinopharm Chemical Reagent Co., Ltd. (Shanghai, China).

2.2. Samples

Two tea oils were prepared in our lab: one was extracted with petroleum ether (bp range 60-90 °C) at room (or low) temperature (TOL) and the other was extracted by the Soxhlet method with petroleum ether (TOS) and then the solvent was removed by a vacuum rotary evaporator in a water bath at 30 °C. Other commercial plant oils were purchased from the local supermarket. The samples were stored at room temperature away from light.

5, 10, 15, 20, 25, 30, 35, 40 and 45% refined tea seed oil were separately added to TOL.

2.3. Sample preparation for NMR analysis

0.1 mL hexafluorobenzene in a stock solution of pyridine and CDCl3 mixed in a ratio of 1:1.5 (v/v) was mixed with 0.5 g 4-tert-butylphenol. Hexafluorobenzene was used as reference material because the chemical shift was observed at δ164.90 ppm n the ^{19}F NMR analysis. And 4-tert-butylphenol was as a quantitative standard in the ^{19}F NMR analysis. 0.1 Gram oil sample was put in a 4 mL centrifuge tube mixed with 0.4 mL stock solution. The resulting solution was transferred to a 5 mm NMR tube and 30 μL of deriving reagent were added. Then the reaction mixture was left to react for 0.5 h in the tube at room temperature away from light. After completion, the ^{19}F NMR spectra of the samples were determined immediately.

20 μL oil sample were dissolved in 0.4 mL $CDCl_3$ with 0.03% trimethylsilane (TMS). The resulting solution was transferred to a NMR tube and then the ^{1}H NMR spectra were recorded.

2.4. NMR spectroscopy experiments

All NMR recordings were conducted on a Bruker AVANCE III HD 600MHz spectrometer, operating at 564 and 600 MHz for the ^{19}F and proton nucleus, respectively. Typical spectral parameters for this ^{19}F NMR experiment were as follows: 90° pulse width = 19.3 μs, sweep width = 100 kHz, relaxation delay = 1 s, memory size = 64 K. 32T transients were accumulated for each spectrum. For all FIDs, line broadening of 0.3 Hz was applied and drift correction was performed prior to Fourier transformation.

Typical spectral parameters for ^{1}H NMR experiment were shown as: 16 scans and 4 dummy scans for each free induction decay, 32K for time domain points with a spectral width of 12.0 ppm, 90° pulse width of 9.0 μs, acquisition time of 2.7 s and relaxation delay of 1.0 s.

2.5. Effect of temperature on tea oil

20 Grams of TOL were divided into two equal parts, one of which was spiked with 0.02% *tert*-butylhydroquinone (TBHQ) and the other without any treatment. The samples were placed on a Rancimat instrument for heating and oil samples were taken every 4 h at 80, 100, 120, 140 °C for a total of 24 h,

2.6. Oven test, reducing autoxidized tea oil, determination of POV

40 Grams of tea oil were placed in a clean beaker, and the beaker was placed in a 63 ± 1 °C oven. The peroxide value was measured every 5 days, and the peak between δ-108 ~ δ-110 ppm on a ^{19}F NMR spectrum was measured and calculated.

Two grams of tea oil were dissolved at 63 °C in the oven after the 35 days in 30 mL solvent (acetic acid: $CHCl_3$ = 3:2) and reduced by KI for 3 min and then washed with 100 mL water 3 times to remove the acetic acid. Anhydrous sodium sulfate was used to dry moisture, while $CHCl_3$ in the solution was dried on a rotary evaporator.

The method of peroxide value measured by titration (Stuffins and Weatherall, 1945) was used according to the following formula:

$$\text{POV}\ \ (\text{g}/100\text{g}) = ((V - V_0) \times \text{c} \times 0.1269)/\text{m} \times 100$$

Where V is the volume of sodium thiosulfate standard solution consumed by the sample, V_0 is the volume of sodium thiosulfate standard solution consumed by blank sample, c is the concentration of sodium thiosulfate standard solution, m is the weight of the oil. The formula for the hydroperoxide value between δ-108 and δ-110 ppm measured by ^{19}F NMR is

$$\text{n}(\text{mmol}/100\text{g}) = ((A/A_i) \times N)/m \times 100$$

Where: A is the area of the peak between δ-108 and δ-110 ppm, Ai is the area of the peak of 4-tert-butylphenol, N is the millimolar amount of 4-tert-butylphenol, m is the weight of oil.

2.7. GC-MS experiments

The methyl esterification method for samples before GC-MS was carried out. 50 Milligrams of oil sample dissolved in 4 mL n-hexane (chromatographic grade) were put in a tube with stopper. Then 200 μL of 2 M KOH-CH_3OH were added and the tube was shaken vigorously for 1 minute for methyl esterification. Then it was left to stand for 5 min to allow solid-liquid separation. One gram of sodium hydrogen sulfate monohydrate was added to the solution to neutralize potassium hydroxide, followed by immediate analysis of the supernatant by GC-MS (ISO 5509:2000, ISO 5508:1990).

The GC-MS analyses were performed on a Shimadzu GC2010A (Kyoto, Japan) gas chromatography. A Rtx®-Wax capillary column (30 m length, 0.25 mm i.d., and 0.25 μm film consisting of cross-bond polyethylene glycol (Restek)) was used. The conditions of the GC-MS analysis were as follow: column temperature = 140 to 250 °C, rate = 4 °C/min, injection temperature = 220 °C, carrier gas = nitrogen, column flow (nitrogen flow rate) = 1.36 mL/min, injection volume = 0.5 μL, split ratio = 30:1.

Mass spectroscopy conditions: ion source temperature = 230 °C, interface temperature = 280 °C, ionization voltage = 0.2 kv.

The peak area normalization method was used to calculate the relative content.

2.8. Statistical analyses

All statistical analyses were determined using IBM SPSS 22.0. The experiments were performed in duplicate, and values were expressed as mean ± standard deviation (SD).

3. RESULTS AND DISCUSSION

3.1. ^{19}F NMR analysis

Our lab previously found a novel method to detect the quality and adulteration of olive oil using the ^{19}F NMR technique (Zhou *et al*., 2015). The main principle of the method is based on the derivatization of the active hydroxy groups like diglycerides (DGs) and water with 4-fluorobenzoyl chloride, and the integration of the appropriate peaks in the ^{19}F NMR spectrum in the MestReNova. The deriving reagent and the intermediate products between 4-fluorobenzoyl chloride and the stock solution peaks were observed at δ-105.05 and δ-103.60 ppm, respectively. The peak at δ-107.45 ppm was attributed to 4-tert-butylphenol, the internal standards in this experiment. The peaks at δ-107.95 and δ-107.86 ppm belong to the α- and β-hydroxyl groups of 1,2-DG and 1,3-DG, respectively. The water peak was attributed to δ-110.42 ppm. The quality of tea oil was analyzed by calculating the characteristic peak appearing on the ^{19}F NMR spectrum.

3.2. Diglyceride content

The DG content is an important indicator of the quality of oil, and it can be detected by ^{19}F NMR. The contents of 1,2-DGs, 1,3-DGs, total diglycerides (TDGs) and the ratio D (1,2-DGs to TDGs) in tea oil and other plant oils are summarized in Table 1. After comparing five different kinds of tea oils, it was found that the fresh TOL had a high D ratio (0.77) and lower TDGs (1.45%). The content of TDGs (2.14%) and D ratio (0.27) of refined tea oil showed the opposite trend. Clearly, the D ratio is a significant indicator for judging the quality of oils because it usually occurs from the isomerization of 1,2-DGs to 1,3-DGs during oil storage and refining. A study by Vigli (Vigli *et al.,* 2003) showed that the D ratio of extra virgin olive

Table 1. Compositional parameters of tea oil and some other plant oils determined by ^{19}F NMR Spectroscopy.

Sample	1,3-DGs	1,2-DGs	Total DGs	D
TOL	0.33 ± 0.01	1.12 ± 0.10	1.45 ± 0.11	0.77 ± 0.01
TOS	0.63 ± 0.06	0.85 ± 0.15	1.49 ± 0.21	0.57 ± 0.02
tea oil from the supermarket 1	1.31 ± 0.07	0.54 ± 0.01	1.86 ± 0.06	0.29 ± 0.02
tea oil from the supermarket 2	1.30 ± 0.09	0.62 ± 0.02	1.92 ± 0.11	0.32 ± 0.01
Refined tea oil	1.57 ± 0.06	0.57 ± 0.01	2.14 ± 0.07	0.27 ± 0.01
Extra virgin olive oil	0.58 ± 0.10	0.68 ± 0.00	1.26 ± 0.10	0.54 ± 0.04
Soybean oil	0.24 ± 0.06	0.10 ± 0.02	0.34 ± 0.08	0.31 ± 0.01
Refined soybean oil	0.67 ± 0.03	0.34 ± 0.02	1.01 ± 0.01	0.34 ± 0.02
Rapeseed oil	2.02 ± 0.22	0.80 ± 0.13	2.82 ± 0.34	0.28 ± 0.01
Palm oil	3.01 ± 0.14	1.09 ± 0.07	4.10 ± 0.10	0.27 ± 0.03
Corn oil	2.16 ± 0.05	1.22 ± 0.11	3.38 ± 0.14	0.36 ± 0.02

[a] Data are expressed as mean ± standard deviation (n=2).
[b] TOL, tea oils extracted at low (room) temperature; TOS tea oils extracted by Soxhlet method.

oil (EVOO) freshly extracted from normal mature olives should be close to 1. Although the D ratio in all oil samples decreases with storage time, the closer the D ratio is to 1, the fresher the oil. When two kinds of tea oil based on extraction temperature were compared, TOL had a higher D ratio, indicating it has better quality and freshness. Usually, commercial tea oil is inevitably affected by temperature during the production process, especially the refining process. Table 1 shows the D ratio of TOL (0.77) > TOS (0.57) > tea oil from the supermarket (0.29, 0.32) > refined tea oil (0.27). This phenomenon is supported by the present results, that is, the quality of tea oil is affected by temperature and freshness. EVOO is a high quality cold-pressed plant oil because of its nutritional value and health benefits. The D ratio of TOL in our lab is much higher than all EVOO samples detected in our previous papers (Zhou *et al*., 2015; Jiang *et al*., 2018b) because all EVOO samples were imported from Spain and Italy to Shanghai at least 1.5 years after being prepared. In addition, the 1,3-DG content of all the other plant oils was higher than 1,2-DGs, and the D ratio D was about 0.3 which is in agreement with the study by Zhou *et al*. (2015). This indicates that the extraction temperature has a great influence on the quality and freshness of plant oil. The lower the extraction temperature is, the better the quality of the oil.

3.3. Moisture content

Moisture content is also a significant indicator for judging the quality of oils (Hu *et al*., 2008). In order to study the moisture content of tea oil by ^{19}F NMR, tea oil was placed in the oven at 63 °C until its mass was constant, then cooled to room temperature. 0, 0.01, 0.02, 0.04, 0.06, 0.08 and 0.1% distilled water was added to the tea oil, and shaken vigorously. ^{19}F NMR was subsequently used to detect the moisture content. The moisture contents in the tea oil were detected at 0, 0.008 ± 0.002, 0.015 ± 0.003, 0.042 ± 0.005, 0.055 ± 0.002, 0.060 ± 0.004, 0.059 ± 0.005%, respectively by ^{19}F NMR. The water contents detected by ^{19}F NMR agree well with those added. The detection of moisture content is usually done together with volatile matters in oils according to the official methods of AOAC (1997, method Cd 8b-90). But in some cases, volatile matters are desired flavors for some edible oils, such as EVOO, or Chinese traditional ground sesames oil. So ^{19}F NMR can directly detect the specific moisture contents in oils. As expected, the solubility of moisture in oil is very low. When the content of added moisture reaches the saturated state of oil dissolution, the excess water will layer from the oil quickly and easily. According to the results of the moisture content detected by ^{19}F NMR, when the content of added water reaches 0.06%, the moisture content becomes saturated in the oil. When over 0.06% water is added to oil, high deviation happens.

3.4. Adulteration of tea oil with refined tea oil

Refined tea oil has the same fatty acid composition of tea oil prepared at a low temperature, but it is much cheaper, so some unscrupulous merchants add refined tea oil to tea oil to make more profit. In addition, there are some minor nutritional components in tea oil that are lost during refining. Some researchers have suggested that the D ratio can be utilized as an index to distinguish different grades of the same kind of oil such as olive oil (Jiang *et al.,* 2018b). Hence, using ^{19}F NMR to detect adulteration in cold-extracted tea oil with refined tea oil is feasible.

In Figure 1, the contents of 1,3-DGs, TDGs increased and D ratio decreased with the adulteration level. The D ratio and the adulteration level showed good correlation (r = 0.9653). It can be seen that it is feasible to use ^{19}F NMR to detect the incorporation of refined tea oil into TOL. Therefore, the D ratio is a key parameter for determining whether TOL is adulterated with refined tea seed oil or not. The higher the D ratio is, the fresher the tea oil.

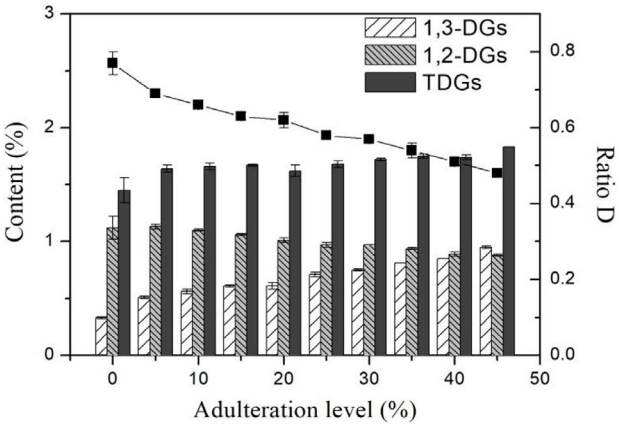

Figure 1. 1,2-DGs (%), 1,3-DGs (%), TDGs content (%), D ratio of the adulteration of tea oil with refined tea oil determined by ^{19}F NMR. Values are mean ± standard deviation (n=2).

3.5. Adulteration of tea oil with other plant oils

3.5.1. Determination of fatty acid composition

^{1}H NMR has been demonstrated as a method for determining the fatty acid composition of oil (Shi *et al.,* 2018). The contents in unsaturated fatty acids (oleic, linoleic and linolenic acids), saturated fatty acids (SFAs) and squalene in plant oils can be obtained by calculating the integral peak area on the ^{1}H NMR spectrum (Figure 2). The assignment of fatty acid signals has been established by Castejón *et al.,* (2014). According to the various signal intensities appearing in the ^{1}H NMR spectra, the peak at δ1.68 ppm in the ^{1}H NMR spectrum of tea oils belongs to squalene. In comparison with another study on the ^{1}H NMR spectrum of squalene, the peak was identified as methyl protons belonging to the CH_3-17 and CH_3-29 of squalene (Mannina *et al.,* 2009; Shi *et al.,* 2019).

According to Jiang *et al.* (2018a), all spectra of different plant oils have similar shape but different peak intensities. So according to the diversity of the fatty acid composition of plant oils, the detection of adulteration in tea oil can be carried out. Then the ^{1}H NMR technique was used to detect the adulteration of tea oil with other plant oils, and GC-MS served as a standard method.

3.5.2. Adulteration of tea oil with soybean oil

Soybean oil, which is much cheaper than TOL and may be used to adulterate TOL, has a different fatty acid composition compared to tea oil. As shown in Figure 3a, in addition to SFAs, the other three parameters, linolenic, linoleic, and oleic acids are all in good agreement with the adulteration level. With an increase in the adulteration level, the contents of linolenic and linoleic acids also increased, whereas the content of oleic acid decreased. GC-MS is a traditional method for detecting oleic acid content in adulterated TOL. The sensitivity and veracity of ^{1}H NMR in determining fatty acid composition can be compared to GC-MS. When the adulteration level reached 45%, the linolenic, linoleic and oleic acid contents according to ^{1}H NMR were 2.63, 28.12 and 52.17%. The content of linolenic, linoleic and oleic acid by GC-MS were 2.53, 29.10 and 54.85%, respectively. The differences in linolenic, linoleic and oleic acid values were 0.1, 0.98 and 2.68%, which showed about 3.95, 3.37 and 4.89% deviation from the data measured by GC-MS. It can be seen that the fatty acid contents measured by ^{1}H NMR were consistent with GC-MS. So ^{1}H NMR can accurately detect the adulteration in tea oil with soybean oil more rapidly than GC-MS.

Comparing the linear equation of linolenic, linoleic and oleic acids by ^{1}H NMR and GC-MS,

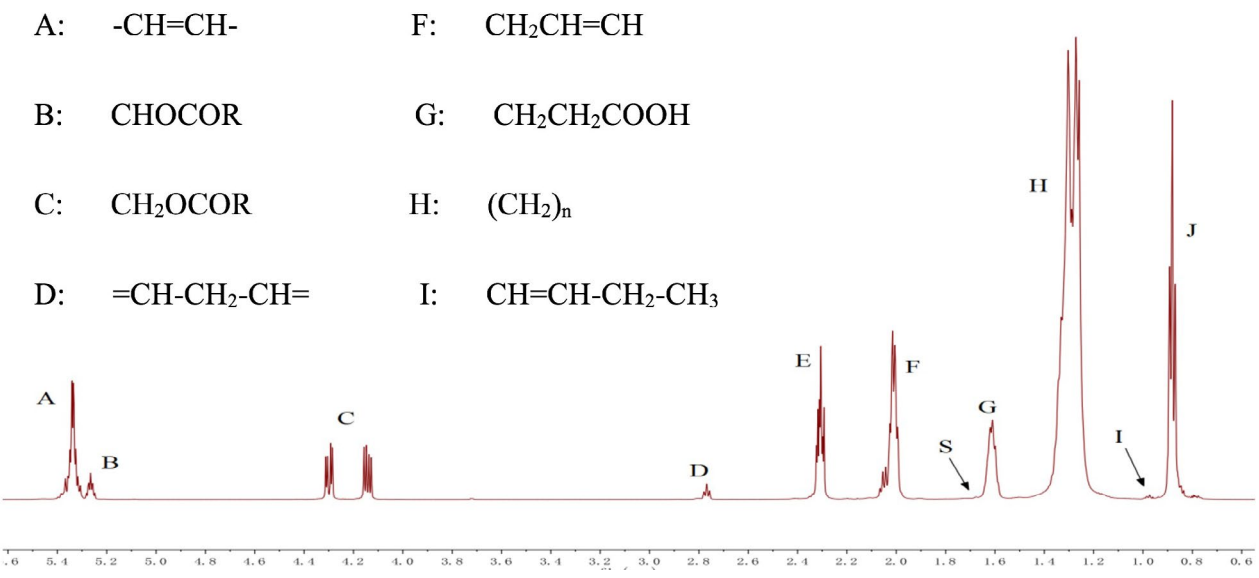

FIGURE 2. 600 MHz ^{1}H NMR spectrum of Camellia Oil.

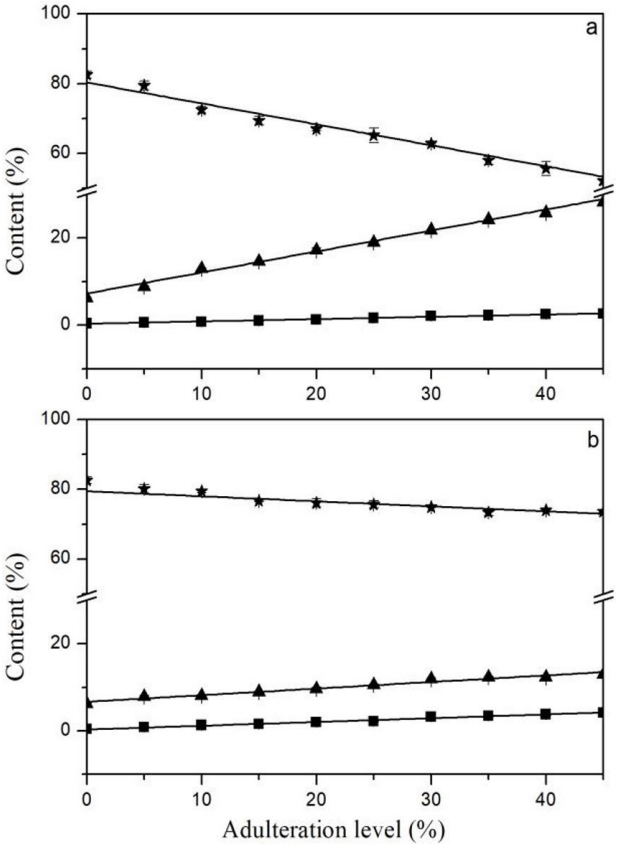

FIGURE 3. Four parameters (oleic, linoleic, linolenic acids and SFAs) in the adulteration of tea oil with other plant oils determined by ^{1}H NMR. (a) adulteration of tea oil with soybean oil, b) adulteration of tea oil with rapeseed oil) (■ linolenic acid, ▲ linoleic acid, ★ oleic acid). Values are mean ± standard deviation (n=2).

it can be found that the contents of linolenic and linoleic acid show the best relationship (R=0.9889) with the adulteration level. According to the linear equation (y = 0.0537x + 0.3111) for linoleic acid, the adulteration level can be accurately calculated.

3.5.3. Adulteration of tea oil with rapeseed oil

Rapeseed oil is an edible oil containing erucic, oleic, linoleic and linolenic acids, tocopherols and sterols (Lambelet *et al.,* 2003). Generally, there are about 14-19% oleic acid and 31-55% erucic acid in traditional rapeseed oil, and erucic acid is bad for the growth and development of the human body (Clement and Renner, 1977). The average content in high-oleic rapeseed oil is about 61%, which is similar to that in tea oil. Therefore, this kind of rapeseed oil was chosen for adulteration to detect the sensitivity of the ^{1}H NMR method. As shown in Figure 3b, the fatty acid composition (oleic, linoleic and linolenic acids), especially the content of oleic acid, are all in good relationship with the adulteration level. The various fatty acid contents were consistent with those detected by GC-MS. When the adulteration level reached 10%, the linolenic acid contents were 1.05 and 1.31% as detected by ^{1}H NMR and GC-MS, respectively. The biggest difference in the linolenic acid value was 0.26%, which was about a 24.62% deviation from the data measured by GC-MS. When the adulteration level reached 45%, the linolenic acid contents were 4.13 and 4.13% as detected by ^{1}H NMR and GC-MS, respectively. This shows no deviation from the data measured by GC-MS. Comparing linoleic oleic acids detected by ^{1}H NMR and GC-MS, the biggest differences in value were 1.65 and 2.29%, which were about 17.40 and 3.21% deviation from the data measured by GC-MS. So ^{1}H NMR can also detect the adulteration of tea oil with rapeseed oil more quickly than GC-MS.

Therefore, there is no significant difference between the two methods used for detecting the adulteration of tea oil. This phenomenon may be applied to determining the content of 18-chain fatty acids in soybean oil and rapeseed oil. Rapeseed oil has more 18 carbon chain fatty acids than soybean oil. The more 18 carbon chain fatty acid content present in oils, the more sensitive the ^{1}H NMR detection method is (Knothe *et al.*, 1996).

3.6. Effect of temperature on the quality of tea oil

The temperature during extraction, transportation and storage of tea oil has a certain impact on its quality. High temperatures can lead to a decline in the quality of tea oil, which often leads to the loss of some nutrients and speedy autoxidation, isomerization. High temperature can also cause an increase in peroxides in oils. All these influences can be detected by ^{19}F NMR.

3.6.1. The content of TDGs

Figure 4 shows the changes in DG contents and D ratio at 80, 100, 120 and 140 °C within 24 hours in the ^{19}F NMR spectrum when the S/N ratio of the peaks is 8. The D ratio steadily decreased for 16 h and then became stable as heating time increased under 80 °C. Whereas, the D ratio decreased sharply in the first 4 h and then remained stable as temperature increased. The results show that the isomerization of 1,2-

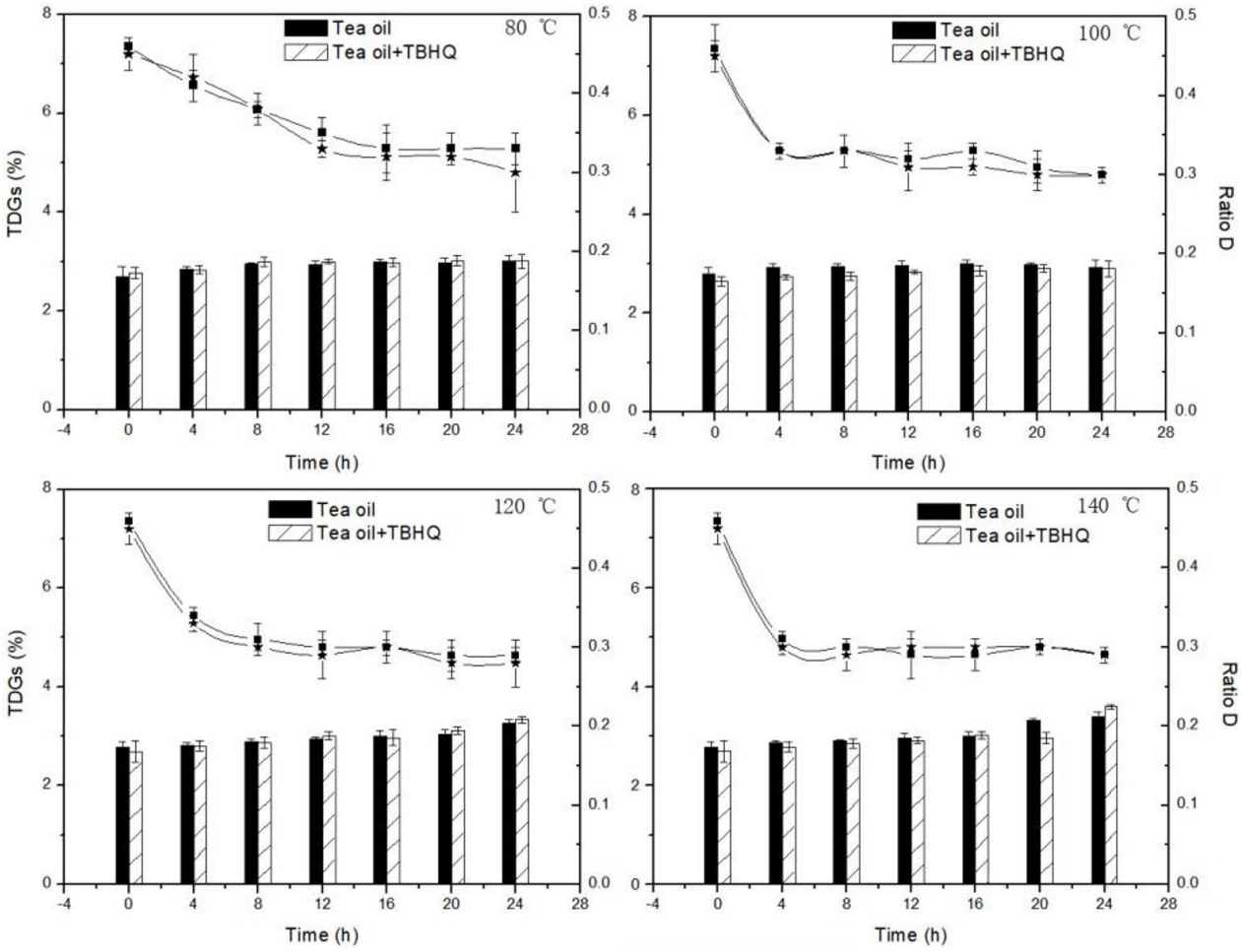

FIGURE 4. The tea oil content of total diglycerides (TDGs) (Columns) and D ratio (Curves) in tea oil and tea oil+tert-butylhydroquinone (TBHQ) heated at 80, 100, 120 and 140 ºC within 24 hours. (■: tea oil; ★: tea oil+TBHQ)

DGs to 1,3-DGs will accelerate when temperature rises. But antioxidants do not affect the speed of the isomerization.

3.6.2. The hydroperoxides

Characteristic peaks at δ-108.21 and δ-109.05 ppm were observed on the ^{19}F NMR spectrum. These peaks are reasoned to belong to the hydroperoxides due to four factors. Firstly, the peak areas of compounds at δ-108.21 and δ-109.05 ppm on the ^{19}F NMR spectrum increased markedly when the heating time increased to 140 °C, as shown in Figure 5. Secondly, the addition of TBHQ to the oil as a positive control greatly inhibited the increase in the peak areas at δ-108.21 and δ-109.05 ppm during 16 to 24 h because TBHQ is a very strong antioxidant and can effectively retard autoxidation of oils, and inhibit the increase in hydroperoxides. But oils commonly contain some natural antioxidants themselves, so oils with and without the addition of antioxidants can retard autoxidation during the first 12 h. But after 12 h, oil without antioxidant addition consumed its own natural antioxidants, and the amount of hydroperoxides increased more rapidly than the oil with the addition of antioxidants. All natural antioxidants, including the ones added, were consumed completely and the hydroperoxides reached maximum levels, as shown in Figure 6. Thirdly, POV (including hydroperoxides and other peroxides), as determined by classic titration is very closely correlated (R2 = 0.943), as shown in Figure 7. Fourthly, it seems that two peaks appear at -109.05 ppm (Figure 8a) after tea oil oxidized for 35 days. But after it was reduced by KI in the acetic acid solution,

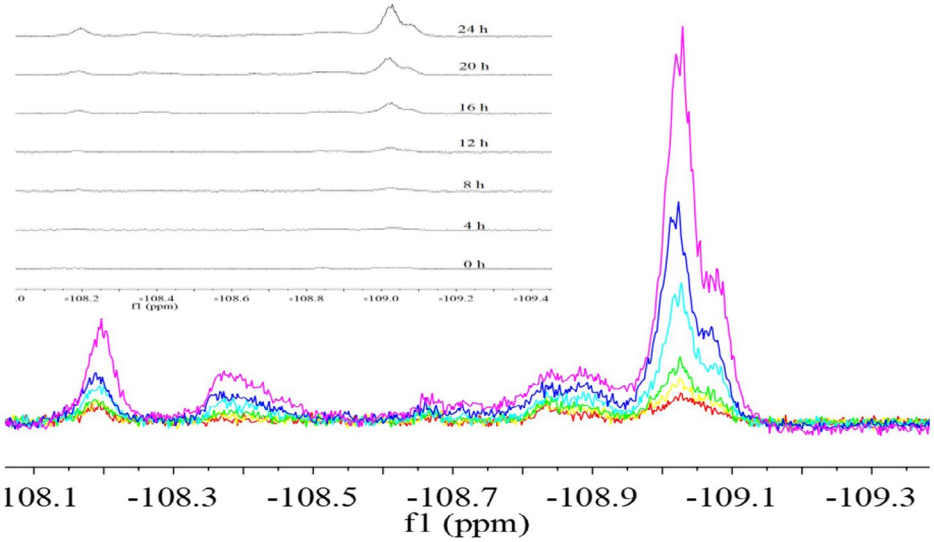

FIGURE 5. 600 MHz ^{19}F NMR spectrum of tea oil heated at 140 °C for 24 h.

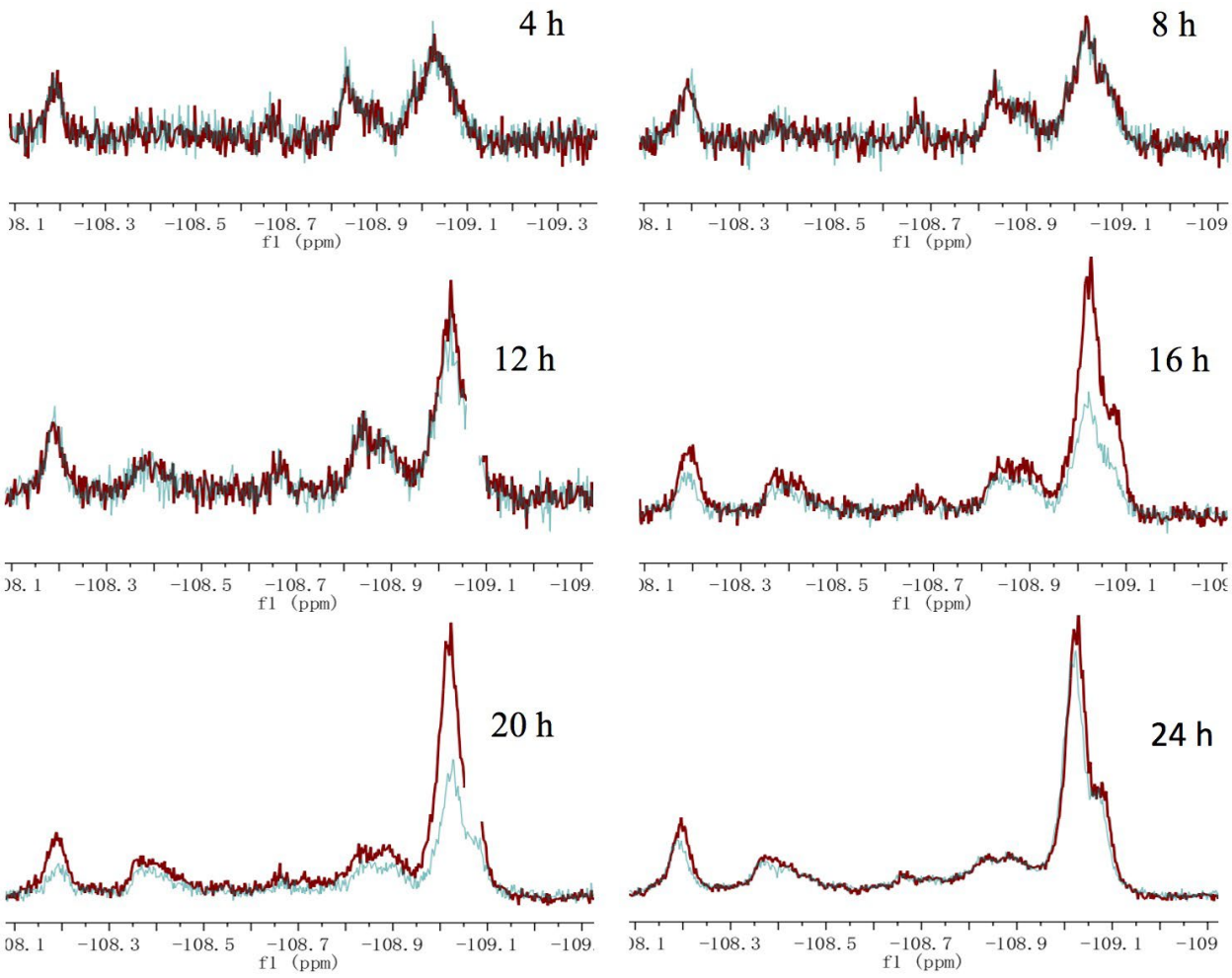

FIGURE 6. The difference between tea oil and tea oil+tert-butylhydroquinone (TBHQ) as detected by ^{19}F NMR during heating at 140 °C for 24 h. (brown: the spectrum of tea oil; blue: the spectrum of tea oil+TBHQ)

two peaks at -109.05 ppm disappeared completely and two new peaks appeared at -109.78 ppm (Figure 8b) and were much more distinguishable than those at -109.05 ppm. This means the hydroperoxides were reduced to related alcohols. The peaks at δ-108.21 ppm showed the same change, disappeared completely and a new peak appeared at δ-109.00 ppm. Figure 9 may explain why the ^{19}F NMR spectrum of autoxidized tea oil appeared in two peaks because the conjugated di-double bonds had a stronger de-shielding effect than the mono-double bond. Also, it is easily explained that two ^{19}F NMR peaks of alcohols are more distinguishable than hydroperoxide ones because the carbon chains of alcohols affect fluorine more than those of hydroperoxides because of one more oxygen atom between fluorine and carbon chains in hydroperoxides.

According to the GB/T11765-2018, the peroxide value for tea oil must be lower than 0.25 g/100g. On the basis of the linear equation y = 7.2077x + 0.1244 for peroxide value measured by titration and ^{19}F NMR, the limit of detection for the hydroperoxide

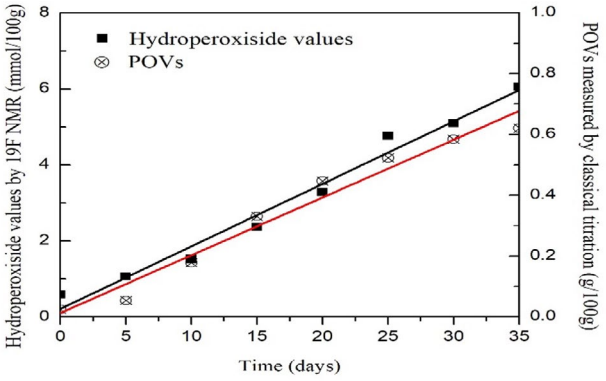

FIGURE 7. The relationship between the peroxide values (POVs) measured by titration and hydroperoxide values by the ^{19}F NMR technique. Values are mean ± standard deviation (n=2).

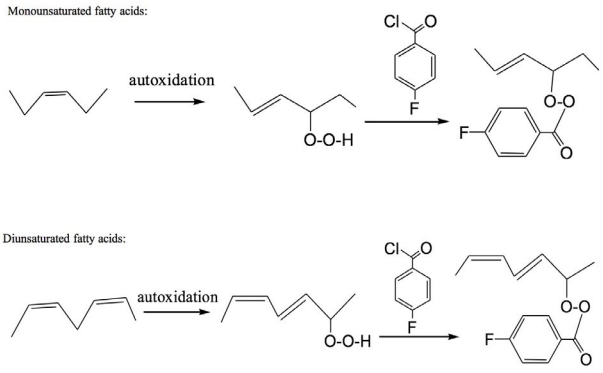

FIGURE 9. Autoxidation of unsaturated fatty acids and the reaction of hydroperoxides of unsaturated fatty acids with 4-fluorobenzoyl chloride.

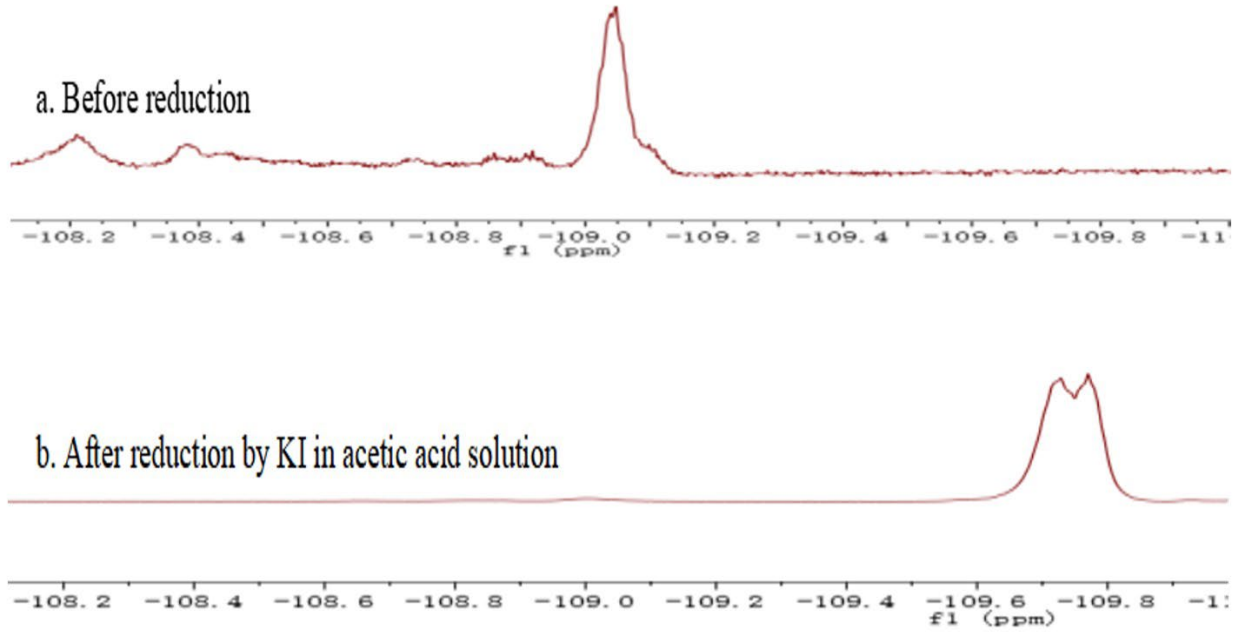

FIGURE 8. The ^{19}F NMR spectra of tea oil stored in the oven at 63 °C for 35 days. (a. Before reduction; b. After reduction by KI in acetic acid solution.)

value level was 1.93 mmol/100g, according to the ^{19}F NMR method. Over this hydroperoxide value (1.93 mmol/100g), the peroxide value for tea oil exceeds regulations and the quality of tea oil is not up to standard.

4. CONCLUSIONS

This is the first time that ^{19}F NMR is used to determine the quality of tea oil, especially the changes in the quality and autoxidation of tea oil. The results from this study demonstrated that ^{19}F NMR and ^{1}H NMR can effectively detect the adulteration of low-temperature extracted tea oil with refined tea oil and other low-price edible oils. The characteristic peaks appearing at δ-108.21 and δ-109.05 ppm on the ^{19}F NMR spectrum belonged to hydroperoxides, and they can be used as an indicator for the determination of the quality and oxidation of tea oil. This phenomenon has great significance for the quality determination of tea oil. Meanwhile, it was found that high temperatures affected the TGDs content and D ratio in tea oil in a short time, and then remained at a certain level within 24 h. In addition, ^{19}F NMR technology can detect long-term dynamic changes of the quality of tea oil. This method is a new, faster and more comprehensive method to determine the quality of tea oil.

ACKNOWLEDGMENTS

The Authors wish to thank Dr. Yan-Hong Song and Dr. Hong-Mei Deng at the Instrumental Analysis and Research Center of Shanghai University for NMR spectra recording and technical assistance, as well as Anhui Xueyan Tea Oil Co., Ltd. for providing research funds and the tea oil samples.

REFERENCES

Andrade DF, Mazzei JL, Kaiser CR. 2012. Assessment of Different Measurement Methods Using 1H-NMR Data for the Analysis of the Transesterification of Vegetable Oils. *J. Am. Oil Chem. Soc*. **89**, 619-630. https://doi.org/10.1007/s11746-011-1951-4

Castejón D, Mateos-Aparicio I, Molero MD, Cambero MI, Herrera A. 2014. Evaluation and optimization of the analysis of fatty acid types in edible oils by ^{1}H NMR. *Food Anal. Methods* **7,** 1285–1297. https://doi.org/10.1007/s12161-013-9747-9

Clement H, Renner R. 1977. Studies of the Utilization of High and Low Erucic Acid Rapeseed Oils by the Chick. *J. Nutr.* **107**, 251-260. https://doi.org/10.1093/jn/107.2.251

GB (national test standard). 2018. Oil-tea camellia seed oil. GB/T11765-2018. Int. Organ. Stand., China.

Gurdeniz G, Ozen B. 2009. Detection of adulteration of extra-virgin olive oil by chemometric analysis of mid-infrared spectral data. *Food Chem.* **116**, 519-525. https://doi.org/10.1016/j.foodchem.2009.02.068

Hu L, Toyoda K, Ihara I. 2008. Dielectric properties of edible oils and fatty acids as a function of frequency, temperature, moisture and composition. *J. Food Eng.* **88**, 151-158. https://doi.org/10.1016/j.jfoodeng.2007.12.035

ISO (International Organization for Standarization). 1990. Animal and vegetable fats and oils—Analysis by gas chromatography of methyl esters of fatty acids. ISO 5508:1990 (IDT.). Int. Organ. Stand., Geneva, Switzerland.

ISO (International Organization for Standarization). 2000. Animal and vegetable fats and oils—Preparation of methyl esters of fatty acids. EN ISO 5509:2000 (E). Int. Organ. Stand., Geneva, Switzerland.

Jiang X, Huang R, Wu S. 2018a. Correlations between ^{1}H NMR and conventional methods for evaluating soybean oil deterioration during deep frying. *J. Food Meas Charact.* **12**, 1420–1426. https://doi.org/10.1007/s11694-018-9757-9

Jiang XY, Li C, Chen QQ, Weng XC. 2018b. Comparison of ^{19}F and ^{1}H NMR spectroscopy with conventional methods for the detection of extra virgin olive oil adulteration. *Grasas Aceites* **69**, 249. https://doi.org/10.3989/gya.1221172

Knothe G, Bagby MO, Weisleder D. 1996. Evaluation of the olefinic proton signals in the ^{1}H-NMR spectra of allylic hydroxy groups in long-chain compounds. *Chem. Phys. Lipids.* **82**, 33-37. https://doi.org/10.1016/0009-3084(96)02559-5

Lambelet P, Grandgirard A, Gregoire S. 2003. Formation of modified fatty acids and oxyphytosterols during refining of low erucic acid rapeseed oil. *J. Agric. Food Chem.* **51,** 4284. https://doi.org/10.1021/jf030091u

Lee CP, Yen GC. 2006. Antioxidant activity and bioactive compounds of tea seed (*Camellia oleifera* Abel.) oil. *J. Agric. Food. Chem.* **54**, 779. https://doi.org/10.1021/jf052325a

Li X, Kong W, Shi W, Shen Q. 2016. A combination of chemometric methods and gc–ms for the classification of edible vegetable oils. *Chemometr Intell. Lab.* **155**, 145-150. https://doi.org/10.1016/j.chemolab.2016.03.028

Mannina L, D'Imperio M, Capitani D, Rezzi S, Aparicio R. 2009. ^{1}H NMR-Based Protocol for the Detection of Adulterations of Refined Olive Oil with Refined Hazelnut Oil. *J. Agric. Food Chem.* **57**, 11550-11556. https://doi.org/10.1021/jf902426b

Memon A. 2011. Phenolic compounds and seed oil characterization of *Ziziphus Mauritiana* L. fruit grown in Pakistan. *FASEB. J.* **25**, 3515-3524. https://doi.org/10.1002/jcb.23318

Qin S, Rong J, Zhang W, Chen J. 2018. Cultivation history of *Camellia oleifera* and genetic resources in the Yangtze River Basin. *Bio. Sci*. https://doi.org/10.17520/biods.2017254

Sacchi R, Addeo F, Paolillo L. 1997. ^{1}H and ^{13}C NMR of virgin olive oil. An overview. *Magn. Reson. Chemi.* **35**, S133–S145. https://doi.org/10.1002/(SICI)1097-458X(199712)35:13<S133::AID-OMR213>3.0.CO;2-K

Santos JS, Escher GB, Marcos DSPJ. 2018. ^{1}H NMR combined with chemometrics tools for rapid characterization of edible oils and their biological properties. *Ind. Crop. Prod.* **116**, 191-200. https://doi.org/10.1016/j.indcrop.2018.02.063

Shi T, Zhu M, Chen Y, Yan X, Chen Q, Wu X, Lin J, Xie M. 2018. ^{1}H NMR combined with chemometrics for the rapid detection of adulteration in camellia oils. *Food Chem.* **242**, 308-315. https://doi.org/10.1016/j.foodchem.2017.09.061

Shi T, Zhu M, Zhou X, Huo X, Long Y, Zeng X, Chen Y. 2019. ^{1}H NMR combined with PLS for the rapid determination of squalene and sterols in vegetable oils. *Food Chem.* **287**, 46-54. https://doi.org/10.1016/j.foodchem.2019.02.072

Stuffins CB, Weatherall H. 1945. Determination of the peroxide value of oils and fats. *Analyst.* **70**, 403-409. https://doi.org/10.1039/AN9457000403

Tu PS, Tung YT, Lee WT, Yen GC. 2017. Protective Effect of Camellia Oil (*Camellia oleifera* Abel.) against Ethanol-induced Acute Oxidative Injury of the Gastric Mucosa in Mice. *J. Agric. Food Chem.* **65**, 4932-4941. https://doi.org/10.1021/acs.jafc.7b01135

Vigli G, Philippidis A, Spyros A, Dais P. 2003. Classification of Edible Oils by Employing ^{31}P and ^{1}H NMR Spectroscopy in Combination with Multivariate Statistical Analysis. A Proposal for the Detection of Seed Oil A. *J. Agric. Food Chem.* **51**, 5715-5722. https://doi.org/10.1021/jf030100z

Wang Y, Huang S, Shao S. 2012. Studies on bioactivities of tea (*Camellia sinensis* L.) fruit peel extracts: Antioxidant activity and inhibitory potential against α-glucosidase and α-amylase in vitro. *Ind. Crop. Prod*. **37,** 520-526. https://doi.org/10.1016/j.indcrop.2011.07.031

Weng X, Yun Z, Zhang C. 2018. Comparison of the Characteristics of Two Kinds of Tea Seed Oils: Oil-tea Seed Oil and Green-Tea Seed Oil. *J. Food Stud.* **7**, 56. https://doi.org/10.5296/jfs.v7i1.12289

Xiao H, Yao Z, Peng Q, Ni F, Sun Y, Zhang CX, Zhong ZX. 2016. Extraction of squalene from camellia oil by silver ion complexation. *Sep. Purif. Technol.* **169**, 196-201. https://doi.org/10.1016/j.seppur.2016.05.041

Zhou LL, Li C, Weng XC, Fang XM, Gu ZH. 2015. ^{19}F NMR method for the determination of quality of virgin olive oil. *Grasas Aceites* **66**, e106. https://doi.org/10.3989/gya.0242151

Zhou X, Xu L, Feng S, Jing L, Zhou L, Yang R, Ding C. 2018. Antioxidant effect of hawk tea extracts on camellia oil oxidation during microwave heating. *J. Consum Prot. Food S.* **13,** 1-8. https://doi.org/10.1007/s00003-018-1167-8

Grasas y aceites

International Journal of Fats and Oils

Volumen 72 | Nº 3 | **July-September 2021** | Sevilla (España) | ISSN-L: 0017-3495

Sumario

INVESTIGACIÓN / *RESEARCH*

GOBIERNO DE ESPAÑA MINISTERIO DE CIENCIA E INNOVACIÓN CSIC

ISSN 0017-3495

http://grasasyaceites.revistas.csic.es

editorial.csic.es